CENTER FOR DRUG EVALUATION AND RESEARCH

APPLICATION NUMBER:

202570Orig1s000

PHARMACOLOGY REVIEW(S)

DEPARTMENT OF HEALTH AND HUMAN SERVICES
PUBLIC HEALTH SERVICE
FOOD AND DRUG ADMINISTRATION
CENTER FOR DRUG EVALUATION AND RESEARCH

PHARMACOLOGY/TOXICOLOGY NDA/BLA REVIEW AND EVALUATION

Application number:	202570
Supporting document/s:	0000
Applicant's letter date:	March 30, 2011
CDER stamp date:	March 30, 2011
Product:	Xalkori® (Crizotinib)
Indication:	ALK-positive non-small cell lung cancer
Applicant:	Pfizer Inc
Review Division:	Division of Drug Oncology Products (HFD-150)
Reviewer:	Brenda J. Gehrke, Ph.D.
Acting Team Leader:	Whitney S. Helms, Ph.D.
Division Director:	Robert Justice, M.D.
Project Manager:	CDR Diane Hanner

Disclaimer

Except as specifically identified, all data and information discussed below and necessary for approval of NDA 202570 are owned by Pfizer Inc or are data for which Pfizer Inc has obtained a written right of reference. Any information or data necessary for approval of NDA 202570 that Pfizer Inc does not own or have a written right to reference constitutes one of the following: (1) published literature, or (2) a prior FDA finding of safety or effectiveness for a listed drug, as reflected in the drug's approved labeling. Any data or information described or referenced below from reviews or publicly available summaries of a previously approved application is for descriptive purposes only and is not relied upon for approval of 202570.

Labeling Review for Xalkori ® (Crizotinib) capsules (NDA 202750):

The Sponsor Proposes:	We recommend:	Justification:
Highlights:		
Indications and Usage TRADENAME is a kinase inhibitor indicated for the treatment of: (b) (4)	**Indications and Usage** XALKORI is a kinase inhibitor indicated for the treatment of patients with locally advanced or metastatic non-small cell lung cancer (NSCLC) that is anaplastic lymphoma kinase (ALK)-positive as detected by an FDA-approved test. (1)	No change was made to the pharmacologic class in the indication statement.
Warnings and Precautions	**Warnings and Precautions** • Pregnancy: XALKORI can cause fetal harm when administered to a pregnant woman. (5.5, 8.1)	The pregnancy category was changed (b) (4) to D, therefore, a Pregnancy section was added to Warnings and Precautions.
5. Warnings and Precautions		
	5.5 Pregnancy XALKORI can cause fetal harm when administered to a pregnant woman based on its mechanism of action. In nonclinical studies in rats crizotinib was embryotoxic and fetotoxic at exposures similar to and above those observed in humans at the recommended clinical dose of 250 mg twice daily. There are no adequate and well-controlled studies in pregnant women using XALKORI. If this drug is used during pregnancy, or if the patient becomes pregnant while taking this drug, the patient should be apprised of the potential hazard to a fetus. *[see Use in Specific Populations (8.1)].*	The pregnancy category was changed (b) (4) to D, therefore, a Pregnancy section was added to Warnings and Precautions. Standard language and formatting for pregnancy category D outlined in the CFR were used to comply with PLR regulations. The phrase" based on its mechanism of action" was added to indicate that the statement is based on the mechanism of action and not human data. The sentence, "In nonclinical studies in rats crizotinib was embryotoxic and fetotoxic at exposures similar to and above those observed in humans at the recommended clinical dose of 250 mg twice daily" was added to briefly describe the animal data.

The Sponsor Proposes:	We recommend:	Justification:
8. Use in Specific Populations		
8.1 Pregnancy (b) (4)	**8.1 Pregnancy** **Pregnancy Category D *[see "Warnings and Precautions" (5.5)]*** XALKORI can cause fetal harm when administered to a pregnant woman based on its mechanism of action. There are no adequate and well-controlled studies of XALKORI in pregnant women. In nonclinical studies in rats, crizotinib was embryotoxic and fetotoxic at exposures similar to and above those observed in humans at the recommended clinical dose of 250 mg twice daily. Crizotinib was administered to pregnant rats and rabbits during organogenesis to study the effects on embryo-fetal development. Postimplantation loss was increased at doses ≥ 50 mg/kg/day (approximately 1.2 times the AUC at the recommended human dose) in rats. No teratogenic effects were observed in rats at doses up to the maternally toxic dose of 200 mg/kg/day (approximately 5 times the AUC at the recommended human dose) or in rabbits at doses of up to 60 mg/kg/day (approximately 3 times the AUC at the recommended human dose), though fetal body weights were reduced at these doses. Women of childbearing potential should be advised to avoid becoming pregnant while receiving XALKORI. Women of childbearing potential who are receiving this drug, or partners of women of childbearing potential receiving this drug, should use adequate contraceptive methods during therapy and for	The pregnancy category was changed (b) (4) to D. Pregnancy Category D was considered appropriate for this drug for the following reasons: • Positive findings of post-implantation loss and low fetal weight in animals at exposures similar to the clinical exposure—based on an ODAC discussion in which it was agreed that based on mechanism of action (targeting rapidly dividing cells and targets that are important in embryogenesis) that Category D was appropriate for many cancer drugs despite the lack of human data. • The importance of ALK in neural development which would not be reflected well in the embryo-fetal development studies—while embryo-fetal studies are the only reproductive toxicology studies required for a drug in this patient population, pregnancy categories are based on an assumption of the full battery of reproductive toxicology studies being performed Language from the Warnings section was repeated based on recommendations from the Maternal Health Team. Additional details of the animal studies conducted and results were added, including doses of crizotinib and the finding of postimplantation loss in rats, in order to communicate all relevant findings.

The Sponsor Proposes:	We recommend:	Justification:
	at least 90 days after completing therapy. If this drug is used during pregnancy, or if the patient or their partner becomes pregnant while taking this drug, the patient should be apprised of the potential hazard to a fetus.	The statement on adequate contraceptive methods was expanded to include partners of women of childbearing potential as an additional precaution to take into account the finding of a miscarriage in 1 of 2 reported pregnancies in partners of patients receiving crizotinib in clinical trials. While these reports were not considered definitive evidence, the team concluded that extra caution might be warranted.
8.2 Nursing Mothers (b) (4)	**8.3 Nursing Mothers** It is not known whether XALKORI is excreted in human milk. Because many drugs are excreted in human milk and because of the potential for serious adverse reactions in nursing infants from XALKORI, a decision should be made whether to discontinue nursing or to discontinue the drug, taking into account the importance of the drug to the mother.	Standard language and formatting outlined in the CFR were used to comply with PLR regulations The cross-reference to section 13.1 was removed since it is not necessary.
8.3 Pediatric Use The safety and efficacy of TRADENAME in pediatric patients has not been established. Decreased bone formation in growing long bones was observed in immature rats at 150 mg/kg/day following once daily dosing for 28 days (approximately (b) (4) times (b) (4) AUC). Other toxicities of potential concern to pediatric patients have not been evaluated in juvenile animals.	**8.4 Pediatric Use** The safety and efficacy of XALKORI in pediatric patients has not been established. Decreased bone formation in growing long bones was observed in immature rats at 150 mg/kg/day following once daily dosing for 28 days (approximately 10 times the AUC in adult patients at the recommended human dose). Other toxicities of potential concern to pediatric patients have not been evaluated in juvenile animals.	As the findings in bone were observed only in male rats, the comparison should be based on the AUC value for the male rats alone. Male rats had a higher exposure than females. This statement also clarifies that the AUC data used for the comparison was from adult patients.

The Sponsor Proposes:	We recommend:	Justification:
12. Clinical Pharmacology		
12.1 Mechanism of Action (b) (4)	**12.1 Mechanism of Action** Crizotinib is an inhibitor of receptor tyrosine kinases including ALK, Hepatocyte Growth Factor Receptor (HGFR, c-Met), and Recepteur d'Origine Nantais (RON). Translocations can affect the ALK gene resulting in the expression of oncogenic fusion proteins. The formation of ALK fusion proteins results in activation and dysregulation of the gene's expression and signaling which can contribute to increased cell proliferation and survival in tumors expressing these proteins. Crizotinib demonstrated concentration-dependent inhibition of ALK and c-Met phosphorylation in cell-based assays using tumor cell lines and demonstrated antitumor activity in mice bearing tumor xenografts that expressed EML4- or NPM-ALK fusion proteins or c-Met.	The word (b) (4) was removed since crizotinib inhibits multiple tyrosine kinases, and (b) (4) was removed because it was considered unnecessary by the review team. The first two sentences were combined and Recepteur d'Origine Nantais (RON) was added to the list of kinases inhibited. The sentences on translocations of the ALK gene and the formation of fusion proteins were added to provide context for why testing is important and to explain the mechanism of crizotinib in the indicated patient population. "Crizotinib demonstrated concentration-dependent inhibition of ALK and c-Met phosphorylation in cell-based assays using tumor cell lines and demonstrated antitumor activity in mice bearing tumor xenografts that expressed EML4- or NPM-ALK fusion proteins or c-Met." This sentence mentions both the *in vitro* and *in vivo* activity of crizotinib without unnecessary details that could have been used promotionally. "or c-Met" was added to the tumor xenograft findings statement to indicate that the drug was studied and had activity in c-Met xenograft models as well.
13. Nonclinical Toxicology		
13.1 Carcinogenesis, Mutagenesis, Impairment of Fertility Carcinogenicity studies with crizotinib have not	**13.1 Carcinogenesis, Mutagenesis, Impairment of Fertility** Carcinogenicity studies with crizotinib have not	

The Sponsor Proposes:	We recommend:	Justification:
been (b) (4).	been conducted.	
(b) (4)	Crizotinib was genotoxic in an *in vitro* micronucleus assay in Chinese Hamster Ovary cultures, in an *in vitro* human lymphocyte chromosome aberration assay, and in *in vivo* rat bone marrow micronucleus assays. Crizotinib was not mutagenic *in vitro* in the bacterial reverse mutation (Ames) assay. No specific studies with crizotinib have been conducted in animals to evaluate the effect on fertility; however, crizotinib is considered to have the potential to impair reproductive function and fertility in humans based on findings in repeat-dose toxicity studies in the rat. Findings observed in the male reproductive tract included testicular pachytene spermatocyte degeneration in rats given greater than or equal to 50 mg/kg/day for 28 days (greater than 3 times the AUC at the recommended human dose). Findings observed in the female reproductive tract included single-cell necrosis of ovarian follicles of a rat given 500 mg/kg/day (approximately 10 times the recommended human daily dose on a mg/m^2 basis) for 3 days.	Crizotinib was positive in 3 assays investigating genotoxicity and should, therefore, be described as genotoxic. The positive findings were listed first.followed by the statement that crizotinib is not mutagenic.. During the labeling revisions, the sponsor wanted to add additional information on the results of the studies in order to explain or minimize the findings. These changes were rejected in order to simply state that crizotinib is genotoxic. (b) (4) was changed to "(greater than 3 times the AUC at the recommended human dose)". The margin of 3 times was used instead of (b) (4) based on the AUC in males at the 50 mg/kg/day dose on study day 26. "(approximately 10 times the recommended human daily dose on a mg/m^2 basis)" was added to compare the dose in rats to the human dose. The margin was based on the recommended human daily dose on a mg/m^2 basis because there were no PK data for the 500 mg/kg/day dose.
17. Patient Counseling Information		

The Sponsor Proposes:	We recommend:	Justification:
	17.6 Pregnancy and Nursing Patients of childbearing potential must be told to use adequate contraceptive methods during therapy and for at least 90 days after completing therapy. (b) (4) [redacted] Patients should also be advised not to breastfeed while taking XALKORI.	This section was added at the request of DMEPA to add discussion on avoiding pregnancy while on the product, based on the information in section 8.1. The last two sentences were proposed by the sponsor and were acceptable to the team.

This is a representation of an electronic record that was signed electronically and this page is the manifestation of the electronic signature.

/s/

BRENDA J GEHRKE
08/24/2011

WHITNEY S HELMS
08/25/2011

MEMORANDUM

Crizotinib (Xalkori)

Date: August 11, 2011
To: File for NDA 202570
From: John K. Leighton, PhD, DABT
Associate Director for Pharmacology/Toxicology
Office of Oncology Drug Products

I have examined pharmacology/toxicology review and labeling provided by Dr. Gehrke and the supporting memorandum provided by Dr. Helms. I concur with their conclusions that Xalkori may be approved for the proposed indication and that no additional nonclinical studies are needed.

This is a representation of an electronic record that was signed electronically and this page is the manifestation of the electronic signature.

/s/

JOHN K LEIGHTON
08/11/2011

MEMORANDUM

Date: August 10, 2011
From: Whitney S. Helms, Ph.D.
Acting Pharmacology Team Leader
Division of Drug Oncology Products
To: File for NDA #202,570
Crizotinib (XALKORI)
Re: Approvability of Pharmacology and Toxicology

Non-clinical studies examining the pharmacology and toxicology of crizotinib provided to support NDA 202570 for the treatment of patients with ALK-positive non-small cell lung cancer were reviewed in detail by Brenda J. Gehrke, Ph.D. The submission included studies of orally administrated crizotinib in rats, dogs, mice, and rabbits that investigated the drug's pharmacology, pharmacokinetics, safety pharmacology, general toxicology, genetic toxicity (*in vivo* and *in vitro*), and reproductive toxicity. The reviewed studies include only original research conducted by the sponsor.

The pharmacology studies submitted to this NDA demonstrate that crizotinib is a kinase inhibitor. Like other approved kinase inhibitors crizotinib targets a several proteins at clinically relevant concentrations including c-Met/hepatocyte growth factor receptor (HGFR), anaplastic lymphoma kinase (ALK), and Recepteur d'Origine Nantais (RON). Though the drug has its strongest potency against c-Met, the clinical development of crizotinib has focused on patients with tumors expressing ALK gene translocation products. ALK has an important role during development, particularly in neural development, but has limited expression in normal cells. Translocations with the *ALK* gene have led to the expression of oncogenic fusion proteins resulting in dysregulated expression of, and increased signaling through this kinase. Crizotinib was able to inhibit the growth of tumors derived from various cell types expressing c-Met/HGFR, and either EML-ALK4 or NPM-ALK4 translocations both *in vitro* and in a series of xenograft experiments conducted in athymic mice. Treatment of these mice with the drug also led to decreased phosphorylation of a number of downstream targets in the tumors, decreases in proliferation markers, and increases in apoptotic markers, further demonstrating the pharmacologic activity of crizotinib.

In a one-month rat toxicology study high dose males displayed a minimal to moderate decrease in bone primary spongiosa. This observation was made in a single study at an exposure approximately 10-fold higher than human exposure at the clinically recommended dose, however, it may have significance for a pediatric population. Major target organs for crizotinib toxicity observed in the 3 month toxicology studies conducted in rats and dogs included the liver, GI tract, and heart. Significant increases in liver enzymes (ALT, AST, and ALP) were observed at the high dose levels in both species. Increases in blood urea nitrogen and creatinine were also noted. These increases correlate with hepatic abnormalities noted clinically. High dose animals of both species also displayed increases in inflammatory cells including neutrophils, eosinophils, and monocytes that may correlate with clinical observations of increased pneuomonitis. In *in vitro* assays investigating hERG and calcium channel signaling, dedicated safety pharmacology

studies examining the effects of crizotinib on cardiovascular function, and ECG examinations conducted during the 3-month general toxicology study in dogs there was evidence of the potential for cardiac toxicity. These findings correlate with clinical findings of QTc prolongation, bradycardia, and cardiac arrest observed occasionally in clinical trials.

Visual disturbances were a frequently reported adverse event in clinical trials. A dedicated study was performed in rats to further examine the basis of these clinically observed visual events. This electroretinography study suggested that treatment with crizotinib leads to differences in light/dark adaptation in animals. In addition, high levels of crizotinib were detected in the eye and eye associated tissue in a distribution study. Detectable levels of crizotinib remained in the eye for at least 504 hours following a single dose of the drug.

During the course of the review, 4 impurities were identified with proposed specifications above the ICH threshold of 0.15%. The sponsor conducted a 1 month daily dose toxicology study in rats to qualify these impurities. For two of the impurities, doses administered to animals in the batch of crizotinib used in the qualification study exceeded the single cycle clinical exposure; these impurities were considered qualified. The 2 other impurities neither met this criteria nor were qualified by any other animal study submitted to the NDA and the sponsor agreed to lower their specification levels to the ICH limit.

Crizotinib was shown to be genotoxic in both *in vitro* and *in vivo* assays. The genotoxic activity of the drug appears to be clastogenic rather than mutagenic. Carcinogenicity studies were not conducted and were not required for approval in this patient population.

Reproductive studies investigating the effects of crizotinib on fertility or on post-natal development were not submitted and were not required for approval in this patient population; however, findings in 1-month and 7-day studies in the rat suggest that crizotinib may have effects on human fertility. In embryo-fetal toxicity studies in rats and rabbits there was increased post-implantation loss and decreased fetal weight at doses resulting in exposures at or above the approximate human exposure at the recommended clinical dose. Pregnancy category D is recommended.

Recommendations: I concur with the conclusion of Dr. Gehrke that the submitted pharmacology and toxicology data support the approval of NDA 202,570 for XALKORI. There are no outstanding nonclinical issues related to the approval of XALKORI for the proposed indication.

This is a representation of an electronic record that was signed electronically and this page is the manifestation of the electronic signature.

/s/

WHITNEY S HELMS
08/10/2011

DEPARTMENT OF HEALTH AND HUMAN SERVICES
PUBLIC HEALTH SERVICE
FOOD AND DRUG ADMINISTRATION
CENTER FOR DRUG EVALUATION AND RESEARCH

PHARMACOLOGY/TOXICOLOGY NDA/BLA REVIEW AND EVALUATION

Application number:	202570
Supporting document/s:	0000
Applicant's letter date:	January 4, 2011
CDER stamp date:	March 30, 2011
Product:	Xalkori® (Crizotinib)
Indication:	ALK-positive non-small cell lung cancer
Applicant:	Pfizer Inc
Review Division:	Division of Drug Oncology Products (HFD-150)
Reviewer:	Brenda J. Gehrke, Ph.D.
Acting Team Leader:	Whitney S. Helms, Ph.D.
Division Director:	Robert Justice, M.D.
Project Manager:	CDR Diane Hanner

Disclaimer

Except as specifically identified, all data and information discussed below and necessary for approval of NDA 202570 are owned by Pfizer Inc or are data for which Pfizer Inc has obtained a written right of reference. Any information or data necessary for approval of NDA 202570 that Pfizer Inc does not own or have a written right to reference constitutes one of the following: (1) published literature, or (2) a prior FDA finding of safety or effectiveness for a listed drug, as reflected in the drug's approved labeling. Any data or information described or referenced below from reviews or publicly available summaries of a previously approved application is for descriptive purposes only and is not relied upon for approval of 202570.

TABLE OF CONTENTS

1 EXECUTIVE SUMMARY 7

1.1 INTRODUCTION 7
1.2 BRIEF DISCUSSION OF NONCLINICAL FINDINGS 7
1.3 RECOMMENDATIONS 10

2 DRUG INFORMATION 10

2.2 RELEVANT INDS, NDAS, BLAS AND DMFS: IND 73544 11
2.3 DRUG FORMULATION 11
2.4 COMMENTS ON NOVEL EXCIPIENTS 13
2.5 COMMENTS ON IMPURITIES/DEGRADANTS OF CONCERN 13
2.6 PROPOSED CLINICAL POPULATION AND DOSING REGIMEN 13
2.7 REGULATORY BACKGROUND 13

3 STUDIES SUBMITTED 14

3.1 STUDIES REVIEWED 14
3.2 STUDIES NOT REVIEWED 16
3.3 PREVIOUS REVIEWS REFERENCED 18

4 PHARMACOLOGY 18

4.1 PRIMARY PHARMACOLOGY 18
4.2 SECONDARY PHARMACOLOGY 47
4.3 SAFETY PHARMACOLOGY 52

5 PHARMACOKINETICS/ADME/TOXICOKINETICS 73

5.1 PK/ADME 73

6 GENERAL TOXICOLOGY 83

6.1 SINGLE-DOSE TOXICITY 83
6.2 REPEAT-DOSE TOXICITY 84

7 GENETIC TOXICOLOGY 107

7.1 *IN VITRO* REVERSE MUTATION ASSAY IN BACTERIAL CELLS (AMES) 107
7.2 *IN VITRO* ASSAYS IN MAMMALIAN CELLS 110
7.3 *IN VIVO* CLASTOGENICITY ASSAY IN RODENT (MICRONUCLEUS ASSAY) 117

8 CARCINOGENICITY 124

9 REPRODUCTIVE AND DEVELOPMENTAL TOXICOLOGY 124

9.1 FERTILITY AND EARLY EMBRYONIC DEVELOPMENT 124
9.2 EMBRYONIC FETAL DEVELOPMENT 124
9.3 PRENATAL AND POSTNATAL DEVELOPMENT 140

10 SPECIAL TOXICOLOGY STUDIES 141

11 INTEGRATED SUMMARY AND SAFETY EVALUATION 152

Table of Tables

Table 1: Upstate 102 kinase panel screening data and kinase hit follow-up 21
Table 2: Pfizer kinase panel screening and kinase hit follow-up 21
Table 3: Selectivity of PF-02341066 in cell-based kinase assays 22
Table 4:Cellular potency of PF-02341066 vs. c-Met/HGFR phosphorylation 23
Table 5: Biochemical potency of crizotinib and its metabolites..... 37
Table 6: Cellular potency of crizotinib..... 38
Table 7: Comparison of cellular potency of crizotinib and its human metabolites 39
Table 8: Immunohistochemistry analysis for caspase3, Ki67, pERK, and pAKT in NCI-H3122 xenograft tumor samples 44
Table 9: Effects of PF-02341066 in binding assays 47
Table 10: Effects of PF-02341066 in enzyme assays 48
Table 11: Antagonist effects of PF-02341066 on the 5-HT4e and 5-HT7 receptors..... 49
Table 12: Effects of PF-02341066 on the 5-HT2B receptor 50
Table 13: % inhibition of Nav1.1 sodium currents 53
Table 14: Mean total activity during the 30-minute session..... 56
Table 15: % inhibition of hERG potassium currents 58
Table 16: % reduction in KCl-induced contraction..... 60
Table 17: % inhibition of L-type calcium current..... 62
Table 18: Effects on the APD_{50} of the cardiac action potential 64
Table 19: Effects on the APD_{90} of the cardiac action potential 65
Table 20: % inhibition of Nav1.5 sodium currents 66
Table 21: Plasma samples 70
Table 22: Unbound fraction (fu) of PF-02341066 in plasma from preclinical species and humans determined using equilibrium dialysis 74
Table 23: Pharmacokinetic parameters for blood and tissues in male Long Evans rats following a single oral administration of [14C] PF-02341066..... 75
Table 24: Concentrations of radioactivity in the right and left eyes at 336 and 504 hours after dosing 76
Table 25: Relative quantitation of PF-02341066 and metabolites in plasma of male and female rats 77
Table 26: Relative quantitation of PF-02341066 and metabolites in feces and bile of male and female rats..... 77
Table 27: Relative quantitation of PF-02341066 and metabolites in plasma of male and female dogs..... 78
Table 28: Relative quantitation of PF-02341066 and metabolites in feces of male and female dogs..... 79
Table 29: Excretion of radioactivity in male and female rats after a single administration of [14C] PF-02341066 (10 mg/kg): Group 1 80
Table 30: Excretion of radioactivity in male and female rats after a single administration of [14C] PF-02341066 (10 mg/kg): Group 2 80
Table 31: Concentrations of radioactivity in blood and plasma of male and female rats after a single administration of [14C] PF-02341066 (10 mg/kg): Group 3 81
Table 32: Pharamacokinetic parameters for radioactivity in plasma of male and female rats after a single administration of [14C] PF-02341066 (10 mg/kg): Group 3 81

Table 33: Excretion of radioactivity in male and female dogs after a single administration of [14C] PF-02341066 (10 mg/kg) 82
Table 34: Concentrations of radioactivity in blood and plasma of male and female dogs after a single administration of [14C] PF-02341066 (10 mg/kg) 83
Table 35: Pharamacokinetic parameters for radioactivity in plasma of male and female dogs after a single administration of [14C] PF-02341066 (10 mg/kg) 83
Table 36: Preliminary Mutagencity 109
Table 37: Definitive Mutagenicity 110
Table 38: 3-Hour Chromasomal Aberration with Metabolic Activation 112
Table 39: 3 Hour Chromosomal Aberration Without Metabolic Activation 113
Table 40: 24 Hour Chromosomal Aberration Without Metabolic Activation 114
Table 41: Male Micronucleus Results 120
Table 42: Female Micronucleus Results 120
Table 43: Male Micronucleus Results (2) 123
Table 44: Mean adjusted body weight change and uterine weight (g) 134
Table 45: Mean adjusted body weight change and uterine weight (g) 138
Table 46: Vitreous Humor to Plasma Ratio 145
Table 47: Impurity Qualification 152

Table of Figures

Figure 1: HGF-stimulated migration and invasion of NCI-H441 lung carcinoma cells .. 24
Figure 2: Vascular sprouting of HMVEC 24
Figure 3: Inhibition of c-Met/HGFR-dependent signaling in A549 human lung carcinoma cells 25
Figure 4: Cell cycle G0/G1 phase arrest and apoptosis 25
Figure 5: Inhibition of NPM-ALK signaling pathways 26
Figure 6: Inhibition of c-Met/HGFR phosphorylation and tumor growth in the GTL-16 xenograft model 29
Figure 7: PK/PD relationship of PF-02341066 in mice bearing GTL-16 tumors 30
Figure 8: Inhibition of tumor growth and c-Met/HGFR phosphorylation in the U87MG Xenograft Model (excerpted from sponsor's submission) 30
Figure 9:Effects of PF-02341066 on tumor volume of large established GTL-16 tumor xenografts 31
Figure 10: Effects of PF-02341066 in the NCI-H441 non-small lung carcinoma (A) or PC-3 prostate carcinoma tumor xenograft models (excerpted from sponsor's submission) 32
Figure 11: Inhibition of signaling proteins in GTL-16 tumors 32
Figure 12: Effects of PF-02341066 on cell proliferation in GTL-16 tumors 33
Figure 13: Effect of PF-02341066 on tumor microvessel density 34
Figure 14: Effects of PF-02341066 on tumor growth and NPM-ALK phosphorylation in the Karpas 299 xenograft model 35
Figure 15: Inhibition of signaling proteins in Karpas 299 tumors 35
Figure 16: Effects of crizotinib on kinase activity of the EML4-ALK variants in human NSCLC and EML4-ALK engineered 3T3 cells 38
Figure 17: Inhibition of cell proliferation and induction of apoptosis in EML4-ALK V1 positive H3122 and H2228 NSCLC in vitro 40
Figure 18: Inhibition of EML4-ALK phosphorylation and tumor growth in the H3122 lung adenocarcinoma model 41
Figure 19: Inhibition of tumor growth in the H3122 lung adenocarcinoma model 42
Figure 20: Crizotinib PK/PD profile in Nude mice 42
Figure 21: Dose-dependent inhibition of EML4-ALK-dependent signaling in H3122 tumors following 4-days of daily crizotinib administration 43
Figure 22: Effect of crizotinib on cellular kinase activity and expression levels of c-Met/HGFR and EGFR in NCI-H3122 tumors 44
Figure 23: Effect of crizotinib on EML4-ALK phosphorylation (upper) and total EML4-ALK levels (lower) in NCI-H3122 tumors by IHC analysis 45
Figure 24: Inhibition of Ki67 immunostaining (cell proliferation) in the H3122 model ... 46
Figure 25: Induction of activated caspase3 levels (cell apoptosis) in the NCI-H3122 model 46
Figure 26: α1a Agonist/Antagonist Curve 52
Figure 27: Concentration-response curve for the closed state 53
Figure 28: Concentration-response curve for the inactivated state 54
Figure 29: Effects of PF-02341066 on total distance traveled 56
Figure 30: Effects of PF-02341066 on number of vertical movements 57

Figure 31: Concentration-response curve (mean + SEM) 59
Figure 32: Concentration-response curve (mean + SEM) 61
Figure 33: Effect of PF-02341066 on ICa,L 62
Figure 34: Concentration-response curve (mean + SEM) 66
Figure 35: Average change in heart rate 68
Figure 36: Average change in left ventricular end diastolic pressure (LVEDP) 68
Figure 37: Average change in left ventricular LV+dP/dt 69
Figure 38: Average change in PR interval 69
Figure 39: Average change in QT interval 69
Figure 40: Average change in QRS interval 70
Figure 41: Effect of PF-2341066 on mean minute volume 72
Figure 42: Effect of PF-2341066 on mean respiratory rate 72
Figure 43: Effect of PF-2341066 on mean tidal volume 72
Figure 44: 7 Day Rat Body Weights 86
Figure 45: 3 Month Body Weight 94
Figure 46: 3 Month Rat Food Consumption 95
Figure 47: Maternal Body Weight (Rabbit Dose Range) 134
Figure 48: ERG b-Wave Amplitude in Male Rats 144

1 Executive Summary

1.1 Introduction

Pfizer has submitted NDA 202570 for crizotinib (Xalkori®), a new molecular entity that is a kinase inhibitor with strongest activity against the c-Met/hepatocyte growth factor receptor (HGFR) and anaplastic lymphoma kinase (ALK). The clinical development of crizotinib has focused on its ability to inhibit ALK, a tyrosine kinase receptor belonging to the insulin growth factor receptor super family. ALK is expressed at high levels in the nervous system during embryogenesis and is involved in neural development and differentiation. In humans, ALK has a restricted distribution in normal cells and is detected in rare scattered neural cells, pericytes, and endothelial cells in the adult brain. Translocations can affect the ALK gene resulting in the expression of oncogenic fusion proteins, including NPM-ALK detected in anaplastic large cell lymphoma and EML4-ALK detected in non-small cell lung cancer. The formation of fusion proteins results in activation and dysregulation of ALK expression and signaling leading to increased cell-proliferation and survival. The proposed clinical dose of 250 mg twice daily (BID) is administered orally as a capsule. Nonclinical pharmacology, pharmacokinetic, and toxicology studies have been submitted to support the approval of crizotinib for the treatment of ALK-positive advanced non-small cell lung cancer.

1.2 Brief Discussion of Nonclinical Findings

Crizotinib is a kinase inhibitor that inhibits c-Met/hepatocyte growth factor receptor (HGFR), anaplastic lymphoma kinase (ALK), and Recepteur d'Origine Nantais (RON) at clinically relevant concentrations. *In vitro*, crizotinib inhibited constitutive or HGF-stimulated tyrosine phosphorylation of wild-type c-Met/HGFR with a mean IC_{50} value of 11 nM across a panel of human tumor and endothelial cell lines. Crizotinib is less potent for ALK with an IC_{50} value of 24 nM in Karpas 299 lymphoma cells. Additionally, crizotinib inhibits RON with an EC_{50} value of 80 nM in NIH-3T3 cells engineered to express human RON. The average C_{max} observed in humans at the recommended clinical dose of 250 mg BID was approximately 1061 nM (478 ng/mL), a concentration that was reached or exceeded in nonclinical studies submitted to support the application. Pharmacokinetic results showed similar levels of protein binding in humans compared to rat, dog, or mouse plasma with free crizotinib representing less than 10% of the total drug in all species. The unbound fraction of crizotinib in human plasma *in vitro* was 0.093 (9.3%), indicating that 91% of crizotinib is bound to human plasma proteins *in vitro*. Based on this information, crizotinib is capable of inhibiting those kinases for which it has an IC_{50} value of less than approximately 114 nM. While crizotinib was shown to have potential activity against other kinases *in vitro*, pharmacokinetic data, suggest that c-Met/HGFR, ALK, and RON are the primary targets of crizotinib *in vivo*. *In vivo* effects of crizotinib were demonstrated in numerous studies using various human xenograft models in athymic mice. Treatment with crizotinib showed a dose-dependent inhibition of c-Met/HGFR, NPM-ALK, and EML4-ALK phosphorylation in xenograft models. These findings provide evidence that crizotinib has *in vivo* activity against c-Met/HGFR and ALK. In the same models the sponsor

demonstrated inhibition of tumor growth, decreased proliferation, and increased apoptosis in tumors of crizotinib treated animals compared to controls.

In vitro pharmacology studies evaluating the potential off-target effects of crizotinib at various receptor subtypes were also included in the submission. Crizotinib showed inhibitory activity at potentially clinically relevant concentrations for a number of receptors including the α_1 (non-selective) adrenergic receptor and the 5-HT_{2B} and 5-HT_{4e} serotonin receptors. Activity of crizotinib at these receptors could result in a wide range of effects including neurologic effects as the drug appears to efficiently cross the blood brain barrier; however, there were no adverse effects noted in clinical trials that clearly relate to the off target binding of crizotinib at these receptors.

The pharmacokinetics of crizotinib were studied in multiple species including the rat and dog, the non-clinical species tested for toxicity. The distribution of crizotinib in the rat was extensive with C_{max} occurring at 4 or 8 hours after dosing in most tissues. High concentrations of crizotinib were observed in the eye and associated tissues (Harderian gland, lacrimal gland, and uveal tract), pituitary gland, liver, kidney, adrenal gland, and spleen. Exposure in the eye was long with crizotinib present through 504 hours after dosing with an estimated elimination $t_{1/2}$ of 576 hours, a half life that is significantly longer than the plasma half-life of crizotinib which ranged from 4.4 to 9.8 hours in rats and was approximately 42 hours in humans. The liver, small intestine, and pituitary were target organs of toxicity in the rat, and visual impairment was observed in rats and in the clinical studies. This finding suggests that crizotinib produces toxicity in organs with high concentrations of the drug. High concentrations of crizotinib and a long half-life in the eye may be contributing to the ocular toxicity/visual impairment observed in humans in clinical trials. Excretion studies in rats and dogs showed that with oral administration crizotinib is primarily eliminated in the feces and bile (62-99% total; 35-53% in feces and 38-62% in bile in rats), with some excretion in the urine (2-6%).

Both *in vitro* and *in vivo* safety pharmacology studies were conducted to assess the effects of crizotinib on neurological, and pulmonary function. Neurological and pulmonary function were assessed in separate *in vivo* studies in Sprague-Dawley rats following single oral doses of crizotinib (0, 10, 75, or 500 mg/kg; 0, 60, 450, or 3000 mg/m^2). Treatment with crizotinib reduced locomotor activity at the mid and high doses (450 and 3000 mg/m^2) in the neurological evaluation study. The high dose of 3000 mg/m^2 also reduced the mean minute volume and mean respiratory rate and increased tidal volume in the pulmonary study. These locomotor and respiratory findings were only observed at doses ≥ 450 mg/m^2 which yielded C_{max} values 2.5-5 times higher than the average C_{max} (1.061 μM; 478 ng/mL) observed in humans at the recommended clinical dose.

Repeat-dose toxicology studies were conducted in both rats and dogs in order to fully characterize crizotinib-induced toxicities. Decreased bone formation in growing long bones was observed in immature rats at 150 mg/kg (900 mg/m^2) in the one month study but only in males, who had a significantly higher exposure to crizotinib than females. This finding may be a concern for pediatric administration of the drug.In a three-month oral study, male and female Sprague-Dawley rats were administered crizotinib daily for 90 days with a 57-day recovery period. Based on the results of the one-month rat study, lower doses of crizotinib were administered to males (0, 10, 30, or 100 mg/kg; 0, 60, 180, or 600 mg/m^2) than females (0, 10, 50, or 250 mg/kg; 0, 60, 300,

or 1500 mg/m^2). In another three-month oral study, male and female beagle dogs were administered crizotinib (0, 1, 5, or 25 mg/kg; 0, 20, 100, or 500 mg/m^2) daily for 91 days with a 57-day recovery period. Target organs of toxicity for both species included the liver, gastrointestinal tract, heart, mesenteric lymph node, and bone marrow. Liver toxicity was reflected in significant increases in liver function enzymes at the high dose levels in both species. Similar increases in liver enzymes have been observed in clinical trials. There were also significant increases in inflammatory cells (neutrophils, monocytes, and eosinophils) noted in these studies at the high dose levels, particularly at late time-points near the end of the study. These increases may correlate with clinical findings of pneumonitis. In the rat studies, the pituitary, mandibular salivary gland, kidney, and thymus were additional target organs for toxicity. The main toxicities in these animals included an increased incidence and severity of myonecrosis in the heart and alveolar histiocytosis in the lung. Vacuolation was observed in multiple organs including the gastrointestinal tract (cecum, colon, duodenum, ileum, and jejunum), liver, pituitary, and prostate, and foamy macrophages were observed in the mesenteric lymph node. Cellular vacuolation and the presence of foamy macrophages observed in the histopathology appear to be due to phospholipidosis.

In the 13 week dog study, males treated with crizotinib at doses ≥ 100 mg/m^2 or females treated at 500 mg/m^2 exhibited increases in QT/QTc intervals at both the Week 6 and Week 13 pre-dose time-points compared to pretreatment. This finding is consistent with increases in QT/QTc intervals observed in a one-month dog study. The effects of crizotinib on cardiovascular function were also assessed in multiple *in vitro* studies and in a single dose *in vivo* study in anesthetized dogs. Crizotinib inhibited the hERG channel at all concentrations tested with an IC_{50} of 1.1 μM, supporting the finding that the drug has the potential to prolong the QT interval. Crizotinib inhibited the Nav1.5 sodium channel current in a concentration-dependent manner with an IC_{50} value of 1.56 μM, indicating that the drug has the potential to prolong the QRS or PR intervals. These effects were observed with IC_{50} values below or similar to the C_{max} (1.061 μM) observed in humans at the recommended clinical dose. Additionally, crizotinib produced a concentration-dependent relaxation of a 45 mM KCl-induced contraction with an IC_{50} of 0.83 μM in the rat aorta isometric tension model and inhibited the L-type calcium channel current in a concentration-dependent manner with an IC_{50} of 14.6 μM indicating that crizotinib is has some calcium channel antagonist activity. Inhbition of calcium signaling is associated with diminished contractile force without major changes in fiber action potentials. At the high concentration of 10 μM crizotinib did show some inhibition of cardiac action potential in an *in vitro* Purkinje fibre assay, however, the drug had no effect on action potential at lower concentrations. In a hemodynamic and electrophysiological study in anesthetized dogs, intravenous administration of crizotinib decreased heart rate and contractility, increased left ventricular end diastolic pressure, and increased the PR-, QRS-, and QT-intervals at the two highest doses. Clinically, cardiac toxicity, including bradycardia, cardiac arrest, and QT prolongation, has been observed following crizotinib treatment.

One of the most common adverse events observed in the clinical studies with crizotinib was vision disorder characterized as diplopia (double vision), photopsia, blurred vision, visual impairment, and vitreous floaters. The median onset was <2 weeks after the initiation of crizotinib treatment. No treatment-related ophthalmic

findings were observed in the one- or three-month general toxicology studies in the rat and dog. An electroretinography study was conducted to evaluate the potential effects of crizotinib on electroretinogram (ERG) measurements as a potential biomarker for changes in ocular/retinal function in male Long-Evans (pigmented) rats after 4-weeks of daily administration of crizotinib (0 or 100 mg/kg; 0 or 600 mg/m^2). Treatment with crizotinib (600 mg/m^2) significantly reduced the rate of retinal dark adaptation, indicating that crizotinib did impair visual function in rats.

Crizotinib was tested for mutagenicity in an *in vitro* reverse mutation (Ames) assay and tested for clastogenicity in both an *in vitro* structural chromosome aberration assay in human peripheral lymphocytes and *in vivo* rat micronucleus assays. At the concentrations and doses tested, crizotinib was not mutagenic, however, crizotinib was shown to be genotoxic based on positive results in the *in vitro* chromosome aberration assay and in the *in vivo* micronucleus assay in male rats. An exploratory *in vitro* micronucleus assay with kinetochore analysis of crizotinib conducted in Chinese hamster ovary (CHO) cultures without metabolic activation, indicated that the genotoxic activity of the drug is aneugenic and not clastogenic in nature.

Reproductive and developmental toxicology studies were conducted in rats and rabbits to assess the effects of crizotinib on embryo-fetal development. Crizotinib produced maternal toxicity including decreases in body weight and food consumption leading to mortality at doses of $\geq$1200 mg/m^2 in rats and $\geq$900 mg/m^2 in rabbits. Post implantation loss was increased compared to controls in rats at doses of $\geq$300 mg/m^2 in rats and 720 mg/m^2 in rabbits. Fetal weight was decreased with treatment of crizotinib compared to controls at doses of ≥1200 mg/m^2 in rats and 720 mg/m^2 in rabbits. No teratogenicity was observed in either rats or rabbits when crizotinib was administered during organogenesis. Pregnancy category D is recommended.

1.3 Recommendations

1.3.1 Approvability

Recommended for approval. The non-clinical studies submitted to this NDA provide sufficient information to support the use of crizotinib in the treatment of anaplastic lymphoma kinase (ALK)-positive advanced non-small cell lung cancer.

1.3.2 Additional Non Clinical Recommendations

None

1.3.3 Labeling

A separate labeling review will be provided.

2 Drug Information

CAS Registry Number	877399-52-5
Generic Name	Crizotinib
Code Name	PF-02341066

Chemical Name	(R)- 3- (1-(2,6- Dichloro- 3-fluoro-phenyl)-ethoxy)- 5-(1-piperidin-4-yl-1H-pyrazol-4-yl)-pyridin-2-ylamine
Molecular Formula/Molecular Weight	$C_{21}H_{22}Cl_2FN_5O$/450.34 g/mol
Structure or Biochemical Description	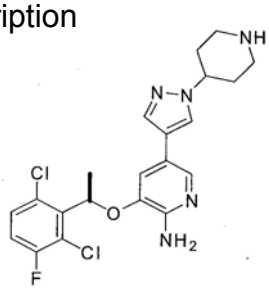
Pharmacologic Class	Kinase inhibitor

2.2 Relevant INDs, NDAs, BLAs and DMFs: IND 73544

2.3 Drug Formulation

Crizotinib is available as 200 and 250 mg hard gelatin capsules. The 200 mg strength is a size 1 white and pink opague capsule with “Pfizer” on the cap and “CRZ 200” on the body. The 250 mg strength is a size 0 pink opaque capsule with “Pfizer” on the cap and “CRZ 250” on the body. The composition and manufacturing descriptions for both strengths are presented in the tables below (excerpted from sponsor’s submission).

200 mg capsule

Name of Ingredients	Function	Reference to Standard	Unit formula	
			Unit	%
(b) (4) **Composition**				
Crizotinib	Active	Pfizer	200.00 mg	50.00
Colloidal Silicon Dioxide	(b) (4)	NF/Ph Eur/JP		(b) (4)
Microcrystalline Cellulose		NF/Ph Eur/JP		
Anhydrous Dibasic Calcium Phosphate		USP/Ph Eur/JP		
Sodium Starch Glycolate		NF/Ph Eur/JP		
Magnesium Stearate [1]		NF/Ph Eur/JP		
(b) (4				
Capsule Shell				
Size 1 White Opaque/ Pink Opaque HG Capsule		Pfizer		
(b) (4				
Gelatin		USP/Ph Eur/JP		
Titanium Dioxide (b) (4)		USP/Ph Eur		
				(b) (4)
Print Ink [2]				
				(b) (4)

N/A is not applicable; HG is hard gelatin

(b) (4)

250 mg capsule

Name of Ingredients	Function	Reference to Standard	Unit formula	
			Unit	%
(b) (4) **Composition**				
Crizotinib	Active	Pfizer	250.00 mg	50.00
Colloidal Silicon Dioxide	(b) (4)	NF/Ph Eur/JP		(b) (4)
Microcrystalline Cellulose		NF/Ph Eur/JP		
Anhydrous Dibasic Calcium Phosphate		USP/Ph Eur/JP		
Sodium Starch Glycolate		NF/Ph Eur/JP		
Magnesium Stearate [1]		NF/Ph Eur/JP		
(b) (4)				
Capsule Shell				
Size 0 Pink Opaque/ Pink Opaque HG Capsule		Pfizer		
(b) (4)				
Gelatin		USP/Ph Eur/JP		
Titanium Dioxide (b) (4)		USP/Ph Eur		
Red Iron Oxide (b) (4)		USP/Ph Eur		
				(b) (4)
Print Ink [2]				
				(b) (4)

N/A is not applicable; HG is hard gelatin

(b) (4)

2.4 Comments on Novel Excipients

None

2.5 Comments on Impurities/Degradants of Concern

The proposed specifications are NMT (b) (4) for impurity (b) (4) and NMT (b) (4) for impurities (b) (4), which are above the ICH qualification threshold of 0.15%. With a clinical dose of 250 mg BID (500 mg/day; 308.33 mg/m^2/day), the dose of (b) (4) and the dose of (b) (4) A one-month toxicology study in rats (Study # 10GR100) was conducted using batch 00703371-053-2 to qualify these impurities that were not present in previous non-clinical toxicology studies. Toxicities observed in this study with 50 mg/kg (300 mg/m^2) were similar to those observed at the mid-dose in males (30 mg/kg; 180 mg/m^2) and females (50 mg/kg; 300 mg/m^2) in the 3-month repeat-dose study in rats (Study # 09GR347). Below is a table with the levels of the impurities present in batch 00703371-053-2. The doses of impurities (b) (4) present in batch 00703371-053-2 were higher than the expected clinical doses at the proposed specifications, therefore, these impurities are qualified. Impurities (b) (4) are not qualified as the doses administered to animals in the toxicology study were lower than the expected clinical doses at doses the proposed specifications for these impurities.

Dose based on BSA (mg/m^2)

Impurity	NDA 202570 Proposed Specifications		Impurity qualification study in rats (10GR100) Batch 00703371-053-2		Qualification Determination
	%	Dose (mg/m^2)	%	Dose (mg/m^2)	
(b) (4)					Not qualified
					Qualified
					Qualified
					Not qualified

The applicant was informed that impurities (b) (4) were not qualified at the proposed specifications and were asked to revise the specifications to meet ICH recommendations. The applicant agreed to lower the specifications for impurities (b) (4) to NMT 0.15%.

2.6 Proposed Clinical Population and Dosing Regimen

The proposed clinical population is patients with anaplastic lymphoma kinase (ALK)-positive advanced non-small cell lung cancer. Crizotinib (250 mg capsule) is to be administered orally twice daily.

2.7 Regulatory Background

Crizotinib has been developed as an anti-cancer drug by Pfizer Inc. and clinical trials have been conducted since December 2005 under IND 73544. Crizotinib was granted

a Fast Track designation for ALK-positive non-small cell lung cancer on December 6, 2010. NDA 202570 was submitted as a rolling submission, with the nonclinical sections including Module 4 submitted first on January 4, 2011 and the final submission with the clinical data submitted on March 30, 2011.

3 Studies Submitted

3.1 Studies Reviewed

Primary Pharmacology

Study#	Title
Pharm001	Kinase target profile and selectivity of PF-02341066 in biochemical and cellular assays and its effect on kinase target-dependent cancer phenotypes *in vitro*
Pharm002	Pharmacodynamic inhibition of target RTKS, elucidation of pharmacokinetic/pharmacodynamic (PK/PD) relationships, and evaluation of antitumor efficacy of PF-02341066 in rodent models of cancer *in vivo*
192308	Characterization of pharmacodynamic inhibition of target RTKS and their oncogenic variants by crizotinib (PF-02341066) and its primary metabolites *in vitro*
192438	Pharmacodynamic inhibition of EML4-ALK, elucidation of pharmacokinetic/pharmacodynamic (PK/PD) relationships, and evaluation of antitumor efficacy of crizotinib (PF-02341066) in a rodent model of EML4-ALK positive lung adenocarcinoma cancer *in vivo*

Secondary Pharmacology

Study#	Title
901036	*In vitro* pharmacology: Pfizer wide ligand profile
8850900-3	*In vitro* pharmacology study of PF-02341066-00
8850568	*In vitro* pharmacology study of PF-02341066-14-0001
SP7610	Assessment of the activity of PF-02341066 at the human 5-HT_{2A}, 5-HT_{1B}, M1, M2, & M3 muscarinic, and the rat adrenergic α_{1A} receptors

Safety Pharmacology

Study #	Title
PF02341066HERG	Assessment of the potential effect of PF-02341066 on hERG potassium current stably expressed in HEK293 cells
PF02341066AORTA Amendment	Assessment of PF-02341066 Ca^{2+} channel antagonism in the rat aorta isometric tension model
04-2796-01	Effect of PF-02341066 on calcium current in freshly isolated guinea pig ventricular myocytes
IC00104	Effects of PF-2,341,066-01 on cardiac action potentials recorded from dog isolated Purkinje fibres *in vitro*
3660	Neurofunctional evaluation of PF-02341066 in Sprague-Dawley rats
3622 (745-04146)	Effect of PF-02341066 on pulmonary function in Sprague-Dawley rats
PF02341066/CG/003/04	To determine the effects of intravenously administered PF-02341066 on haemodynamic and electrophysical parameters in the isoflurane anaesthetized dog
PF02341066NA15	Effect of PF-02341066 on Nav1.5 sodium current stably expressed in CHO cells
PF02341066NA15 Amendment 1	Effect of PF-02341066 on Nav1.5 sodium current stably expressed in CHO cells, Final report amendment #1

PF02341066NA11	Effect of PF-02341066 on Nav1.1 sodium current stably expressed in HEK293 cells

Pharmacokinetics

Study #	Title
	Distribution
8215155	Quantitative whole body autoradiography of rats following oral administration of [^{14}C]PF-02341066
PDM-014	Equilibrium dialysis determination of unbound fraction of PF-02341066 in rat, mouse, dog, monkey, and human plasma
	Metabolism
122138	Metabolism of [^{14}C]PF-02341066 following oral administration to dogs
133625	Metabolism of [^{14}C]PF-02341066 following oral administration to rats
	Excretion
8215153	Pharmacokinetics and excretion of [^{14}C]PF-02341066 following oral administration to rats
8220895	Pharmacokinetics and excretion of [^{14}C]PF-02341066 following oral administration to dogs

Repeat-Dose Toxicology

Study#	Title
04HGF004	A 7-day PO toxicology study of PF-02341066 in male and female Sprague-Dawley rats
05137	1-month oral toxicity study of PF-02341066 in rats
09GR347	3-month oral toxicity study of PF-02341066 in rats with a 2-month recovery
09GR347 Amendment 1	Final report amendment #1: 3-month oral toxicity study of PF-02341066 in rats with a 2-month recovery
05162	1-month oral toxicity study of PF-02341066 in dogs
09GR346	3-month oral toxicity study of PF-02341066 in dogs with a 2-month recovery

Genetic Toxicology

Study#	Title
3565	Bacterial reverse mutation assay of PF-2341066
3554	*In vitro* structural chromosome aberration assay of PF-2341066 in human peripheral lymphocytes
PG 0135	*In vitro* micronucleus assay with kinetochore analysis of PF-2341066 in Chinese hamster ovary (CHO) cultures
3746	*In vivo* micronucleus study of PF-2341066 in male rats
3665	*In vivo* micronucleus study of PF-2341066 in rats

Reproductive Toxicology

Study#	Title
09GR345	Oral dose range-finding study of PF-02341066 in pregnant rats
10GR072	Oral embryo-fetal development study of PF-02341066 in rats
09GR350	Oral dose range-finding study of PF-02341066 in pregnant rabbits
10GR073	Oral embryo-fetal development study of PF-02341066 in rabbits

Special Toxicology

Study#	Title
10GR201	4-week oral gavage exploratory electroretinography study of PF-02341066 in male Long-Evans rats

10GR100	1-month oral toxicity study of PF-02341066 in rats (impurity study)
05195	Determination of the phototoxic potential of PF-02341066 in the 3T3 neutral red uptake (NRU) phototoxicity assay

3.2 Studies Not Reviewed

Primary Pharmacology

Study#	Title
124928	Preliminary pharmacokinetic-pharmacodynamic modeling of PF-02341066 for inhibition of anaplastic lymphoma kinase in athymic mice implanted with H3122 non-small cell lung carcinomas
213230	Pharmacokinetic-pharmacodynamic modeling of PF-02341066 for inhibition of anaplastic lymphoma kinase and anti-tumor efficacy in athymic mice implanted with H3122 non-small cell lung carcinomas

Pharmacokinetics

Study #	Title
	Analytical methods and validation reports
15-0937 VA Amendment 2	Partial validation of a method for the determination of PF-02341066 in rat plasma by LC-MS/MS
15-0938 Amendment 1	Partial validation of a method for determination of PF-02341066 in dog plasma by LC-MS/MS
15-0950 VA Amendment 2	Partial validation of a method for determination of PF-02341066 in rabbit plasma by LC-MS/MS
764-04982	Method validation report: LC/MS/MS analysis of PF-02341066 in EDTA rat plasma
764-04983	Method validation report: LC/MS/MS analysis of PF-02341066 in EDTA dog plasma
BA00105	Validation of an assay for PF-02341,066 in dog plasma using SPE followed by LC-MS-MS
	Absorption
PDM-012	Pharmacokinetics of PF-02341066 in male Beagle dogs following a single intravenous or oral dose of PF-02341066
PDM-013	Pharmacokinetics of PF-02341066 in male Cynomolgus monkeys following a single intravenous or oral dose of PF-02341066
174737	MDR1 and BCRP transport evaluation of PF-02341066
194244	PF-02341066: *In vitro* assessment of hepatic uptake in human hepatocyte suspensions
PDM-011	Pharmacokinetics of PF-02341066 in male Sprague-Dawley rats following a single intravenous or oral dose of PF-02341066
	Distribution
202638	PF-02341066 protein binding in rabbit plasma
145554	Determination of protein binding in rat and human plasma for PF-06260182 and its diastereomers PF-06270079 and PF-06270080, lactam metabolites of PF-02341066
144558	*In vitro* binding of PF-02341066 in human albumin and human α_1-acid glycoprotein
PDM-015	Red blood cell distribution of [^{3}H]PF-02341066 in whole blood of mouse, rat, dog, monkey, and human
	Metabolism
A8081008-Lactam	Pharmacokinetics of the crizotinib lactam diastereomers (PF-06270079 and PF-06270080) in a Phase 1 relative bioavailability study of PF-02341066 at 250 mg

	powder-in-capsule (A8081008)
174623	Assessment of *in vitro* metabolism of PF-02341066 by recombinant human cytochrome P450 3A4 and 3A5 enzymes
163819	Assessment of *in vitro* metabolism of PF-02341066 by recombinant human cytochrome P450 enzymes
PDM-019	Identification of human cytochrome P450 isoforms involved in the metabolism of PF-02341066
145505	Involvement of P450 isoforms and aldehyde oxidase in the formation of lactam and ether derived metabolites of PF-02341066
PDM-018	*In vitro* metabolic stability and *in vitro* and *in vivo* metabolite profiles of PF-02341066 in various species
PDM-024	Preliminary evaluation of PF-02341066 metabolism in male and female rat and human liver S9
123536	The metabolism of [^{14}C]PF-02341066 in humans following a single oral (250 mg) administration to healthy male volunteers
Excretion	
8225214	Radioanalysis support for clinical study A8081009
Pharmacokinetic drug interactions	
095303	*In vitro* inhibition of OATP 1B3 by PF-02341066
153034	Effect of PF-02341066 on human drug metabolizing enzymes *in vitro*
182103	PF-02341066: BCRP inhibition evaluation
181858	*In vitro* inhibition of OATP 1B1 by PF-01341066
141847	The *in vitro* study of P-glycoprotein inhibition by PF-02341066 in CACO-2 cells
153446	An investigation of the potential for PF-02341066 to induce CYP3A4 and CYP1A2 in human hepatocytes
PDM-017	Evaluation of time-dependent inhibition of CYP3A isozymes by PF-02341066 in human liver microsomes

Repeat-Dose Toxicology

Study#	Title
PDM-010	Toxicokinetic report for a 2-day oral toxicology study of PF-02341066 in male and female Sprague-Dawley rats
05HGF006	A two day PO toxicology study of PF-02341066 in male/female Sprague-Dawley rats
764-04988	Toxicokinetic report for 1-month oral toxicity study of PF-02341066 in rats
04HGF003	A toxicity study of B6 mice treated with PF-02341066
04HGF003 Amendment 2	Amendment 2: A toxicity study of B6 mice treated with PF-02341066
05079	Oral escalating dose toxicity study followed by a 7-day repeat dose period of PF-02341066 in dogs
PDM 001	Toxicokinetic report for an oral escalating dose toxicity study followed by a 7-day repeat dose period of PF-02341066 in dogs
3584	28-day exploratory oral toxicity study of PF-02341066 in monkeys

Special Toxicology

Study#	Title
10LJ027 Amendment 1	Final report amendment #1: Local vascular tissue irritation study of PF-02341066 in female New Zealand white rabbits
10LJ017	*In vitro* compatibility of PF-02341066 with human blood
10LJ022	PF-02341066: Analytical report for the *in vitro* compatibility with rabbit blood

3.3 Previous Reviews Referenced

IND 73544, pharmacology/toxicology review #1 (Robeena Aziz, Ph.D.)

4 Pharmacology

4.1 Primary Pharmacology

Study title: Kinase target profile and selectivity of PF-02341066 in biochemical and cellular assays and its effect on kinase target-dependent cancer phenotypes in vitro
Study no.: Pharm001
Study report location: M4.2.1.1

Key Findings

- PF-02341066 inhibited HGF-stimulated or constitutive total tyrosine autophosphorylation of wild-type c-Met/HGFR with a mean IC_{50} value of 11 nM across a panel of human tumor and endothelial cell lines
- PF-02341066 inhibited ALK in a human lymphoma cell line (Karpas 299 cells) with an IC_{50} of 24 nM
- PF-02341066 inhibited HGF-stimulated human NCI-H441 lung carcinoma cell migration (IC_{50}=11 nM) and invasion (IC_{50}=6.1 nM)
- PF-02341066 demonstrated concentration-dependent inhibition of HGF-stimulated phosphorylation of signaling molecules implicated in transduction of signals through c-Met/HGFR including Gab1, AKT, Raf, Mek, MAPK1/2, p90RSK, and STAT5 in A549 human NSCLC cells
- PF-02341066 inhibited proliferation of Karpas 299 cells with an IC_{50} of approximately 60 nM and induced cell cycle G0/G1 phase arrest and apoptosis in Karpas 299 and SU-DHL-1 lymphoma cells

A series of studies were conducted to characterize PF-02341066 for 1) potency against c-Met/HGFR in both biochemical enzyme assays and cell assays, 2) selectivity against a series of other RTKs, non-receptor tyrosine kinases and serine-threonine kinases, and 3) effects on c-Met/HGFR- and NPM-ALK-dependent cellular functions that are altered during cancer progression. These studies were summarized in the Pharm001 report.

Biochemical kinase assays
In vitro biochemical kinase assays were conducted at both Pfizer Global Research and [redacted] (b) (4) To investigate kinase selectivity, PF-02341066 was evaluated against a panel of 102 human kinases from [redacted] (b) (4). and a panel of 19 kinases at Pfizer. For the studies conducted at Pfizer, the biochemical K_i values of PF-02341066 for the inhibition of the c-Met/HGFR kinase were determined using a general procedure with a continuous-coupled spectrophotometic assay to monitor NADH oxidation that is coupled to ATP turnover. For the studies conducted at [redacted] (b) (4), the biochemical enzyme of interest was assayed in a final volume of 25 µL containing 5-10

mU of the enzyme of choice incubated with 8 mM MOPS pH 7.0, 0.2 mM EDTA, 50 μM EAIYAAPFAKKK, 10 mM MgAcetate and [^{32}P-ATP]. (b) (4) and scintillation counting. For Upstate assays, the concentration of ATP is equal to the K_M for ATP in these assays, therefore, the IC_{50} of the compounds measured in the biochemical assay will be lower than for cell based IC_{50}s.

Cellular kinase phosphorylation assays

ELISA and immunoblotting assays were used to directly determine the ability of PF-02341066 to inhibit ligand-dependent or constitutive kinase phosphorylation using a variety of serum-starved cells. A sandwich ELISA method with capture antibodies specific for each protein and a detection antibody specific for phosphorylated tyrosine residues was used to assess phosphorylation of protein kinases. In each ELISA assay, protein lysates generated from various cell lines treated with appropriate RTK ligands and/or PF-02341066 were transferred to a 96 well plate that was pre-coated with the corresponding antibodies including anti-c-Met/HGFR, -Ron, -Axl, -Sky, -IR, -Tie2, -KDR, -PDGFR β, -Zap70, and etc. Plates were measured at OD-450 nm using a spectrophotometer. IC_{50} values were calculated by concentration-response curve fitting utilizing a four-parameter analytical method in an Excel-based template. In the immunoblotting assays, cells were treated with dilutions of PF-02341066 in serum-free media and lysed for protein extraction. Cell lysates were normalized for protein concentration by BSA assay (b) (4)) and specific antibodies were used to immunoprecipitate proteins of interest. Immunoprecipitated proteins were separated by SDS-PAGE and immunoblotting with anti-phosphotyrosine antibodies was performed to determine relative levels of phosphorylated proteins at each drug concentration. This immunoblotting method was also used to determine total protein levels for the molecules of interest.

Cell proliferation and survival assays

Cell proliferation and HGF-stimulated HUVEC survival assays were conducted using 96 well plates. Serial dilutions of PF-02341066 were conducted and appropriate controls or designated concentrations of PF-02341066 were added to each well. A MTT assay (b) (4) was performed to determine the relative cell numbers and IC_{50} values were calculated by concentration-response curve fitting utilizing a four-parameter analytical method.

HGF-dependent cell migration and invasion assays

HGF-dependent cell migration and invasion assays were also conducted with PF-02341066. The effect of PF-02341066 on HGF-stimulated NCI-H441 human non-small cell lung carcinoma cell migration and matrigel invasion was determined using a commercially available cell migration and invasion system ((b) (4)). Designated control or treated suspended cells (0.5 mL) were added to each migration or invasion chamber and 25 ng/mL HGF (0.75 mL) was added to the lower well of each companion plate as a chemoattractant to attract cells from migration or invasion chamber inserts inserted at the top of the companion plate. Cells that invaded

or migrated to the lower well of the plate were then fixed and nuclei were stained. Five microscopic images were taken from each well and the cell number for migration or invasion was determined under each condition using Image-Pro Plus software (Media Cybernetics, Silver Spring, MD). IC_{50} values were calculated by concentration-response curve fitting utilizing a four-parameter analytical method.

An *in vitro* HUVEC matrigel invasion assay was conducted using an ACEA RT-CES system (ACEA biologicals, San Diego, CA) with ACEA electro-sensing 96-well plates. HUVEC cells were treated with 100 ng/mL HGF and/or different concentrations of PF-02341066. Electronic sensors embedded on the bottom of the ACEA plates detected HUVEC cells that invaded through Matrigel. The relative number (cell index) of invaded HUVEC cells was determined utilizing ACEA RT-CES™ Integrated Software and IC_{50} values were calculated by concentration-response curve fitting utilizing a four-parameter analytical method.

In an MDCK cell scattering assay in a 96-well plate, MDCK cells were stimulated with HGF (50 ng/mL) in the presence of various concentrations of PF-02341066 diluted in growth medium. Colonies were fixed and stained with 0.2% crystal violet in 10% buffered formalin and assessed for scattering at each concentration visually.

An HMVEC vascular sprouting assay was conducted using 96- and 48-well plates. Endothelial tube formation was observed daily under an inverted microscope, and images were captured on Day 7 by a digital camera [redacted] (b) (4) connected to the microscope. PF-02341066 was added at several concentrations and vascular sprouting was visually assessed.

The effect of PF-02341066 on NPM-ALK-dependent cell cycle distribution and apoptosis of human lymphoma cells was evaluated by flow cytometric analysis ([redacted] (b) (4) Karpas 299 and SU-DHL-1 human lymphoma cells were treated with PF-02341066 for 24-48 hours in growth media (RPMI + 10% FBS). Cell cycle distribution and apoptosis of lymphoma cells was assessed utilizing the CycloTest Plus DNA Reagent Kit [redacted] (b) (4) and cells were analyzed by flow cytometry. DNA content (ploidy analysis to determine percent cell number in each cell cycle) was assessed using Cell Quest Pro and analyzed with ModFit LT software ([redacted] (b) (4)). The apoptotic peak (A_0) was defined as the peak that occurs in channel numbers lower than G_0/G_1 peak. Apoptosis was also determined by flow cytometric analysis using Annexin V-FITC staining ([redacted] (b) (4)) and also analyzed using FACSCalibur.

Results

Kinase selectivity profile of PF-02341066 in biochemical enzyme and cell-based assays

Results indicate that PF-02341066 is an ATP-competitive inhibitor of recombinant, human c-Met/HGFR kinase activity with a mean K_i of 4 nM. In preliminary biochemical

kinase selectivity screens, PF-02341066 showed activity in the nM range for 13 kinases from the 102 tested at (b) (4) and 6 kinases of the 19 tested at Pfizer.

Table 1: (b) (4) 102 kinase panel screening data and kinase hit follow-up

Kinase	(b) (4) % inhibition	(b) (4) enzyme IC_{50}	Pfizer cell IC_{50}
c-Met/HGFR		<1 nM	9.5 nM
Tie2	103	5 nM	448 nM
TrkA	102	<1 nM	580 nM
ALK	100	<1 nM	20 nM
TrkB	100	<1 nM	399 nM
Abl(T315I)	98	2 nM	NA
Yes	96	23 nM	NA
Lck	95	<1 nM	2741 nM
Rse [SKY]	94	310 nM	NA
Axl	93	<1 nM	300 nM
Fes	93	32 nM	NA
Lyn	93	128 nM	NA
Arg	91	3 nM	NA
Ros	90	60 nM	NA

NA= not available

Table 2: Pfizer kinase panel screening and kinase hit follow-up

Kinase	Enzyme EC_{50}	Cell EC_{50}
c-Met/HGFR	0.008 µM (8 nM)	0.011 µM (11 nM)
RON	0.027 µM (27 nM)	0.189 µM 189 nM
Abl	0.06 µM (60 nM)	1.159 µM (1159 nM)
Lck	0.067 µM (67 nM)	2.741 µM (2741 nM)
Mer	0.074 µM (74 nM)	NA
Rse [SKY]	0.151 µM (151 nM)	>10 µM (>10,000 nM)
Axl	0.463 µM (463 nM)	0.294 µM (294 nM)

NA= not available

The selectivity of PF-02341066 was evaluated in a panel of cell based kinase activity assays for the potential targets identified in the biochemical assays and other related RTKs (e.g., RON, SKY, IR). The IC_{50} for c-Met/HGFR in A549 lung carcinoma cells was

8.6 nM and this value was used for the selectivity ratios in the table below. PF-02341066 showed similar inhibitory activity for Anaplastic Lymphoma Kinase (ALK) in a human lymphoma cell line (Karpas 299 cells) with an IC_{50} of 24 nM.

Table 3: Selectivity of PF-02341066 in cell-based kinase assays

(excerpted from Sponsor)

Kinase	Kinase form	Assay	Cell Line	IC50 (nM)[b] Mean ± STD	Selectivity Ratio[a]
ALK	Human NPM-ALK	Constitutive ALK Phosphorylation	KARPAS 299 Lymphoma	24 ± 6 (n = 6)	2.8X
RON	Human kinase domain	Constitutive Ron Phosphorylation	Engineered Ron-CHO-B	298 ± 65 (n = 2)	33X
	Human full length	MSP-stimulated Ron Phosphorylation	Engineered Ron-NIH3T3	189 ± 34 (n = 6)	21X
Axl	Human full length	H_2O_2-stimulated Axl Phosphorylation	HUVEC	294 (n = 1)	33X
	Mouse full length	Gas6-stimulated Axl Phosphorylation	Engineered Axl-NIH3T3	322 ± 75 (n = 3)	37X
Tie-2	Human EGF/Tie2 chimera	EGF-stimulated Tie-2 Phosphorylation	Engineered EGFR/Tie-2-NIH3T3	448 ± 83 (n = 8)	52X
Trk A	Human full length	NGF-stimulated Trk A Phosphorylation	Engineered TrkA-PAE	580 ± 222 (n = 5)	67X
Trk B	Human full length	BDNF-stimulated TrkB Phosphorylation	Engineered TrkB-PAE	399 ± 172 (n = 5)	46X
Abl	Human BCR-Abl	Constitutive BCR-Abl Phosphorylation	Engineered BCR-Abl BaF3	1045 ± 25 (n = 3)	121X
IRK	Human full length	Insulin-stimulated IRK Phosphorylation	Engineered 293-IRK	2887 ± 882 (n = 4)	334X
Lck	Human full	Anti-CD3-stimulated Zap70 Phosphorylation	Jurkat	2741 ± 434	283X
	length			(n = 2)	
Sky	Human full length	Gas6-stimulated Sky Phosphorylation	Engineered Sky-NIH3T3	>10000 (n = 1)	>1000X
VEGFR2	Human full length	$VEGF_{165}$-stimulated VEGFR2 Phosphorylation	Engineered PAE-VEGFR2	>10000 (n = 1)	>1000X
PDGFRβ	Human full length	PDGF bb-stimulated PDGFRβ Phosphorylation	Engineered PAE-PDGFRβ	>10000 (n = 1)	>1000X

a. A549 cell c-Met/HGFR IC_{50} was used to calculate the selectivity ratio for cell assays. Selectivity Index was calculated as $IC_{50,\ (HGFR)}/IC_{50,\ (target)}$.
b. Data are referenced in Appendix Table 3.

Inhibition of cMet/HGFR phosphorylation

The ability of PF-02341066 to inhibit cMet/HGFR phosphorylation was evaluated to confirm that enzymatic activity translated into inhibition of c-Met/HGFR in cells. PF-02341066 inhibited constitutive or HGF-stimulated tyrosine phosphorylation of wild-type c-Met/HGFR with a mean IC_{50} value of 11 nM across a panel of human tumor and endothelial cell lines (Table 4). RTK phosphorylation was also evaluated in PF-02341066-treated NIH3T3 cells engineered to express wild-type c-Met/HGFR or a series of representative c-Met/HGFR active-site mutations. The IC_{50} for the wild-type receptor was 12.6 nM. PF-02341066 showed greater or similar activity for the ATP

mutants (H1094R, 2.2 nM and V1092I, 19 nM) or P-loop mutants (M1250T, 15 nM), however, the potency was 10-fold lower for the activation loop mutant (Y1230C, 127 nM).

Overexpression of ABC transporters such as MDR1, MRP1, and MXR by tumor cells has been frequently associated with decreased cellular accumulation of several classes of anticancer drugs. The potential for efflux transporter-mediated drug resistance with PF-02341066 was evaluated by testing an isogenic pair of MDCK cells engineered to express high levels of MDR1 and tumor cell lines from the NCI60 panel with the highest reported expression of each ABC transporters. The IC_{50} of PF-02341066 in MDCK cells with high levels of MDR1 (112 nM) was 4.5-fold less potent than in wild-type MDCK cells (24 nM; see table below). Tumor cells expressing high levels of MDR1 (A498), MRP1 (786-0), MXP (HT29), or a combination of all 3 transporters (Colo205) showed minimal decreases in potency compared with a cell line that does not express ABC transporters (MBA-MD-231) (Table 4). Therefore, there is a moderate potential for resistance to PF-02341066 due to expression of efflux transporters.

Table 4:Cellular potency of PF-02341066 vs. c-Met/HGFR phosphorylation

(excerpted from Sponsor)

Kinase	Cell Line	Stimulus	IC_{50} (nM) [a] Mean ± STD
Human WT HGFR	A549 Lung Carcinoma	HGF	8.6 ± 2 (n = 11)
Human WT HGFR	GTL-16 Gastric carcinoma	Constitut.	13 ± 4 (n = 7)
Human WT HGFR	HT29 Colon Carcinoma	HGF	11 ± 2.6 (n = 8)
Human WT HGFR	Colo205 Colon Carcinoma	HGF	10 ± 1 (n = 2)
Human WT HGFR	A498 Renal Carcinoma	HGF	13 ± 1.4 (n = 4)
Human WT HGFR	786-O Renal Carcinoma	HGF	19 ± 1.5 (n = 4)
Human WT HGFR	MBA-MD-231 Breast CA	HGF	5.1 ± 1.5 (n = 4)
Canine WT HGFR	MDCK Kidney Epithelial	HGF	24 ± 5 (n = 7)
Canine WT HGFR	MDCK-MDR1	HGF	112 ± 34 (n = 6)
Murine WT HGFR	mIMCD3 Kidney Epithelial	HGF	5.0 ± 0.4 (n = 4)
Receptor Phosphorylation of c-Met/HGFR Mutants			
HGFR V1092I	NIH3T3-HGFR- V1092I	HGF	19 (n = 1)
HGFR-H1094R	NIH3T3-HGFR- H1094R	HGF	2.2 ± 0.3 (n = 3)
HGFR-Y1230C	NIH3T3-HGFR- Y1230C	HGF	127 ± 29 (n = 5)
HGFR-M1250T	NIH3T3-HGFR- M1250T	HGF	15 ± 3 (n = 4)
HGFR WT	NIH3T3-stable-hHGFR	HGF	12.6 ± 3.4 (n = 6)

a. Data are referenced in Appendix Table 3.

Effects of PF-02341066 on c-Met/HGFR-dependent phenotypes and HGF-stimulated signal transduction pathways in cells

PF-02341066 inhibited human GTL-16 gastric carcinoma cell growth/proliferation (IC_{50}= 9.7 nM), HGF-stimulated human NCI-H441 lung carcinoma cell migration and invasion (IC_{50s} of 11 nM and 6.1 nM, respectively; Figure 1), and MDCK cell scattering (IC_{50}=15.6 nM). Inhibition of HGF-stimulated c-Met/HGFR autophosphorylation in HUVEC cells (IC_{50}=14 nM) correlated with inhibition of HGF-mediated HUVEC cell survival (IC_{50}=11 nM) and matrigel invasion (IC_{50}=35 nM, n=2).

Figure 1: HGF-stimulated migration and invasion of NCI-H441 lung carcinoma cells

(excerpted from sponsor's submission)

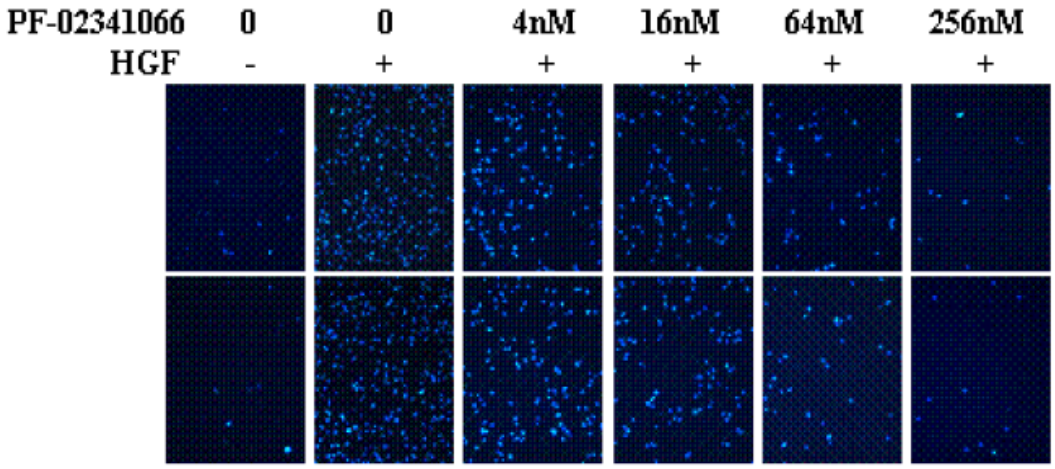

PF-02341066 also inhibited vascular sprouting in Human Microvascular Endothelial cells (HMVEC) (Figure 2),. These data suggest that PF-02341066 may inhibit angiogenesis.

Figure 2: Vascular sprouting of HMVEC

(excerpted from sponsor's submission)

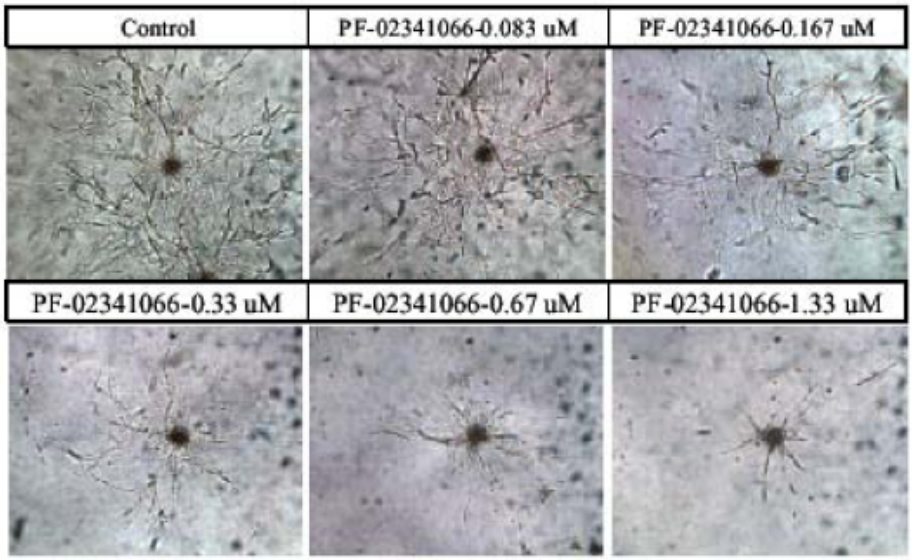

PF-02341066 was evaluated for its ability to inhibit c-Met/HGFR-dependent signaling. PF-02341066 demonstrated concentration-dependent inhibition of HGF-stimulated phosphorylation of signaling molecules implicated in transduction of signals through c-Met/HGFR including Gab1, AKT, Raf, Mek, MAPK1/2, p90RSK, and STAT5 in A549 human NSCLC cells.

Figure 3: Inhibition of c-Met/HGFR-dependent signaling in A549 human lung carcinoma cells

(excerpted from sponsor's submission)

(b) (4)

Effects of PF-02341066 against oncogenic ALK, ALK dependent phenotypes and signal transduction pathways in cells

Based on the inhibition of NPM-ALK observed in Karpas 299 lymphoma cells discussed above (IC_{50}=24 nM), the effects of PF-02341066 on NPM-ALK-dependent cell functions were investigated. PF-02341066 inhibited proliferation of Karpas 299 cells with an IC_{50} of approximately 60 nM and induced cell cycle G0/G1 phase arrest and apoptosis in Karpas 299 and SU-DHL-1 lymphoma cells (Figure 4).

Figure 4: Cell cycle G0/G1 phase arrest and apoptosis

(excerpted from sponsor's submission)

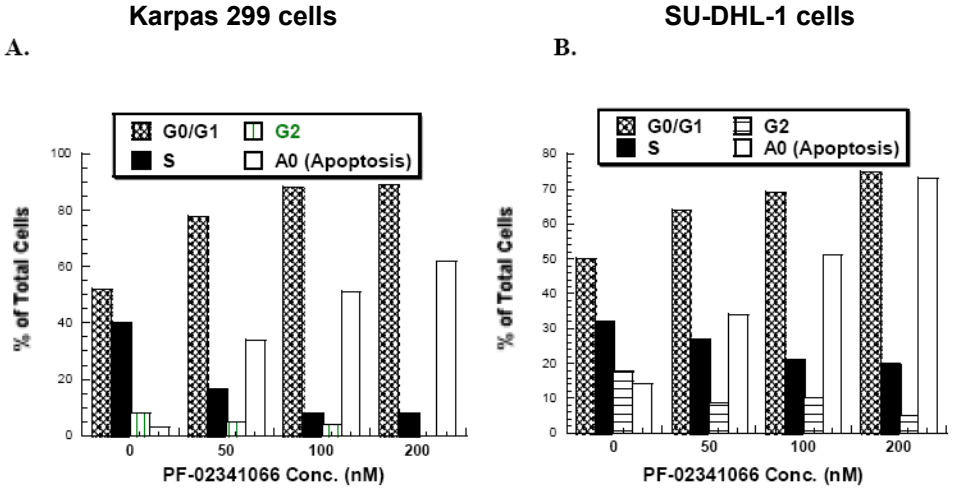

The effects of PF-02341066 on a variety of downstream effector molecules involved in tumor cell growth and survival were evaluated *in vitro* in Karpas 299 cells. PF-02341066 demonstrated dose-dependent inhibition of phosphorylation of multiple signaling molecules including PLC-γl, MAPK, cyclin-A, c-myc, c-fos, c-jun, AKT and STAT3 (Figure 5 A and B).

Figure 5: Inhibition of NPM-ALK signaling pathways

(excerpted from sponsor's submission)

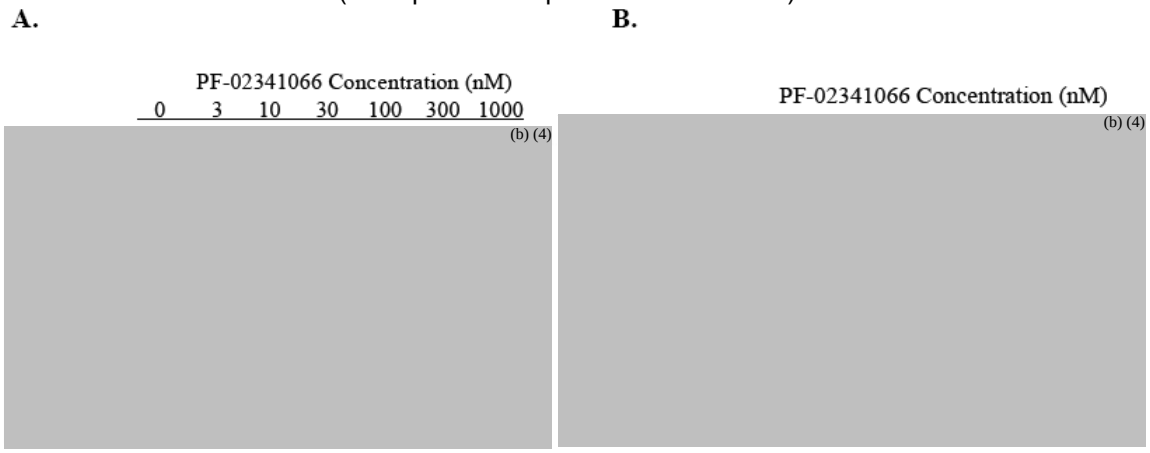

Study title: Pharmacodynamic inhibition of target RTKS, elucidation of pharmacokinetic/pharmacodynamic (PK/PD) relationships, and evaluation of antitumor efficacy of PF-02341066 in rodent models of cancer *in vivo*
Study no.: Pharm002
Study report location: M4.2.1.1

Key Findings

- PF-02341066 dose-dependently inhibited tumor growth and c-Met/HGFR phosphorylation in the GTL-16 gastric carcinoma and U87MG glioblastoma tumor xenograft models
- PF-02341066 also inhibited tumor growth in the NCI-H441 non-small cell lung carcinoma and PC-3 prostate carcinoma tumor xenograft models
- PF-02341066 produced dose-dependent inhibition of phosphorylated HGFR (activation loop and docking site), Erk, AKT, and Gab-1 in GTL-16 tumors
- PF-02341066 inhibited cell proliferation in the GTL-16 xenograft model as measured by significant reduction in levels of Ki67, a marker of mitotic index, in immunohistochemical studies
- PF-02341066 demonstrated a dose-dependent reduction in immunostaining for CD31, a tumor endothelial cell marker, in GTL-16 tumors, indicating that crizotinib may have anti-angiogenic effects
- PF-02341066 dose-dependently inhibited tumor growth and NPM-ALK phosphorylation in the Karpas human lymphoma xenograft model
- PF-02341066 demonstrated dose-dependent inhibition of PLC-γ1, MAPK 44/42, AKT and STAT3 phosphorylation and inhibition of Cyclin-A, -B, and -D1, c-myc, c-fos, and c-jun in Karpas 299 human lymphoma xenografts

Following the identification of c-Met/HGFR and ALK kinase as targets of PF-02341066 in *in vitro* assays, several objectives were pursued *in vivo* including 1) demonstration of kinase target inhibition by PF-02341066 *in vivo*, 2) demonstration of antitumor efficacy in relevant tumor models by PF-02341066, 3) establishing pharmacokinetic/pharmacodynamic (PK/PD) relationships to aid in the determination of

the target plasma concentration of PF-02341066, and 4) characterization of the antitumor mechanism of action of this compound *in vivo*. An additional objective was to determine the most effective dose levels and administration schedules for the clinical dose schedule projection and to aid in the determination of a therapeutic index. Nonclincal pharmacology studies with PF-02341066 were conducted in a variety of rodent models of cancer to study these objectives and were summarized in the Pharm002 report.

Subcutaneous xenograft models in Athymic mice

Tumor cells were supplemented with 30-50% Matrigel (b) (4) to facilitate tumor take and growth of selected tumor cells as xenografts. Cells (2-5 x 10^6 in 100 µL) were implanted subcutaneously into the hindflank region of female or male nu/nu or SCID/Beige mice (5-8 weeks old) and allowed to grow to a designated size prior to the administration of compound for each experiment. Tumor size was determined by measurement with electronic calipers and tumor volume was calculated as the product of its length x width^2 x 0.4.

Ex vivo target modulation (PK/PD) studies

Tumor cells expressing constitutively phosphorylated c-Met/HGFR or ALK were implanted subcutaneously in nude mice and allowed to grow untreated to a size of 300-800 mm^3. PF-02341066 was administered to mice at the designated dose levels as a single oral dose for acute PK/PD studies or multiple oral doses for steady state PK/PD studies. At indicated times following PF-02341066 administration, individual mice were euthanized, a blood sample was isolated from the cardiac left ventricle using a syringe primed with heparin sulfate, and tumors were resected. Plasma samples were analyzed for PF-02341066 concentration using LCMS analysis. (b) (4) The level of total and/or phosphorylated proteins of interest in each vehicle- or PF-02341066-treated tumor sample was determined using a capture ELISA method using a 96 well plates pre-coated with either anti-c-Met/HGFR (b) (4) or anti-ALK capture antibodies (b) (4). The optical density (OD) of each vehicle or PF-02341066-treated well was measured at 450 nm using a spectrometer. Total phosphorylation of c-Met/HGFR or ALK in tumors resected from PF-02341066-treated animals was compared with that in tumors resected from vehicle-treated animals at the same time point based on the OD readings. Inhibition of kinase target phosphorylation by PF-02341066 in tumors was calculated using the following equation: % inhibition= 100-[(Mean OD treated/ Mean OD untreated) X 100].

Immunoblotting

Immunoblotting method was also used to determine relative kinase phosphorylation status and total protein levels in tumor samples. Tumor bearing mice were treated with different doses of PF-02341066 and tumor lysates and protein samples were prepared. Specific antibodies (anti-total human c-Met/HGFR, anti-phospho-c-Met/HGFR, anti-total and -phospho ALK, anti-total and phosphor Gab1, anti-total and phospho AKT, anti-total and phosphor-MAPK44/42, STAT5) were used to immunoprecipitate proteins of interest. Immunoprecipitated proteins were separated by SDS-PAGE and immunoblotting was conducted with anti-phosphotyrosine or total antibodies.

Tumor histology and immunohistochemistry (ICH)

Tumor specimens to be evaluated for immunohistochemical endpoints were harvested, fixed in 10% buffered formalin with protease and phosphotase inhibitors, subsequently paraffin-embedded, and 4 µM sections were [redacted] (b) (4) Tumor OCT frozen samples were also collected and sectioned for CD-31 staining. For immunostaining, slides were incubated with the primary antibodies then secondary antibodies, and visualized using either a colorimetric method [redacted] (b) (4), or a fluoremetric method ([redacted] (b) (4)). All of the immunostained sections were counterstained using hematoxylin. Automated [redacted] (b) (4) Staining Module [redacted] (b) (4)) was also used to conduct histological staining. Stained sections were analyzed using an [redacted] (b) (4) microscope and quantitative analysis of section staining was performed utilizing the [redacted] (b) (4). The slides were also analyzed by in house pathologists using standard clinical methods. Immunohistochemistry studies were conducted on tumor tissue using anti-phospho-c-Met/HGFR, anti-Ki67, and anti-CD31 antibodies.

Results

PK/PD relationship of c-Met/HGFR activity, tumor growth, and plasma exposure of PF-02341066 in GTL-16 model

The GTL-16 human gastric carcinoma model was used extensively for c-Met/HGFR PK/PD studies. In steady state PD studies, athymic mice bearing established GTL-16 tumors (250 mm^3) were administered PF-02341066 (3.125, 6.25, 12.5, 25, or 50 mg/kg/day) or vehicle orally for 11 days. For studies investigating inhibition of c-Met/HGFR phosphorylation, mice were euthanized at 1, 4, 8, 16, and 24 hours after administration of PF-02341066 and phosphorylation in vehicle and treated groups was quantitated by ELISA. The effects of PF-02341066 on c-Met/HGFR phosphorylation and tumor growth in the GTL-16 xenograft model are shown in the figure below. Inhibition of tumor growth was dose-dependent and corresponded to both the amount of inhibition (percentage) and duration of inhibition of c-Met/HGFR phosphorylation. At a dose of

6.25 mg/kg/day 34% inhibition of tumor growth corresponded with 30-50% inhibition of c-Met/HGFR phosphorylation at 1-8 hours with full recovery by 16 hours. At 12.5 mg/kg/day 60% inhibition of tumor growth corresponded with 80-90% inhibition of c-Met/HGFR phosphorylation at 1-8 hours which decreased to 50-60% inhibition by 16-24 hours. A dose of 25 mg/kg/day inhibited tumor growth by 89% with near complete inhibition of phosphorylation, and the highest dose of 50 mg/kg/day demonstrated 100% tumor growth inhibition which corresponded with complete inhibition of c-Met/HGFR phosphorylation for 24 hours. These findings suggest that the duration of c-Met/HGFR inhibition is important to maximize the anti-tumor efficacy of PF-02341066.

Figure 6: Inhibition of c-Met/HGFR phosphorylation and tumor growth in the GTL-16 xenograft model

(excerpted from sponsor's submission)

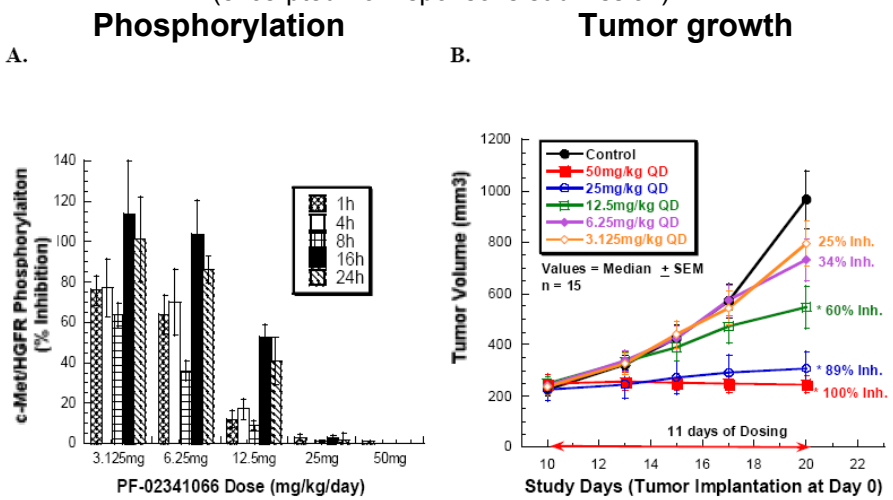

* denotes median tumor volumes significantly less in treated group compared to control group ($p<0.001$)

The relationship of plasma exposure of PF-02341066 and inhibition of c-Met/HGFR phosphorylation at various dose levels was evaluated in mice bearing GTL-16 tumors (250 mm^3) administered PF-02341066 (8.6, 17.2, or 34 mg/kg/day) orally for 10 days. In Figure A below, the relationship of free plasma concentration of PF-02341066 (corrected for mouse plasma protein binding) and c-Met/HGFR phosphorylation in tumors (% inhibition) is expressed as a Hill Function plot at 1, 4, 8, and 24 hours. Figure B below shows plasma levels (red solid line) as determined by HPLC and c-Met/HGFR phosphorylation (blue dotted line) as determined by ELISA at 1, 4, 8, and 24 hours after dosing.

Figure 7: PK/PD relationship of PF-02341066 in mice bearing GTL-16 tumors

(excerpted from sponsor's submission)

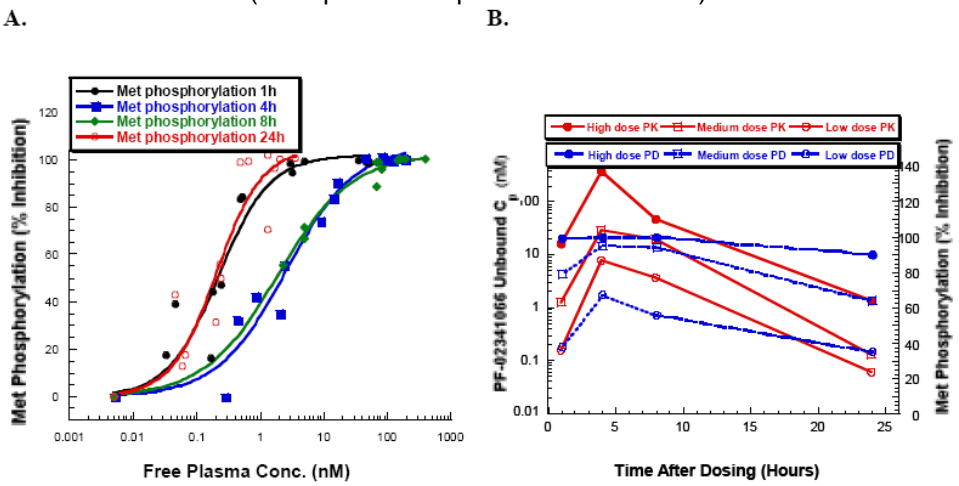

Effects of PF-02341066 on tumor growth and c-Met/HGFR phosphorylation in the U87MG model

A dose-dependent effect of PF-02341066 on tumor growth and c-Met/HGFR phosphorylation was also observed in the U87MG glioblastoma human tumor xenograft model. Athymic mice bearing established U87MG tumors (150 mm^3) were administered PF-02341066 (3.125, 6.25, 12.5, 25, or 50 mg/kg/day) or vehicle orally for 9 days. For studies investigating inhibition of c-Met/HGFR phosphorylation, mice were euthanized 4 hours after the 4th administration of PF-02341066 and phosphorylation in vehicle and treated groups was quantitated by ELISA. The effects of PF-02341066 on tumor growth and c-Met/HGFR phosphorylation in the U87MG xenograft model (Figure 8). It was reported that PF-02341066 did not inhibit Tie-2 phosphorylation in U87MG xenografts at dose levels up to 100 mg/kg, however, these results were not shown.

Figure 8: Inhibition of tumor growth and c-Met/HGFR phosphorylation in the U87MG Xenograft Model (excerpted from sponsor's submission)

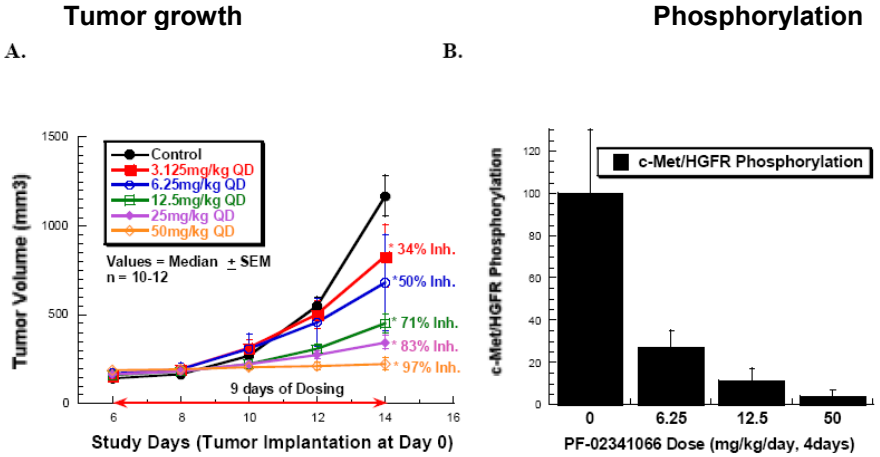

* denotes median tumor volumes significantly less in treated group compared to control group ($p<0.001$)

Antitumor efficacy of PF-02341066 in human xenograft models

The antitumor efficacy of PF-02341066 was evaluated in human tumor xenograft models of cancer indications in which dysregulation of c-Met/HGFR is implicated including GTL-16 gastric carcinoma, U87MG glioblastoma, NCI-H441 NSCLC, and PC-3 prostate carcinoma. The effects of PF-02341066 on large established tumors (> 600 mm^3) were studied in the GTL-16 model. Athymic mice bearing GTL-16 tumors (620 mm^3) were administered PF-02341066 (50 or 75 mg/kg/day) or vehicle orally for 43 days. The effects of PF-02341066 on tumor volume are shown in the figure below. A mean tumor regression of 60% was observed in both the 50 and 75 mg/kg/day treatment groups after 43 days of PF-02341066 administration.

Figure 9:Effects of PF-02341066 on tumor volume of large established GTL-16 tumor xenografts

(excerpted from sponsor's submission)

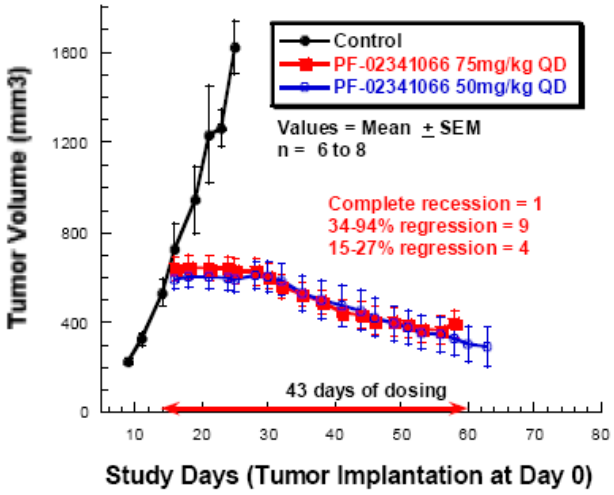

In the NCI-H441 non-small cell lung cancer model, athymic mice bearing established NCI-H441 tumor xenografts (100 mm^3) were administered PF-02341066 (15 or 50 mg/kg/day) or vehicle orally for 38 days. The effects of PF-02341066 on tumor volume were dose-dependent with a 59% mean inhibition of tumor growth at 15 mg/kg/day and complete inhibition of tumor growth and a 48% mean regression in tumor volume at 50 mg/kg/day (Figure 10 A). In the PC-3 prostate carcinoma tumor model, athymic mice bearing established PC-3 tumor xenografts were administered PF-02341066 (50 mg/kg/day) or vehicle orally for 20 days. Treatment with PF-02341066 (50 mg/kg/day) inhibited tumor growth by 84% in the PC-3 model (Figure 10,B).

Figure 10: Effects of PF-02341066 in the NCI-H441 non-small lung carcinoma (A) or PC-3 prostate carcinoma tumor xenograft models (excerpted from sponsor's submission)

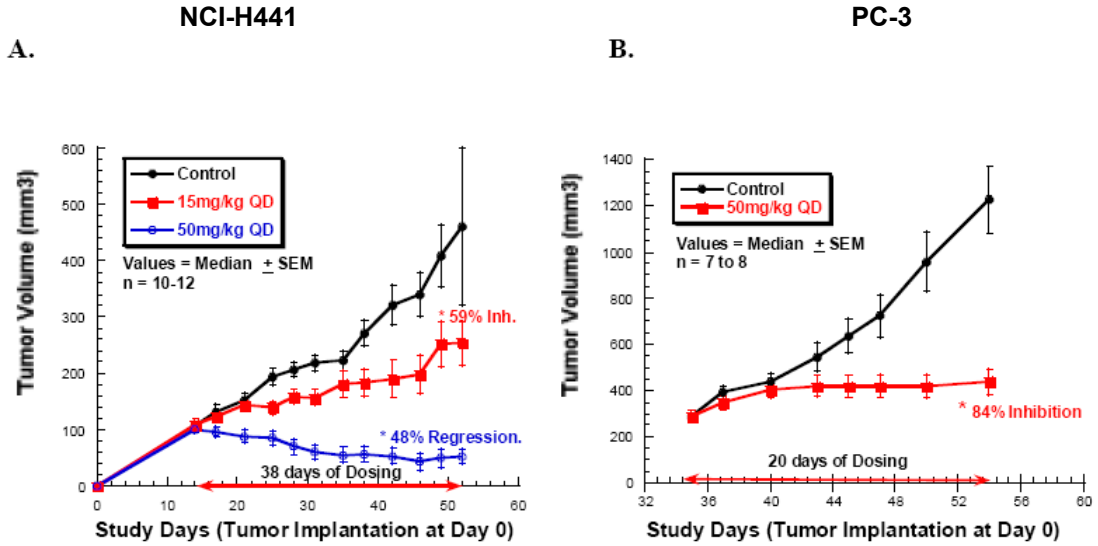

* denotes median tumor volumes significantly less in treated group compared to control group ($p<0.001$)

PF-02341066 mechanism of action studies in c-Met/HGFR-dependent tumor models

Immunoblotting studies were conducted with PF-02341066 using the GTL-16 xenograft model in order to identify signaling proteins corresponding to the inhibitory and anti-tumor activity of PF-02341066. Athymic mice bearing established GTL-16 xenografts were administered PF-02341066 (12.5, 25 or 50 mg/kg/day) or vehicle orally for 12 days. After 12 days, mice were euthanized at 4 hours after PF-02341066 administration and immunoblotting was conducted for proteins of interest. Treatment with 25 or 50 mg/kg/day PF-02341066 produced dose-dependent inhibition of phosphorylated HGFR (activation loop and docking site), Erk, AKT, and Gab-1 in the GTL-16 tumors (Figure 11).

Figure 11: Inhibition of signaling proteins in GTL-16 tumors

(excerpted from sponsor's submission)

PF-02341066 was evaluated for time- and dose-dependent modulation of Ki67, a marker of mitotic index, and caspase-3, a marker of apoptosis, using immunohistochemical methods in tumor sections. For these studies, athymic mice bearing established GTL-16 xenografts were administered PF-02341066 (12.5, 25, or 50 mg/kg/day) or vehicle orally for up to 11 days. Mice were euthanized at the indicated study day (Day 1, 2, 3, 4, or 11) 4 hours after PF-02341066 administration. A significant dose-dependent inhibition of Ki67 was observed at 25 and 50 mg/kg/day in the GTL-16 model (Figure 12 A and C). The time course data for the 50 mg/kg/day dose indicates that inhibition of mitogenesis was greater at Days 3 and 4 (Figure 12 B). Inhibition of Ki67 was also observed at 50 mg/kg/day in the U87MG model according to the report, but these data were not shown. Additionally, a qualitative induction of caspase-3 at 25 and 50 mg/kg/day was reportedly observed in the GTL-16 model and at 50 mg/kg/day in the U87MG model, suggesting that PF-02341066 may also increase apoptosis in these models. The apoptotic response was not quantified and time-dependence could not be established.

Figure 12: Effects of PF-02341066 on cell proliferation in GTL-16 tumors

(excerpted from sponsor's submission)

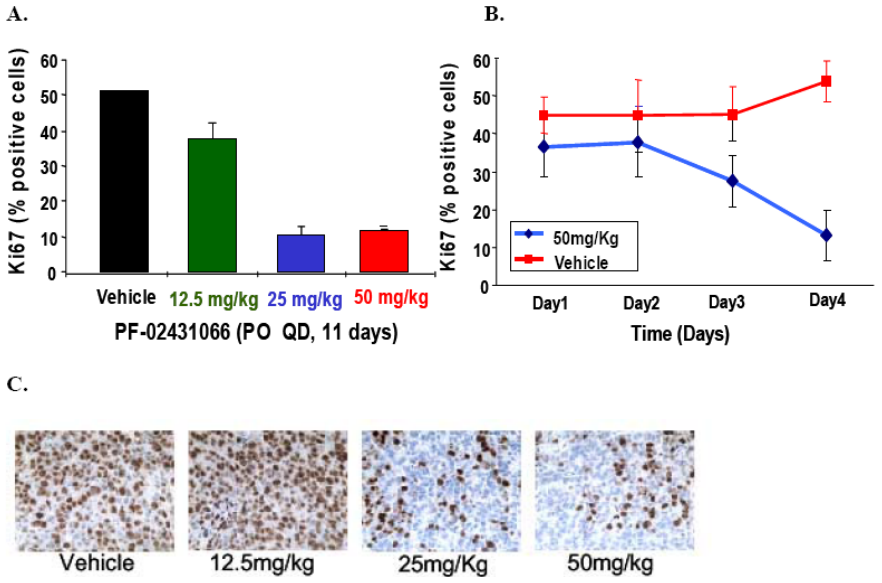

The possible anti-angiogenic effects of PF-02341066 were studied *in vivo* by evaluating time- and dose-dependent modulation of tumor microvessel density (MVD) assessed by immunostaining for CD31 (PECAM1) as a tumor endothelial cell marker. For these studies, athymic mice bearing established GTL-16 xenografts were administered PF-02341066 (12.5, 25, or 50 mg/kg/day) or vehicle orally for 12 days. Mice were euthanized on study Day 12 at 4 hours after PF-02341066 administration. A significant dose-dependent reduction of CD31 positive endothelial cells was observed at 12.5, 25, and 50 mg/kg/day in GTL-16 tumors (Figure 13).

Figure 13: Effect of PF-02341066 on tumor microvessel density

(excerpted from sponsor's submission)

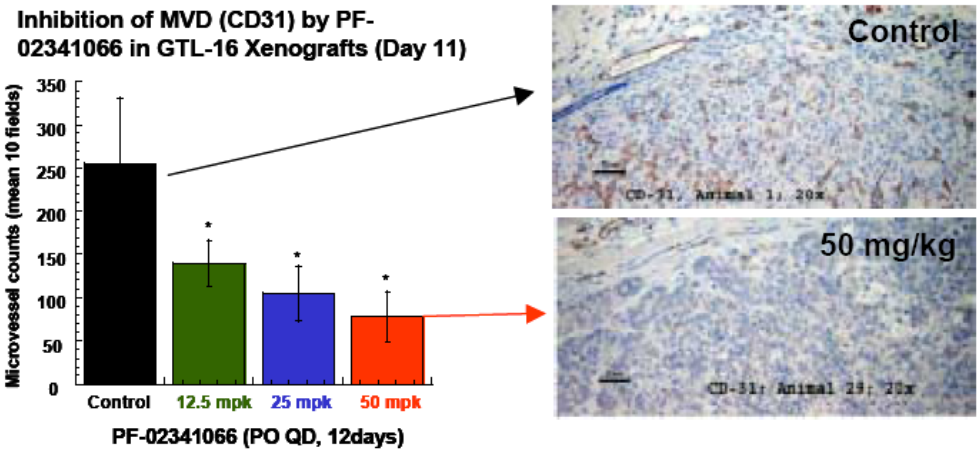

Antitumor efficacy and PK/PD relationships of PF-02341066 in an NPM-ALK dependent lymphoma model

The Karpas 299 human lymphoma xenograft model was used to evaluate the antitumor activity and pharmacodynamic inhibition of NPM-ALK by PF-02341066 *in vivo*. SCID-beige mice bearing established Karpas 299 tumors (220 mm^3) were administered PF-02341066 (25, 50, or 100 mg/kg/day) or vehicle orally for designated time periods. For studies investigating inhibition of NPM-ALK phosphorylation, mice were euthanized at 1, 4, 8, and 24 hours after the 4th administration of PF-02341066 and ALK phosphorylation in vehicle and treated groups was quantitated by ELISA. Complete regression of tumors was observed in the 100 mg/kg/day group within 15 days of the initiation of PF-02341066. After 17 days, PF-02341066 treatment was stopped, resulting in tumor re-growth. When tumors grew to a larger size (>600 mm^3), PF-02341066 treatment was reinitiated for an additional 13 days and complete regression of tumors was observed once again (Figure 14 A). As observed in the GTL-16 xenograft model with c-Met/HGFR phosphorylation, inhibition of tumor growth was dose-dependent and corresponded to the amount of inhibition of NPM-ALK phosphorylation in Karpas 299 tumors. It is important to note that the phosphorylation study had a shorter period of treatment (4 days) than the tumor volume study. At 25 mg/kg/day, 57% tumor growth inhibition was observed in 10 days and corresponded with $\geq$ 50% inhibition of NPM-ALK phosphorylation, while at 50 mg/kg/day, 96% tumor growth inhibition in 10 days corresponded with approximately 80% inhibition of NPM-ALK phosphorylation. The 100% tumor regression observed at 100 mg/kg/day corresponded to almost complete inhibition of NPM-ALK phosphorylation in Karpas 299 tumors. In the Karpas 299 model associated with ALK activity, the maximally efficacious dose of PF-02341066 was 100 mg/kg/day, which was lower than the 50 mg/kg/day maximally efficacious dose in the c-Met associated models.

Figure 14: Effects of PF-02341066 on tumor growth and NPM-ALK phosphorylation in the Karpas 299 xenograft model

(excerpted from sponsor's submission)

Tumor growth **Phosphorylation**

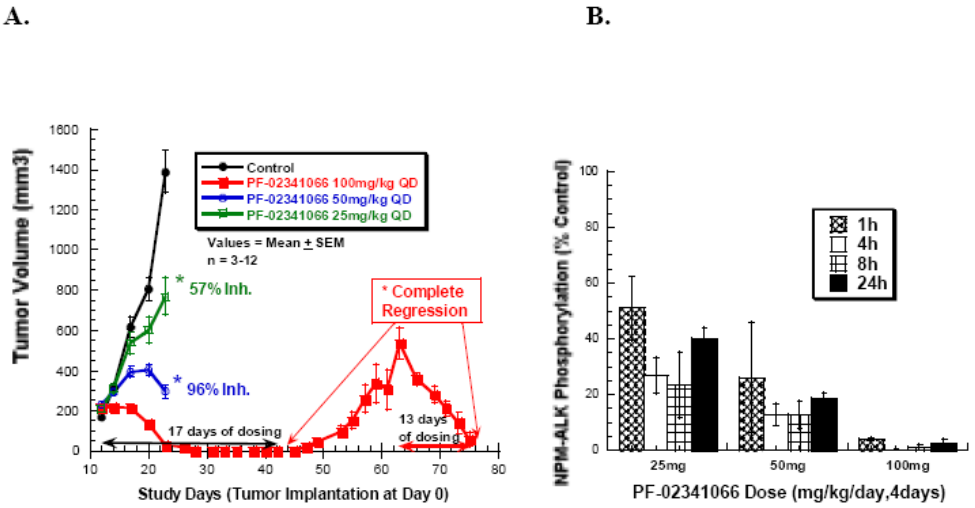

* denotes median tumor volumes significantly less in treated group compared to control group ($p<0.001$)

Immunoblotting studies were conducted with PF-02341066 using the Karpas 299 xenograft model to evaluate the effect of PF-02341066 on NPM-ALK-dependent signal transduction. Athymic mice bearing established Karpas 299 xenografts were administered PF-02341066 (25, 50, or 100 mg/kg/day) or vehicle orally for 4 days. After 4 days, mice were euthanized at 4 hours after PF-02341066 administration and immunoblotting was conducted for proteins of interest. PF-02341066 demonstrated dose-dependent inhibition of PLC-γ1, MAPK 44/42, AKT and STAT3 phosphorylation and inhibition of Cyclin-A, -B, and -D1, c-myc, c-fos, and c-jun in Karpas 299 human lymphoma xenografts (Figure 15). Inhibition of these proteins appears to correspond with NPM-ALK inhibition and anti-tumor efficacy in the Karpas 299 xenograft model.

Figure 15: Inhibition of signaling proteins in Karpas 299 tumors

(excerpted from sponsor's submission)

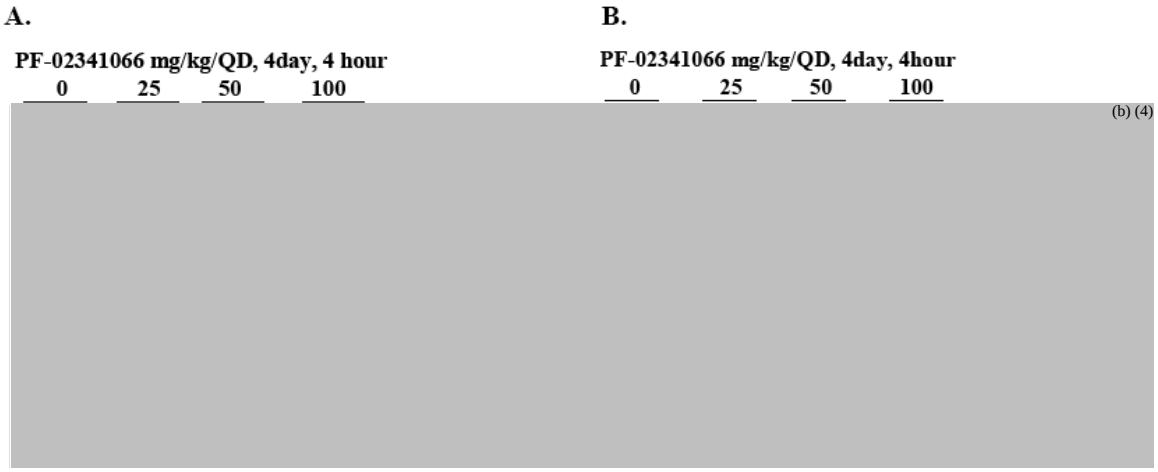

Study title: Characterization of pharmacodynamic inhibition of target RTKS and their oncogenic variants by crizotinib (PF-02341066) and its primary metabolites *in vitro*
Study no.: 192308
Study report location: M4.2.1.1

The objectives of this study were to characterize crizotinib and its metabolites for 1) potency against its RTK targets EML4-ALK, c-Met/HGFR, RON, and their oncogenic variants in biochemical enzyme assays and cell assays, 2) the effects on EML4-ALK-dependent cellular functions that are altered during cancer progression in the EML4-ALK positive NSCLC cell lines. Metabolites tested were the crizotinib lactam diasteromers (PF-06270079 and PF-06270080), pO-desalkyl crizotinib (PF-03255243), and O-desalkyl lactam crizotinib (PF-06268935).

Enzymatic potencies of crizotinib and its human metabolites against ALK and other kinase targets

Biochemical kinase assays were conducted for ALK, c-Met/HGFR, and RON with 11 concentrations of inhibitor (crizotinib or its metabolites) and DMSO control. The enzyme inhibition values (Ki) were calculated by fitting initial rates of enzymatic reactions (<20% peptide phosphorylation) to a tight binding equation for competitive inhibition by the method of nonlinear least-squares using SIGHTS in-house software or GraphPad Prism (GraphPad software, San Diego, CA). The biochemical Ki values for the inhibition of ALK and c-Met/HGFR were determined by a fluorescence based off-chip mobility shift assay, and RON Ki values were determined using a continuous fluorometric assay.

Crizotinib was shown to be an ATP-competitive inhibitor of recombinant, human ALK kinase activity with a mean Ki value of 0.50 nM and also inhibited human recombinant full length EML4-ALK V3 activity with a Ki value of 0.5 nM. Crizotinib also inhibited the catalytic activity of recombinant human c-Met/HGFR and RON kinases with mean values of 0.62 nM and 9.1 nM, respectively. These Ki values for the wild-type ALK, c-Met, and RON kinases are listed below (Table 5) along with values for the crizotinib metabolites. Compared to crizotinib, PF-06270079 and PF-06270080 exhibited approximately 5- and 3-fold higher Ki values against ALK, respectively. The activity of these metabolites against c-Met/HGFR was similar to that of crizotinib. PF-06270080 was approximately 3-fold more potent than crizotinib against RON kinase. The two O-desalkyl crizotinib metabolites, PF-06268935 and PF-03255243, showed only weak inhibitory activity against EML4-ALK, c-Met/HGFR, or RON activity in the recombinant enzyme activity assays.

Table 5: Biochemical potency of crizotinib and its metabolites

(excerpted from sponsor's submission)

Compound	Biochemical Enzyme Assays								
	Wild-type ALK kinase Domain			Wild-type c-Met kinase domain			Wild-type RON kinase domain		
	Ki (nM) Mean ± STD	n	M/P Ratio[a]	Ki (nM) Mean ± STD	n	M/P Ratio[a]	Ki (nM) Mean ± STD	n	M/P Ratio[a]
Crizotinib	0.50 ± 0.17	28		0.62 ± 0.70	3		9.1 ± 3.6	4	
PF-06270079	2.41	1	4.8	0.45 ± 0.16	2	0.73	7.74	1	0.85
PF-06270080	1.61	1	3.2	0.56 ± 0.26	4	0.90	2.83	1	0.31
PF-06268935	>2,000	1	>4,000	>1,500	1	>2000	970	1	107
PF-03255243	>3,000	1	>6,000	1,250	1	312	492	1	54

[a] : M/P Ration = Metabolite Ki divided by the Parent (Crizotinib) Ki
Data are referenced in Archiving, section 9.

Pharmacodynamic inhibition of target RTK activities in cells

Cellular assays were conducted to assess the ability of crizotinib to inhibit the phosphorylation of EML4-ALK variants, NPM-ALK, c-Met/HGFR and RON in cell lines expressing these targets. NCI-H3122 and NCI-H2228 are human lung adenocarcinoma cell lines harboring chromosomal inversion events resulting in the expression of EML4-ALK fusion protein variant 1 (V1) and variant (V3a/b), respectively. NCI-H3122 and NCI-H2228 cells were treated with designated concentrations of crizotinib for one hour, cells were then lysed and lysates used for ELISA analysis. Studies were also conducted with NIH3T3 fibroblasts engineered to express the EML4-ALK variants V1, V2, V3A, or V3B. The effect of crizotinib on EML4-ALK phosphorylation was determined using a commercially available [redacted] (b) (4) Phospho-ALK (Tyr1604) Chemiluminescent Sandwich ELISA kit ([redacted] (b) (4)). EC_{50} values were calculated by concentration-response curve fitting using a four-parameter analytical method. The EC_{50} values for inhibition of phosphoryaltion by crizotinib in the various cell lines expressing EML4-ALK variants, NPM-ALK, c-Met/HGFR, and RON are listed in Table 6. The percent of inhibition of ALK phosphorylation by crizotinib in H3122 and H2228 cells and EML4-ALK engineered 3T3 cells is shown in Figure 16. Crizotinib showed similar inhibition of the variants of EML4-ALK (V1, V2, V3a, and V3b) with EC_{50} values ranging from 27-74 nM. Additionally, crizotinib inhibited RON and RONΔ160 autophosphorylation (EC_{50}=80 nM and 65 nM) in NIH-3T3 cells engineered to express human RON or RONΔ160.

Table 6: Cellular potency of crizotinib

(excerpted from sponsor's submission)

Cell-based Kinase Phosphorylation Assays	EC_{50} (nM) Mean ± STD	n
Endogenous wild-type EML4-ALK V1 phosphorylation/H3122 NSCLC cells	63 ± 31	20
Endogenous wild-type EML4-ALK V3a/b phosphorylation/H2228 NSCLC cells	74 ± 23	6
Exogenous wild-type EML4-ALK V1 phosphorylation/3T3EML4-ALK V1 cells	60 ± 10	2
Exogenous wild-type EML4-ALK V2 phosphorylation/3T3EML4-ALK V2 cells	69 ± 1	2
Exogenous wild-type EML4-ALK V3a phosphorylation/3T3EML4-ALK V3a cells	27 ± 2	2
Exogenous wild-type EML4-ALK V3b phosphorylation/3T3EML4-ALK V3b cells	41 ± 7	2
Endogenous NPM-ALK phosphorylation in Kapass299 ALCL cells	35 ± 17	41
HGF stimulated wild-type c-Met phosphorylation in A549 NSCLC cells	5.0 ± 3.8	164
MSP stimulated wild-type RON phosphorylation in 3T3-RON cells	80 ± 31	269
MSP stimulated wild-type RON phosphorylation in 3T3-RONΔ160 cells	65 ± 4	2
Data are referenced in the archiving, section 9.		

Figure 16: Effects of crizotinib on kinase activity of the EML4-ALK variants in human NSCLC and EML4-ALK engineered 3T3 cells

(excerpted from sponsor's submission)

NSCLC **EML4-ALK engineered 3T3 cells**

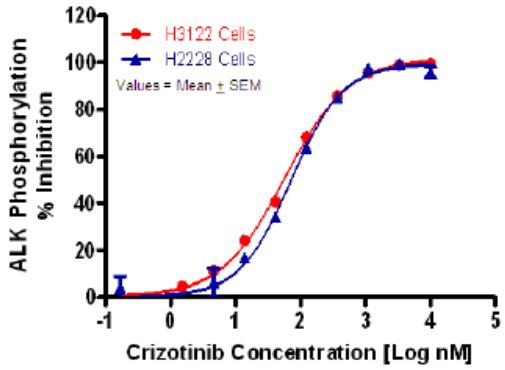

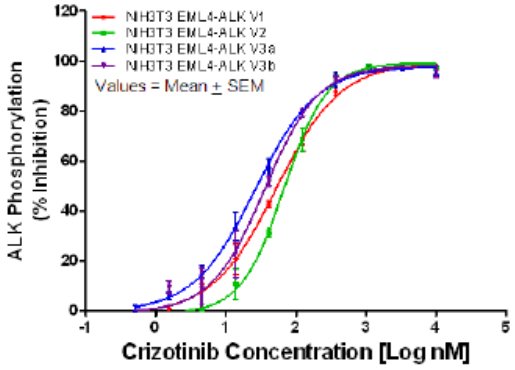

The EC_{50} values of the crizotinib human metabolites for inhibition of phosphorylation of the crizotinib targets in cell-based assays are listed in the table below. The activities of the metabolites in the cell-based assays were consistent with those observed in the enzyme assays. The two O-desalkyl crizotinib metabolites (PF-06268935 and PF-03255234) did not inhibit EML4-ALK, c-Met/HGFR, or RON activity at concentrations up to 10 µM, however, the two lactam metabolites (PF-06270079 and PF-06270080) demonstrated potentially pharmacologically relevant inhibitory activity for

phosphorylation of EMLK-ALK, c-Met/HGFR and RON kinase in cell-based assays. The data indicate that PF-06270079 and PF-06270080 are less potent for ALK and c-Met/HGFR inhibition than crizotinib with EC_{50} values 3-7 fold higher in the ALK assays and 3-4-fold higher against c-Met/HGFR in A549 cells compared to crizotinib. PF-06270079 and crizotinib showed similar potencies for the inhibition of RON phosphorylation in MSP stimulated 3T3-RON cells, while PF-06270080 was 2-fold more potent than crizotinib against RON in these cells.

Table 7: Comparison of cellular potency of crizotinib and its human metabolites

(excerpted from sponsor's submission)

Cellular Kinase Assays	Compound	EC_{50} (nM) Mean ± STD	n	p value# vs. C	Metabolite/Crizotinib (C) Ratio#			
					Ratio#	n	p value# vs. C	p value# vs. -079
Endogenous wild-type EML4-ALK V1 phosphorylation in H3122 NSCLC cells	Crizotinib	63 ± 31	20					
	PF-06270079	284 ± 182	7	0.0002	3.7#	7	<0.0001	
	PF-06270080	194 ± 118	6	0.0030	2.5#	6	<0.0001	<0.0001
	PF-06268935	>10,000	3	<0.0001	>137#	3	<0.0001	
	PF-03255243	>10,000	3	<0.0001	>137#	3	<0.0001	
Endogenous wild-type EML4-ALK V3a/b phosphorylation in H2228 NSCLC cells	Crizotinib	74 ± 23	6					
	PF-06270079	554 ± 102	3	<0.0001	7.5#	3	<0.0001	
	PF-06270080	355 ± 66	3	0.0026	5.0#	3	0.0026	0.0414
	PF-06268935	ND						
	PF-03255243	ND						
HGF stimulated wild-type c-Met phosphorylation in A549 NSCLC cells	Crizotinib	5.0 + 3.8	164					
	PF-06270079	18.5 ± 7.3	3	0.0065	4.0#	3	0.0065	
	PF-06270080	11.8 ± 2.7	3	0.0308	2.5#	3	0.0308	0.25
	PF-06268935	>10,000	6	<0.0001	>2000#	3	<0.0001	
	PF-03255243	>10,000	6	<0.0001	>2000#	3	<0.0001	
MSP stimulated wild-type Ron phosphorylation in 3T3-Ron-R4 cells	Crizotinib	80 ± 31	269					
	PF-06270079	85 ± 14	3	0.828	1.0#	3	0.828	
	PF-06270080	40 ± 17	3	0.025	0.5#	3	0.025	0.019
	PF-06268935	>10,000	6	<0.0001	>118#	6	<0.0001	
	PF-03255243	>10,000	6	<0.0001	>118#	6	<0.0001	
#: p values and ratios on EC_{50} values of crizotinib vs. metabolites were derived by utilizing EC_{50} values of crizotinib and the metabolites generated in the same experiment.								
Data are referenced in Archiving, section 9.								

Effect of crizotinib on EML4-ALK-dependent phenotypes in NSCLC *in vitro*

The effects of crizotinib on cell proliferation and survival/apoptosis were studied in the EML4-ALK V1 positive NCI-H3122 and EML4-ALK V3a/b positive NCI-H2228 human lung adenocarcinoma cell lines. The effect of crizotinib on cell proliferation was determined using a commercially available [redacted] (b) (4), which measures the relative number of live cells in the assay wells. The effect of crizotinib on cell apoptosis was determined by using a commercially available [redacted] (b) (4), which measures the ability of caspase 3/7 from the cells to cleave the specific caspase 3/7 substrate that was added into the assay wells. H3122 and H2228 cells were treated with designated concentrations of crizotinib for 72 hours for

cell proliferation and 48 hours for cell apoptosis. EC_{50} values were calculated by concentration-response curve fitting using a four-parameter analytical method. In the EML4-ALK V1 positive NCI-H3122 cell line, crizotinib completely inhibited cell proliferation (EC_{50}=54 nM) and induced apoptosis associated with a 4-fold increase in Caspase 3/7 activity with a mean EC_{50} value of 110 nM. In the EML4-ALK V3a/b positive NCI-H2228 cell line, crizotinib only partially inhibited cell proliferation with a mean EC_{50} value of 34 nM and induced apoptosis associated with a 2-fold increase in Caspase 3/7 activity.

Figure 17: Inhibition of cell proliferation and induction of apoptosis in EML4-ALK V1 positive H3122 and H2228 NSCLC in vitro

(excerpted from sponsor's submission)

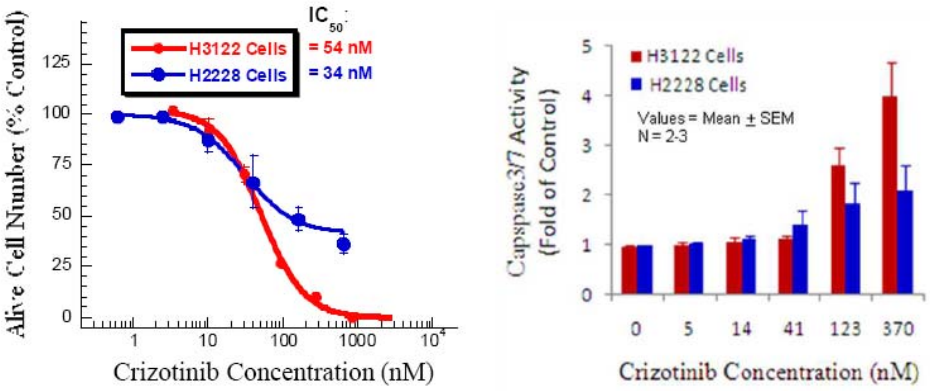

Study title: Pharmacodynamic inhibition of EML4-ALK, elucidation of pharmacokinetic/pharmacodynamic (PK/PD) relationships, and evaluation of antitumor efficacy of crizotinib (PF-02341066) in a rodent model of EML4-ALK positive lung adenocarcinoma cancer *in vivo*
Study no.: 192438
Study report location: M4.2.1.1

Crizotinib was studied *in vivo* in a series of experiments using the NCI-H3122 lung adenocarcinoma model harboring EML4-ALK V1 fusion gene to investigate the following objectives: 1) demonstration of EML4-ALK inhibition of crizotinib *in vivo*, 2) demonstration of antitumor efficacy in established tumors, 3) establishing pharmacokinetic/pharmacodynamic (PK/PD) relationships for inhibition of EML4-ALK and tumor growth, 4) characterization of the antitumor mechanism of action of this compound *in vivo*.

The human NCI-H3122 NSCLC tumor xenograft model was used to evaluate the antitumor efficacy and PK/PD relationship of crizotinib. Tumor cells were supplemented with 50% Matrigel ((b) (4) to facilitate tumor take. Cells (2 x 10^6 in 100 µL) were implanted subcutaneously into the hindflank region of female or male nu/nu mice (5-8 weeks old) and allowed to grow to the designated size prior to the administration of compound for each experiment. Tumor size was determined by

measurement with electronic calipers and tumor volume was calculated as the product of its length x width^2 x 0.4.

Antitumor efficacy and relationship to EML4-ALK inhibition

To evaluate inhibition of EML4-ALK by crizotinib, crizotinib (25, 50, 100, or 200 mg/kg/day) or vehicle was administered orally to mice for 13 days and NCI-H3122 xenografts were harvested at 1, 4, 7, and 23 hours following the final administration. Tumor volume was measured and EML4-ALK phosphorylation in tumors was quantitated by ELISA. The effects of crizotinib on EML4-ALK phosphorylation and tumor growth in the H3122 model are shown below. Crizotinib dose-dependently inhibited both tumor growth and EML4-ALK phosphorylation. At the lowest dose tested (25 mg/kg/day) a 38% inhibition of tumor growth corresponded with 27% inhibition of EML4-ALK phosphorylation at 1 hour, 55-66% at 4-7 hours, and 41% at 24 hours. At the 50 mg/kg/day dose level, a 40% inhibition of tumor growth corresponded with 62-74% inhibition of EML4-ALK phosphorylation at 1-7 hours and 59% inhibition at 24 hours. At the 100 mg/kg/day dose level, a 74% inhibition of tumor growth corresponded with 77-85% inhibition of EML4-ALK phosphorylation during the entire dosing interval (24 hours). The highest dose tested (200 mg/kg/day) inhibited tumor growth by 94%, which corresponded with 83-86% inhibition of EML4-ALK phosphorylation during the entire dosing interval (24 hours).

Figure 18: Inhibition of EML4-ALK phosphorylation and tumor growth in the H3122 lung adenocarcinoma model

(excerpted from sponsor's submission)

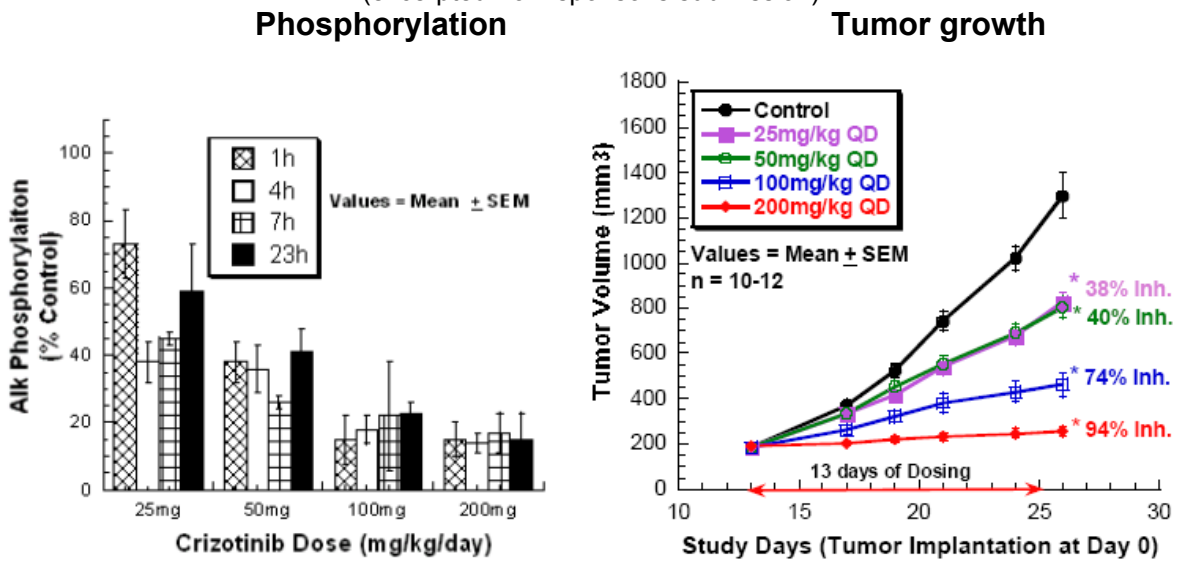

* denotes mean tumor volumes significantly less in treated group compared to control group ($p<0.00001$)

Dose-dependent inhibition of tumor growth by crizotinib in the NCI-HI322 model was demonstrated again in a repeat study in which athymic mice bearing established H3122 tumors (140 mm^3) were administered crizotinib (25, 50, 100, or 200 mg/kg/day) or

vehicle orally for 17 days. Treatment with the highest dose of crizotinib (200 mg/kg/day) for 17 days resulted in complete inhibition of tumor growth.

Figure 19: Inhibition of tumor growth in the H3122 lung adenocarcinoma model

(excerpted from sponsor's submission)

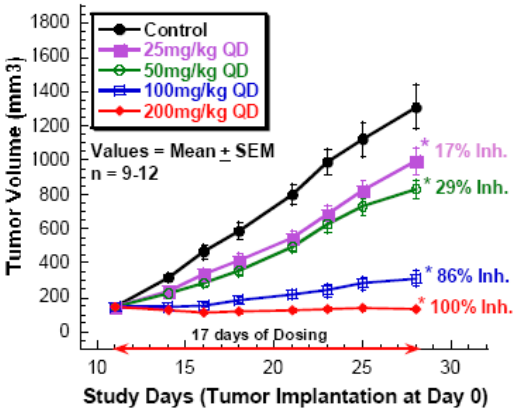

* denotes tumor volumes significantly less in treated group compared to control group ($p<0.001$)

PK/PD relationship for EML4-ALK target inhibition

Two independent dose-response studies were conducted to investigate the relationship of crizotinib plasma concentration to inhibition of EML4-ALK phosphorylation in the NCI-H3122 lung adenocarcinoma model. In one study, mice bearing established H32122 tumors (320 mm^3) were administered crizotinib or vehicle orally for 4 days. The left figure below shows the PK/PD time profile for crizotinib treatment with plasma levels of crizotinib determined by LCMS (red line) and EML4-ALK phosphorylation determined by ELISA (blueline) at 3 doses and at 1, 4, 7, and 24 hours after dosing on Day 4. In the right figure below, the relationship of free plasma concentration of crizotinib to EML4-ALK phosphorylation in tumors (% inhibition) is expressed as a Hill Function plot at 1, 4, 7, and 24 hours after dosing. A similar study was conducted with 14 days of crizotinib treatment, however, results were not shown.

Figure 20: Crizotinib PK/PD profile in Nude mice

(excerpted from sponsor submission)

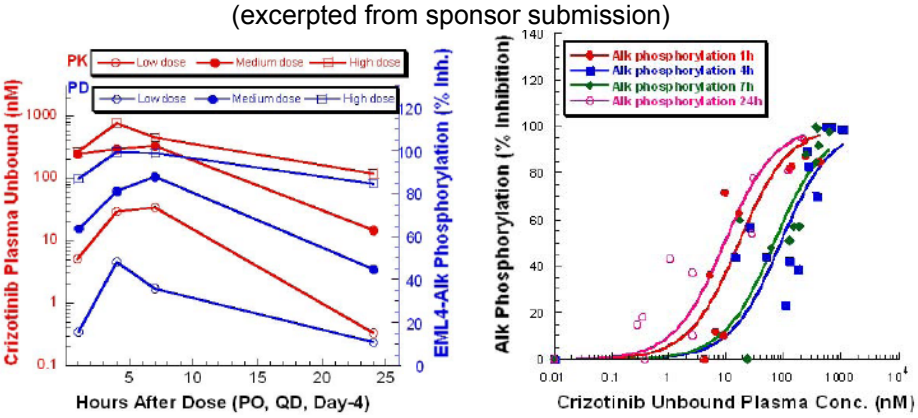

Anti-tumor mechanism of action and biomarker studies *in vivo*

Crizotinib was evaluated for its ability to inhibit EML4-ALK-dependent signaling pathways in order to further understand the anti-tumor mechanism of action and confirm that inhibition of EML4-ALK kinase activity correlates with downstream signal transduction. Crizotinib (0, 50, 100, or 200 mg/kg/day) was administered orally to mice bearing NCI-H3122 tumors for 4 days. Tumors were collected 7 hours following crizotinib administration on Day 4. Tumors were snap-frozen and pulverized, protein lysates were generated from tumor samples and resolved by SDS-PAGE, and proteins of interest were evaluated by immunoblotting. As shown in the immunoblot below, crizotinib dose-dependently inhibited phosphorylated EML4-ALK (activation loop and docking site), STAT3, ERK1/2, AKT, PLCγ, and c-Myc in NIH-H3122 xenografts following 4 days of crizotinib administration. A reduction in total ALK levels was also observed at 100 and 200 mg/kg/day compared to the control group following 4 days of crizotinib treatment.

Figure 21: Dose-dependent inhibition of EML4-ALK-dependent signaling in H3122 tumors following 4-days of daily crizotinib administration

(excerpted from sponsor's submission)

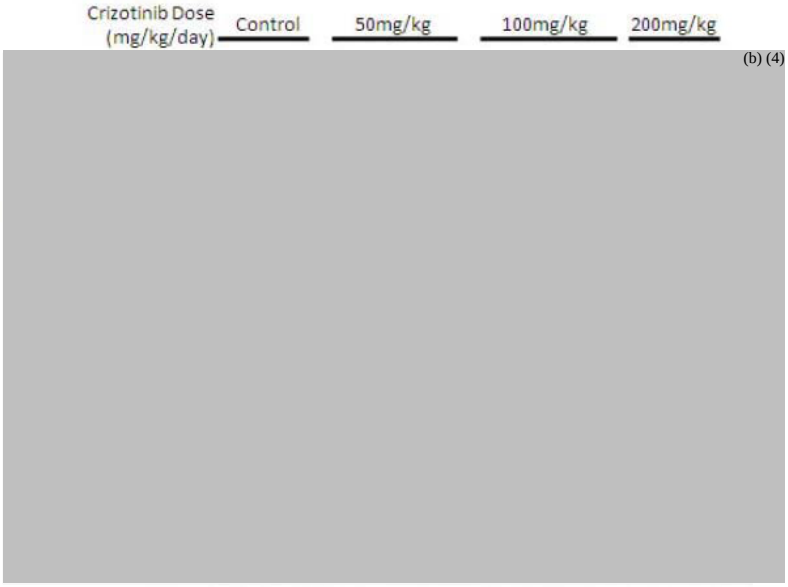

The inhibitory effect on phosphorylated ERK and AKT levels were confirmed by immunohistochemical (IHC) analysis in a separate study in which crizotinib was administered for 14 days in the NCI-H3122 model and showed dose-dependent inhibition of tumor growth (Table 8).

Table 8: Immunohistochemistry analysis for caspase3, Ki67, pERK, and pAKT in NCI-H3122 xenograft tumor samples

(excerpted from sponsor's submission)

Immunohistochemistry Mean Score by Group									
Group	**Treatment**	**Drug Dose (mg/kg)**	Caspase 3	Ki67	pERK				pAKT*
					Tumor		Endothelium		Tumor
					N	C	N**	C	C
1	Vehicle (water)	0	1.0	3.0	1.2	3.4	3.9	3.9	2.5/2.0
2	PF-02341066	25	1.0	3.1	**2.3**	3.8	3.6	3.6	2.5/2.0
3	PF-02341066	50	1.0	3.3	**1.8**	3.8	2.9	2.9	**1.8**/1.7
4	PF-02341066	100	1.0	2.5	**1.6**	**2.3**	3.5	3.5	**1.2/1.6**
5	PF-02341066	200	**1.8**	**2.0**	**2.3**	**1.6**	**2.3**	**2.3**	**0.3/0.4**

Treatment: NCI-H3122 tumors (180mm^3) were orally administered with vehicle or various dose levels of crizotinib once a day for 14 days, and tumor FFPE samples were collected after the last day of treatment.
Bolded scores reflect notable changes from the vehicle control
Caspase 3 Scoring (% of positive cells in tumor staining positive) – 1 = rare; 2 = scattered; 3 = clustered
Ki-67 Scoring (% of viable cells in tumor staining positive) – 1 = 0-50%; 2 = 51-75%; 3 = 76-90%; 4 = >90%
pERK Scoring (% of viable positive cells exhibiting nuclear and/or cytoplasmic staining – tumor or endothelium) – 1 = <10%; 2 = 10-25%; 3 = 26-50%; 4 = >50%
pAKT Scoring (% of viable positive cells) – 1 = <5%; 2 = 5-20%; 3 = 20-50%; 4 = >50%
AND pAKT Mean Staining Intensity – 1 = very faint; 2 = faint; 3 = mild; 4 = moderate

N – nuclear staining
C – cytoplasmic staining

* each mean pAKT score (X/Y) reflects the **frequency of stained cells/mean staining intensity**
** minor dose-related reductions in mean staining intensity also noted (See Appendix 2)

Lappin, Pfizer DSRD study report 10-281a

Crizotinib was also evaluated for its ability to inhibit c-Met/HGFR phosphorylation and cellular EGFR activities in the NCI-H3122 model. In this study, crizotinib (50, 100, or 200 mg/kg/day) or vehicle was administered orally to mice bearing NCI-H3122 tumors for 4 days. Tumors were collected 4-7 hours following crizotinib administration on Day 4, and proteins of interest were evaluated by immunoblotting. Crizotinib inhibited c-Met/HGFR phosphorylation at all dose levels following 4 days of administration. Crizotinib actually dose-dependently increased phospho-EGFR levels and decreased total EGFR levels in the same study (Figure 22).

Figure 22: Effect of crizotinib on cellular kinase activity and expression levels of c-Met/HGFR and EGFR in NCI-H3122 tumors

(excerpted from sponsor's submission)

Immunohistochemistry (IHC) methods were used to detect EML4-ALK phosphorylation in formalin fixed and paraffin embedded NCI-H3122 tumor xenograft samples. Crizotinib (25, 50, 100, or 200 mg/kg/day) or vehicle was orally administered to mice bearing H3122 tumors for 14 days and tumors were collected 7 hours following crizotinib administration at Day 14. Phospho-ALK levels were determined by IHC analysis using an anti-phospho ALK Tyr1278/1282/1283 antibody and total-ALK levels were determined by ICH using an anti-total ALK antibody. Consistent with the immunoblot results, crizotinib demonstrated dose-dependent inhibition of phospho-ALK staining at dose levels ranging from 25-200 mg/kg/day following 14 days of treatment. The reduction in total EML4-ALK levels observed in the immunoblot study was also observed in the IHC analysis in this study.

Figure 23: Effect of crizotinib on EML4-ALK phosphorylation (upper) and total EML4-ALK levels (lower) in NCI-H3122 tumors by IHC analysis

(excerpted from sponsor's submission)

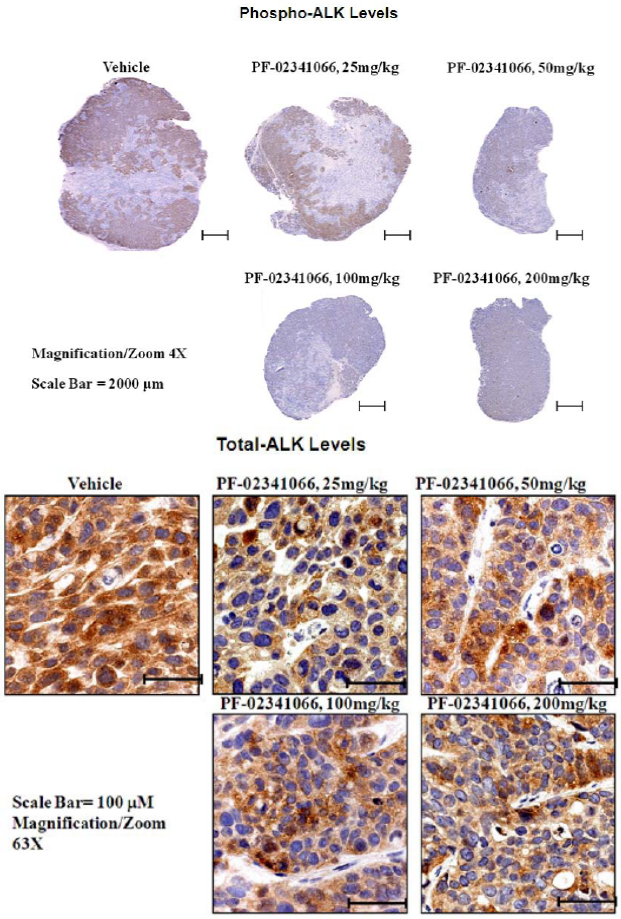

Crizotinib was evaluated for modulation of the Ki67 marker of mitotic index and the caspase-3 marker of apoptosis using IHC methods in tumor sections in the 14-day study mentioned above. Following 14 days of crizotinib administration to mice bearing

NCI-H3122 tumors, a significant reduction in the number of Ki67 positive tumor cells was observed at 200 mg/kg/day. There was a trend of Ki67 reduction at 100 mg/kg/day (Figure 24). The results corresponded with the significant tumor growth inhibition of 74% and 94% observed in the 100 mg/kg/day and 200 mg/kg/day groups, respectively, shown above (Figure 18). Therefore, inhibition of cell mitogenesis appears to be correlated with anti-tumor efficacy.

Figure 24: Inhibition of Ki67 immunostaining (cell proliferation) in the H3122 model

(excerpted from sponsor's submission)

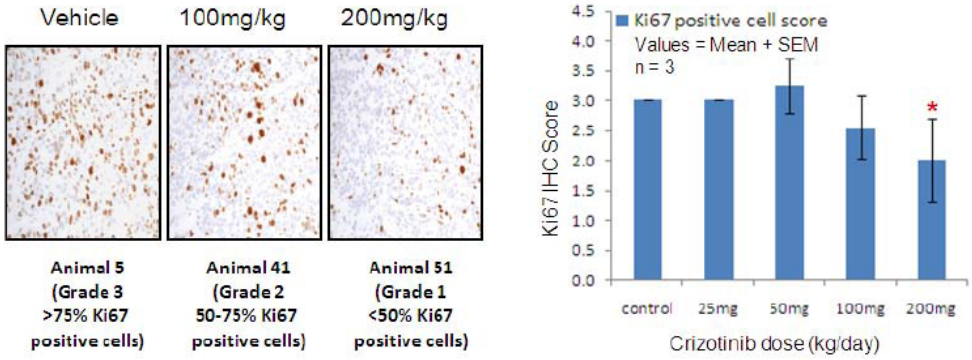

Additionally, a significant dose-dependent induction of activated caspase-3 levels was observed at 50, 100, and 200 mg/kg/day crizotinib in the NCI-H3122 model in mice orally administered crizotinib for 4 days (tumors harvested 7 hours after last dose).

Figure 25: Induction of activated caspase3 levels (cell apoptosis) in the NCI-H3122 model

(excerpted from sponsor's submission)

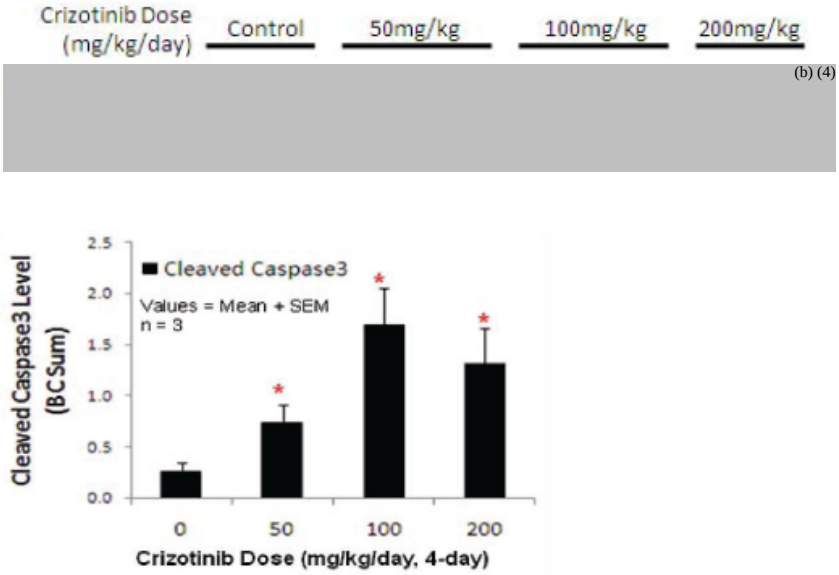

4.2 Secondary Pharmacology

Study title: *In vitro* pharmacology: Pfizer wide ligand profile
Study no.: 901036
Study report location: M4.2.1.3

Key Study Findings

- PF-02341066 showed inhibitory activity for a number of receptors and channels in binding assays including the α_1 (non-selective), H_1 (central), 5-HT_{2B}, and 5-HT_{4e} receptors, and L type Ca^{2+} and Na^+ channels.

The effects of PF-02341066 on various receptors, channels, and transporters, including receptors for neurotransmitters, were investigated using *in vitro* receptor binding and enzyme assays. In each experiment, a respective reference compound was tested concurrently with PF-02341066 in order to assess the assay suitability. The specific ligand binding to the receptors is defined as the difference between the total binding and the nonspecific binding determined in the presence of an excess of unlabelled ligand. The results were expressed as a percent of control specific binding and as a percent inhibition of control specific binding obtained in the presence of PF-02341066. IC_{50} values and Hill coefficients (n_H) were determined by non-linear regression analysis of the competition curves using Hill equation curve fitting. The inhibition constants (K_i) were calculated from the Cheng Prusoff equation ($K_i=IC_{50}/(1+(L/K_D))$, where L= concentration of radioligand in the assay, and K_D= affinity of the radioligand for the receptor).

Results

Binding assays

Of the receptors, channels, and transporters tested in the binding assays, PF-02341066 showed >50% inhibition of control specific binding for those listed in the table below. The IC_{50} and K_i values for both the reference compound tested and PF-02341066 are presented.

Table 9: Effects of PF-02341066 in binding assays

Assay	Reference compound	Reference compound results		PF-02341066 results		
		IC_{50} (M)	K_i (M)	% inhibition of control specific binding	IC_{50} (M)	K_i (M)
α_1 (non-selective)	Prazosin	2.3 E-09	6.0 E-10	74	6.6 E-07	1.7 E-07
α_{2B}	Yohimbine	1.4 E-08	5.3 E-09	51	1.7 E-05	6.5 E-06
ET_A	Endothelin-1	1.5 E-10	1.4 E-10	61	5.0 E-06	4.6 E-06
H_1 (central)	Pyrilamine	1.3 E-09	5.4 E-10	99	3.7 E-09	1.6 E-09
M1	Pirenzepine	9.3 E-09	8.0 E-09	75	2.7 E-06	2.4 E-06
M2	Methoctramine	3.2 E-08	2.2 E-08	84	1.9 E-06	1.3 E-06

Assay	Reference compound	Reference compound results		PF-02341066 results		
		IC_{50} (M)	K_i (M)	% inhibition of control specific binding	IC_{50} (M)	K_i (M)
M3	4-DAMP	1.3 E-09	9.2 E-10	86	2.9 E-06	2.1 E-06
N (neuronal) (α-BGTX-insensitive)	Nicotine	7.7 E-09	4.2 E-09	84	3.6 E-06	2.0 E-06
$5\text{-}HT_{1B}$	Serotonin (5-HT)	1.2 E-08	7.6 E-09	82	4.0 E-06	2.4 E-06
$5\text{-}HT_{2A}$	Ketanserin	4.7 E-09	2.5 E-09	87	4.5 E-06	2.5 E-06
$5\text{-}HT_{2B}$	Serotonin (5-HT)	4.0 E-08	1.4 E-08	92	2.6 E-07	9.0 E-08
$5\text{-}HT_{4e}$	Serotonin (5-HT)	3.6 E-07	1.2 E-07	104	3.2 E-07	1.1 E-07
$5\text{-}HT_{7}$	Serotonin (5-HT)	1.1 E-09	4.6 E-10	76	1.5 E-06	6.3 E-07
Ca^{2+} channel (L, DHP site)	Nitrendipine	8.0 E-10	2.7 E-10	94	3.9 E-07	1.3 E-07
Ca^{2+} channel (L, diltiazem site)	Diltiazem	3.5 E-08	3.2 E-08	106	7.7 E-08	7.1 E-08
Ca^{2+} channel (L, verapamil site)	D 600	1.3 E-08	2.1 E-09	107	1.6 E-07	2.7 E-08
Na^{+} channel (site 2)	Veratridine	4.1 E-06	3.7 E-06	105	2.5 E-07	2.3 E-07
NE transporter	Protriptyline	1.4 E-08	1.1 E-08	82	4.8 E-06	3.7 E-06
DA transporter	BTCP	1.9 E-08	1.1 E-08	92	9.8 E-07	5.9 E-07
Choline transporter	Hemicholinium-3	1.9 E-08	1.3 E-08	56	6.2 E-06	4.2 E-06
5-HT transporter	Imipramine	7.3 E-09	4.3 E-09	65	3.7 E-06	2.2 E-06

Enzyme assays

PF-02341066 showed >50% inhibition of control specific binding for phosphodiesterase 4 and $p55^{fyn}$kinase. The IC_{50} values for both the reference compound tested and PF-02341066 are presented below.

Table 10: Effects of PF-02341066 in enzyme assays

Assay	Reference compound	Reference compound results	PF-02341066 results	
		IC_{50} (M)	% inhibition of control specific binding	IC_{50} (M)
Phosphodiesterase 4	Rolipram	4.8 E-07	53	7.8 E-06
$p55^{fyn}$kinase	Staurosporine	2.1 E-08	83	2.9 E-07

Study title: *In vitro* pharmacology study of PF-02341066-00
Study no.: 8850900-3
Study report location: M4.2.1.3

Key Study Findings

- PF-02341066 showed antagonist activity for the 5-HT_{4e} receptor (IC_{50}= 9.07 E-07 M) and inhibited dopamine (IC_{50}= 6.3E-07 M) and serotonin (IC_{50}= 8.3 E-07 M) uptake all at higher than clinically relevant concentrations.

This study was conducted to investigate the effects of PF-02341066 in various *in vitro* cellular function and uptake assays at concentrations ranging from 3.0 E-09 to 3.0 E-05 M. Cellular function assays were conducted for 5-HT_{4e} and 5-HT_7 receptors using human recombinant CHO cells and uptake assays were conducted for dopamine and 5-HT uptake in rat striatum synaptosomes. In each experiment, the respective reference compound was tested concurrently with PF-02341066. For the cellular function assays, the results are expressed as a percent of control specific agonist response ((measured specific response/control specific agonist response) x 100) obtained in the presence of PF-02341066. The EC_{50} and IC_{50} values were determined by non-linear regression analysis of the concentration-response curves generated with mean replicate values using Hill equation fitting. For antagonists, the apparent dissociation constants (K_B) were calculated using the modified Cheng Prusoff equation (K_B=IC_{50}/(1+(A/EC_{50}A)), where A= concentration of reference agonist in the assay, and EC_{50}A= EC_{50} value of the reference agonist). For the uptake assays, the results are expressed as a percent of control specific activity ((measured specific activity/control specific activity) x 100) obtained in the presence of PF-02341066. The IC_{50} values and Hill coefficients (nH) were determined by non-linear regression analysis of the inhibition curves generated with mean replicate values using Hill equation fitting.

Results

The agonist effect of PF-02341066 for the 5-HT_7 receptor was tested and the concentration-response curve shows no effect at any of the concentrations tested, therefore, an EC_{50} value was not calculable. The EC_{50} for the reference compound serotonin was 1.8 E -08 M. Results for the antagonist effects of PF-02341066 for the 5-HT_{4e} and 5-HT_7 receptors indicate that PF-02341066 has antagonist activity for the 5-HT_{4e} receptor at higher than clinically relevant concentrations. The IC_{50} for dopamine uptake was 6.3E-07 M and the IC_{50} for serotonin uptake was 8.3 E-07 M.

Table 11: Antagonist effects of PF-02341066 on the 5-HT4e and 5-HT7 receptors

Assay	Reference compound	Reference compound results		PF-02341066 results	
		IC_{50} (M)	K_B (M)	IC_{50} (M)	K_B (M)
5-HT_{4e}	GR113808	2.8 E-10	4.1 E-11	9.07 E-07	1.4 E-07
5-HT_7	Musulergine	3.0 E-07	2.3 E-08	2.8 E-05	2.2 E-06

Study title: *In vitro* pharmacology study of PF-02341066-14-0001
Study no.: 8850568
Study report location: M4.2.1.3

Key Study Findings

- PF-02341066 inhibited agonist binding at the 5-HT_{2B} receptor with an IC_{50} of 1.7 E-07 M (170 nM) and Ki of 1.6 E-07 M (160 nM).

This study was conducted to investigate the effects of PF-02341066 on the 5-HT_{2B} receptor in *in vitro* receptor binding assays and the effects of PF-02341066 on the H_1 receptor mediated Ca^{2+} mobilization in cell biology assays. The concentrations of PF-02341066 used in the assays ranged from 1.0 E-10 to 1.0 E-05. In each experiment, the respective reference compound was tested concurrently with PF-02341066 in order to assess the assay suitability. For the binding assays, the results were expressed as a percent of control specific obtained in the presence of PF-02341066. The IC_{50} values and Hill coefficients (n_H) were determined by non-linear regression analysis of the competition curves using Hill equation fitting. The inhibition constants (K_i) were calculated from the Cheng Prusoff equation ($K_i=IC_{50}/(1+(L/K_D))$, where L= concentration of radioligand in the assay, and K_D= affinity of the radioligand for the receptor). For cell-based assays, the results were expressed as a percent of control values obtained in the presence of PF-02341066. The IC_{50} values and Hill coefficients (n_H) were determined by non-linear regression analysis of the inhibiton curves using Hill equation fitting.

Results

The IC_{50} and Ki values of PF-02341066 for the 5-HT_{2B} receptor are in the table below and indicate that PF-02341066 may inhibit activation of the 5-HT_{2B} receptor at concentrations similar to clinically relevant concentrations of <114 nM. PF-02341066 did not have an effect on H1-stimulated Ca^{2+} mobilization in HEK293 cells at any concentration tested and therefore, an IC_{50} value could not be calculated.

Table 12: Effects of PF-02341066 on the 5-HT2B receptor

Assay	Reference compound	Reference compound results		PF-02341066 results	
		IC_{50} (M)	K_i (M)	IC_{50} (M)	K_i (M)
5-HT_{2B}	±DOI	5.1 E-09	4.9E-09	1.7 E-07	1.6 E-07

Study title: Assessment of the activity of PF-02341066 at the human 5-HT_{2A}, 5-HT_{1B}, M1, M2, & M3 muscarinic, and the rat adrenergic α_{1A} receptors
Study no.: SP7610
Study report location: M4.2.1.3

Key Study Findings

- PF-02341066 did not demonstrate any agonist activity at any of the receptors at the concentrations tested in this study and did not demonstrate antagonist activity at the 5-HT_{2A} (tested up to 10 μM), 5-HT_{1B} (tested up to 1 μM), or M1, M2, and M3 muscarinic (tested up to 1 μM) receptor subtypes.
- PF-02341066 was shown to be an antagonist at the rat adrenergic α_{1A} receptor with an EC_{50} value of 159.73 nM and a calculated K_B value of 40.73 nM.

PF-02341066 was found to have activity at the 5-HT_{2A} and 5-HT_{1B} serotonin receptors, the M1, M2, and M3 muscarinic, and the rat adrenergic α_{1A} receptor in a previous study. Due to concerns regarding potential off-target activity, this follow-up study was conducted to determine the pharmacological properties of PF-02341066 at this subset of seven transmembrane receptors. For each receptor subtype, *in vitro* studies were conducted to construct agonist concentration response curves with a known agonist of the receptor alone and PF-02341066 alone; EC_{50} values were calculated. The agonist/antagonist shift for each receptor was studied by constructing concentration response curves with a known agonist alone, the agonist plus one or more concentrations of PF-02341066, and the agonist plus a known antagonist; EC_{50} and K_B values were calculated. The agonists, antagonists, and concentrations of PF-02341066 used in the agonist/antagonist shift assays for each receptor are listed in the table below.

Receptor studied	Agonist	Antagonist	Concentration(s) of PF-02341066 for agonist/antagonist shift
5-HT_{2A} serotonin	5-HT	Butaclamol (3 nM)	10 μM
5-HT_{1B} serotonin	5-HT	SB224289 (10 nM)	1 μM
M1 muscarinic	Oxotremorine M	Atropine (10 nM)	1 μM
M2 muscarinic	Oxotremorine S	Atropine (10 nM)	0.1, 0.3, and 1 μM
M3 muscarinic	Oxotremorine M	Atropine (10 nM)	1 μM
rat adrenergic α_{1A}	Phenylephrine	Prazosin (5 nM)	1 μM

Results

PF-02341066 did not demonstrate agonist activity at any of the receptors at the concentrations tested in this study. Similarly, PF-02341066 did not demonstrate antagonist activity at the 5-HT_{2A} (tested up to 10 μM), 5-HT_{1B} (tested up to 1 μM), or M1, M2, and M3 muscarinic (tested up to 1 μM) receptor subtypes, though at 10 μM there was some mild antagonistic activity at the M2 receptor. PF-02341066 was shown to be an antagonist at the rat adrenergic α_{1A} receptor with an EC_{50} value of 159.73 nM and a calculated K_B value of 40.73 nM. The antagonist shift of the phenylephrine (PE) concentration response curve with 1 μM PF-02341066 or 5 nM prazosin is shown in the figure below (excerpted from sponsor's submission).

Figure 26: α1a Agonist/Antagonist Curve

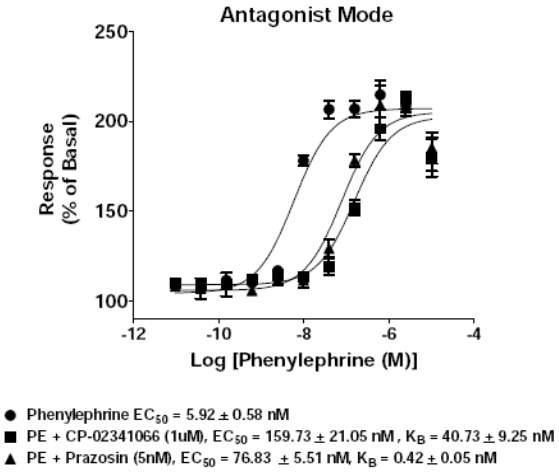

4.3 Safety Pharmacology

Neurological effects:

Study title: Effect of PF-02341066 on Nav1.1 sodium current stably expressed in HEK293 cells

Study no.:	PF02341066NA11
Study report location:	M4.2.1.3
Conducting laboratory and location:	Pfizer Global Research & Development Drug Safety Research & Development Eastern Point Rd. Groton, CT
Date of study initiation:	Not provided, study report approved by senior scientist on September 8, 2010
GLP compliance:	No
QA statement:	No
Drug, lot #, and % purity:	PF-02341066, lot # E010009648

Key Study Findings

- PF-02341066 produced a concentration-dependent inhibition of the Nav1.1 current with an IC_{50} of 0.85 μM and 0.87 μM for the closed state and inactivated state of the Nav1.1 channels, respectively

Methods

Positive control:	Tetrodotoxin (3, 10, and 30 nM)
Vehicle:	DMSO (0.1%)
Cell line:	HEK293 cells transfected with the human Nav1.1 gene
Concentrations of PF-02341066:	0.3, 1, and 3 μM PF-02341066

To assess the potential for seizures, the effects of PF-02341066 (0.3, 1, and 3 μM) on the neuronal Nav1.1 sodium channel were studied in an *in vitro* assay. The whole-cell planar patch clamp technique was used to record Nav1.1 currents in HEK293 cells expressing the Nav1.1 sodium channel. Percent inhibition was determined by taking the ratio of the current at steady state compound block ($I_{Compound}$) versus the control current ($I_{Control}$), and expressed as: % inhibition = 100- ($I_{Compound}/I_{Control}$) x 100.

Results

PF-02341066 significantly inhibited the closed state Nav1.1 current in a concentration-dependent manner at all concentrations tested with an IC_{50} value of 0.85 μM. PF-02341066 also significantly inhibited the inactivated state Nav1.1 current in a concentration-dependent manner at all concentrations tested with an IC_{50} value of 0.87 μM. The mean % inhibition of the closed state and inactivated state Nav1.1 sodium currents for each concentration is listed in the table below and the concentration response curves are shown in the figures below. The positive control, tetrodotoxin, inhibited the Nav1.1 current with IC_{50} values of 4.28 nM and 4.11 nM for the closed state and inactivated state of Nav1.1 channels, respectively.

Table 13: % inhibition of Nav1.1 sodium currents

Concentration (μM) of PF-02341066	Closed state current (Mean ± SEM)	Inactivated state current (Mean ± SEM)
0.3	26.2 ± 3.5	22.6 ± 4.7
1	53.2 ± 3.0	53.2 ± 4.2
3	80.6 ± 3.9	82.3 ± 3.9

Figure 27: Concentration-response curve for the closed state

(excerpted from sponsor's submission)

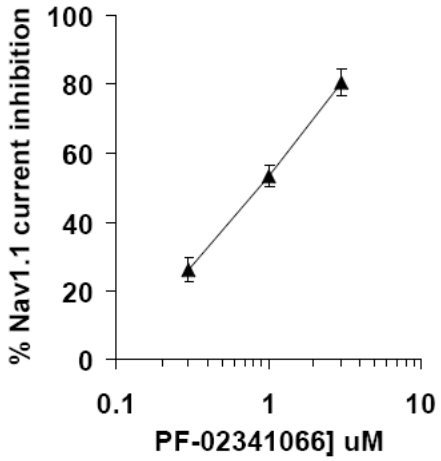

Figure 28: Concentration-response curve for the inactivated state

(excerpted from sponsor's submission)

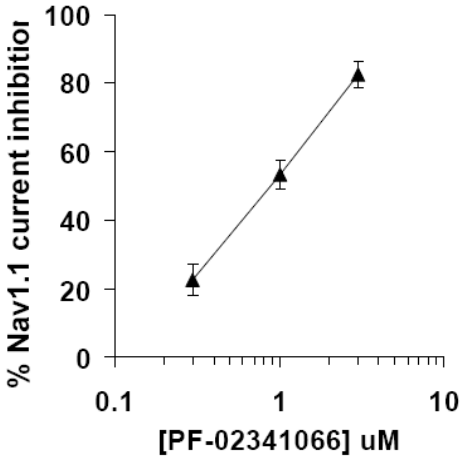

Study title: Neurofunctional evaluation of PF-2341066 in Sprague-Dawley rats

Study no.:	3660
Study report location:	M4.2.1.3
Conducting laboratory and location:	Pfizer Global Research & Development Safety Sciences 2800 Plymouth Rd. Ann Arbor, MI
Date of study initiation:	June 16, 2005
GLP compliance:	Yes
QA statement:	Yes
Drug, lot #, and % purity:	PF-02341066, lot # AK-100830-53-5, Purity: 99.91%

Key Study Findings

- Treatment with a single dose of PF-02341066 reduced locomotor activity at 75 and 500 mg/kg, and produced salivation and dyspnea at 500 mg/kg.

Methods

Doses:	0, 10, 75, or 500 mg/kg
Frequency of dosing:	Single dose
Route of administration:	Oral gavage
Dose volume:	10 mL/kg
Formulation/Vehicle:	0.5% methylcellulose
Species/Strain:	Sprague-Dawley rat
Number/Sex/Group:	8 males/group, 12 groups total
Age:	48-55 days at dose initiation
Weight:	184-207 g

Male Sprague-Dawley rats (n=8) were administered a single oral dose of vehicle or PF-02341066 (10, 75, or 500 mg/kg), with three separate groups of rats administered each dose. Separate groups at each dose were used for observational assessment, neuromuscular testing, and reflex/activity monitoring. Although the low dose group is presented as 10 mg/kg, analysis of dosing suspensions indicated the actual dose was 8 mg/kg. For observational assessment, rats were observed for clinical signs of toxicity cage-side immediately (~10 minutes) after dosing and every 15 minutes for a 60-minute period starting 3 hours after dosing. At the anticipated t_{max} of 4 hours after dosing, rats were evaluated in an open-field environment for appearance, exploratory behavior, gait, and general activity for approximately 5 minutes. Neuromuscular and reflex parameters were assessed at 4 hours after dosing. During neuromuscular testing, rats were assessed for air-righting reflex, visual placing, acoustic startle, forelimb grip strength, hindlimb foot splay, thermal response, and catalepsy. During reflex testing, corneal and papillary reflexes were evaluated following a 10-minute dark adaptation, and body temperature was measured. Total distance and number of vertical movements in an automated activity monitor were recorded for 30 minutes following reflex testing. Subsequent to the neurofunctional evaluation, 12 vehicle-control rats were dosed at 10, 75, or 500 mg/kg PF-02341066 (4 rats/dose) for determination of plasma concentrations and calculation of toxicokinetic parameters. Blood samples were collected at approximately 1, 4, 7, and 24 hours after dosing.

Results

Observational assessment

During the 60-minute period starting 3 hours after dosing, clinical signs were observed at 500 mg/kg PF-02341066. During the cage-side and open-field observations, 2 of 8 rats at the 500 mg/kg dose level (Animals # 7980 and 7985) had salivation and dyspnea and another HD rat (Animal # 7981) had red muzzle staining. Salivation was also observed 10 minutes after dosing in Animal # 7985. Hypoactivity was observed in this same rat along with the salivation and dyspnea during the open-field assessment.

Neuromuscular testing

Unremarkable

Reflex testing/activity monitoring

There were no effects of PF-02341066 on reflex parameters. Statistically significant decreases in body temperature were observed at 75 and 500 mg/kg, however, the decreases were slight compared to controls, 0.73° C and 1.13° C, respectively. Since the decreases were less than 2 ° C, PF-02341066 does not appear to produce hypothermia. PF-02341066 reduced locomotor activity at both 75 and 500 mg/kg, with a statistically significant reduction in both total distance and the number of vertical movements at 500 mg/kg compared to controls. The means for the total activity during

the 30-minute session are presented in the table below and the time-course for the data is shown in the figures below.

Table 14: Mean total activity during the 30-minute session

Dose (mg/kg)	Total distance (cm)	No. of vertical movements
0	2550.5	536.5
10	2201.3	470.1
75	1704.5	377.8
500	1316.9*	189.8*

* p <0.0354

Figure 29: Effects of PF-02341066 on total distance traveled

(excerpted from sponsor's submission)

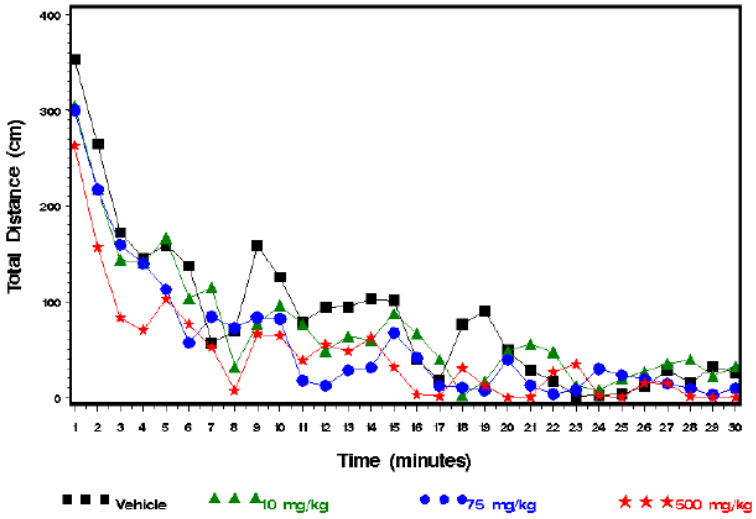

Figure 30: Effects of PF-02341066 on number of vertical movements

(excerpted from sponsor's submission)

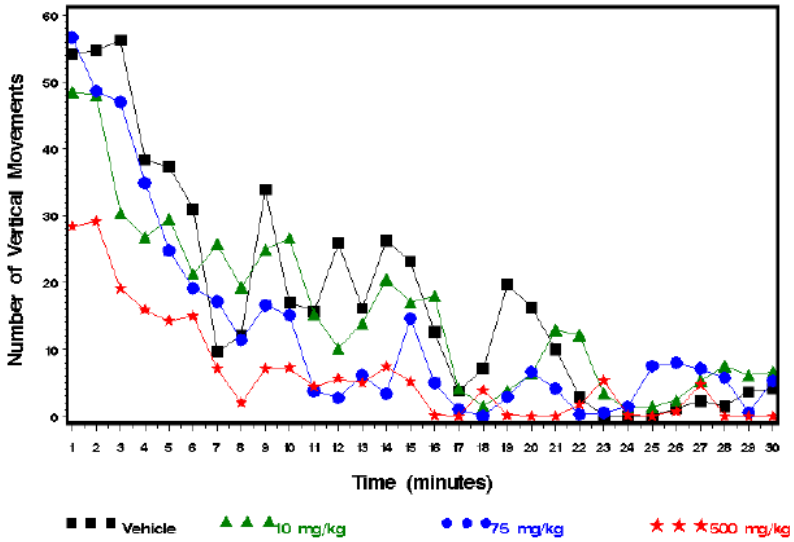

Toxicokinetics

The plama toxicokinetic parameters for PF-02341066 are presented in the table below (excerpted from sponsor's submission). The C_{max} values observed at the mid (2.57 µM) and high dose (5 µM), were higher than the C_{max} (1.061 µM; 478 ng/mL) observed in humans at the recommended clinical dose.

Dose (mg/kg)	Cmax (µg/mL)	tmax (hr)	AUC(0-24) (µg·hr/mL)
10	0.109±0.0586	4.00±0.00	0.984±0.611
75	1.16±0.156	4.75±1.50	17.9±2.55
500	2.26±0.361	19.8±8.50	45.0±7.20

[a] Data presented as mean values ± SD; n = 4.

<u>Cardiovascular effects</u>:

Study title: Assessment of the potential effect of PF-02341066 on hERG potassium current stably expressed in HEK293 cells

Study no.: PF02341066HERG
Study report location: M4.2.1.3
Conducting laboratory and location: Safety Pharmacology, Safety Sciences
La Jolla
Pfizer Global Research & Development
Agouron Pharmaceuticals, Inc.,
"d/b/a PGRD-La Jolla, a wholly owned subsidiary of Pfizer Inc"
10646 Science Center Drive

	San Diego, CA 92121
Date of study initiation:	Not provided, study report approved by director on June 28, 2004
GLP compliance:	No
QA statement:	No
Drug, lot #, and % purity:	PF-02341066, lot # PF-02341066-14-0001

Key Study Findings

- PF-02341066 inhibited the hERG channel at all concentrations tested (0.1, 0.3, 1, 3, and 10 μM) with an IC_{50} of 1.1 μM.

Methods

Positive control:	Dofetilide (UK-068798; 25 nM)
Vehicle:	DMSO (0.1%)
Cell line:	HEK293 cells transfected with hERG gene
Concentrations of PF-02341066:	0.1, 0.3, 1, 3, and 10 μM PF-02341066

To assess the potential for delayed repolarization and prolongation of the QT interval, the effects of PF-02341066 (0.1, 0.3, 1, 3, and 10 μM) on the human ether-a-go-go related gene (HERG) potassium channel were studied in an *in vitro* hERG assay. The whole-cell patch clamp technique was used to record hERG currents in HEK293 cells expressing the hERG potassium channel. The percent inhibition after 5 minutes of drug exposure was calculated based on the ratio of the current in the presence of drug relative to the extrapolated control amplitude using the following formula: % inhibition= $100 – (I_{drug}/I_{control}) \times 100$.

Results

PF-02341066 produced a concentration-dependent inhibition of the hERG current, with statistically significant inhibition at all concentrations. The IC_{20} for hERG current inhibition was 0.30 μM and the IC_{50} for hERG current inhibition was 1.1 μM. The mean % inhibition of the hERG current for each concentration is listed in the table below and the concentration response curve is shown in the figure below. The results of this assay suggest that crizotinib has some potential to cause QTc prolongation, but low potential at clinically relevant exposures..

Table 15: % inhibition of hERG potassium currents

Concentration (μM) of PF-02341066	Mean ± SEM
0.1	9.8 ± 2.7
0.3	18.8 ± 4.6
1	48.2 ± 5.1
3	73.4 ± 5.9
10	95.5 ± 1.0

Figure 31: Concentration-response curve (mean + SEM)

(excerpted from sponsor's submission)

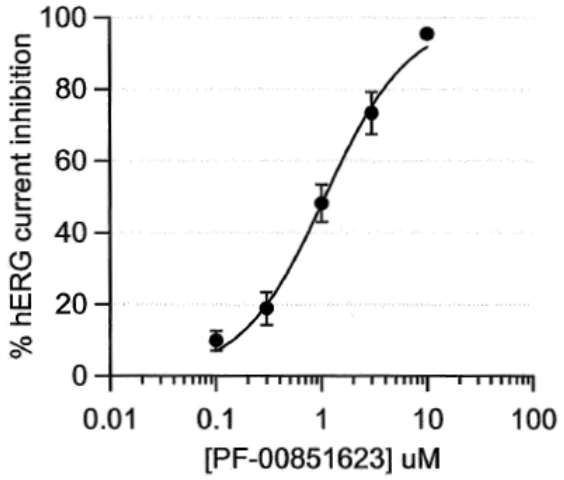

Study title: Assessment of PF-02341066 Ca^{2+} channel antagonism in the rat aorta isometric tension model

Study no.:	PF02341066AORTA Amendment
Study report location:	M4.2.1.3
Conducting laboratory and location:	Safety Pharmacology, Safety Sciences La Jolla Pfizer Global Research & Development 10646 Science Center Drive San Diego, CA 92121
Date of study initiation:	Not provided, study report approved by director on April 27, 2005
GLP compliance:	No
QA statement:	No
Drug, lot #, and % purity:	PF-02341066, lot # PF-02341066-01-0004, Purity: 98.84%

Key Study Findings

- PF-02341066 produced a concentration-dependent relaxation of a 45 mM KCl-induced contraction with an IC_{50} of 0.83 µM, indicating that PF-02341066 is a calcium channel antagonist.

Methods

Controls:	Phenylephrine (100 nM; contractile response) carbachol (10 µM; relaxation response)
Vehicle:	DMSO (0.1%)
Tissue:	Descending thoracic aorta of male Sprague Dawley rats
Concentrations of PF-02341066:	0.1, 1, and 10 µM PF-02341066

To evaluate the potential for blood pressure changes, the effects of PF-02341066 on vascular Ca^{2+} channel were studied in the rat aorta isometric tension model. For assessment of aortic ring viability, 100 nM phenylephrine was applied to each tissue preparation for approximately 10-15 minutes to elicit a contractile response. Once the maximum response was induced by 100 nM phenylephrine, tissues were exposed to 10 µM carbachol to assess whether the endothelium was intact and functional. For the assessment of calcium channel antagonism, aortic rings were exposed to 45 mM KCl to elicit a contractile response and each tissue was then exposed to PF-02341066 or vehicle (2 tissues per treatment) by direct addition to the static tissue baths. Percent reduction on contraction by addition of carbachol or PF-02341066 was calculated by normalizing the magnitude of tension reduction to the amount initially induced by the constricting agents (phenylephrine or KCl).

Results

PF-02341066 produced a concentration-dependent relaxation of a 45 mM KCl-induced contraction with an IC_{50} of 0.83 µM, indicating that PF-02341066 is a calcium channel antagonist. The mean % reduction in KCl-induced contraction for each concentration is listed in the table below and the concentration response curve is shown in the figure below.

Table 16: % reduction in KCl-induced contraction

Treatment	Mean ± SEM
Control (0.1%) DMSO	3.0 ± 1.5
0.1 µM PF-02341066	7.7 ± 2.9
1 µM PF-02341066	56.0 ± 4.2
10 µM PF-02341066	94.2 ± 2.2

Figure 32: Concentration-response curve (mean + SEM)

(excerpted from sponsor's submission)

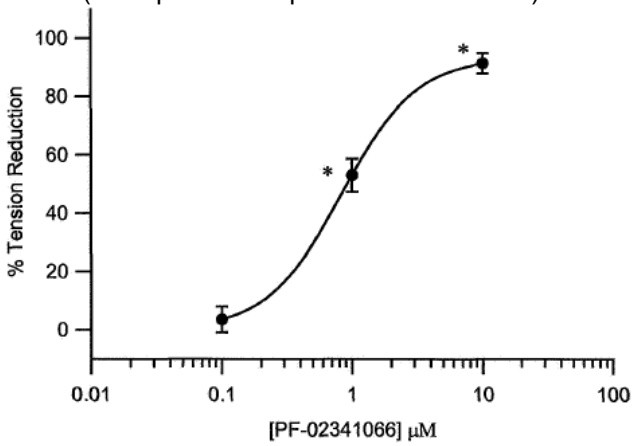

* p<0.05

Study title: Effect of PF-02341066 on calcium current in freshly isolated guinea pig ventricular myocytes

Study no.:	04-2796-01
Study report location:	M4.2.1.3
Conducting laboratory and location:	Safety Pharmacology, Safety Sciences Pfizer Global Research & Development Groton, Connecticut 06340
Date of study initiation:	November 30, 2004
GLP compliance:	No
QA statement:	No
Drug, lot #, and % purity:	PF-02341066, lot # PF-02341066-01-0004, Purity: 98.84%

Key Study Findings

- PF-02341066 inhibited the L-type calcium channel current in a concentration-dependent manner with an IC_{50} of 14.6 µM.

Methods

Positive control:	Nifedipine (10 µM)
Vehicle:	DMSO
Tissue:	Guinea pig ventricular myocytes
Concentrations of PF-02341066:	1, 3, 10, 30, and 100 µM PF-02341066

The effects of PF-02341066 (1, 3, 10, 30, and 100 µM) on the cardiac L-type calcium channel current ($I_{Ca,L}$) were investigated using the whole-cell patch clamp technique to record $I_{Ca,L}$ in freshly isolated guinea pig ventricular myocytes. The calcium channel current was activated by a voltage step to 0 mV for 300 ms after a 10-ms interval at -80 mV that was preceded by a 3-ms prepulse to +30 mV from a holding potential of -80 mV

with a stimulation frequency of 0.25 Hz. In the presence of the test compound, a steady-state response was achieved before a subsequent concentration was applied. At the end of each experiment, 10 µM nifedipine, a selective $I_{Ca,L}$ blocker, was applied to block the $I_{Ca,L}$. The remaining nifepipine-insensitive current was subtracted from the experimental data to eliminate leakage current. Percent block of the compound was computed from the predicted current after linear extrapolation as a control ($I_{Control}$) and the corresponding steady-state current in the presence of the compound (I_{Drug}).

Results

PF-02341066 inhibited the $I_{Ca,L}$ in a concentration-dependent manner with an IC_{50} of 14.6 µM. The mean % inhibition of the L-type calcium current for each concentration is listed in the table below and the concentration response curve is shown in the figure below.

Table 17: % inhibition of L-type calcium current

Concentration (µM) of PF-02341066	Mean ± SEM
1	9.3 ± 0.5
3	17.3 ± 2.7
10	36.0 ± 1.9
30	67.7 ± 7.8
100	95.6 ± 3.6

Figure 33: Effect of PF-02341066 on ICa,L

(excerpted from sponsor's submission)

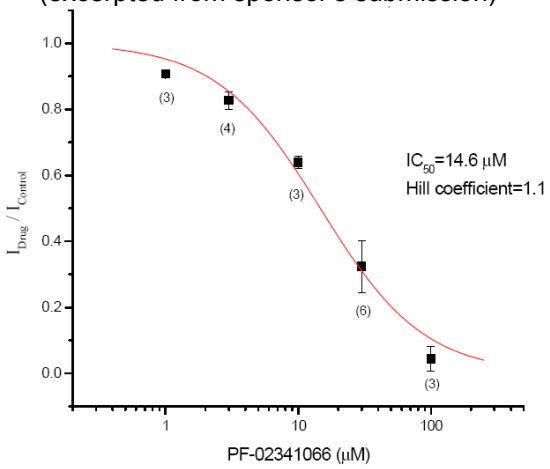

Study title: Effects of PF-2,341,066-01 on cardiac action potentials recorded from dog isolated Purkinje fibres *in vitro*

Study no.:	IC00104
Study report location:	M4.2.1.3
Conducting laboratory and location:	(b) (4) [redacted] Pfizer Global Research & Development Sandwich Laboratories Ramsgate Road Kent CT13 9NJ United Kingdom
Date of study initiation:	August 25, 2004
GLP compliance:	Yes
QA statement:	Yes
Drug, lot #, and % purity:	PF-02341066, lot # PF-02341066-01-0001

Key Study Findings

- At the highest concentration tested (10 µM), PF-02341066 produced effects on the cardiac action potential including reductions in the APD_{50} at all stimulation frequencies and APD_{90} at 1 and 3 Hz.

Methods

Positive control:	Dofetilide (10 nM)
Vehicle:	DMSO (1%)
Tissue:	Beagle dog Purkinje fibres
Concentrations of PF-02341066:	0.01, 0.1, 1, and 10 µM PF-02341066

The effects of PF-02341066 (0.01, 0.1, 1, and 10 µM) on cardiac action potentials evoked at stimulation frequencies of 0.3, 1, and 3 Hz in dog isolated Purkinje fibres were studied *in vitro*. Following an equilibration period, intracellular recordings were made from the Purkinje fibres. Each experiment consisted of an initial 5 minute segment with superfusion of physiological salt solution (PSS) only followed by five 34 minute segments: 1) control solution (vehicle; 1% DMSO), 2) 0.01 µM PF-02341066 or vehicle, 3) 0.1 µM PF-02341066 or vehicle, 4) 1 µM PF-02341066 or vehicle, 5) 10 µM PF-02341066 or vehicle. Then, vehicle-treated preparations were exposed to the positive control dofetilide (10 nM) for 34 minutes and the PF-02341066-treated preparations were exposed to vehicle for 34 minutes. During each of the 34 minute periods, preparations were stimulated at 1 Hz for the first 25 minutes, then 3 Hz for 3 minutes, 1 Hz for 3 minutes, and 0.3 Hz for 3 minutes. The parameters determined were resting membrane potential, action potential amplitude, maximum rate of depolarization (Vmax) and the action potential duration at 50% and 90% repolarization (APD_{50} and APD_{90} respectively). The data were expressed as the percentage change from the 36 minute time point (i.e. after 5 minutes exposure in PSS only and 31 minutes

in vehicle) for all data collected at a stimulation frequency of 1 Hz. Data collected at 3 Hz were expressed as the percentage change from the 33 minute time point (i.e. after 5 minutes in PSS and 28 minutes in vehicle) and the data collected at 0.3 Hz were expressed as the percentage change from the 39 minute time point (i.e. after 5 minutes in PSS and 34 minutes in vehicle).

Results

At all stimulation frequencies, PF-02341066 had no statistically significant effect on action potential amplitude or Vmax at any concentration tested compared to the vehicle control. PF-02341066 had no effects on cardiac action potential at concentrations up to 1 µM, however, the highest concentration of PF-02341066 tested (10 µM) did produce effects on the cardiac action potential. At 10 µM, PF-02341066 significantly reduced the resting membrane potential at a stimulation frequency of 3 Hz (-2.2 at 10 µM compared to 3.2 for vehicle). Significant reductions in APD_{50} were observed at all stimulation frequencies at 10 µM PF-02341066, with the largest reduction at 3 Hz (-18.4). Additionally, significant reductions in APD_{90} were observed at 1 and 3 Hz at 10 µM PF-02341066, with the largest reduction at 3 Hz (-8.1). The values for APD_{50} and APD_{90} are presented in the tables below.

Table 18: Effects on the APD_{50} of the cardiac action potential

(excerpted from sponsor's submission)

3Hz			
Vehicle		PF-2,341,066	
	Mean ± SEM (n)	Conc (µM)	Mean ± SEM (n)
V1	1.1 ± 0.6 (5)	0.01	0.5 ± 0.5 (5)
V2	0.9 ± 0.7 (5)	0.1	0.2 ± 1.0 (5)
V3	0.8 ± 0.6 (5)	1	-1.6 ± 1.1 (5)
V4	0.8 ± 1.0 (5)	10	-18.4 ± 2.9 (5)***
1Hz			
Vehicle		PF-2,341,066	
	Mean ± SEM (n)	Conc (µM)	Mean ± SEM (n)
V1	1.7 ± 0.5 (5)	0.01	1.5 ± 1.0 (5)
V2	1.2 ± 0.7 (5)	0.1	1.2 ± 1.7 (5)
V3	0.7 ± 0.9 (5)	1	0.7 ± 1.1 (5)
V4	0.9 ± 1.2 (5)	10	-13.4 ± 1.9 (5)***
0.3Hz			
Vehicle		PF-2,341,066	
	Mean ± SEM (n)	Conc (µM)	Mean ± SEM (n)
V1	2.1 ± 1.4 (5)	0.01	0.3 ± 0.6 (5)
V2	0.9 ± 1.6 (5)	0.1	6.9 ± 5.8 (5)
V3	1.5 ± 2.2 (5)	1	6.8 ± 7.0 (5)
V4	2.7 ± 2.1 (5)	10	-6.3 ± 1.9 (5)*

V1, V2, V3 and V4 = time-matched vehicle controls; n = number of tissues; values obtained from action potentials evoked in dog isolated Purkinje fibres *in vitro*. *** P<0.001, * P<0.05, compared to time-matched vehicle control data (Student's unpaired t-test).

Table 19: Effects on the APD_{90} of the cardiac action potential

(excerpted from sponsor's submission)

3Hz			
Vehicle		PF-2,341,066	
	Mean ± SEM (n)	Conc (μM)	Mean ± SEM (n)
V1	0.7 ± 0.5 (5)	0.01	1.0 ± 0.6 (5)
V2	0.4 ± 0.4 (5)	0.1	1.0 ± 1.0 (5)
V3	0.4 ± 0.4 (5)	1	-0.3 ± 1.1 (5)
V4	0.7 ± 0.4 (5)	10	-8.1 ± 1.7 (5)**
1Hz			
Vehicle		PF-2,341,066	
	Mean ± SEM (n)	Conc (μM)	Mean ± SEM (n)
V1	1.2 ± 0.4 (5)	0.01	2.0 ± 1.1 (5)
V2	0.9 ± 0.3 (5)	0.1	1.6 ± 1.7 (5)
V3	0.5 ± 0.4 (5)	1	1.5 ± 1.2 (5)
V4	1.2 ± 0.4 (5)	10	-6.3 ± 2.2 (5)*
0.3Hz			
Vehicle		PF-2,341,066	
	Mean ± SEM (n)	Conc (μM)	Mean ± SEM (n)
V1	1.8 ± 0.8 (5)	0.01	1.1 ± 0.5 (5)
V2	0.7 ± 0.8 (5)	0.1	7.2 ± 6.0 (5)
V3	1.1 ± 1.4 (5)	1	8.0 ± 6.5 (5)
V4	2.9 ± 1.2 (5)	10	4.0 ± 5.7 (5)

V1, V2, V3 and V4 = time-matched vehicle controls; n = number of tissues; values obtained from action potentials evoked in dog isolated Purkinje fibres *in vitro*; ** P<0.01, * P<0.05, compared to time-matched vehicle control data (Student's unpaired t-test).

Study title: Effect of PF-02341066 on Nav1.5 sodium current stably expressed in CHO cells

Study no.:	PF02341066NA15 and PF02341066NA15 Amendment 1
Study report location:	M4.2.1.3
Conducting laboratory and location:	Pfizer Global Research & Development Drug Safety Research & Development Eastern Point Rd. Groton, CT
Date of study initiation:	Not provided, study report approved by senior scientist on September 9, 2010 Amendment signed September 24, 2010
GLP compliance:	No
QA statement:	No
Drug, lot #, and % purity:	PF-02341066, lot # E010009648

Key Study Findings

- PF-02341066 inhibited the Nav1.5 current in a concentration-dependent manner with an IC_{50} value of 1.56 μM

Methods

Positive control:	Propafenone (0.3, 1, and 3 μM)
Vehicle:	DMSO (0.1%)
Cell line:	CHO cells transfected with the human Nav1.5 gene
Concentrations of PF-02341066:	0.3, 1, 3, and 10 μM PF-02341066

To assess the potential for prolongation of the QRS or PR intervals, the effects of PF-02341066 (0.3, 1, 3, and 10 μM) on the Nav1.5 sodium channel were studied in an *in vitro* assay. The whole-cell planar patch clamp technique was used to record Nav1.5 currents in CHO cells expressing the Nav1.5 sodium channel. Percent inhibition was determined by taking the ratio of the current at steady state compound block ($I_{Compound}$) versus the control current ($I_{Control}$), and expressed as: % inhibition = 100-($I_{Compound}/I_{Control}$) x 100.

Results

PF-02341066 inhibited the Nav1.5 current in a concentration-dependent manner with an IC_{50} value of 1.56 μM. The mean % inhibition of the Nav1.5 sodium current for each concentration is listed in the table below and the concentration response curve is shown in the figure below. The positive control, propafenone, inhibited the Nav1.5 current with an IC_{50} value of 1.8 μM.

Table 20: % inhibition of Nav1.5 sodium currents

Concentration (μM) of PF-02341066	Mean ± SEM
0.3	16.4 ± 5.7
1	35.0 ± 4.3
3	68.7 ± 2.2
10	95.7

Figure 34: Concentration-response curve (mean + SEM)

(excerpted from sponsor's submission)

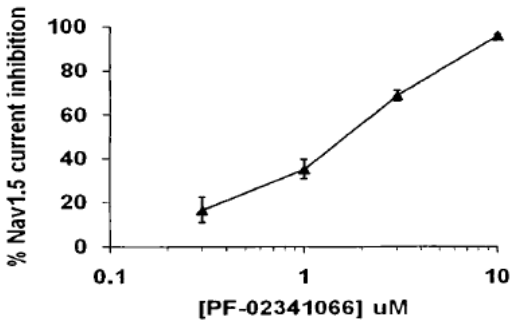

Study title: To determine the effects of intravenously administered PF-02341066 on haemodynamic and electrophysiological parameters in the isoflurane anaethetised dog

Study no.:	PF02341066/CG/003/04
Study report location:	M4.2.1.3
Conducting laboratory and location:	(b) (4) [redacted]. Pfizer Global Research & Development Ramsgate Rd. Sandwich, Kent CT13 9NJ United Kingdom
Date of study initiation:	November 19, 2004
GLP compliance:	Yes
QA statement:	Yes
Drug, lot #, and % purity:	PF-02341066, batch # PF-02341066-01-0005

Key Study Findings

- Hemodynamic parameters: There were significant decreases in heart rate and increases in left ventricular end diastolic pressure (LVEDP) at the two highest doses of PF-02341066 compared to vehicle treatment. Additionally, there were significant differences in myocardial contractility (LV+dP/dt) at the highest dose.
- ECG parameters: There were significant increases in PR-interval, QRS-interval, and QT-interval at the two highest doses of PF-02341066.

Methods

Doses:	Loading infusions: 0, 0.134, 0.295, 1.192, and 1.907 mg/kg over 10 minutes Maintenance infusions: 0.00939, 0.0207, 0.0834, 0.134 mg/kg/min for ~25 minutes
Route of administration:	Intravenous
Dose volume:	Loading infusions: 0.0536 mL/minute/kg Maintenance infusions: 0.0375 mL/minute/kg
Formulation/Vehicle:	0.9% w/v saline
Species/Strain:	Beagle dog
Number/Sex/Group:	4 males/group (2 groups, PF-02341066-treated and vehicle-treated)
Weight:	11.6-14.7 kg

Male beagle dogs (n=4/group) were anesthetized with isoflurane and were administered PF-02341066 or vehicle intravenously into the left femoral vein. Each dose of PF-02341066 was administered as an intravenous infusion lasting approximately 35

minutes (10 minute loading infusion and approximately 25 minute maintenance infusion). The same infusion rates and times were used in the vehicle experiments. Arterial blood pressure, left ventricular pressure, monophasic action potentials, and lead II ECG were recorded continuously throughout the experiment. From these signals the following parameters were derived: systolic, diastolic, and mean blood pressure, systolic and end diastolic left ventricular pressure (LVP), LV+dP/dt (an index of myocardial contractility), heart rate, monophasic action potential (MAP) duration (MAPD) to 90 and 100% of repolarization and ECG PR, QT, and QRS intervals, and T wave amplitudes. The effects of PF-02341066 and vehicle treatment were monitored during sinus rhythem and also at paced frequencies of 150, 160, 170, 180, 190, and 200 beats/minute (bpm). Approximately 2 mL of arterial blood was collected pre-dose, at the end of each loading infusion, 10 minutes after the start of each maintenance infusion, and approximately 5 minutes before the end of each maintenance infusion.

Results

The main hemodynamic effects of PF-02341066 treatment were significant decreases in heart rate and increases in left ventricular end diastolic pressure (LVEDP) at the 3rd and 4th dose levels compared to vehicle treatment. Additionally, there were significant differences in myocardial contractility (LV+dP/dt) at the 4th dose level. These findings are shown in the figures below.

Figure 35: Average change in heart rate

(excerpted from sponsor's submission)

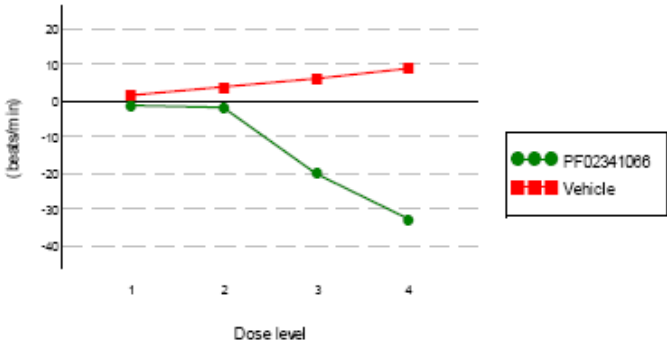

Figure 36: Average change in left ventricular end diastolic pressure (LVEDP)

(excerpted from sponsor's submission)

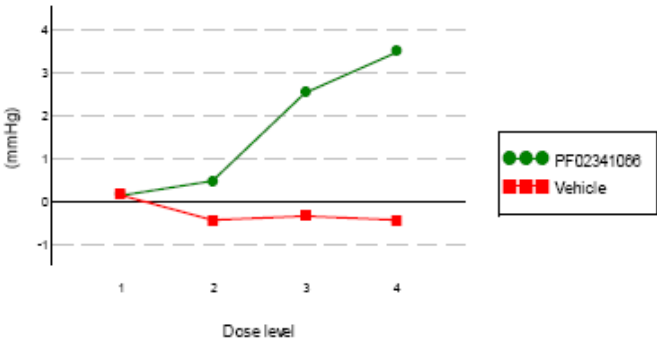

Figure 37: Average change in left ventricular LV+dP/dt

(excerpted from sponsor's submission)

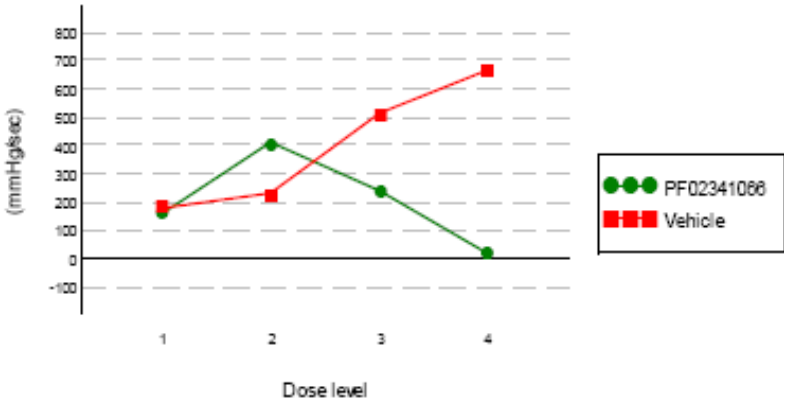

The main effects on ECG parameters were significant increases in PR-interval, QRS, and QT-interval at the 3rd and 4th dose levels; these increases correlate with the decreases in heart rate.

Figure 38: Average change in PR interval

(excerpted from sponsor's submission)

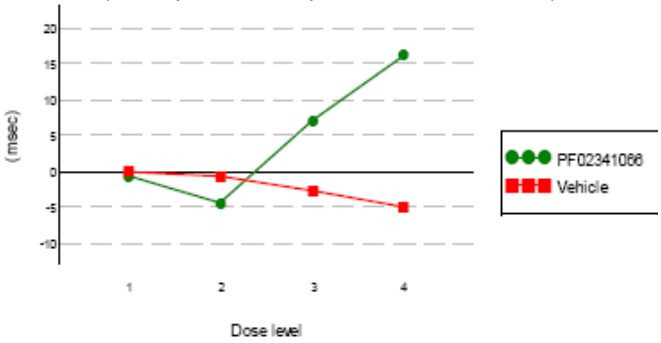

Figure 39: Average change in QT interval

(excerpted from sponsor's submission)

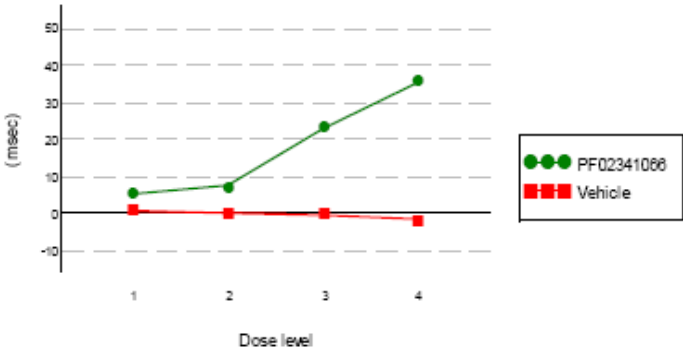

Figure 40: Average change in QRS interval

(excerpted from sponsor's submission)

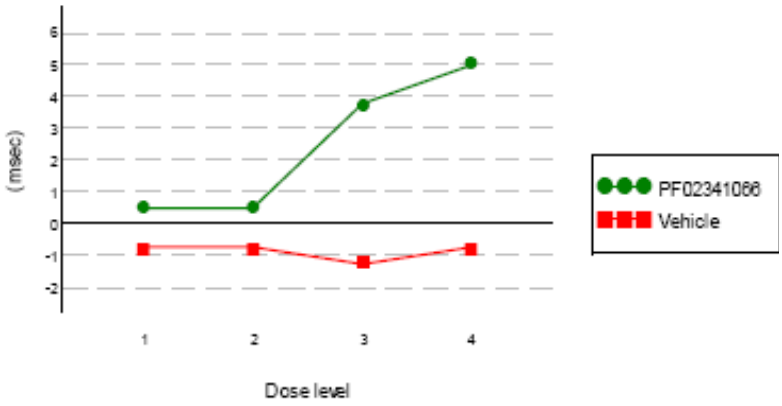

The mean plasma concentrations observed at the end of the loading infusion and following the maintenance infusion are listed in the table below. The plasma concentrations for the two highest doses, which produced cardiovascular effects, ranged from 4.353 µM to 8.477 µM and were higher than the than the C_{max} (1.061 µM; 478 ng/mL) observed in humans at the recommended clinical dose.

Table 21: Plasma samples

Dose (loading infusion /maintenance infusion)	Mean total plasma concentrations (ng/mL)	
	End of loading infusion	Following maintenance infusion
0.134 mg/kg / 0.00939 mg/kg/minute	218 ng/mL (484 nM)	196 ng/mL (435 nM)
0.295 mg/kg / 0.0207 mg/kg/minute	521 ng/mL (1156 nM)	557 ng/mL (1236 nM)
1.192 mg/kg / 0.0834 mg/kg/minute	2210 ng/mL (4913 nM)	1963 ng/mL (4353 nM)
1.907 mg/kg / 0.134 mg/kg/minute	3363 ng/mL (7467 nM)	3817 ng/mL (8477 nM)

Pulmonary effects:

Study title: Effect of PF-2341066 on pulmonary function in Sprague-Dawley rats

Study no.: 3622
Study report location: M4.2.1.3
Conducting laboratory and location: Pfizer Global Research & Development
Safety Sciences
2800 Plymouth Rd.
Ann Arbor, MI
Date of study initiation: May 18, 2005

GLP compliance:	Yes
QA statement:	Yes
Drug, lot #, and % purity:	PF-02341066, lot # AK-100830-53-5, Purity: 99.91%

Key Study Findings

- At the high dose of 500 mg/kg PF-02341066, mean minute volume and mean respiratory rate were significantly lower and tidal volume was significantly increased compared to vehicle controls during the first 24 minute observation interval starting 3 hours after dosing.

Methods

Doses:	0, 10, 75, or 500 mg/kg
Frequency of dosing:	Single dose
Route of administration:	Oral gavage
Dose volume:	10 mL/kg
Formulation/Vehicle:	0.5% methylcellulose
Species/Strain:	Sprague-Dawley rat
Number/Sex/Group:	8 males/group
Age:	~50-53 days old
Weight:	217-238 g

Male Sprague-Dawley rats (n=8) were administered a single oral dose of vehicle or PF-02341066 (10, 75, or 500 mg/kg). Approximately 3 hours after dosing, the unrestrained rats were placed in whole body plethysmographs fitted with flow transducers. Pulmonary function data for minute volume, respiratory rate, and tidal volume were collected for approximately 120 minutes. Means for each parameter were calculated over five 24-minute intervals. Rats were observed for clinical signs predose and immediately following pulmonary evaluation (~5 hours after dosing).

Results

Clinical signs

At 500 mg/kg, red staining of the muzzle was observed in 2 rats 5 hours after dosing, and dyspnea and salivation were observed in another rat 5 hours after dosing and at an unscheduled observation time.

Pulmonary assessment

Mean minute volume and mean respiratory rate were significantly lower in rats treated with 500 mg/kg compared to vehicle controls by 28% and 47%, respectively, during the 1-24 minute interval. Mean tidal volume was significantly increased by 65% at the same dose and time interval compared to vehicle controls. The diminished respiratory rates observed in the initial 1-24 minute interval at 500 mg/kg correlate with the decreased activity and dyspnea observed in the neurofunctional evaluation study. The effects of

PF-2341066 on mean minute volume, respiratory rate, and tidal volume are shown in the figures below (*= p < 0.022).

Figure 41: Effect of PF-2341066 on mean minute volume

(excerpted from sponsor's submission)

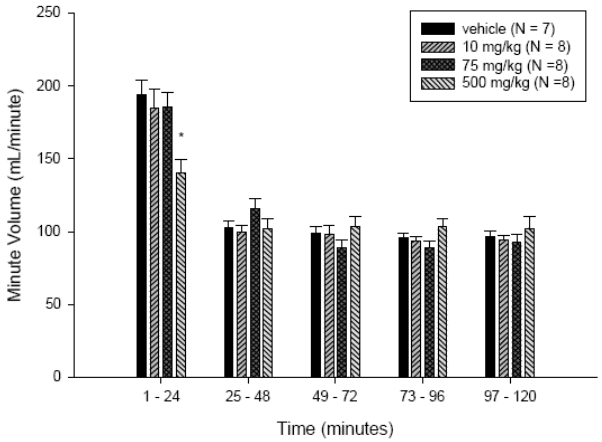

Figure 42: Effect of PF-2341066 on mean respiratory rate

(excerpted from sponsor's submission)

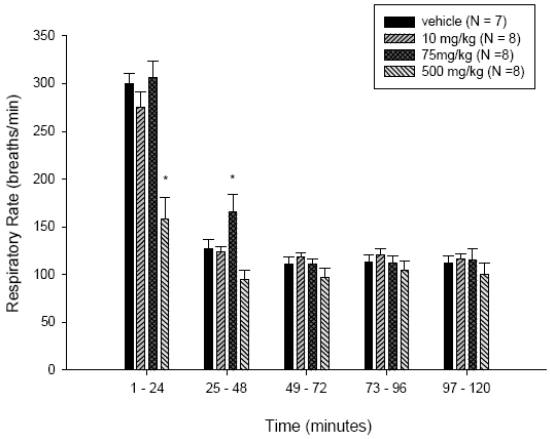

Figure 43: Effect of PF-2341066 on mean tidal volume

(excerpted from sponsor's submission)

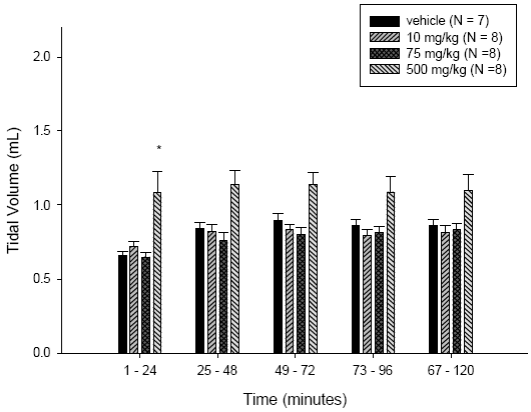

Renal effects:
No studies submitted

Gastrointestinal effects:
No studies submitted

Abuse liability:
No studies submitted

5 Pharmacokinetics/ADME/Toxicokinetics

5.1 PK/ADME

Distribution

Study title: Equilibrium dialysis determination of unbound fraction of PF-02341066 in rat, mouse, dog, monkey, and human plasma
Study no.: PF02341066-PDM-014
Study report location: M4.2.2.3

In this study, the *in vitro* binding of PF-02341066 to rat, mouse, dog, monkey, and human plasma proteins was investigated by initial determination of the time-course to binding equilibrium followed by protein binding experiments across species using the equilibrium dialysis technique. Plasma protein binding studies were performed using a 96-well Teflon® equilibrium dialysis chamber apparatus. The time-course of protein binding equilibration was assessed in human and rat plasma over 24 hours at 4, 7, and 24 hours at a concentration of 1 µM PF-02341066 (in triplicate). Since PF-02341066 was found to be unstable in mouse plasma after a 7-hour incubation, the time-course of protein binding equilibration in mouse plasma was assessed over 7 hours at 2, 4, and 7 hours at a concentration of 5 µM PF-02341066. Based on the binding equilibration time-course, the subsequent cross-species assessment of unbound fraction was conducted with 7 hours equilibration in rat, dog, monkey, and human plasma, and 4 hours equilibration in mouse plasma at PF-02341066 concentrations of 0.5, 5, and 20 µM (0.23, 2.3, and 9 µg/mL). Concentrations of PF-02341066 in plasma and buffer were assayed by LC-MS/MS with sample workup employing protein precipitation. The value of unbound fraction (f_u) was determined using the following equation: $f_u = (C_{buffer} / C_{plasma}) \times 100\%$, where C_{buffer} is the concentration of analyte in the buffer half of the equilibrium dialysis chamber and C_{plasma} the concentration of analyte in the plasma side, respectively.

The unbound fraction of PF-02341066 at each concentration (0.5, 5, and 20 µM) in mouse, rat, dog, monkey, and human plasma are presented in the table below. The average unbound fraction of PF-02341066 was 0.057 in the rat plasma, 0.043 in the dog plasma, and 0.093 in human plasma.

Table 22: Unbound fraction (fu) of PF-02341066 in plasma from preclinical species and humans determined using equilibrium dialysis

(excerpted from sponsor's submission)

Concentration (µM)	Mouse[a]	Rat[b]	Dog[b]	Monkey[b]	Human[b]
0.5	0.028 ± 0.007	0.029 ± 0.003	0.045 ± 0.021	0.049 ± 0.022	0.058 ± 0.043
5	0.047 ± 0.008	0.044 ± 0.010	0.042 ± 0.003	0.030 ± 0.007	0.113 ± 0.004
20	0.033 ± 0.009	0.097 ± 0.023	0.043 ± 0.016	0.137 ± 0.085	0.108 ± 0.010
Mean (f_u)	0.036 ± 0.010	0.057 ± 0.036	0.043 ± 0.001	0.072 ± 0.057	0.093 ± 0.031
Mean Recovery (%)	63	107	67	124	151

Note: Data presented are mean ± SD (Mean of triplicate determinations at each concentration).
[a]Using 4 hours equilibrium time.
[b]Using 7 hours equilibrium time.

Study title: Quantitative whole body autoradiography of rats following oral administration of [^{14}C] PF-02341066
Study no.: 8215155
Study report location: M4.2.2.3

Absorption and tissue distribution of drug-derived radioactivity was assessed in Long Evans male rats following oral administration of [^{14}C] PF-02341066 (10 mg/kg) using quantitative whole-body autoradiography. Rats were euthanized at 1, 4, 8, 24, 48, 96, and 168 hours after dosing (1 rat/time point); the right eye from each rat was collected and carcasses were prepared for whole-body autoradiography. Concentrations of radioactivity were determined in tissues, organs, and biological fluids for each time point. Additionally, radioanalysis was conducted on both eyes from one rat each at 336 and 504 hours after dosing.

The distribution of drug-derived radioactivity was extensive with C_{max} occurring at 4 or 8 hours after dosing in most tissues. [^{14}C] PF-02341066-derived radioactivity was present in most tissues for at least 48 hours with measurable amounts of radioactivity still present in 17 tissues at 168 hours after dosing. Excluding bile and urine, the highest C_{max} values of radioactivity were observed in the eye and associated tissues (Harderian gland, lacrimal gland, and uveal tract), pituitary gland, liver, kidney, adrenal gland, and spleen. In the eye, [^{14}C] PF-02341066-derived radioactivity was present through 504 hours after dosing with an estimated elimination $t_{1/2}$ of 576 hours. The presence of radioactivity in bile and urine indicated that biliary and renal excretion were routes of elimination for [^{14}C] PF-02341066-derived radioactivity.

Table 23: Pharmacokinetic parameters for blood and tissues in male Long Evans rats following a single oral administration of [14C] PF-02341066

(excerpted from sponsor's submission)

Matrix or Tissue	AUC_{0-t} (ng eq·hour/g)	$AUC_{0-\infty}$ (ng eq·hour/g)	C_{max} (ng eq/g)	T_{max} (Hours)	Half-Life (Hours)	xy corr Coefficient (Elimination Phase)	Dose Exposure (µCi·Hour)	Radiation Absorbed Dose (mRad or mrem)[a]
Adrenal gland(s)[b]	153931	166763	7900	8.00	96.6	0.780	0.299	2.24
Bile	130300	478230	21400	4.00	13.8	1.00	NC[c]	NC[c]
Blood	777	1569	165	4.00	5.50	1.00	1.10	0.0207
Bone	686	NC	125	4.00	NC	NC	0.344	0.00656
Bone marrow	55932	57367	2920	8.00	20.2	0.980	2.01	0.163
Brain choroid plexus	64273	73141	3010	8.00	14.5	0.984	NC[c]	NC[c]
Bulbo-urethral gland	32113	32688	2040	4.00	7.83	0.981	NC[c]	NC[c]
Cecum	36974	38126	2010	8.00	8.99	0.996	1.39	NC[c]
Diaphragm	16598	16993	1860	4.00	4.17	1.00	NC[c]	NC[c]
Epididymis[b]	13444	58211	234	8.00	252[d]	0.816	0.910	23.9
Esophagus	18835	19796	1270	4.00	5.55	0.987	NC[c]	NC[c]
Exorbital lacrimal gland	145766	151439	2940	8.00	27.5	1.00	NC[c]	NC[c]
Eye(s)[e]	215725	NC	1460	96.0	NC	NC	NC[c]	NC[c]

LSC Liquid scintillation counting.
NC Not calculated.
xy corr xy correlation; this coefficient predicts the goodness-of-fit for the concentration-time line (theoretical vs. observed).
Note: When $AUC_{0-\infty}$ is not calculated, AUC_{0-t} is used to calculate the absorbed dose.
a Calculated for a 100-µCi dose of [^{14}C]PF-02341066 in humans.
b Pharmacokinetic data should be interpreted with caution because R^2 adjusted value (goodness-of-fit statistic) was <0.7.
c No theoretical organ weight and/or S-factor available to calculate this value.
d As sampling is through 168 hours postdose, this estimated half life provided the most conservative assessment of potential exposure for dosimetry.
e Based on the pharmacokinetic results, dosimetry calculations were applied to Eye (LSC) rather than Eye(s) in order to determine the best conservative estimation of radiation absorbed dose in the eye.

Matrix or Tissue	AUC_{0-t} (ng eq·hour/g)	$AUC_{0-\infty}$ (ng eq·hour/g)	C_{max} (ng eq/g)	T_{max} (Hours)	Half-Life (Hours)	xy corr Coefficient (Elimination Phase)	Dose Exposure (µCi·Hour)	Radiation Absorbed Dose (mRad or mrem)[a]
Eye (LSC)[b,c]	914025	2147307	2710	48.0	576[d]	0.943	20.1	141
Eye uveal tract	1218624	NC	8300	48.0	NC	NC	11.4	80.0
Fat (abdominal)	601	3938	114	4.00	22.9	1.00	2.85	0.0205
Fat (brown)[e,f]	39298	51494	2600	4.00	118	0.763	0.671	0.00483
Harderian gland	292035	438535	2500	48.0	96.7	0.997	4.01	NC[g]
Intra-orbital lacrimal gland	164264	176098	2530	8.00	33.2	1.00	NC[g]	NC[g]
Kidney(s)[e]	169045	212653	6910	4.00	89.7	0.995	18.1	6.12
Kidney cortex	192391	279198	6850	4.00	119	0.995	23.7	8.04
Kidney medulla	130635	141685	6770	4.00	70.3	1.00	12.0	4.08
Large intestine	69432	71519	2760	24.0	6.58	1.00	4.95	1.73
Liver	320770	354194	12900	4.00	57.2	0.998	179	10.4
Lungs	68279	68730	4330	8.00	6.27	0.997	3.31	0.289
Lymph node(s)	56668	62511	2430	8.00	30.7	0.982	NC[g]	NC[g]

NC Not calculated.
xy corr xy correlation; this coefficient predicts the goodness-of-fit for the concentration-time line (theoretical vs. observed).
Note: When $AUC_{0-\infty}$ is not calculated, AUC_{0-t} is used to calculate the absorbed dose.
a Calculated for a 100-µCi dose of [^{14}C]PF-02341066 in humans.
b Based on the pharmacokinetic results, dosimetry calculations were applied to Eye (LSC) rather than Eye(s) in order to determine the best conservative estimation of radiation absorbed dose in the eye.
c The right eye was analyzed for [^{14}C]PF-02341066 concentrations for the 1- through 168-hour collection time points. For the 336- and 504-hour collection time points, both eyes were analyzed for [^{14}C]PF-02341066 concentrations and the average concentration of the right and left eye at each time point was used to calculate pharmacokinetic parameters.
d As sampling is through 504 hours postdose, this estimated half life provided the most conservative assessment of potential exposure for dosimetry.
e Pharmacokinetic data should be interpreted with caution because the %AUC extrapolated value was >20% but <30%.
f Pharmacokinetic data should be interpreted with caution because R^2 adjusted value (goodness-of-fit statistic) was <0.7.
g No theoretical organ weight and/or S-factor available to calculate this value.

Matrix or Tissue	AUC_{0-t} (ng eq·hour/g)	$AUC_{0-\infty}$ (ng eq·hour/g)	C_{max} (ng eq/g)	T_{max} (Hours)	Half-Life (Hours)	xy corr Coefficient (Elimination Phase)	Dose Exposure (µCi·Hour)	Radiation Absorbed Dose (mRad or mrem)[a]
Muscle	3227	16000	578	4.00	17.9	1.00	73.0	0.263
Myocardium	15319	16052	1570	4.00	5.08	1.00	0.520	0.165
Nasal turbinates	14107	16215	526	8.00	15.8	0.994	NC[b]	NC[b]
Pancreas	38658	39247	2860	4.00	7.42	0.972	1.38	1.04
Periosteum	38901	56680	1070	4.00	57.1	1.00	NC[b]	NC[b]
Pituitary gland	682644	838978	7380	48.0	60.5	0.966	0.241	42.1
Preputial gland	108510	116226	1270	8.00	49.1	0.941	0.551	NC[b]
Prostate gland	18083	18738	1080	8.00	9.14	0.992	0.152	0.936
Salivary gland(s)	52045	57351	2980	8.00	80.5	1.00	1.20	1.48
Seminal vesicle(s)	4818	7876	321	8.00	14.3	1.00	0.125	NC[b]
Skin (nonpigmented)	7263	8294	507	8.00	8.22	0.943	19.6	0.624
Skin (pigmented)	63765	110113	650	8.00	133	0.993	261	8.28
Small intestine	72947	75826	7670	1.00	5.27	0.998	16.7	2.70
Spleen	115131	124416	5450	4.00	54.1	0.961	3.28	2.30
Stomach	28669	30364	1710	4.00	10.7	0.970	1.56	1.10
Testis(es)[c]	14304	28516	135	8.00	169	0.901	2.94	8.83
Thymus	26142	28515	1260	8.00	12.4	1.00	0.557	2.34
Thyroid[c]	70381	78528	5110	4.00	82.9	0.784	0.0444	0.233
Urinary bladder	5343	NC	1490	8.00	NC	NC	0.0166	0.0349
Urine	114428	115574	12600	4.00	6.68	0.999	NC[b]	NC[b]

NC Not calculated.
xy corr xy correlation; this coefficient predicts the goodness-of-fit for the concentration-time line (theoretical vs. observed).
Note: When $AUC_{0-\infty}$ is not calculated, AUC_{0-t} is used to calculate the absorbed dose.
a Calculated for a 100-µCi dose of [^{14}C]PF-02341066 in humans.
b No theoretical organ weight and/or S-factor available to calculate this value.
c Pharmacokinetic data should be interpreted with caution because R^2 adjusted value (goodness-of-fit statistic) was <0.7.

Table 24: Concentrations of radioactivity in the right and left eyes at 336 and 504 hours after dosing

Collection time point (hours)	Radioactivity (ng eq/g)	
	Right eye	Left eye
336	1590	1650
504	1440	1530

Metabolism

Study title: Metabolism of [^{14}C] PF-02341066 following oral administration to rats
Study no.: 133625
Study report location: M4.2.2.4

Radio-HPLC profiling and metabolite identification were performed on plasma, feces, urine, and bile samples collected from male and female rats following a single oral administration of [^{14}C] PF-02341066 (10 mg/kg). Urine was collected at 0-8 and 8-24 hours after dosing and at 24 hour intervals through 168 hours after dosing. Feces were collected at 24 hour intervals through 168 hours after dosing in the same rats. In a second group of rats, bile was collected at 0-8, 8-24, and 24-48 hours after dosing. In a third group of rats, blood was collected at time of euthanasia at 1, 2, 4, 6, 8, and 24 hours after dosing to obtain plasma. Samples were analyzed for total radioactivity using HPLC and metabolite identification in plasma, feces, and bile was conducted by mass spectrometry using HPLC-MS/MS. No single radioactive component of urine accounted for ≥1% of the administered dose, therefore, metabolite identification was not conducted for urine samples.

The major drug-related component observed in radio-HPLC profiles of pooled plasma was PF-02341066, which accounted for 53.4% and 44.2% of the recovered radioactivity in male and female rat plasma, respectively. Other components present in the plasma were the lactam metabolite (M10; PF-06260182), a sulfate conjugate of PF-02341066 (M19), and a nitrone metabolite (M21; PF-06248761). Two early eluting peaks that could not be characterized were also observed in the plasma in both males and females.

Table 25: Relative quantitation of PF-02341066 and metabolites in plasma of male and female rats

excerpted from sponsor's submission)

Sex	% Radioactivity in Plasma					
	PF-02341066	Uncharacterized	Uncharacterized	M10 (PF-06260182)	M19	M21 (PF-06248761)
Male	53.4	4.4	7.0	7.6	3.2	14.4
Female	44.2	2.8	2.7	16.4	17.7	8.5

The major component observed in radio-HPLC profiles of the feces was PF-02341066, which accounted for 78.6% and 60.4% of the dose in male and female feces, respectively. M19 was also present in the feces, particularly in females. One unknown component present in male feces was detected but not characterized. The major component observed in female bile was M19, which accounted for 47.1% of the dose in bile. M19 was also present in male bile (7%). Other components present in the bile were two different glucuronides of *O*-dealkylated PF-02341066 (M1 and M20), *O*-dealkylated lactum (M2; primarily in males), and a sulfate conjugate of the *O*-dealkylated lactum (M8).

Table 26: Relative quantitation of PF-02341066 and metabolites in feces and bile of male and female rats

(excerpted from sponsor's submission)

	% of Dose													
	PF-02341066		Uncharacterized		M1		M2		M8		M19		M20	
Sex	Feces	Bile	Feces	Bile	Feces	Bile	Feces	Bile	Feces	Bile	Feces	Bile	Feces	Bile
M	78.6	<1	1.9	4.1	<1	6.7	<1	2.7	<1	8.7	1.3	7.0	<1	2.9
F	60.4	<1	<1	<1	<1	2.9	<1	<1	<1	10.1	23.9	47.1	<1	<1

Abbreviations: M = Male; F = Female.
Average of 2 animals/sex reported.
If metabolite was <1% of dose in an animal, a value of 0 was used in calculating the average

The metabolite profiling data indicated that PF-02341066 underwent oxidation of the piperdine ring, direct sulfate conjugation, and *O*-dealkylation, with subsequent Phase 2 conjugation of *O*-dealkylated metabolites. Overall, the metabolite profiles in male and female rats were qualitatively similar, however, there was a quantitative difference between males and females in metabolism of PF-02341066. The pathway involving the

formation of a direct sulfate conjugate of PF-02341066 (M19) is much more prevalent in female than male rats.

Study title: Metabolism of [^{14}C] PF-02341066 following oral administration to dogs
Study no.: 122138
Study report location: M4.2.2.4

Radio-HPLC profiling and metabolite identification were performed on plasma, feces, and urine samples collected from male and female dogs following a single oral administration of [^{14}C] PF-02341066 (10 mg/kg). Urine was collected at 0-8 and 8-24 hours after dosing and at 24 hour intervals through 168 hours after dosing. Feces were collected at 24 hour intervals through 168 hours after dosing. Blood was collected via a jugular vein at 1, 2, 4, 6, 8, 24, 48, 72, 96, and 120 hours after dosing. Samples were analyzed for total radioactivity using HPLC and metabolite identification in plasma and feces was conducted by mass spectrometry using HPLC-MS/MS. No single radioactive component of urine represented $\geq$1% of the administered dose, therefore, metabolite identification was not conducted for urine samples.

The major drug-related component observed in radio-HPLC profiles of pooled plasma was PF-02341066, which accounted for 58.6% and 71% of the radioactivity in male and female dog plasma, respectively. Other components present in the plasma were a hydroxyl metabolite of the lactam metabolite (M15; females only), a nitrone metabolite (M21; PF-06248761), the *N*-dealkylated metabolite (M16; males only), and a dicarbanyl metabolite (M17 or M18; males only).

Table 27: Relative quantitation of PF-02341066 and metabolites in plasma of male and female dogs

(excerpted from sponsor's submission)

	% Radioactivity in Plasma					
Gender	PF-02341066	M15	M16	M17 or M18	M21 (PF-06248761)	Uncharacterized
Male	58.6	-	3.4	3.2	7.9	3.0
Female	71.0	2.8	-	-	4.6	-

The major component observed in radio-HPLC profiles of the feces was PF-02341066, which accounted for 47.2% and 69.8% of the dose in male and female feces, respectively. M17 and M18 were also present in the feces of both males and females.

Table 28: Relative quantitation of PF-02341066 and metabolites in feces of male and female dogs

(excerpted from sponsor's submission)

Gender	% of Dose	
	PF-02341066	M17/M18
Male	47.2	3.2
Female	69.8	3.1

The metabolite profiling data indicated that PF-02341066 underwent metabolism on the piperdine ring by oxidative pathways and *N*-dealkylation.

Excretion

Study title: Pharmacokinetics and excretion of [^{14}C] PF-02341066 following oral administration to rats
Study no.: 8215153
Study report location: M4.2.2.5

The pharmacokinetics and excretion of drug-derived radioactivity were investigated in male and female Sprague-Dawley rats following a single oral administration of [^{14}C] PF-02341066 (10 mg/kg). Rats were assigned to one of three groups for the study. From rats in group 1 (n=3/sex), urine was collected at 0-8 and 8-24 hours after dosing and at 24 hour intervals through 168 hours after dosing, and feces were collected at 24 hour intervals through 168 hours after dosing. From bile duct cannulated rats in group 2 (n=3/sex), urine and bile were collected at 0-8, 8-24, and 24-48 hours after dosing, and feces were at 0-24 and 24-48 hours after dosing. For groups 1 and 2, cage rinses, cage wash, and cage wipe were also conducted to collect radioactivity, and bile cannula and jacket used for bile collection for group 2 were saved for radioanalysis. From rats in group 3 (n=2/sex/time point) blood was collected at the time of euthanasia at 1, 2, 4, 6, 8, and 24 hours after dosing to obtain blood and plasma. Urine, feces, bile, blood, and plasma were analyzed for radioactivity by liquid scintillation counting.

The major excretion routes of [^{14}C] PF-02341066-derived radioactivity were via feces and bile in male and female rats, while urinary excretion was a minor route of elimination. Group 2 data shows that biliary excretion was higher in females than males, while fecal excretion was higher in males than females. Elimination of [^{14}C] PF-02341066-derived radioactivity mainly occurred over the first 24 hours after dosing and was complete by 168 hours after dosing. The concentrations of drug-derived radioactivity in blood and plasma following a single oral administration of [^{14}C] PF-02341066 reached C_{max} at 8 hours after dosing in males and 4 hours after dosing in females. There were no other notable differences in plasma concentrations and pharmacokinetic parameters between males and females.

Table 29: Excretion of radioactivity in male and female rats after a single administration of [14C] PF-02341066 (10 mg/kg): Group 1

Sample	Mean percent excreted (% of the administered dose)	
	Males	Females
Urine	3.19	2.17
Feces	99.60	98.40
Cage rinse	0.13	0.06
Cage wash	0.01	0.01
Cage wipe	0.04	0.01
Total recovery	102.97	100.65

Table 30: Excretion of radioactivity in male and female rats after a single administration of [14C] PF-02341066 (10 mg/kg): Group 2

Sample	Time point (hours after dosing)	Mean percent excreted (% of the administered dose)	
		Males	Females
Urine	8	1.35	0.0
	24	3.55	2.24
	48	0.71	0.28
	Subtotal	5.61	2.52
Feces	24	38.90	23.60
	48	14.40	11.40
	Subtotal	53.30	35.0
Bile	8	16.60	43.70
	24	18.30	14.80
	48	2.82	3.30
	Subtotal	37.80	61.80
Cage rinse	24	0.10	0.07
Cage wash	48	0.07	0.05
Cage wipe	48	0.06	0.22
Bile cannula	48	0.01	0.02
Jacket rinse	48	0.00	0.00
Total recovery		96.95	99.68

Table 31: Concentrations of radioactivity in blood and plasma of male and female rats after a single administration of [14C] PF-02341066 (10 mg/kg): Group 3

Sample	Time point (hours after dosing)	Mean radioactivity level (ng eq/g)	
		Males	Females
Blood	1	42.9	26.3
	2	56.3	68.8
	4	163	160
	6	139	149
	8	190	143
	24	18.6	17.5
Plasma	1	57.7	41.2
	2	68.1	83.5
	4	192	204
	6	156	189
	8	220	167
	24	19.6	17.1

Table 32: Pharamacokinetic parameters for radioactivity in plasma of male and female rats after a single administration of [14C] PF-02341066 (10 mg/kg): Group 3

Pharmacokinetic parameters	Males	Females
C_{max} (ng eq/g)	220	204
T_{max} (hours)	8	4
$AUC_{(0-t)}$ (ng eq·hours/g)	2990	2590
$AUC_{(0-\infty)}$ (ng eq·hours/g)	3160	2720
$t_{1/2}$ (hours)	5.76	5.06

Study title: Pharmacokinetics and excretion of [^{14}C] PF-02341066 following oral administration to dogs
Study no.: 8220895
Study report location: M4.2.2.5

The pharmacokinetics and excretion of drug-derived radioactivity were investigated following a single oral administration of [^{14}C] PF-02341066 (10 mg/kg) to male and female beagle dogs (n=2/sex). Blood was collected from all dogs at 1, 2, 4, 6, 8, 24, 48, 72, 96, and 120 hours after dosing. Urine was collected from all dogs at 0-8 and 8-24 hours after dosing and at 24 hour intervals through 168 hours after dosing, and feces was collected at 24 hour intervals through 168 hours after dosing. Cage rinses, cage wash, cage wipe, and urine wipe were conducted and cage debris and vomitus were collected to quantify radioactivity. Urine, feces, blood, and plasma were analyzed for radioactivity by liquid scintillation counting.

Following a single oral administration of [^{14}C] PF-02341066 (10 mg/kg), the average total recoveries of the administered dose were 86.12% and 92.7% from male and female dogs, respectively. Excretion of radioactivity occurred primarily within the first 72 hours after dosing. The major excretion route of [^{14}C] PF-02341066-derived radioactivity was via the feces in male and female dogs, while urinary excretion was a

minor route of elimination. Emesis was observed in 3 of the 4 dogs, and radioactivity was present in vomitus. The concentrations of drug-derived radioactivity in blood and plasma following a single oral administration of [^{14}C] PF-02341066 reached C_{max} at 6 hours after dosing in males and 1 hour after dosing in females. Exposure to [^{14}C] PF-02341066 in the plasma was slightly higher in males than females.

Table 33: Excretion of radioactivity in male and female dogs after a single administration of [14C] PF-02341066 (10 mg/kg)

Sample	Time point (hours after dosing)	Mean percent excreted (% of the administered dose)	
		Males	Females
Urine	8	0.51	0.36
	24	0.57	0.76
	48	0.46	0.51
	72	0.20	0.24
	96	0.14	0.12
	120	0.10	0.09
	144	0.09	0.06
	168	0.08	0.04
	Subtotal	2.15	2.18
Feces	24	28.40	38.90
	48	21.20	36.50
	72	6.03	6.33
	96	2.84	1.51
	120	1.23	1.44
	144	0.74	0.40
	168	2.03	0.28
	Subtotal	62.47	85.36
Cage debris	Subtotal	0.29	0.09
Cage rinse	Subtotal	2.61	0.63
Cage wash	Subtotal	0.14	0.05
Cage wipe	Subtotal	1.70	0.23
Urine wipe	Subtotal	0.00	0.12
Vomitus	0.32	0.56	0.00
Vomitus/emesis	6	16.20	4.04
Total recovery		86.12	92.70

Table 34: Concentrations of radioactivity in blood and plasma of male and female dogs after a single administration of [14C] PF-02341066 (10 mg/kg)

Sample	Time point (hours after dosing)	Mean radioactivity level (ng eq/g)	
		Males	Females
Blood	1	510	509
	2	591	494
	4	603	479
	6	629	417
	8	532	405
	24	189	152
	48	78.8	31.8
	72	55.4	21.1
	96	23.0	0.00
	120	0.00	0.00
Plasma	1	617	691
	2	668	660
	4	699	618
	6	763	544
	8	577	487
	24	232	195
	48	67.5	42.6
	72	40.2	0.00
	96	0.00	0.00
	120	0.00	0.00

Table 35: Pharamacokinetic parameters for radioactivity in plasma of male and female dogs after a single administration of [14C] PF-02341066 (10 mg/kg)

Pharmacokinetic parameters	Males	Females
C_{max} (ng eq/g)	938	781
T_{max} (hours)	6	1
$AUC_{(0-t)}$ (ng eq·hours/g)	15900	12000
$AUC_{(0-\infty)}$ (ng eq·hours/g)	17600	13900
$t_{1/2}$ (hours)	14.0	12.4

6 General Toxicology

6.1 Single-Dose Toxicity

No single-dose toxicity studies were submitted.

6.2 Repeat-Dose Toxicity

Study title: A 7-day PO toxicology study of PF-02341066 in male and female Sprague Dawley rats

Study no.:	04HGF004
Study report location:	M4.2.3.2
Conducting laboratory and location:	Pfizer Central Research Drug Safety Evaluation Department Groton, CT
Date of study initiation:	September 14, 2004 (Study start date)
GLP compliance:	No
QA statement:	No
Drug, lot #, and % purity:	PF-02341066, lot and purity not provided

Key Study Findings

- Mortality: One male in the 500 mg/kg dose group was found dead on Day 4. The remaining males and females treated with 500 mg/kg were euthanized on Day 4 due to poor clinical condition.
- Target organs of toxicity included the bone marrow (sternum), gastrointestinal tract (ileum, jejunum, and stomach), kidney, liver, ovary, pancreas, spleen, salivary gland, and thymus.
- Hematology changes included decreases in WBC count and lymphocytes and increases in neutrophils and monocytes.
- Clinical chemistry changes included increases in ALT, AST, glucose, and creatine kinase and decreases in total protein and albumin.

Methods

Doses:	0, 50, 150, or 500 mg/kg
Frequency of dosing:	Once daily for 7 days
Route of administration:	Oral gavage
Dose volume:	10 mL/kg
Formulation/Vehicle:	Sterile water
Species/Strain:	Sprague-Dawley rat
Number/Sex/Group:	3/sex/group
Age:	8 weeks on Day 1
Weight:	Males: 178.53-203.01 g on Day 1 Females: 121.23-140.87 g on Day 1
Satellite groups:	None

Note: One female treated with 150 mg/kg (Animal # 3F01) was not treated on Day 6

Observations and times:

Mortality:	Daily
Clinical signs:	Daily
Body weights:	Day -4, every other day beginning on Day 1, and Day 8
Food consumption:	Not conducted

ECG:	Not conducted
Ophthalmoscopy:	Not conducted
Hematology:	Conducted full CBC, times not provided
Clinical chemistry:	Conducted full rat clinical chemistry panel including troponin 1 and CK isoenzymes, times not provided
Coagulation:	Not conducted
Urinalysis:	Days -1, 1, 2, and 6
Gross pathology:	At necropsy*
Organ weights:	At necropsy*
Histopathology:	At necropsy*
Toxicokinetics:	Day -1: Predose Day 1: 4 and 24 hours after dosing Day 4: Predose and 4 hours after dosing Day 7: 1, 4, 7, and 24 hours after dosing

* Necropsy on Day 8

Results

Mortality

One male treated with 150 mg/kg (Animal # 3M03) was misdosed and subsequently euthanized on Day 5. No tissues were collected for this animal. One male in the 500 mg/kg dose group (Animal # 4M03) was found dead on Day 4 and was also not necropsied. The remaining males and females treated with 500 mg/kg were euthanized on Day 4 due to poor clinical condition.

Clinical Signs

Clinical signs	No. of animals affected (No. of days observed)							
	Males				**Females**			
Dose (mg/kg)	0	50	150	500	0	50	150	500
Number of animals examined	3	3	3	3	3	3	3	3
Diarrhea	-	-	-	1 (1)	-	-	-	1 (1)
Dyspnea	-	-	1 (6)	3 (3)	-	-	1 (6)	3 (2)
Lethargy	-	-	1 (1)	-	-	-	-	-
Oral discharge	-	-	1 (5)	3 (3)	-	-	1 (4)	2 (2)
Gurgled, raspy breathing	-	1 (1)	1 (1)	-	-	-	-	-

- = Clinical sign not observed in this group

One female treated with 150 mg/kg (Animal # 3F01) was having difficulty breathing and appeared to be gasping. The animal was left on study but was not treated on Day 6.

Body Weights

Body weights were lower at all dose levels of PF-02341066 compared to controls. At 500 mg/kg, body weight was decreased by 10% in males and 3% in females on Day 4 compared to Day 1.

Figure 44: 7 Day Rat Body Weights

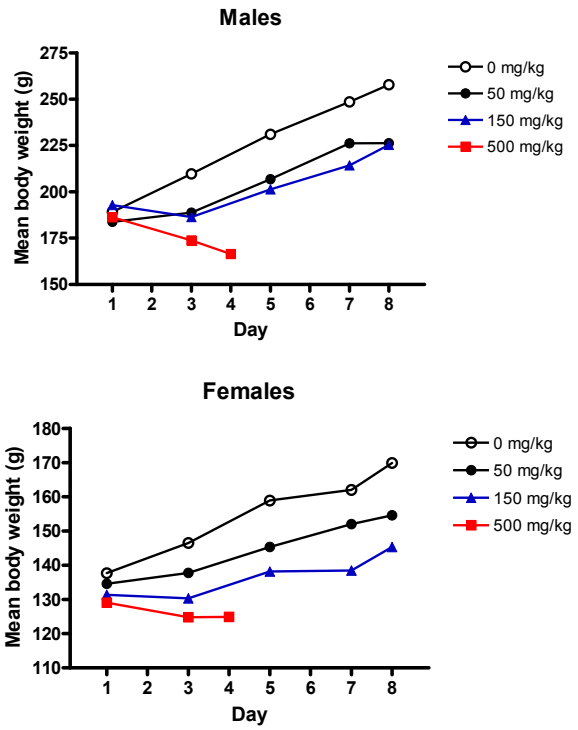

Food Consumption

Not conducted

Ophthalmoscopy

Not conducted

ECG

Not conducted

Hematology

These changes in hematology parameters for the 500 mg/kg group were in a table provided in the study report; actual data was not provided. These changes may be compared to controls, however, this is not clearly stated in the table.

Index	Change in index 500 mg/kg	
	Males	Females
WBC	↓28%	↓58%
Neutrophils %	↑4.6 fold	↑1.3 fold
Lymphocytes %	↓60%	↓25%
Monocytes %	↑ 2.6 fold	↑ 2.6 fold

↑= increase ↓=decrease

Clinical Chemistry

These changes in clinical chemistry parameters for the 500 mg/kg group were in a table provided in the study report; actual data was not provided. These changes may be compared to controls, however, this is not clearly stated in the table.

Index	Change in index 500 mg/kg	
	Males	Females
ALT	↑2.6 fold	↑2.0 fold
AST	↑2.1 fold	↑2.0 fold
Glucose	↑65%	-
Total protein	↓25%	↓15%
Albumin	↓25%	↓15%
Sodium	↓3%	↓2%
Chloride	↓4%	↓4%
Creatine kinase	↑4.0 fold	↑2.5 fold

↑= increase ↓=decrease - = no test-article related changes

Urinalysis

Urine volume was increased in rats treated at 500 mg/kg on Days 1 and 2 compared to both controls and pretreatment (Day -1). The mean values for urine volume for controls and the 500 mg/kg group are presented in the table below.

	Urine volume (mL)					
Group/dose	0 mg/kg			500 mg/kg		
Day	-1	1	2	-1	1	2
Males	3.8	6.8	7.8	4.2	20.0	21.9
Females	5.6	7.6	7.9	9.7	13.5	16.4

Gross Pathology

Treatment-Related Macroscopic Findings		No. of animals affected							
		Males				**Females**			
Dose (mg/kg)		0	50	150	500*	0	50	150	500*
Number of animals examined		3	3	2	2	3	3	3	3
Kidney	Hydronephrosis	-	-	1	-	-	-	-	-
Salivary glands	Pale	-	-	-	2	-	-	-	1
Spleen	Decreased size	-	-	-	1	-	-	-	-

- = no test-article related changes; * Necropsy conducted on Day 4

Organ Weights

Group and Dose		Mean		Percentage deviation from Control					
		Control 0 mg/kg		50 mg/kg		150 mg/kg		500 mg/kg*	
Sex		Males	Females	Males	Females	Males	Females	Males	Females
Number of animals examined		3	3	3	3	2	3	2	3
Kidney	Absolute (g)	2.65	1.77	↓14	↓17	↓21	↓16	↓37	↓34
	Relative Brain (%)	156.85	103.06	↓19	↓14	↓21	↓15	↓41	↓33
Liver	Absolute (g)	12.63	8.25	↓26	↓19	↓24	↓25	↓53	↓42
	Relative Brain (%)	742.09	477.12	↓29	↓16	↓24	↓24	↓55	↓41
Ovaries	Absolute (g)	NA	0.07	NA	-	NA	-	NA	↓29
	Relative Brain (%)	NA	3.95	NA	-	NA	-	NA	↓25
Spleen	Absolute (g)	0.68	0.40	↓19	-	↓24	-	↓68	↓33
	Relative Brain (%)	40.30	22.94	↓23	-	↓23	-	↓69	↓31
Thymus	Absolute (g)	0.70	0.44	↓27	-	↓56	-	↓34	-
	Relative Brain (%)	40.64	42.80	↓30	-	↓53	-	↓37	-

↑= increase ↓=decrease - = no test-article related changes* Necropsy conducted on Day 4; NA= Not Applicable, tissue does not exist in this sex

Histopathology

One male in the 500 mg/kg dose group was found dead on Day 4 and was not necropsied. The remaining males and females treated with 500 mg/kg were euthanized on Day 4, histopathological examination was conducted for these 2 males and 3 females. No tissues were examined for the 3 males treated with 50 mg/kg, however, there is no explanation why.

Adequate Battery: Yes
Peer Review: No

Histological Findings

Treatment-Related Microscopic Findings			No. of animals affected							
			Males				Females			
Dose (mg/kg)			0	50	150	500*	0	50	150	500*
Number of animals examined			3	0	2	2	3	3	3	3
Organ	Finding									
Bone marrow, sternum	Hypocellularity	Total	-	NE	-	2	-	-	-	3
		Minimal	-	NE	-	1	-	-	-	3
		Mild	-	NE	-	1	-	-	-	-
Ileum	Lymphoid depletion	Minimal	-	NE	-	2	-	NE	NE	-
	Inflammation	Minimal	-	NE	-	1	-	NE	NE	-
	Necrosis	Minimal	-	NE	-	2	-	NE	NE	-
Jejunum	Lymphoid depletion	Minimal	-	NE	-	1	-	NE	NE	-
	Necrosis	Minimal	-	NE	-	1	-	NE	NE	-
Kidney	Hydronephrosis	Mild	-	NE	1	-	-	NE	-	-
Liver	Glycogen depletion	Total	-	NE	-	2	-	1	3	3
		Mild	-	NE	-	-	-	1	2	-
		Moderate	-	NE	-	-	-	-	1	1
		Marked	-	NE	-	2	-	-	-	2
Lung	Lymphoid depletion	Minimal	-	NE	-	1	-	NE	NE	-
Ovary	Necrosis	Minimal	NA	NA	NA	NA	-	NE	NE	1
Pancreas	Zymogen depletion	Minimal	-	NE	-	2	-	NE	-	1
Spleen	Lymphoid depletion	Total	-	NE	-	2	-	-	-	-
		Minimal	-	NE	-	1	-	-	-	-
		Mild	-	NE	-	1	-	-	-	-
	Depletion extramedullary hematopoiesis	Total	-	NE	-	2	-	-	1	2
		Minimal	-	NE	-	-	-	-	1	2
		Moderate	-	NE	-	2	-	-	-	-
Salivary gland	Secretory depletion	Mild	-	NE	-	2	-	NE	-	1
	Single cell necrosis	Minimal	-	NE	-	2	-	NE	-	-
Stomach	Edema	Minimal	-	NE	NE	1	-	NE	-	3
	Hyperkeratosis	Minimal	-	NE	NE	-	-	NE	-	1
	Erosion/ulcer	Minimal	-	NE	NE	-	-	NE	-	1
	Inflammation	Minimal	-	NE	NE	-	-	NE	-	1
	Glandular hyperplasia	Mild	-	NE	NE	-	-	NE	-	1
Thymus	Atrophy	Total	-	NE	-	2	-	-	1	3
		Minimal	-	NE	-	-	-	-	1	-
		Mild	-	NE	-	-	-	-	-	1
		Moderate	-	NE	-	-	-	-	-	1
		Marked	-	NE	-	2	-	-	-	1

- = no test-article related changes; NA= Not Applicable, tissue does not exist in this sex; NE=Not examined, tissue not examined in this group; * Necropsy conducted on Day 4

Toxicokinetics

The toxicokinetics of PF-02341066 (0, 50, 150 and 500 mg/kg) were evaluated Days 1, 4, and 7. The most complete data was collected on Day 7 with samples collected 1, 4, 7, and 24 hours after dosing. C_{max}, AUC, and $T_{1/2}$ were presented for Day 7 only and since the 500 mg/kg group was euthanized on Day 4, these data are only available for the 50 and 150 mg/kg groups. The limited information in the study report is presented in the table below.

- C_{max} and AUC increased with an increase in dose; increases were less than dose proportional
- Exposure to PF-02341066 was higher in males than females

Toxicokinetic parameters on Day 7

Group/dose	Sex	C_{max}	AUC	$T_{1/2}$ (hours)
50 mg/kg	Males	0.90	13	6
	Females	0.51	5.9	4.4
150 mg/kg	Males	1.9	31	9.8
	Females	1.4	17	6.9

Study title: 1-month oral toxicity study of PF-02341066 in rats
Study no.: 05137
Study report location: M4.2.3.2
Previously reviewed in IND 73544 by Robeena Aziz, MPH, Ph.D.

Study title: 1-month oral toxicity study of PF-02341066 in dogs
Study no.: 05162
Study report location: M4.2.3.2
Previously reviewed in IND 73544 by Robeena Aziz, MPH, Ph.D.

The one month repeat dose toxicology studies in rats (Study 05137) and dogs (Study 05162) were previously reviewed under IND 73544. In the one month studies PF-02341066 was administered by oral gavage daily for 28 days in rats (0, 10, 50, or 150 mg/kg) and dogs (0, 1, 6, or 20 mg/kg). Recovery was not assessed in either study and there were no treatment related mortalities. In the rat study, target organs of toxicity were the bone marrow, bone (joint), kidney, prostate, spleen, seminal vesicle, testes, and thymus in male rats only. Vacuolation of renal cortical tubules, atrophy of the prostate and thymus, and degeneration of pachytene spermatocytes in the testes were observed at $\geq$ 50 mg/kg. At the 150 mg/kg dose level, hypocellularity of the bone marrow, decreased bone primary spongiosa of the joint, atrophy of the seminal vesicle, and lymphoid depletion of the spleen were also observed. The rats were 7 weeks of age at dose initiation, therefore, the finding of decreased bone primary spongiosa of the joint was observed in immature rats in this study. In the dog study, effects included emesis and diarrhea in both males and females at $\geq$ 6 mg/kg, and decreased cellularity of the thymus in males at 20 mg/kg. ECG results showed that QT/QTc intervals before or after dosing on Day 22 were increased compared to pre-study values in 2 dogs (1 male and 1 female) at the 20 mg/kg dose level.

Study title: 3-month oral toxicity study of PF-02341066 in rats with a 2-month recovery

Study no.:	09GR347
Study report location:	M4.2.3.2
Conducting laboratory and location:	Pfizer Global Research & Development Drug Safety Research & Development Eastern Point Rd. Groton, CT and (b) (4) (Toxicokinetics)
Date of study initiation:	September 24, 2009
GLP compliance:	Yes
QA statement:	Yes
Drug, lot #, and % purity:	PF-02341066, lot # E010009648, Purity: 99.6%

Key Study Findings

- Target organs of toxicity included the bone marrow, gastrointestinal tract (cecum, colon, duodenum, ileum, and jejunum), heart, liver, lung, mesenteric lymph node, pituitary, mandibular salivary gland, and thymus
- Cellular vacuolation due to phospholipidosis was observed in multiple organs including the liver (bile duct), pituitary, prostate, and gastrointestinal tract (cecum, colon, duodenum, ileum, and jejunum)
- Hematology changes included decreases in reticulocytes and increases in platelets, WBC count, neutrophils, and monocytes
- Clinical chemistry changes included increases in ALT, AST, ALP, BUN, and creatinine

Methods

Doses:	0, 10, 30, or 100 mg/kg (males), 0, 10, 50, or 250 mg/kg (females)
Frequency of dosing:	Once daily for 3 months (90 consecutive days), 2-month (57-day) recovery period
Route of administration:	Oral gavage
Dose volume:	10 mL/kg
Formulation/Vehicle:	0.5% methylcellulose
Species/Strain:	Sprague-Dawley rat
Number/Sex/Group:	10/sex/group (main study) 5/sex/group (recovery)
Age:	~9 weeks at dose initiation
Weight:	Males: 271.4-336.7 g at dose initiation Females: 183.9-232.0 g at dose initiation
Satellite groups:	None

Observations and times:

Mortality:	Once daily during the pretreatment and recovery periods, twice daily during the treatment period
Clinical signs:	Once daily during the pretreatment and recovery periods, twice daily during the treatment period
Body weights:	During the pretreatment period, Day 1, weekly, and prior to necropsy
Food consumption:	Weekly
ECG:	Not conducted
Ophthalmoscopy:	During the pretreatment period and near the end of Week 13
Hematology:	On day of necropsy*
Clinical chemistry:	On day of necropsy*
Coagulation:	On day of necropsy*
Urinalysis:	On day of necropsy*
Gross pathology:	At necropsy*
Organ weights:	At necropsy*
Histopathology:	At necropsy*
Toxicokinetics:	Days 1 and 88 at ~1, 2, 4, 7, and 24 hours after dosing

* Necropsy on Day 91 for main study animals and on Day 147 for recovery animals

Results

Mortality

Four females treated with 250 mg/kg were found dead or euthanized during the treatment period. According to the pathologist's report, the mortalities of animals # 109, 114, and 118 were attributed to gavage trauma or dose administration errors. The cause of death was unknown for animal #111. Clinical signs and histopathology

findings possibly related to death/euthanization are listed in the table below. The mortalities could possibly be due to gavage or dose administration errors, however, it is not completely clear, especially for animal #114, the animal that was euthanized. The temporal relationship between the dosing and deaths or euthanization is not provided.

Dose of PF-02341066	Animal #	Sex	Found Dead or Euthanized	Day	Important observations related to euthanization or death
250 mg/kg	109	Female	Found dead	21	• Left eye partially closed, haircoat stained on nose (red) • Gross pathology/ histopathology findings: multiple white materials attached to lung, inflammation in esophagus, gavage trauma in thymus (crystal-like eosinophilic foreign material mixed with inflammatory infiltrate on the thymic capsule)
	111	Female	Found dead	21	• No clinical signs • Gross pathology/ histopathology findings: abnormal color (red) and congestion in lung
	114	Female	Euthanized	44	• Activity decreased, thorax edema, left eye partially closed, haircoat rough, haircoat stained on nose (red), lame/limping • Gross pathology/ histopathology findings: Submucosal infiltration of brown pigment laden macrophages in esophagus, inflammation in trachea
	118	Female	Found dead	44	• Chromodacryorrhea • Gross pathology/ histopathology findings: submucosal hemorrhage in esophagus, inflammation in trachea and lung, gavage trauma in thymus (crystal-like eosinophilic foreign material mixed with inflammatory infiltrate on the thymic capsule)

Clinical Signs

Clinical signs for animals found dead or euthanized are listed in the mortality table. Clinical signs for all animals during the treatment period are listed in the table below.

Clinical signs	No. of animals affected (No. of Observations)							
	Males				**Females**			
Dose (mg/kg)	0	10	30	100	0	10	50	250
Number of animals examined	15	15	15	15	15	15	15	15
Activity decreased	-	-	-	-	-	-	-	1 (3)
Chromodacryorrhea, left	-	-	-	-	-	-	-	1 (3)
Decreased skin tugor	-	2(2)	1(2)	-	-	-	-	1(2)
Decreased skin turgor, mild	-	-	-	1(6)	-	-	-	-
Edema, left cervical	-	-	-	-	-	-	-	1(13)
Edema, left thorax	-	-	-	-	-	-	-	2(12)
Eye partially closed, left	-	-	-	-	-	-	-	2(3)
Haircoat rough	-	-	-	-	-	-	-	1(2)
Haircoat, stained, nose (red)	-	-	-	-	-	-	-	1(3)
Lame/limping, left forelimb (mild)	-	-	-	-	-	-	-	1(22)
Lame/limping, left forelimb	-	-	-	-	-	-	-	1(2)
Hunched posture	-	-	-	-	-	-	-	2(3)

- = Clinical sign not observed in this group

Body Weights

Body weights were significantly lower than controls in males treated with 100 mg/kg and females treated with 250 mg/kg during the treatment period. These decreases in body weight gain corresponded to decreases in food consumption.

Figure 45: 3 Month Body Weight

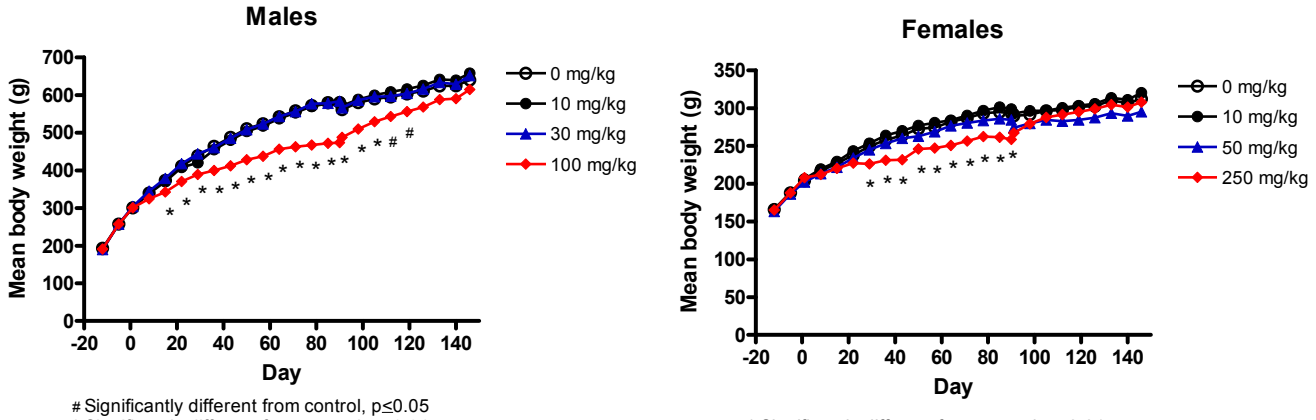

Significantly different from control, p≤0.05
* Significantly different from control, p≤0.01

* Significantly different from control, p≤0.01

Food Consumption

Food consumption was significantly decreased by 6-13% compared to controls in males treated with 100 mg/kg Days 1-8, 9-15, 16-22, 30-36, and 37-43, with a 7% decrease for the entire treatment period (Days 1-90). In females treated with 250 mg/kg, food consumption was significantly decreased 11-19% compared to controls Days 1-8, 16-22, 23-29, 30-36, 37-43, and 58-64, with a 10% decrease for the entire treatment period (Days 1-90).

Figure 46: 3 Month Rat Food Consumption

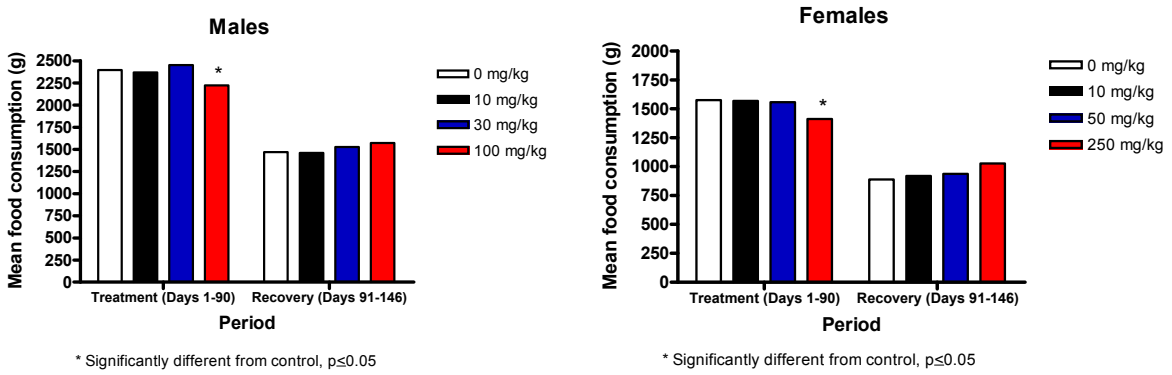

Ophthalmoscopy

Unremarkable

ECG

Not conducted

Hematology

Males

Index	Mean		Percentage deviation from Control					
	Control 0 mg/kg		10 mg/kg		30 mg/kg		100 mg/kg	
	Day 91	Day 147 (Recovery)	Day 91	Day 147 (Recovery)	Day 91	Day 147 (Recovery)	Day 91	Day 147 (Recovery)
Hemoglobin	14.50	15.06	-	-	-	-	↓5**	-
Hematocrit	43.44	45.90	-	-	-	-	↓5**	-
MCV	50.43	50.56	-	-	-	-	↓4**	-
MCH	16.84	16.58	-	-	-	-	↓4**	-
Reticulocytes	139.2	148.6	-	-	-	-	↓10	↓14
Platelets	1181.5	1182.4	-	-	-	-	↑24**	-
Neutrophils	1.077	1.248	-	-	-	-	↑110**	-

↑= increase ↓=decrease - = no test-article related changes; Significantly different from Control, * p<0.05, ** p<0.01

While the group means for reticulocytes were not significantly decreased in the 100 mg/kg group, decreases were observed in 2 individual males (Animal #49 and 52). The reticulocyte counts for these animals were 80 and 88 (10e3/µL), respectively, and were 43 and 37% lower than the control group mean of 139.2 (10e3/µL) and 35 and 29% lower than 100 mg/kg group mean of 124.8 (10e3/µL) on Day 91.

Females

Index	Mean		Percentage deviation from Control					
	Control 0 mg/kg		10 mg/kg		50 mg/kg		250 mg/kg	
	Day 91	Day 147 (Recovery)	Day 91	Day 147 (Recovery)	Day 91	Day 147 (Recovery)	Day 91	Day 147 (Recovery)
MCV	52.53	52.94	-	-	-	-	↓4*	-
MCH	17.85	17.78	-	-	-	-	↓6**	-
Platelets	1187.0	1107.8	-	-	-	↑11*	↑35**	↑16*
WBC	4.96	5.38	-	-	-	-	↑65*	-
Neutrophils	0.734	0.670	-	-	-	-	↑233**	↑111
Monocytes	0.142	0.186	-	-	-	-	↑125**	↑72

↑= increase ↓=decrease - = no test-article related changes, Significantly different from Control, * p<0.05, ** p<0.01

Clinical Chemistry

Males

Index	Mean		Percentage deviation from Control					
	Control 0 mg/kg		10 mg/kg		30 mg/kg		100 mg/kg	
	Day 91	Day 147 (Recovery)	Day 91	Day 147 (Recovery)	Day 91	Day 147 (Recovery)	Day 91	Day 147 (Recovery)
ALT	33.8	31.0	↑26**	-	↑170**	-	↑547**	-
AST	94.6	73.6	↑35*	-	↑90**	-	↑315**	-
ALP	82.6	66.6	-	-	-	-	↑42**	-
Glucose	189.7	185.2	-	-	-	-	↓23**	-
BUN	16.5	<13.2	-	-	-	↑26*	↑15*	↑24*
Creatinine	0.36	0.32	-	-	-	-	↑11*	-

↑= increase ↓=decrease - = no test-article related changes, Significantly different from Control, * p<0.05, ** p<0.01

Females

Index	Mean		Percentage deviation from Control					
	Control 0 mg/kg		10 mg/kg		50 mg/kg		250 mg/kg	
	Day 91	Day 147 (Recovery)	Day 91	Day 147 (Recovery)	Day 91	Day 147 (Recovery)	Day 91	Day 147 (Recovery)
ALT	36.2	57.0	-	-	-	-	↑205**	-
AST	110.1	115.8	-	-	-	-	↑93**	-
ALP	47.7	44.4	-	-	-	-	↑150**	-
Glucose	153.8	143.0	-	-	-	-	↓16*	-
BUN	15.9	<15.8	-	-	↑15*	-	↑34**	-

↑= increase ↓=decrease - = no test-article related changes
Significantly different from Control, * p<0.05, ** p<0.01

Urinalysis

The urinary pH was slightly decreased in males treated with 30 and 100 mg/kg PF-02341066 on Day 91. No treatment-related effect on urinary pH was observed in females.

Males

Index	Mean		Percentage deviation from Control					
	Control 0 mg/kg		10 mg/kg		30 mg/kg		100 mg/kg	
	Day 91	Day 147 (Recovery)	Day 91	Day 147 (Recovery)	Day 91	Day 147 (Recovery)	Day 91	Day 147 (Recovery)
pH	7.15	6.90	-	-	↓6**	-	↓11**	-

↑= increase ↓=decrease - = no test-article related changes; Significantly different from Control, * p<0.05, ** p<0.01

Gross Pathology

Treatment-Related Macroscopic Findings		No. of animals affected							
		Males				**Females**			
Dose (mg/kg)		0	10	30	100	0	10	50	250
Number of animals examined		0/10/**5**	0/10/**5**	0/10/**5**	0/10/**5**	0/10/**5**	0/10/**5**	0/10/**5**	4*/7/**4**
Ileum	Dilatation	-	**-**	**-**	0/2/**0**	-	-	-	0/1/**0**
Jejunum	Dilatation	-	-	-	0/1/**0**	-	-	-	0/1/**0**
Kidney	Mass/abscess, subcutaneous	-	-	-	-	-	-	-	1*/0/**0**
Lung	Abnormal color	-	-	-	-	-	-	-	2*/0/**0**

Number of animals examined and affected: Early deaths*/ Terminal necropsy / **Recovery necropsy**
- = no test-article related changes

Organ Weights

Males

Group and Dose		Mean		Percentage deviation from Control					
		Control 0 mg/kg		10 mg/kg		30 mg/kg		100 mg/kg	
Necropsy		Terminal	Recovery	Terminal	Recovery	Terminal	Recovery	Terminal	Recovery
Number of animals examined		10	5	10	5	10	5	10	5
Kidney	Absolute (g)	3.78	4.01	-	-	-	-	↓21**	-
	Relative Brain (%)	1.66	1.85	-	-	-	-	↓16*	-
Liver	Absolute (g)	13.88	14.29	-	-	-	-	↓15*	-
	Relative Brain (%)	6.08	6.57	-	-	-	-	↓10*	-
Spleen	Absolute (g)	0.864	0.819	-	-	-	-	↓20**	-
	Relative Brain (%)	0.380	0.377	-	-	-	-	↓15*	-
Thymus	Absolute (g)	0.3828	0.3430	-	-	-	-	↓26**	-
	Relative Brain (%)	0.1686	0.1585	-	-	-	-	↓21**	-

↑= increase ↓=decrease - = no test-article related changes, Significantly different from Control, * p<0.05, ** p<0.01

Females

Group and Dose		Mean		Percentage deviation from Control					
		Control 0 mg/kg		10 mg/kg		50 mg/kg		250 mg/kg	
Necropsy		Terminal	Recovery	Terminal	Recovery	Terminal	Recovery	Terminal	Recovery
Number of animals examined		10	5	10	5	10	5	7	4
Heart	Absolute (g)	1.03	1.12	-	-	-	-	↑14*	↑17*
	Relative Brain (%)	0.52	0.55	-	-	-	-	↑15	↑20
Kidney	Absolute (g)	1.93	1.92	-	-	↓8*	-	↓12*	-
	Relative Brain (%)	0.99	0.94	-	-	↓6	-	↓12*	-
Spleen	Absolute (g)	0.531	0.530	-	-	-	-	↓16*	-
	Relative Brain (%)	0.272	0.260	-	-	-	-	↓16*	-
Thymus	Absolute (g)	0.3273	0.2630	-	-	-	-	↓38**	-
	Relative Brain (%)	0.1672	0.1292	-	-	-	-	↓38**	-

↑= increase ↓=decrease - = no test-article related changes, Significantly different from Control, * p<0.05, ** p<0.01

Histopathology

Histopathologic examination of all tissues was conducted for all main study animals in the control and high dose groups. Target organs were examined in the main study animals in the low and mid dose groups and recovery animals in all groups. Gross lesions were collected and processed at the discretion of the study pathologist. Histopathology findings possibly related to the early mortalities are listed in the mortality table and treatment-related findings are listed in the table below.

Adequate Battery: Yes
Peer Review: Yes

Histological Findings

Treatment-Related Microscopic Findings			No. of animals affected							
			Males				**Females**			
Dose (mg/kg)			0	10	30	100	0	10	50	250
Number of animals examined			0/10/**5**	0/10/**5**	0/10/**5**	0/10/**5**	0/10/**5**	0/10/**5**	0/10/**5**	4*/7/**4**
Organ	Finding									
Bone marrow	Cell debris, myeloid	Minimal	-	-	0/1/**0**	0/10/**0**	**-**	-	-	0/7/**0**
	Increased cellularity	Mild	-	-	-	-	**-**	-	-	1*/1/**0**
Cecum	Vacuolation	Minimal	-	-	-	0/3/**0**	**-**	-	-	0/4/**0**
Colon	Vacuolation	Minimal	-	-	-	0/2/**0**	**-**	-	-	0/1/**0**
Duodenum	Vacuolation	Minimal	-	-	-	0/9/**0**	**-**	-	-	0/7/**0**
	Vacuolation, extrahepatic bile duct	Minimal	-	-	0/2/**0**	0/8/**0**	**-**	-	0/3/**0**	1*/5/**0**
Heart	Chronic inflammation	Minimal	-	-	-	-	**-**	-	-	0/1/**0**
	Myonecrosis	Total	0/6/**3**	0/5/**1**	0/10/**1**	0/9/**1**	0/1/**3**	0/4/**0**	0/1/**1**	0/2/**0**
		Minimal	0/6/**2**	0/4/**1**	0/9/**1**	0/4/**1**	0/0/**3**	0/4/**0**	0/1/**1**	0/2/**0**
		Mild	0/0/**1**	0/1/**0**	0/1/**0**	0/5/**0**	0/1/**0**	-	-	-
Ileum	Vacuolation	Minimal	-	-	0/5/**0**	0/9/**0**	-	-	0/2/**0**	0/6/**0**
Jejunum	Dilatation	Minimal	-	-	-	-	-	-	-	0/1/**0**
	Vacuolation	Minimal	-	-	-	0/6/**0**	-	-	-	0/6/**0**
Liver	Vacuolation, bile duct	Total	-	-	0/10/**NE**	0/10/**0**	-	**-**	0/10/**NE**	4*/7/**0**
		Minimal	-	-	0/10/**NE**	-	-	-	0/10/**NE**	2*/0/**0**
		Mild	-	-	-	0/10/**0**	-	**-**	-	2*/7/**0**
Lung	Alveolar histiocytosis	Total	0/5/**4**	0/3/ **NE**	0/5/ **NE**	0/10/**2**	0/6/**3**	0/6/ **NE**	0/6/ **NE**	4*/7/**2**
		Minimal	0/5/**4**	0/3/ **NE**	0/5/ **NE**	0/1/**2**	0/6/**3**	0/6/ **NE**	0/6/ **NE**	2*/1/**2**
		Mild	-	-	-	0/2/**0**	-	-	-	1*/1/**0**
		Moderate	-	-	-	0/7/**0**	-	-	-	1*/5/**0**
	Conges ion	Minimal	-	-	**-**	**-**	-	-	-	2*/0/**0**
Mesenteric lymph node	Foamy macrophages	Total	0/0/**4**	0/0/**5**	0/0/**5**	0/10/**5**	0/0/**4**	0/0/**5**	0/0/**5**	3*/7/**4**
		Mininmal	0/0/**4**	0/0/**5**	0/0/**5**	0/0/**2**	0/0/**3**	0/0/**5**	0/0/**5**	0/0/**1**
		Mild	-	-	**-**	0/4/**3**	0/0/**1**	**-**	**-**	0/1/**3**
		Moderate	-	-	-	0/6/**0**		-	-	3*/6/**0**
Pituitary	Vacuolation, pars distalis	Minimal	-	-	-	0/10/**0**	-	-	-	2*/7/**0**
Prostate	Vacuolation	Minimal	-	-	-	0/1/**1**	NA	NA	NA	NA
Salivary gland, mandibular	Swelling, acinar cells	Minimal	-	**-**	-	0/6/**1**	-	-	-	1*/5/**0**
Thymus	Lymphocytolysis	Total	-	-	-	0/10/**0**	-	-	-	4*/7/**0**
		Minimal	-	-	-	0/10/**0**	-	-	-	2*/7/**0**
		Moderate	-	-	-	-	-	-	-	1*/0/**0**
		Marked	-	-	-	-	-	-	-	1*/0/**0**

Number of animals examined and affected: Early deaths*/ Terminal necropsy / **Recovery necropsy**
- = no test-article related changes NA= Not Applicable, tissue does not exist in this sex; NE=Not examined, tissue not examined in this group

In order to further characterize the microscopic vacuolar findings, ultrastructural evaluation and immunohistochemical staining for adipophilin (a protein that forms the membrane around non-lysosomal lipid droplets) were conducted on representative tissues of the liver (bile duct), duodenum (enterocyte) and mesenteric lymph node (macrophage) from animal # 46 and/or 47 in the 100 mg/kg group. Control tissues from animal #4 were used for comparison. Ultrastructural investigation revealed the presence of intracytoplasmic multiple membrane-bound variably sized multi- or uni-centric myelin figures in the bile duct epithelial cells, enterocytes, and macrophages. These multiple lamellar structures corresponded to the intracytoplasmic vacuoles (bile duct and enterocyte) or foamy cytoplasm (macrophage) seen microscopically, and were consistent with phospholipid accumulation. Adipophilin staining was negative for these vacuoles. Therefore, cellular vacuolation and the presence of foamy macrophages observed in the histopathology were considered to be due to phospholipidosis by the pathologist.

Toxicokinetics

The toxicokinetics of PF-02341066 (0, 10, 30 and 100 mg/kg in males and 0, 10, 50 and 250 mg/kg in females) were evaluated Days 1 and 88 with samples collected at 1, 2, 4, 7, and 24 hours after dosing (see table excerpted from the sponsor's submission).

- C_{max} and $AUC_{(0-24)}$ increased with increasing dose.
- C_{max} and $AUC_{(0-24)}$ values were higher on Day 88 compared to Day 1.
- Exposure to PF-02341066 was higher in males than females with C_{max} and $AUC_{(0-24)}$ values similar between males and females or higher in males than females despite higher mid and high doses in females than males.
- T_{max} ranged from 1-7 hours.

Gender	Dose (mg/kg/day)	Study Day	Cmax (ng/mL)	tmax (h)	AUC(0-24) (ng*h/mL)
Males	10	1	84.9	4	835
		88	343	4	3750
	30	1	564	4	5900
		88	1290	4	14300
	100	1	1350	7	20500
		88	2090	4	37600
Females	10	1	87.9	2	588
		88	120	4	1060
	50	1	721	2	6130
		88	813	4	10100
	250	1	978	1	15300
		88	2090	4	32700

Study title: 3-month oral toxicity study of PF-02341066 in dogs with a 2-month recovery

Study no.:	09GR346
Study report location:	M4.2.3.2
Conducting laboratory and location:	Pfizer Global Research & Development Drug Safety Research & Development Eastern Point Rd. Groton, CT and (b) (4) (Toxicokinetics)
Date of study initiation:	October 8, 2009
GLP compliance:	Yes
QA statement:	Yes
Drug, lot #, and % purity:	PF-02341066, lot # E010009648, Purity: 99.6%

Key Study Findings

- Target organs of toxicity included the bone marrow, mesenteric lymph node, jejunum, and stomach
- Hematology changes included a decrease in RBC parameters (RBC count, hemoglobin, and hematocrit) and increases in white blood cell parameters (WBC count, neutrophils, lymphocytes, monocytes, and eosinophils), platelets, and fibrinogen
- Clinical chemistry changes included increases in ALT, AST, ALP, and GGT and decreases in albumin and calcium
- QT interval was increased from pretreatment levels in males treated with 5 and 25 mg/kg and females treated with 25 mg/kg at Weeks 6 and 13

Methods

Doses:	0, 1, 5, or 25 mg/kg
Frequency of dosing:	Once daily for 3 months (91 consecutive days), 2-month (57-day) recovery period
Route of administration:	Oral gavage
Dose volume:	1 mL/kg
Formulation/Vehicle:	0.5% methylcellulose
Species/Strain:	Beagle dog
Number/Sex/Group:	3/sex/group (main study) 2/sex/group (recovery)
Age:	>8 months at dose initiation
Weight:	Males: 6.9-11.6 kg at dose initiation Females: 5.9-8.5 kg at dose initiation
Satellite groups:	None

Observations and times:

Mortality:	Once daily during the pretreatment and recovery periods, twice daily during the treatment period
Clinical signs:	Once daily during the pretreatment and recovery periods, twice daily during the treatment period
Body weights:	During the pretreatment period, Day 1, weekly, and prior to necropsy
Food consumption:	Visually estimated ~1 week during the pretreatment and daily during the treatment and recovery periods
ECG:	Once during pretreatment, and predose and ~4 hours after dosing Weeks 6 and 13, and Day 146
Ophthalmoscopy:	During the pretreatment period and Weeks 13 and 21
Hematology:	During pretreatment period, and Days 48, 91, and 148
Clinical chemistry:	During pretreatment period, and Days 48, 91, and 148
Coagulation:	During pretreatment period, and Days 48, 91, and 148
Urinalysis:	Days 92 and Day 148
Gross pathology:	At necropsy*
Organ weights:	At necropsy*
Histopathology:	At necropsy*
Toxicokinetics:	Days 1 and 91 at 1, 2, 4, 7, and 24 hours after dosing

* Necropsy on Day 92 for main study animals and on Day 148 for recovery animals

Results

Mortality

No mortality was observed in this study.

Clinical Signs

Clinical signs for all animals during the treatment period are listed in the table below.

Clinical signs	No. of animals affected (No. of Observations)							
	Males				**Females**			
Dose (mg/kg)	0	1	5	25	0	1	5	25
Number of animals examined	5	5	5	5	5	5	5	5
Emesis, yellow	1 (2)	1 (1)	3 (8)	5 (19)	1 (1)	-	2 (10)	5 (16)
Emesis, white foamy	-	-	4 (16)	5 (43)	1 (1)	-	4 (9)	5 (19)
Emesis post-dose, food-like material	-	-	1 (1)	2 (2)	-	-	-	-
Emesis, food-like material	1 (1)	-	1 (1)	4 (16)	-	-	1 (1)	4 (6)
Feces, mucoid	-	-	1 (1)	1 (3)	1 (1)	-	-	3 (5)
Feces, watery	-	-	1 (3)	5 (55)	2 (6)	-	1 (11)	5 (24)
Salivation, clear	-	-	-	3 (28)	-	-	-	2 (31)

- = Clinical sign not observed in this group

Body Weights

Unremarkable

Food Consumption

Report states that there were no treatment-related changes in food consumption, however, data are not provided.

Ophthalmoscopy

Unremarkable

ECG

By the pre-dose time-points in Weeks 6 and 13, QT interval was increased in males treated with ≥ 5 mg/kg and in females treated with 25 mg/kg compared to baseline pretreatment (Day -10 for males and Day -9 for females) measurments. These increases in QT interval were not observed following the 2-month recovery period. There were no changes in mean pre-dose to post-dose QTc at either Week 6 or 13.

Males

Index	Mean change from pretreatment to pre-dose							
	Control 0 mg/kg		1 mg/kg		5 mg/kg		25 mg/kg	
	Week 6	Week 13	Week 6	Week 13	Week 6	Week 13	Week 6	Week 13
QTc (msec)	-0.856	-3.862	2.888	2.330	11.714*	7.384*	19.262**	13.322**
QT interval (msec)	-0.20	-4.92	3.86	0.12	16.92*	16.70**	21.58*	18.24**

Significantly different from Control, * $p<0.05$, ** $p<0.01$

Females

Index	Mean change from pretreatment to pre-dose							
	Control 0 mg/kg		1 mg/kg		5 mg/kg		25 mg/kg	
	Week 6	Week 13	Week 6	Week 13	Week 6	Week 13	Week 6	Week 13
QTc (msec)	1.920	1.434	1.030	0.994	-0.718	0.846	11.280	16.688*
QT interval (msec)	7.20	7.18	-4.46	-8.60	8.74	11.04	23.30*	26.70**

Significantly different from Control, * p<0.05, ** p<0.01

Hematology

Males

Index	Mean			Percentage deviation from Control								
	Control 0 mg/kg			1 mg/kg			5 mg/kg			25 mg/kg		
	Day 48	Day 91	Day 148 (Recovery)	Day 48	Day 91	Day 148 (Recovery)	Day 48	Day 91	Day 148 (Recovery)	Day 48	Day 91	Day 148 (Recovery)
RBC	7.882	7.614	7.725	-	-	-	-	-	-	↓12*	↓14	-
Hemoglobin	18.18	17.54	17.85	-	-	-	-	-	-	↓14**	↓14*	-
Hematocrit %	53.68	52.02	55.05	-	-	-	-	-	-	↓13*	↓13	-
Reticulocytes	64.0	64.8	50.5	-	-	-	-	-	-	-	↑38*	↑24
Platelets	263.4	243.2	247.0	-	-	-	-	-	-	↑65**	↑104**	-
WBC	7.74	7.90	6.55	-	-	-	-	-	-	↑64*	↑53	-
Neutrophils	4.572	4.932	3.725	-	-	-	-	-	-	↑53	↑47	-
Lymphocytes	2.458	2.266	2.205	-	-	-	-	-	-	↑54*	-	-
Monocytes	0.380	0.346	0.190	-	-	-	-	-	-	↑128**	↑83	-
Eosinophils	0.240	0.236	0.285	-	-	-	-	-	-	↑275*	↑289*	-
F brinogen	204.8	242.0	154.0	-	-	-	-	-	-	↑45	↑20	-

↑= increase ↓=decrease - = no test-article related changes
Significantly different from Control, * p<0.05, ** p<0.01

Females

Index	Mean			Percentage deviation from Control								
	Control 0 mg/kg			1 mg/kg			5 mg/kg			25 mg/kg		
	Day 48	Day 91	Day 148 (Recovery)	Day 48	Day 91	Day 148 (Recovery)	Day 48	Day 91	Day 148 (Recovery)	Day 48	Day 91	Day 148 (Recovery)
RBC	7.106	7.278	6.970	-	-	-	-	-	-	-	↓16*	-
Hemoglobin	16.18	16.46	15.60	-	-	-	-	-	-	-	↓14*	-
Hematocrit %	47.58	49.42	47.65	-	-	-	-	-	-	-	↓14*	-
Platelets	305.2	316.4	319.5	-	-	-	-	-	-	↑76**	↑101**	↑45
WBC	7.64	8.68	7.20	-	-	-	-	-	-	↑73*	↑37**	-
Neutrophils	4.490	5.228	4.215	-	-	-	-	-	-	↑68	↑31*	-
Lymphocytes	2.450	2.620	2.295	-	-	-	-	-	-	↑42*	↑24	-
Monocytes	0.334	0.328	0.325	-	-	-	-	-	-	↑211**	↑151	-
Eosinophils	0.286	0.298	0.320	-	-	-	-	↑50	-	↑231**	↑199*	-
Fibrinogen	195.0	184.8	239.5	-	-	-	-	-	-	↑51**	↑94**	-

↑= increase ↓=decrease - = no test-article related changes; Significantly different from Control, * p<0.05, ** p<0.01

Clinical Chemistry

Males

Index	Mean			Percentage deviation from Control								
	Control 0 mg/kg			1 mg/kg			5 mg/kg			25 mg/kg		
	Day 48	Day 91	Day 148 (Recovery)	Day 48	Day 91	Day 148 (Recovery)	Day 48	Day 91	Day 148 (Recovery)	Day 48	Day 91	Day 148 (Recovery)
ALT	34.8	33.0	37.5	-	-	-	-	-	-	↑136*	↑42*	-
AST	35.4	32.8	32.0	-	-	-	-	-	-	↑102**	↑107**	-
ALP	56.8	55.4	39.0	↑32	-	-	↑30	↑24	-	↑76	↑80*	-
GGT	<2.0	<2.0	<2.0	-	-	-	-	-	-	↑110*	-	-
Total protein	6.12	5.88	6.00	-	↓6*	-	-	↓6*	-	↓10**	↓8*	-
Albumin	3.54	3.34	3.40	-	↓5	-	↓6*	↓5	-	↓16**	↓18**	-
Calcium	10.84	10.20	10.35	-	-	-	-	-	-	↓8**	↓8**	-
BUN	15.4	14.2	12.0	-	-	-	-	-	-	↑17	↑30*	-

↑= increase ↓=decrease - = no test-article related changes; Significantly different from Control, * p<0.05, ** p<0.01

Females

Index	Mean			Percentage deviation from Control								
	Control 0 mg/kg			1 mg/kg			5 mg/kg			25 mg/kg		
	Day 48	Day 91	Day 148 (Recovery)	Day 48	Day 91	Day 148 (Recovery)	Day 48	Day 91	Day 148 (Recovery)	Day 48	Day 91	Day 148 (Recovery)
ALT	27.6	29.4	27.5	-	-	-	-	-	-	↑32	↑39	-
AST	29.8	30.0	29.5	-	-	-	↑26*	↑24*	-	↑99**	↑107**	-
ALP	55.2	55.6	51.0	-	-	-	↑33	↑17	-	↑47	↑46	↑73
GGT	<2.0	<2.0	<2.0	↑40	↑40*	-	-	↑20*	-	-	↑40*	-
Albumin	3.42	3.32	3.40	-	-	-	-	-	-	↓8	↓14*	-

↑= increase ↓=decrease - = no test-article related changes; Significantly different from Control, * p<0.05, ** p<0.01

Urinalysis

Unremarkable

Gross Pathology

Treatment-Related Macroscopic Findings		No. of animals affected							
		Males				**Females**			
Dose (mg/kg)		0	1	5	25	0	1	5	25
Number of animals examined		3/**2**	3/**2**	3/**2**	3/**2**	3/**2**	3/**2**	3/**2**	3/**2**
Jejunum	Abnormal color	-	-	1/**0**	-	-	-	1/**0**	**-**
Mesenteric lymph node	Abnormal color	-	-	-	3/**0**	-	-	-	-
Skin	Abrasion	-	-	-	-	-	-	-	1/**0**
Stomach	Abnormal color	-	-	1/**0**	-	-	-	-	-

Number of animals examined and affected: Terminal necropsy / **Recovery necropsy** - = no test-article related changes

Organ Weights

Unremarkable

Histopathology

Histopathologic examination of all tissues was conducted for all main study animals. No tissues were examined from recovery animals because no target organs were identified by the sponsor at the end of the treatment phase. Gross lesions were examined at the discretion of the study pathologist. Histopathology findings for the terminal necropsy are in the table below.

Adequate Battery: Yes
Peer Review: Yes

Histological Findings

Treatment-Related Microscopic Findings			No. of animals affected							
			Males				Females			
Dose (mg/kg)			0	1	5	25	0	1	5	25
Number of animals examined			3	3	3	3	3	3	3	3
Organ	Finding									
Bone marrow	Increased cellularity, eosinophil	Minimal	-	1	-	1	-	-	-	2
Jejunum	Conges ion	Minimal	-	-	-	-	-	-	1	-
Mesenteric lymph node	Erythrophagocytosis, sinus	Total	-	2	3	3	1	1	3	2
		Mininmal	-	1	3	2	1	1	3	-
		Mild	-	1	-	1	-	-	-	2
Skin	Ulcer	Mild	-	-	-	-	-	-	-	1
Stomach	Conges ion	Minimal	-	-	1	-	-	-	-	-

Number of animals examined and affected: Terminal necropsy - = no test-article related changes

Toxicokinetics

The toxicokinetics of PF-02341066 (0, 1, 5, and 25 mg/kg) were evaluated Days 1 and 91 with samples collected at 1, 2, 4, 7, and 24 hours after dosing (see table excerpted from the sponsor's submission).

- C_{max} and $AUC_{(0-24)}$ increased with increasing dose; increases were greater than dose proportional between 1 and 5 mg/kg and less than dose proportional between 5 and 25 mg/kg
- C_{max} and $AUC_{(0-24)}$ values were higher on Day 91 compared to Day 1, $AUC_{(0-24)}$ values were approximately 2-3 fold higher on Day 91 than on Day 1
- T_{max} ranged from 1.2-6.0 hours.

Dose (mg/kg/day)	Study Day	Gender	Cmax (ng/mL)			tmax (h)			AUC(0-24) (ng*h/mL)		
			Mean	SD	n	Mean	SD	n	Mean	SD	n
1	1	Male	40.4	12.9	5	2.6	1.3	5	518	149	5
		Female	44.8	13.1	5	2.0	0.0	5	502	118	5
		Overall	42.6	12.5	10	2.3	0.95	10	510	127	10
	91	Male	78.8	16.6	5	3.0	1.4	5	1220	277	5
		Female	82.6	4.12	5	3.2	1.1	5	1280	119	5
		Overall	80.7	11.6	10	3.1	1.2	10	1250	204	10
5	1	Male	300	250	5	1.2	0.45	5	3930	3220	5
		Female	322	63.1	5	1.4	0.55	5	4150	686	5
		Overall	311	172	10	1.3	0.48	10	4040	2200	10
	91	Male	614	238	5	4.0	2.1	5	10200	3740	5
		Female	475	64.2	5	1.6	1.3	5	7570	1720	5
		Overall	545	180	10	2.8	2.1	10	8900	3080	10
25	1	Male	739	655	5	1.6	1.3	5	9270	7490	5
		Female	889	442	5	1.8	1.3	5	12800	6620	5
		Overall	814	532	10	1.7	1.3	10	11100	6920	10
	91	Male	1440	547	5	4.8	3.0	5	25900	10100	5
		Female	2200	748	5	6.0	2.2	5	43400	13700	5
		Overall	1820	737	10	5.4	2.6	10	34600	14600	10

Overall = Males and Females Combined

Histopathology inventory

Study	04HGF004	09GR347	09GR346
Species	Rat	Rat	Dog
Adrenals		X*	X*
Aorta		X	X
Bone Marrow smear	X	X	X
Bone	X		
Brain	X*	X*	X*
Cecum	X	X	X
Cervix		X	X
Colon	X	X	X
Duodenum	X	X	X
Epididymis		X*	X
Esophagus		X	X
Eye	X	X	X
Fallopian tube			
Gall bladder			X
Gross lesions		X	X
Harderian gland		X	
Heart	X*	X*	X*
Ileum	X	X	X
Injection site			
Jejunum	X	X	X
Kidneys	X*	X*	X*
Lachrymal gland			
Larynx			
Liver	X*	X*	X*
Lungs	X	X	X
Lymph nodes, cervical			
Lymph nodes mandibular			
Lymph nodes, mesenteric		X	X
Mammary Gland		X	X
Nasal cavity			
Optic nerves	X	X	X
Ovaries	X*	X*	X
Pancreas	X	X	X
Parathyroid		X	X
Peripheral nerve		X	X
Pharynx			

Study	04HGF004	09GR347	09GR346
Species	Rat	Rat	Dog
Pituitary		X	X
Prostate		X*	X
Rectum			
Salivary gland	X	X	X
Sciatic nerve	X		
Seminal vesicles		X	
Skeletal muscle		X	X
Skin		X	X
Spinal cord		X	X
Spleen	X*	X*	X*
Sternum	X	X	X
Stomach	X	X	X
Teeth			
Testes	X*	X*	X*
Thymus	X*	X*	X*
Thyroid		X	X
Tongue		X	X
Trachea		X	X
Urinary bladder		X	X
Uterus		X	X
Vagina		X	X
Zymbal gland			

X, histopathology performed
*, organ weight obtained

7 Genetic Toxicology

7.1 *In Vitro* Reverse Mutation Assay in Bacterial Cells (Ames)

Study title: Bacterial reverse mutation assay of PF-2341066

Study no.:	3565
Study report location:	M4.2.3.3.1
Conducting laboratory and location:	Pfizer Global Research & Development Safety Sciences 2800 Plymouth Rd. Ann Arbor, MI
Date of study initiation:	March 11, 2005
GLP compliance:	Yes
QA statement:	Yes
Drug, lot #, and % purity:	PF-02341066, lot # AK-100830-26-42, Purity: 97.25%

Key Study Findings

- PF-02341066 did not increase the number of revertant colony counts of any strain in the absence or presence of S-9 activation, therefore, PF-02341066 was not mutagenic in this valid assay.

Methods

Strains:	*Salmonella typhimurium* TA98, TA100, TA1535, TA1537 *Escherichia coli* WP2*uvr*A
Concentrations in definitive study:	TA98, TA100, TA1535, and TA1537: 0, 31.3, 62.5, 125, 250, and 500 µg/plate WP2*uvr*A: 0, 62.5, 125, 250, 500, and 1000 µg/plate
Basis of concentration selection:	Results of preliminary mutagenicity assay: Excessive cytotoxicity was observed at concentrations ≥500 µg/plate in TA98, TA100, TA1535, and TA1537 both with and without S-9 and ≥1600 µg/plate in WP2uvrA without S-9
Negative control:	DMSO (0.1 mL/plate)
Positive control:	2-aminoanthracene, 9-aminoacridine, 2-nitrofluorene, 4-nitroquinoline-N-oxide, Benzo[a]pyrene, and Sodium azide (see table below)
Formulation/Vehicle:	DMSO (0.1 mL/plate)
Incubation & sampling time:	Plates incubated for ~69 hours at 37°C prior to scoring for revertants

Positive control	Solvent	Strain	+/- S9
2-aminoanthracene	DMSO	TA100, TA1535, TA1537, and WP2*uvr*A	+
9-aminoacridine	Ethanol	TA1537	-
2-nitrofluorene	DMSO	TA98	-
4-nitroquinoline-N-oxide	DMSO	WP2*uvr*A	-
Benzo[a]pyrene	DMSO	TA98	+
Sodium azide	DMSO	TA100 and TA1535	-

Study Validity

Each concentration of PF-02341066 and positive controls was tested in triplicate in the definitive assay. Samples were considered positive for mutagenicity if they had at least a 2-fold increase in revertants compared with the respective vehicle control in strains TA98, TA100, or WP2*uvr*A, or at least a 3-fold increase in revertants compared with the respective vehicle control in strains TA1535 or TA1537. Tester strain integrity,

spontaneous revertant background frequency, positive control values, and toxicity were all valid, therefore, the test is valid.

Results

Preliminary mutagenicity assay

Excessive cytotoxicity was observed at concentrations ≥500 µg/plate PF-02341066 in TA98, TA100, TA1535, and TA1537 both with and without S-9 and ≥1600 µg/plate PF-02341066 in WP2*uvr*A without S-9. No precipitation was observed at any concentration. The number of revertants was no greater than 1.7-fold of vehicle controls in any strain with or without S-9. The data are presented in the table below (excerpted from sponsor's submission). Based on these results, the highest concentration of PF-02341066 chosen for the definitive assay was 500 µg/plate for the *Salmonella typhimurium* strains and 1000 µg/plate for WP2*uvr*A.

Table 36: Preliminary Mutagencity

		TA-1535		TA-1537		TA-98		TA-100		WP2*uvr*A	
Phase	Dose (µg/plate)	Mean[c]	Fold of Control	Mean[c]	Fold of Control	Mean[c]	Fold of Control	Mean[c]	Fold of Control	Mean[c]	Fold of Control
S9-	Vehicle Control[d]	10.0	n/a	6.5	n/a	21.5	n/a	115.0	n/a	261.5	n/a
	16	15.5	1.6	8.5	1.3	21.5	1.0	125.5	1.1	274.5	1.0
	50	15.0	1.5	10.0	1.5	21.5	1.0	114.5	1.0	282.0	1.1
	160	16.5	1.7	7.5	1.2	22.5	1.0	87.0	0.8	283.0	1.1
	500	X	X	X	X	X	X	X	X	161.0	0.6
	1600	X	X	X	X	X	X	X	X	X	X
	5000	X	X	X	X	X	X	X	X	X	X
	Positive Control[e]	474.0	47.4	615.5	94.7	280.0	13.0	871.5	7.6	1966.0	7.5
S9+	Vehicle Control[d]	12.5	n/a	11.5	n/a	25.0	n/a	127.5	n/a	280.0	n/a
	16	14.5	1.2	11.5	1.0	36.5	1.5	122.0	1.0	262.0	0.9
	50	16.5	1.3	7.0	0.6	37.5	1.5	125.5	1.0	288.5	1.0
	160	13.0	1.0	12.0	1.0	42.0	1.7	130.5	1.0	274.5	1.0
	500	X	X	X	X	X	X	X	X	225.0	0.8
	1600	X	X	X	X	X	X	X	X	X	X
	5000	X	X	X	X	X	X	X	X	X	X
	Positive Control[e]	449.5	36.0	301.5	26.2	474.0	19.0	1891.5	14.8	1568.5	5.6

n/a = Not applicable
X = Not analyzed due to toxicity to the background lawn.
[a] Data represent the mean of 2 plates.
[b] Fold of control refers to comparison with corresponding vehicle control.
[c] Mean refers to the mean number of colonies/plate.
[d] DMSO
[e] See page 11 for positive control compounds.

Definitive mutagenicity assay

The number of revertants observed in the vehicle controls was consistent with historical reference ranges in all bacterial strains. Positive controls increased the number of revertants by 5.4- to 94.8-fold of vehicle controls. Excessive cytotoxicity was observed at PF-02341066 concentrations ≥250 µg/plate in TA100 and TA1537 without S-9, at 500 µg/plate in TA98 and TA1535 with and without S-9 and TA100 and TA1537 with S-9, and at 1000 µg/plate in WP2*uvr*A with and without S-9. No precipitation was observed at any concentration. The number of revertants was no greater than 1.9-fold of vehicle controls in TA1537 and 1.2-fold of vehicle controls in TA98, TA100, TA1535, and WP2*uvr*A with or without S-9. The data are presented in the table below (excerpted from sponsor's submission).

Table 37: Definitive Mutagenicity

Table 2: Definitive Mutagenicity Assay – Plate Incorporation[a]

Phase	Dose (µg/plate)	TA-1535[b] Mean[c]	TA-1535[b] Fold of Control	TA-1537[b] Mean[c]	TA-1537[b] Fold of Control	TA-98[b] Mean[c]	TA-98[b] Fold of Control	TA-100[b] Mean[c]	TA-100[b] Fold of Control	WP2*uvr*A[b] Mean[c]	WP2*uvr*A[b] Fold of Control
S9-	Vehicle Control[d]	16.3	n/a	7.7	n/a	31.0	n/a	86.3	n/a	255.3	n/a
	31.3	15.3	0.9	10.3	1.3	28.3	0.9	79.3	0.9	--	--
	62.5	15.7	1.0	14.7	1.9	32.0	1.0	81.7	0.9	269.3	1.1
	125	16.7	1.0	11.3	1.5	23.0	0.7	93.0	1.1	277.7	1.1
	250	16.0	1.0	X	X	15.7	0.5	X	X	246.7	1.0
	500	X	X	X	X	X	X	X	X	164.0	0.6
	1000	--	--	--	--	--	--	--	--	X	X
	Positive Control[e]	445.7	27.3	727.0	94.8	255.7	8.2	963.7	11.2	1924.3	7.5
S9+	Vehicle Control[d]	15.7	n/a	11.3	n/a	38.7	n/a	97.3	n/a	279.7	n/a
	31.3	15.3	1.0	13.0	1.1	43.3	1.1	97.3	1.0	--	--
	62.5	13.3	0.9	16.7	1.5	40.0	1.0	103.0	1.1	276.3	1.0
	125	12.3	0.8	14.3	1.3	42.7	1.1	106.3	1.1	285.7	1.0
	250	12.0	0.8	13.3	1.2	44.7	1.2	103.7	1.1	268.0	1.0
	500	X	X	X	X	X	X	X	X	251.0	0.9
	1000	--	--	--	--	--	--	--	--	X	X
	Positive Control[e]	357.7	22.8	351.3	31.0	540.0	14.0	1877.7	19.3	1507.3	5.4

n/a = Not applicable
X = Not analyzed due to toxicity to the background lawn.
-- = Not tested
[a] Data represent the mean of 3 plates.
[b] Fold of control refers to comparison with corresponding vehicle control.
[c] Mean refers to the mean number of colonies/plate.
[d] DMSO
[e] See page 11 for positive control compounds.

Conclusion: PF-02341066 was not mutagenic under the conditions of this valid assay.

7.2 *In Vitro* Assays in Mammalian Cells

Study title: *In vitro* structural chromosome aberration assay of PF-2341066 in human peripheral lymphocytes

Study no.:	3554
Study report location:	M4.2.3.3.1
Conducting laboratory and location:	Pfizer Global Research & Development Safety Sciences 2800 Plymouth Rd. Ann Arbor, MI
Date of study initiation:	February 24, 2005
GLP compliance:	Yes
QA statement:	Yes
Drug, lot #, and % purity:	PF-02341066, lot # AK-100830-26-42, Purity: 97.25%

Key Study Findings

- PF-02341066 was genotoxic as evidenced by significant increases in the percentage of structural and numerical chromosomal aberrations both with and without S-9 activation in human peripheral lymphocytes in this valid assay.
- PF-02341066 increased the number of cells with structural chromosomal aberrations at 3 hours both with and without S-9 activation.
- PF-02341066 increased the number of cells with numerical chromosomal aberrations at 3 hours both with and without S-9 activation and at 24 hours without S-9 activation.

Methods

Cell line:	Human peripheral lymphocytes
Concentrations in definitive study:	See concentration table below
Basis of concentration selection:	Cytotoxicity results of range-finding assay
Negative control:	DMSO
Positive control:	Without S-9: Mitomycin C (0.4 µg/mL for 3 hour incubation and 0.1 µg/mL for 24 hour incubation) With S-9: Cyclophosphamide (10 µg/mL)
Formulation/Vehicle:	DMSO
Incubation & sampling time:	Incubation: 3 hours with and without S-9 and 24 hours without S-9 Harvest time: 24 hours

Concentrations used in definitive study

	Exposure period	Concentrations of PF-02341066 (µg/mL) tested	Concentrations of PF-02341066 (µg/mL) scored
Without S-9 (-)	3 hours	2.5, 5.0, 7.5, 10.0, 12.5, and 15.0	2.5, 5.0, and 7.5
	24 hours	0.10, 0.25, 1.0, 1.5, 2.0, and 2.5	1.0, 1.5, and 2.5
With S-9 (+)	3 hours	1.0, 2.5, 5.0, 7.5, 10.0, and 12.5	1.0, 5.0, and 10.0

Study Validity

In the definitive assay, each dose of PF-02341066 was tested in duplicate with 100 cells per culture scored for structural chromosomal aberrations, therefore, there were 200 cells scored per treatment. The criteria for a positive response were a statistically significant dose-related increase in aberrant cells in the treated samples relative to the concurrent vehicle control with the increases reproducible between replicate cultures. The criteria for a positive result are adequate, and positive controls produced significant increases in the percentage of cells with structural aberrations compared to the vehicle controls. The study appears to be valid.

Results

Concentration range-finding assay

For the 3-hour treatment, concentrations of 2.5 to 20 µg/mL PF-02341066 produced mitotic index suppressions of 36-74% with S-9 activation and 2-75% without S-9 activation. The 24-hour treatment without S-9 activation produced mitotic index suppressions of 0-74% with concentrations of 0.05 to 5.0 µg/mL PF-02341066. Based on these cytotoxicity results, the highest concentrations chosen for the definitive study were 12.5 µg/mL for the 3-hour treatment with S-9, 15.0 µg/mL for the 3-hour treatment without S-9, and 2.5 µg/mL for the 24-hour treatment without S-9.

Definitive chromosome aberration assay

Vehicle control aberration frequencies ranged from 0-1%, which were within reported literature values and historical reference ranges. Positive controls (cyclophosphamide and mitomycin C), induced aberrations in 25-42% of cells. In the 3-hour assay with S-9 activation, PF-02341066 induced mitotic index suppressions of approximately 28%, 41%, and 56% at 1, 5, and 10 µg/mL, respectively. The percentage of cells with structural chromosome aberrations ranged from 0.5-6% with a statistically significant increase observed at 10 µg/mL (6% abnormal cells). The percentages of cells with numerical aberrations ranged from 0.6-13.4% polyploid cells with increases at 5 and 10 µg/mL. Data for the 3-hour assay with S-9 activation are present in the table below (excerpted from sponsor's submission).

Table 38: 3-Hour Chromasomal Aberration with Metabolic Activation

Treatment[a]	Concentration	Mean (%) Mitotic Suppression[b]	Mean (%) Abnormal Cells[c]	p-value[d]	Mean (%) PE cells[e]
DMSO	1%	NA	1	NA	0.05
PF-2341066 (µg/mL)	1	27.63	0.5	0.88	0.6
	5	41.23	3	0.14	1.4
	10	56.14	6	0.006*	13.4
Cyclophosphamide (µg/mL)	10	46.93	42	<0.001*	0.1

[a]Two replicate cultures evaluated for each treatment group; when possible 100 cells per culture are analyzed for chromosome damage.
[b]Mean (%) Mitotic Suppression = [One minus the quotient (Mean Test Article Mitotic Index/Mean Vehicle Control Mitotic Index)] (x) 100.
[c]Mean (%) Abnormal Cells = (Sum of abnormal cells excluding gaps for duplicate cultures/Sum of cells scored) (x) 100.
[d]Data analyzed by one-tailed Fisher's Exact test for increases in abnormal cells excluding gaps compared to the vehicle control value.
[e]Mean (%) PE cells = (Sum of polyploidy (P) and endoreduplication (E) for duplicate cultures/Sum of cells scored) (x) 100.
*Statistically significant at the 5% level

DMSO= Dimethylsulfoxide
NA=Not Applicable

Treatment	Concentration	total # cells analyzed for abs	Chromatid			Chromosome					total abnormal cells	total # cells analyzed for PE	P	E
			Gaps	Ct Brk	Ct Frg	R	Cs Brk	Cs Frg	R	M	PV				
DMSO	1.0%	100		1								1	1000	1	0
		100		1								1	1000	0	0
PF-2341066 (µg/mL)	1	100	1	1								1	1000	5	0
		100	1									0	1000	7	0
	5	100	1	2			1					3	1000	17	0
		100					1	2				3	1000	11	0
	10	100		3			1	3				7	1000	135	0
		100		5								5	1000	133	0
Cyclophosphamide (µg/mL)	10	50		18			1	3	3			22*	1000	1	0
		50		16			2	2	2			20*	1000	1	0

*At least one cell had more than 1 aberration.
Ct brk- Chromatid Break; Ct Frg- Chromatid Fragment; R- Chromatid damage (exchange, ring, dicentric and translocation)
Cs Brk- Chromosome Break; Cs Frg- Chromosome Fragment; M- Multiple Aberration; PV- Pulverized
PE- Polyploidy (P) or Endoreduplication (E) present.
DMSO- Dimethylsulfoxide

In the 3-hour assay without S-9 activation, PF-02341066 induced mitotic index suppressions of approximately 26%, 35%, and 55% at 2.5, 5.0, and 7.5 µg/mL, respectively. The percentage of cells with structural chromosome aberrations ranged from 1.5-3.5% with statistically significant increases observed at 2.5 and 7.5 µg/mL. It is important to note that 0% abnormal cells were observed in the concurrent vehicle control, making these slight increases statistically significant. The percentages of cells with numerical aberrations ranged from 1.05-27.1% polyploid cells with increases at all concentrations evaluated. Data for the 3-hour assay without S-9 activation are present in Table 39 (excerpted from sponsor's submission).

Table 39: 3 Hour Chromosomal Aberration Without Metabolic Activation

Treatment[a]	Concentration	Mean (%) Mitotic Suppression[b]	Mean (%) Abnormal Cells[c]	p-value[d]	Mean (%) PE cells[e]
DMSO	1%	NA	0	NA	0.1
PF-2341066 (µg/mL)	2.5	25.54	2.5	0.030*	1.05
	5	35.33	1.5	0.12	3.65
	7.5	54.89	3.5	0.007*	27.1
Mitomycin C (µg/mL)	0.4	39.67	31	<0.001*	0.2

[a]Two replicate cultures evaluated for each treatment group; when possible 100 cells per culture are analyzed for chromosome damage.
[b]Mean (%) Mitotic Suppression = [One minus the quotient (Mean Test Article Mitotic Index/Mean Vehicle Control Mitotic Index)] (x) 100.
[c]Mean (%) Abnormal Cells = (Sum of abnormal cells excluding gaps for duplicate cultures/Sum of cells scored) (x) 100.
[d]Data analyzed by one-tailed Fisher's Exact test for increases in abnormal cells excluding gaps compared to the vehicle control value.
[e]Mean (%) PE cells = (Sum of polyploidy (P) and endoreduplication (E) for duplicate cultures/Sum of cells scored) (x) 100.
*Statistically significant at the 5% level

DMSO= Dimethylsulfoxide
NA=Not Applicable

Treatment	Concentration	total # cells analyzed for abs	Chromatid			Chromosome					total abnormal cells	total # cells analyzed for PE	P	E
			Gaps	Ct Brk	Ct Frg	R	Cs Brk	Cs Frg	R	M	PV				
DMSO	1.0%	100	1									0	1000	0	0
		100										0	1000	2	0
PF-2341066 (µg/mL)	2.5	100	1	2				1				3	1000	10	0
		100		2								2	1000	11	0
	5	100	1					1				1	1000	39	0
		100		2								2	1000	34	0
	7.5	100		1				1				2	1000	282	0
		100		5								5	1000	260	0
Mitomycin C (µg/mL)	0.4	50		12				1	2			14*	1000	2	0
		50	1	10			2	5	3			17*	1000	2	0

*At least one cell had more than 1 aberration.
Ct brk- Chromatid Break; Ct Frg- Chromatid Fragment; R- Chromatid damage (exchange, ring, dicentric and translocation)
Cs Brk- Chromosome Break; Cs Frg- Chromosome Fragment; M- Multiple Aberration; PV- Pulverized
PE- Polyploidy (P) or Endoreduplication (E) present.
DMSO- Dimethylsulfoxide

In the 24-hour assay without S-9 activation, PF-02341066 induced mitotic index suppressions of approximately 8%, 30%, and 52% at 1, 1.5, and 2.5 µg/mL,

respectively. The percentage of cells with structural chromosome aberrations ranged from 0.5-2.0% with no statistically significant increases. The percentages of cells with numerical aberrations ranged from 1.35-85% polyploid cells with increases at all concentrations evaluated. Data for the 24-hour assay without S-9 activation are present in the table below (excerpted from sponsor's submission).

Table 40: 24 Hour Chromosomal Aberration Without Metabolic Activation

Treatment[a]	Concentration	Mean (%) Mitotic Suppression[b]	Mean (%) Abnormal Cells[c]	p-value[d]	Mean (%) PE cells[e]
DMSO	1%	NA	0.5	NA	0
PF-2341066 (μg/mL)	1	7.76	1	0.50	1.35
	1.5	30.17	0.5	0.75	12.5
	2.5	51.72	2	0.19	85
Mitomycin C (μg/mL)	0.1	19.83	25	<0.001*	0.1

[a]Two replicate cultures evaluated for each treatment group; when possible 100 cells per culture are analyzed for chromosome damage.
[b]Mean (%) Mitotic Suppression = [One minus the quotient (Mean Test Article Mitotic Index/Mean Vehicle Control Mitotic Index)] (x) 100.
[c]Mean (%) Abnormal Cells = (Sum of abnormal cells excluding gaps for duplicate cultures/Sum of cells scored) (x) 100.
[d]Data analyzed by one-tailed Fisher's Exact test for increases in abnormal cells excluding gaps compared to the vehicle control value.
[e]Mean (%) PE cells = (Sum of polyploidy (P) and endoreduplication (E) for duplicate cultures/Sum of cells scored) (x) 100.
*Statistically significant at the 5% level

DMSO= Dimethylsulfoxide
NA=Not Applicable

Treatment	Concentration	total # cells analyzed for abs	Gaps	Chromatid: Ct Brk	Chromatid: Ct Frg	Chromatid: R	Chromosome: Cs Brk	Chromosome: Cs Frg	Chromosome: R	Chromosome: M	Chromosome: PV	total abnormal cells	total # cells analyzed for PE	P	E
DMSO	1.0%	100						1				1	1000	0	0
		100										0	1000	0	0
PF-2341066 (μg/mL)	1	100										0	1000	15	0
		100		2								2	1000	12	0
	1.5	100										0	1000	96	0
		100		1								1	1000	154	0
	2.5	100		2				2				3*	1000	856	0
		100		1								1	1000	844	0
Mitomycin C (μg/mL)	0.1	50		8				3	1			12	1000	1	0
		50	1	6	1	2	3	2				13*	1000	1	0

*At least one cell had more than 1 aberration.
Ct brk- Chromatid Break; Ct Frg- Chromatid Fragment; R- Chromatid damage (exchange, ring, dicentric and translocation)
Cs Brk- Chromosome Break; Cs Frg- Chromosome Fragment; M- Multiple Aberration; PV- Pulverized
PE- Polyploidy (P) or Endoreduplication (E) present.
DMSO- Dimethylsulfoxide

Conclusion: PF-02341066 induced structural and numerical chromosome aberrations in human peripheral lymphocytes.

Study title: *In vitro* micronucleus assay with kinetochore analysis of PF-2341066 in Chinese hamster ovary (CHO) cultures

Study no.:	PG 0135
Study report location:	M4.2.3.3.1
Conducting laboratory and location:	Pfizer Global Research & Development Safety Sciences 2800 Plymouth Rd. Ann Arbor, MI
Date of study initiation:	Date not provided, study director signature on October 12, 2005
GLP compliance:	No
QA statement:	No
Drug, lot #, and % purity:	PF-02341066, lot # AK-100830-26-42, Purity: 97.25%

Key Study Findings

- PF-02341066 induced micronuclei in CHO-WBL cells with the presence of kinetochore staining, indicating that the genotoxic activity of the drug is aneugenic and not clastogenic in nature.

Methods

Cell line:	CHO-WBL cells
Concentrations in definitive study:	0.15-0.30 µg/mL tested; 0.20, 0.27, and 0.30 µg/mL scored
Basis of concentration selection:	Increases observed in the *in vitro* micronucleus assay (Lu, 2004), not submitted
Negative control:	DMSO
Positive control:	Clastogenicity without S-9: Mitomycin C (0.05 µg/mL) Aneugenicity: Noscapine (15 µg/mL)
Formulation/Vehicle:	DMSO
Incubation & sampling time:	24 hours without S-9

The objective of this assay was to discern clastogenic (chromosome breakage) versus aneugenic (whole chromosome loss) chromosomal events in micronuclei of CHO-WBL cells treated with PF-02341066 without metabolic activation. Cytochalasin B was used to prevent cytokinesis. Following treatment and cell fixation, slides were coated with anti-centromere (kinetochore) serum, allowing for the binding of an antihuman IgG antibody to the kinetochores. The antibody, which was conjugated with a fluorescent marker to stain kinetochores, was applied to the slides. Propidium iodide stain was applied to stain the nuclear DNA of the cells. Slides were evaluated microscopically for nuclear division (>100 cells scored) and micronucleus frequency in binucleated cells (500-2000 binucleated cells scored). A minimum of 500 binucleated cells or >70 micronuclei at a single concentration were evaluated microscopically for the presence of micronuclei containing kinetochores.

Study Validity

Criteria for a positive response included at least 2% micronucleated binucleate cells accompanied by a ≥ 2-fold increase in micronucleated binucleate cells compared to the vehicle control. The criterion for aneugenicity was a greater percent incidence of kinetochore positive micronuclei (K^+; indicating the presence of whole chromosomes) over kinetochore negative micronuclei (K^-; indicating the presence of chromosomal fragments) in micronucleated binucleate cells. Positive controls produced significant increases in the percentage of micronucleated binucleate cells compared to the vehicle controls. The study appears to be valid, but was exploratory.

Results

The results of this assay are shown in the table below (excerpted from sponsor's submission). The frequency of binucleated cells containing micronuclei was 6-fold higher in the mitomycin C positive control than the vehicle control. Mitomycin C had 84% K^- cells and 16% K^+ cells, confirming its clastogenic activity, and noscapine had 2% K^- cells and 98% K^+ cells, confirming its aneugenic activity. The percent micronucleated binucleate cells was 3- to 4-fold of the vehicle control at concentrations of 0.20-0.30 µg/mL PF-02341066, with 67-84% of the cells staining positive for K^+ cells.

Table 1. 24-Hour Assay Without Metabolic Activation

Treatment	Concentration (µg/mL)	%ND	%RND	%MN BNC	Fold of Control	%K^-	%K^+
DMSO	0	78		2		75	25
Mitomycin C	0.05	54	69	11	6	84	16
Noscapine	15	53	68	51	25	2	98
PF-2341066	0.15	--	--	--	--	--	--
PF-2341066	0.20	62	80	5	3	33	67
PF-2341066	0.27	53	68	8	4	16	84
PF-2341066	0.30	48	62	9	4	23	77

%ND = Percent nuclear division = (Cells with ≥2 nuclei/total number of cells analyzed) × 100; %RND = Percent relative nuclear division = (%ND per culture/mean %ND of vehicle controls) × 100; %MN BNC = Percent micronucleated binucleated cells = (number of micronucleated binucleate cells/total number binucleate cells scored) × 100; %K^- = Kinetochore negative micronuclei/total number of micronucleated binucleate cells scored) × 100; %K^+ = (Kinetochore positive micronuclei/total number of micronucleated binucleate cells scored) × 100; -- = Not scored.

Conclusion: PF-02341066 induced micronuclei in CHO-WBL cells with the presence of kinetochore staining, indicating aneugenicity.

7.3 *In Vivo* Clastogenicity Assay in Rodent (Micronucleus Assay)

Study title: *In vivo* micronucleus study of PF-2341066 in rats

Study no:	3665
Study report location:	M4.2.3.3.2
Conducting laboratory and location:	Pfizer Global Research & Development Safety Sciences 2800 Plymouth Rd. Ann Arbor, MI
Date of study initiation:	July 11, 2005
GLP compliance:	Yes
QA statement:	Yes
Drug, lot #, and % purity:	PF-02341066, lot # AK-100830-85-10, Purity: 99.77%

Key Study Findings

- PF-2341066 was positive for micronucleus induction in male rats treated with ≥250 mg/kg as evidenced by significant increases in micronucleated polychromatic erythrocytes in bone marrow.
- Treatment with PF-2341066 (250-1000 mg/kg) did not significantly increase micronucleated polychromatic erythrocytes in the bone marrow of female rats.
- Following a single administration of PF-2341066, exposure to PF-02341066 was higher in males than females. Sex-related differences in exposure may have contributed to differential effects on micronucleus formation in males and females.
- Bone marrow was collected for micronucleus assessment at a single time point, 24 hours after the second dose of PF-02341066, therefore, the study is invalid

Methods

Doses in definitive study:	0, 125, 250, 500, or 1000 mg/kg; micronucleus assessment conducted in 0, 250, 500, or 1000 mg/kg
Frequency of dosing:	Once per day for 2 days for micronucleus assessment and 1 day for toxicokinetic assessment
Route of administration:	Oral gavage
Dose volume:	10 mL/kg
Formulation/Vehicle:	0.5% methylcellulose
Species/Strain:	Sprague-Dawley rats
Number/Sex/Group:	5/sex/group
Satellite groups:	Toxicokinetics: 3/sex/group for vehicle group, 4/sex/group for PF-02341066-treated groups
Basis of dose selection:	7-day repeat dose oral toxicity study in male and female rats 50, 150, and 500 mg/kg) and a 2-day oral exploratory study in male and female rats (2000 mg/kg)
Negative control:	0.5% methylcellulose
Positive control:	Cyclophosphamide (20 mg/kg; 2 mg/mL)

Bone marrow was collected for micronucleus assessment at a single time point, 24 hours after the second dose of PF-02341066.

Study Validity

Criteria for a positive response included a reproducible, statistically significant, dose-related increase in the mean percentage of micronucleated polychromatic erythrocytes (%MNPCE) frequency in drug-treated groups compared to concurrent controls of the same sex, with at least one value exceeding the historical vehicle control range. Positive controls showed a significant increase in the mean percentage of micronucleated polychromatic erythrocytes compared to vehicle controls. Two treatments of PF-02341066 were administered in this study and bone marrow should have been collected at two time points for a valid study. Since bone marrow was collected at a single time point, the study appears to be invalid.

Results

Clinical signs and body weight

One male treated with 1000 mg/kg was found dead on Day 3. Clinical signs observed in this animal prior to death were dyspnea, salivation, hypoactivity, fecal staining, absent feces, and red staining of the muzzle. Clinical signs observed in the study are listed in the table below.

Clinical signs	No. of animals affected (No. of Observations)									
	Males					**Females**				
Dose (mg/kg)	0	125	250	500	1000	0	125	250	500	1000
Number of animals examined	5	5	5	5	5	5	5	5	5	5
Feces reduced	-	1(1)	5(9)	5(9)	4(8)	-	1(1)	3(4)	4(6)	5(9)
Feces absent	-	-	-	1(1)	1(1)	-	-	-	-	-
Fecal staining	-	1(1)	-	-	5(9)	-	-	-	1(1)	2(3)
Urine staining	-	-	-	-	-	-	-	-	1(1)	1(2)
Diarrhea	-	-	-	1(1)	3(4)	-	-	-	1(2)	3(4)
Decreased skin turgor	-	-	-	1(1)	3(4)	-	-	-	-	-
Abdominal distension	-	-	-	2(4)	3(3)	-	-	-	2(3)	2(3)
Dyspnea	-	-	-	-	2(3)	-	-	-	-	-
Hypoactive	-	-	-	-	3(7)	-	-	-	-	1(1)
Ptosis	-	-	-	-	1(3)	-	-	-	-	-
Red staining (muzzle)	-	1(1)	1(1)	2(3)	2(3)	-	-	-	2(3)	4(5)
Salivation	-	-	-	-	1(1)	-	-	-	-	-

- = Clinical sign not observed in this group

Body weight was decreased in rats treated with PF-02341066, with males at all doses losing 8.5 to 20.9 g compared with a mean weight gain of 18.3 in controls, and females losing a mean of 5.1 to 10.1 g at ≥250 mg/kg compared to a mean weight gain of 2.8 g in controls.

Micronucleus assay

The mean percentage of micronucleated polychromatic erythrocytes for the cyclophosphamide positive controls was 3.3- to 4.2-fold greater than vehicle controls. The vehicle control values were within the historical control range. In male rats treated with PF-02341066, the mean percentage of micronucleated polychromatic erythrocytes was significantly increased by 2.2- to 2.6-fold at all doses of PF-02341066 (≥250 mg/kg). There was a trend for an increase in the mean percentage of micronucleated polychromatic erythrocytes in females, however, the increases did not reach levels that were beyond the range for historical controls. Significant increases in mean percentage micronucleated normochromatic erythrocytes of 2.4- to 2.6-fold were also seen in males at all doses of PF-02341066. Micronucleus assessment data for males and females are presented in the tables below (excerpted from sponsor's submission).

Table 41: Male Micronucleus Results

	0 mg/kg	250 mg/kg	500 mg/kg	1000 mg/kg	20 mg/kg (CP)
Micronucleus TNC (10e6/femur)					
Day 3	(5) 163.86+21.215	(5) 130.08+22.754*	(5) 109.96+11.139**	(4) 105.65+18.070**	(5) 49.72+11.710**
Polychromatic Erythrocytes (%)					
Day 3	(5) 78.18+ 5.297	(5) 61.50+ 6.876*	(5) 58.94+ 4.846**	(4) 55.78+14.695**	(5) 55.78+ 5.640**
Micronucleated Polychromatic Erythrocytes (%)					
Day 3	(5) 0.64+ 0.288	(5) 1.46+ 0.508**	(5) 1.38+ 0.295*	(4) 1.68+ 0.685**	(5) 2.70+ 0.758**
Normochromatic Erythrocytes (%)					
Day 3	(5) 21.82+ 5.297	(5) 38.50+ 6.876*	(5) 41.06+ 4.846**	(4) 44.23+14.695**	(5) 44.22+ 5.640**
Micronucleated Normochromatic Erythrocytes (%)					
Day 3	(5) 0.20+ 0.122	(5) 0.48+ 0.130*	(5) 0.52+ 0.228**	(4) 0.48+ 0.263*	(5) 1.28+ 0.179**
Total Nucleated Cells (%)					
Day 3	(5) 82.64+ 4.364	(5) 66.36+ 4.929**	(5) 64.04+ 4.751**	(4) 70.05+ 6.693**	(5) 54.86+ 7.702**
Total Erythrocytes (%)					
Day 3	(5) 17.36+ 4.364	(5) 33.64+ 4.929**	(5) 35.96+ 4.751**	(4) 29.95+ 6.693**	(5) 45.14+ 7.702**
Mean Fluorescence (DNA channel / control)					
Day 3	(5) 99.98+ 9.742	(5) 61.28+ 7.598**	(5) 57.44+ 8.677**	(4) 44.75+ 8.977**	(5) 22.20+13.804**

For each group, values expressed are (N) mean + standard deviation.
Mean value significantly different from primary control mean at 1% level (**) or 5% level (*) by sequential trend test (treated groups) or pairwise test (positive control group) within one factor analysis of variance.
Dunnett's test (D) replaces sequential trend test if the linear trend test is not significant at 5% level and the quadratic trend is significant at 1% level.
. Value not applicable or not available.

Table 42: Female Micronucleus Results

	0 mg/kg	250 mg/kg	500 mg/kg	1000 mg/kg	20 mg/kg (CP)
Micronucleus TNC (10e6/femur)					
Day 3	(5) 96.06+ 6.603	(5) 72.84+ 7.519	(5) 69.18+ 9.831	(5) 82.58+19.948	(5) 22.96+ 3.625**
Polychromatic Erythrocytes (%)					
Day 3	(5) 60.86+ 7.401	(5) 54.72+ 3.634	(5) 57.90+ 7.474	(5) 52.28+ 3.363*	(5) 36.24+ 8.650**
Micronucleated Polychromatic Erythrocytes (%)					
Day 3	(5) 0.54+ 0.207	(5) 0.58+ 0.164	(5) 0.74+ 0.207	(5) 0.82+ 0.327	(5) 1.80+ 0.324**
Normochromatic Erythrocytes (%)					
Day 3	(5) 39.14+ 7.401	(5) 45.28+ 3.634	(5) 42.10+ 7.474	(5) 47.72+ 3.363*	(5) 63.76+ 8.650**
Micronucleated Normochromatic Erythrocytes (%)					
Day 3	(5) 0.26+ 0.089	(5) 0.24+ 0.089	(5) 0.28+ 0.130	(5) 0.34+ 0.167	(5) 0.80+ 0.200**
Total Nucleated Cells (%)					
Day 3	(5) 66.96+ 8.705	(5) 62.02+ 6.607	(5) 64.10+ 2.735	(5) 61.04+ 5.146	(5) 39.38+ 5.661**
Total Erythrocytes (%)					
Day 3	(5) 33.04+ 8.705	(5) 37.98+ 6.607	(5) 35.90+ 2.735	(5) 38.96+ 5.146	(5) 60.62+ 5.661**
Mean Fluorescence (DNA channel / control)					
Day 3	(5) 100.00+19.637	(5) 63.44+ 8.267**	(5) 53.84+ 6.915**	(5) 54.70+11.841**	(5) 11.58+ 2.064**

For each group, values expressed are (N) mean + standard deviation.
Mean value significantly different from primary control mean at 1% level (**) or 5% level (*) by sequential trend test (treated groups) or pairwise test (positive control group) within one factor analysis of variance.
Dunnett's test (D) replaces sequential trend test if the linear trend test is not significant at 5% level and the quadratic trend is significant at 1% level.
. Value not applicable or not available.

Toxicokinetics

Plasma was collected for evaluation of toxicokinetic parameters from PF-02341066-treated toxicokinetic animals at approximately 1, 4, 7, and 24 hours after dosing and from vehicle control animals at 4, 7, and 24 after dosing following a single dose of PF-02341066 (table excerpted from sponsor's submission).

- C_{max} and $AUC_{(0-24)}$ values increased with an increase in dose; increases were less than dose proportional
- Exposure to PF-02341066 was higher in males, with C_{max} and $AUC_{(0-24)}$ values 1.5 to 2.4 times higher in males than females
- T_{max} ranged from approximately 5 hours at 125 mg/kg to approximately 22 hours at 1000 mg/kg

Dose (mg/kg)	Sex	Cmax (µg/mL)	Tmax (hr)	AUC(0-24) (µg·hr/mL)
125	Male	1.8	5.5	35.1
	Female	1.0	4.8	14.7
250	Male	2.3	18.3	43.7
	Female	1.3	6.8	20.2
500	Male	2.6	14.8	50.4
	Female	1.7	18.3	30.6
1000	Male	3.4	24	63.8
	Female	2.0	19.8	35.9

Conclusion: PF-2341066 was positive for micronucleus induction in males treated with ≥250 mg/kg.

Study title: *In vivo* micronucleus study of PF-2341066 in male rats

Study no:	3746
Study report location:	M4.2.3.3.2
Conducting laboratory and location:	Pfizer Global Research & Development Drug Safety Research & Development 2800 Plymouth Rd. Ann Arbor, MI
Date of study initiation:	November 3, 2005
GLP compliance:	Yes
QA statement:	Yes
Drug, lot #, and % purity:	PF-02341066, lot # AK-100830-85-10, Purity: 99.77%

Key Study Findings

- PF-2341066 caused an increase in micronucleus induction in male rats treated with 250 mg/kg as evidenced by significant increases in micronucleated polychromatic erythrocytes in bone marrow, however, the value was within the historic control range.
- Bone marrow was collected for micronucleus assessment at a single time point, 24 hours after the second dose of PF-02341066, therefore, the study is invalid

Methods

Doses in definitive study:	0, 25, 100, or 250 mg/kg
Frequency of dosing:	Once per day for 2 days for micronucleus assessment and 1 day for toxicokinetic assessment
Route of administration:	Oral gavage
Dose volume:	10 mL/kg
Formulation/Vehicle:	0.5% methylcellulose
Species/Strain:	Sprague-Dawley rats
Number/Sex/Group:	5 males/group
Satellite groups:	Toxicokinetics: 3 males/group for vehicle group, 4 males/group for PF-02341066-treated groups
Basis of dose selection:	*In vivo* micronucleus study (Study 3665) conducted in male and females rats in which doses ≥250 mg/kg increased the frequency of micronucleated polychromatic erythrocytes in male rats
Negative control:	0.5% methylcellulose
Positive control:	Cyclophosphamide (20 mg/kg; 2 mg/mL)

Bone marrow was collected for micronucleus assessment at a single time point, 24 hours after the second dose of PF-02341066.

Study Validity

Criteria for a positive response included a reproducible, statistically significant, dose-related increase in the mean percentage of micronucleated polychromatic erythrocytes (%MNPCE) frequency in drug-treated groups compared to concurrent controls, with at least one value exceeding the historical vehicle control range. Positive controls showed a significant increase in the mean percentage of micronucleated polychromatic erythrocytes compared to vehicle controls. Two treatments of PF-02341066 were administered in this study and bone marrow should have been collected at two time points for a valid study. Since bone marrow was collected at a single time point, the study appears to be invalid.

Results

Clinical signs and body weight

Clinical signs observed in the study are listed in the table below.

Clinical signs	No. of animals affected (No. of Observations)			
Dose (mg/kg)	0	25	100	250
Number of animals examined	5	5	5	5
Feces decreased	-	-	-	5(8)
Haircoat stained (muzzle-red)	-	-	-	2(2)
Chromorhinorrhea	-	-	-	2(3)
Noisy respiration	-	-	-	2(2)

- = Clinical sign not observed in this group

Body weight gain was decreased 66% in rats treated with 100 mg/kg PF-02341066 compared to controls. Rats treated with 250 mg/kg PF-02341066 lost a mean of 18.5 g in body weight compared with a mean weight gain of 20 g in controls.

Micronucleus assay

The mean percentage of micronucleated polychromatic erythrocytes for the cyclophosphamide positive controls was 3.4-fold greater than vehicle controls. The vehicle control values were within the historical control range. In male rats treated with PF-02341066, the mean percentage of micronucleated polychromatic erythrocytes was significantly increased by 2-fold at 250 mg/kg PF-02341066, however, the value was within the historic control range (0.1-1.0 %). Therefore, the increase in micronucleated polychromatic erythrocytes was not considered a positive response according to the criteria. Micronucleus assessment data are presented in the table below (excerpted from sponsor's submission).

Table 43: Male Micronucleus Results (2)

	0 mg/kg	25 mg/kg	100 mg/kg	250 mg/kg	20 mg/kg (CP)
Micronucleus TNC (10e6/femur)					
Day 3	(5) 144.60+22.770	(5) 133.82+25.837	(5) 112.74+ 9.754*	(5) 102.20+20.160**	(5) 49.20+ 9.544**
Polychromatic Erythrocytes (%)					
Day 3	(5) 70.32+ 8.029	(5) 75.78+ 3.751	(5) 71.80+ 5.024	(5) 57.16+10.955**	(5) 51.44+ 7.444**
Micronucleated Polychromatic Erythrocytes (%)					
Day 3	(5) 0.44+ 0.089	(5) 0.54+ 0.182	(5) 0.62+ 0.239	(5) 0.98+ 0.502*	(5) 1.48+ 0.444**
Normochromatic Erythrocytes (%)					
Day 3	(5) 29.68+ 8.029	(5) 24.22+ 3.751	(5) 28.20+ 5.024	(5) 42.84+10.955**	(5) 48.56+ 7.444**
Micronucleated Normochromatic Erythrocytes (%)					
Day 3	(5) 0.06+ 0.055	(5) 0.06+ 0.089	(5) 0.08+ 0.045	(5) 0.14+ 0.207	(5) 0.12+ 0.110
Total Nucleated Cells (%)					
Day 3	(5) 74.30+ 4.563	(5) 76.88+ 5.829	(5) 71.26+ 5.783	(5) 54.36+ 8.680**	(5) 27.24+ 2.428**
Total Erythrocytes (%)					
Day 3	(5) 25.70+ 4.563	(5) 23.12+ 5.829	(5) 28.74+ 5.783	(5) 45.64+ 8.680**	(5) 72.76+ 2.428**
Mean Fluorescence (DNA channel / control)					
Day 3	(5) 102.96+ 6.649	(5) 97.30+ 8.029	(5) 82.96+ 7.166**	(5) 67.02+ 8.748**	(5) 55.18+ 2.415**

For each group, values expressed are (N) mean + standard deviation.
Mean value significantly different from primary control mean at 1% level (**) or 5% level (*) by sequential trend test (treated groups) or pairwise test (positive control group) within one factor analysis of variance.
Dunnett's test (D) replaces sequential trend test if the linear trend test is not significant at 5% level and the quadratic trend is significant at 1% level.
. Value not applicable or not available.

Toxicokinetics

Plasma was collected for evaluation of toxicokinetic parameters from PF-02341066-treated toxicokinetic animals at approximately 1, 4, 7, and 24 hours after dosing and from vehicle control animals at 4, 7, and 24 after dosing following a single dose of PF-02341066 (table excerpted from sponsor's submission).

- C_{max} and $AUC_{(0-24)}$ values increased with an increase in dose
- T_{max} increased with dose, ranging from 4 hours at 25 mg/kg to approximately 24 hours at 250 mg/kg. Since the observed T_{max} at 250 mg/kg was the last toxicokinetic time point, the actual T_{max} may be later for this dose.

Dose (mg/kg)	Cmax (µg/mL)	Tmax (hr)	AUC(0-24) (µg·hr/mL)
25	0.412	4.0	4.32
100	1.42	4.75	22.2
250	2.06	24.0	38.9

Conclusion: PF-2341066 significantly increased micronucleated polychromatic erythrocytes in males treated with 250 mg/kg, however, the value was within the historic control range.

8 Carcinogenicity

Carcinogenicity studies have not been conducted.

9 Reproductive and Developmental Toxicology

9.1 Fertility and Early Embryonic Development

No fertility and early embryonic development studies were submitted.

9.2 Embryonic Fetal Development

Study title: Oral dose range-finding study of PF-02341066 in pregnant rats

Study no.:	09GR345
Study report location:	M4.2.3.5.2
Conducting laboratory and location:	Pfizer Global Research & Development Drug Safety Research & Development Eastern Point Rd. Groton, CT
Date of study initiation:	September 29, 2009
GLP compliance:	No
QA statement:	No
Drug, lot #, and % purity:	PF-02341066, lot # GR02806, purity: 99.7%

Key Study Findings

- PF-02341066 produced maternal toxicity including decreased body weight and food consumption at 250 and 500 mg/kg
- All females in the 500 mg/kg group were euthanized on GD 12
- Fetal body weight was decreased by 15% in the 250 mg/kg group compared to controls
- Forelimb hyperflexion was observed in all 14 fetuses of a single litter in the 250 mg/kg group; all fetuses in this litter were unusually small

Methods

Doses:	0, 50, 250, or 500 mg/kg
Frequency of dosing:	Once daily gestation days (GD) 6-17
Dose volume:	10 mL/kg
Route of administration:	Oral gavage
Formulation/Vehicle:	0.5% methylcellulose
Species/Strain:	Sprague-Dawley rats (Crl:CD®[SD]
Number/Sex/Group:	6 females/group
Satellite groups:	None
Study design:	6 females/group were dosed GD 6-17 with the day that a sperm plug was observed as GD 0 and euthanized on GD 21
Parameters and endpoints evaluated:	Females: Clinical signs, body weight, gravid uterine weights, food consumption, necropsy, and number of corpora lutea, implantation sites, late and early resorptions, and viable and dead fetuses Fetuses: Fetal weight and external examinations

Results

Mortality

- Due to clinical signs, declining maternal body weights, and food consumption, all females in the 500 mg/kg group were euthanized on GD 12.

Clinical Signs

Clinical signs		Dose (mg/kg)			
		0	50	250	500
Activity decreased	No. of animals	-	-	-	1
	No. of observations	-	-	-	2
	Days observed	-	-	-	11-12
Oral/nasal chromorhinorrhea	No. of animals	-	-	-	2
	No. of observations	-	-	-	5
	Days observed	-	-	-	7-12
Piloerection	No. of animals	-	-	-	1
	No. of observations	-	-	-	2
	Days observed	-	-	-	11-12

- = clinical sign not observed in this group

Body Weight

- The 500 mg/kg group lost weight during treatment of PF-02341066. On GD 12, the day the group was euthanized, mean body weight was decreased by 16% compared to the mean weight on GD 6 and by 26% compared to controls.
- The 250 mg/kg group lost weight between GD 6-8 and had reduced body weight gain compared to controls throughout the dosing period. Average maternal net

weight gain corrected for the gravid uterine weight was reduced for the 250 mg/kg group compared to controls.

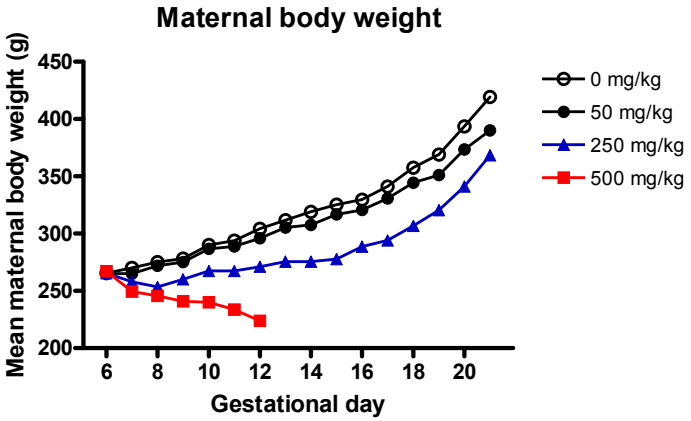

Mean adjusted body weight change and uterine weight (g)

Parameter	Dose (mg/kg)		
	0	50	250
Uterus weight (g)	99.38	74.27	83.61
Carcass weight (g)	319.96	315.83	284.92
Net weight change (g) from GD 6	54.49	50.86	19.32

Food Consumption

- Food consumption was decreased compared to controls in the 250 and 500 mg/kg groups.

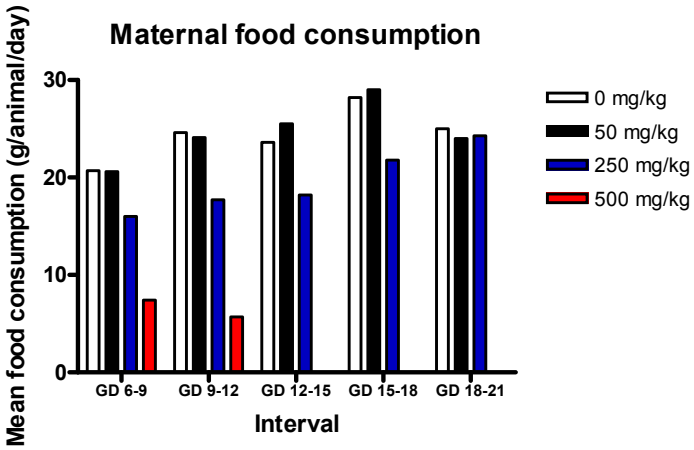

Toxicokinetics

Not conducted

Necropsy

- In the 500 mg/kg group euthanized on GD 12, dilated stomach was observed in two females and dilated cecum was observed in another female.

Cesarean Section Data

Results of the uterine examinations are presented in the table below. There is no data for the 500 mg/kg group, since all females were euthanized on GD 12.

Dose (mg/kg)	0	50	250
Number of pregnant females	6	6	6
Number of corpora lutea			
Total	85	76	88
Mean number per female	14.2	12.7	14.7
Number of implantations			
Total	76	58	78
Mean number per female	12.7	9.7	13.0
Pre-implantation loss			
Total	9	18	10
Mean number per female	1.5	3.0	1.7
Post-implantation loss			
Early resorptions	1	3	6
Late resorptions	0	0	0
Dead fetuses	0	0	0
Total	1	3	6
Mean number per female	0.2	0.5	1.0
Number of live fetuses			
Total	75	55	72
Mean number per female	12.5	9.2	12.0

Offspring

Fetal observations are presented in the tables below.

Number of fetuses and weights

Dose (mg/kg)	0	50	250
Number of live fetuses			
Total	75	55	72
Mean number per female	12.5	9.2	12.0
Sex distribution			
Males	43	33	27
Females	32	22	45
Mean % male fetuses	56.9	59.4	38.6
Mean fetal weight			
Males only	6.0	6.1	5.2
Females only	5.8	5.8	4.8
Combined	5.9	6.0	5.0

Fetal external examinations

	No. of fetuses affected (No. of litters affected)		
Dose (mg/kg)	0	50	250
Litters examined (N)	6	6	6
Fetuses examined (N)	75	55	72
Forelimb hyperflexion	-	-	14 (1)

The finding of forelimb hyperflexion was observed in all fetuses of a single litter in the 250 mg/kg group. All fetuses in this litter were unusually small with a mean of 3.6 g.

Study title: Oral embryo-fetal development study of PF-02341066 in rats

Study no.:	10GR072
Study report location:	M4.2.3.5.2
Conducting laboratory and location:	Pfizer Global Research & Development Drug Safety Research & Development Eastern Point Rd. Groton, CT
Date of study initiation:	May 19, 2010
GLP compliance:	Yes
QA statement:	Yes
Drug, lot #, and % purity:	PF-02341066, lot # 902/2341066/F/X/3 (also assigned 902/2341066/F/X/3/1 and E010010728), purity: 99.7%

Key Study Findings

- PF-02341066 produced maternal toxicity including decreased body weight and food consumption at 200 mg/kg. One female treated with 200 mg/kg was euthanized on GD 12.
- Increased post-implantation loss consisting of early resorptions was observed in the 50 and 200 mg/kg groups.
- Fetal body weight was significantly decreased in the 200 mg/kg group compared to controls.
- A skeletal variation of unossified metatarsals was observed in the 200 mg/kg group, however, the incidence was minimal.
- No teratogenicity was observed in this study.

Methods

Doses:	0, 10, 50, or 200 mg/kg
Frequency of dosing:	Once daily gestation days (GD) 6-17
Dose volume:	10 mL/kg
Route of administration:	Oral gavage
Formulation/Vehicle:	0.5% methylcellulose
Species/Strain:	Sprague-Dawley rats (Crl:CD®[SD]
Number/Sex/Group:	20 females/group
Satellite groups:	Toxicokinetic groups: 3 females/group for 0 mg/kg group, 5 females/group for 10, 50, and 200 mg/kg groups
Study design:	20 females/group were dosed GD 6-17 with the day that a sperm plug was observed as GD 0 and euthanized on GD 21; toxicokinetic groups were dosed GD 6-17 and euthanized on GD18 following the collection of blood samples
Parameters and endpoints evaluated:	Females: Clinical signs, body weight, gravid uterine weights, food consumption, necropsy,

and number of corpora lutea, implantation sites, late and early resorptions, and viable and dead fetuses
Fetuses: Fetal weight and fetal examinations (external, visceral, and skeletal abnormalities)

Results

Mortality

- One female treated with 200 mg/kg (animal # 78) was euthanized on GD 12 due to declining body weight and food consumption.

Clinical Signs

- Oral/nasal chromorhinorrhea and rough haircoat were observed on GD 10-12 in the female treated with 200 mg/kg euthanized on GD 12.

Body Weight

- Body weight was significantly lower in the 200 mg/kg group compared to controls from GD 7-21.
- Gravid uterine weight, corrected maternal body weight (carcass weight), and net body weight change were significantly reduced for the 200 mg/kg group compared to controls.

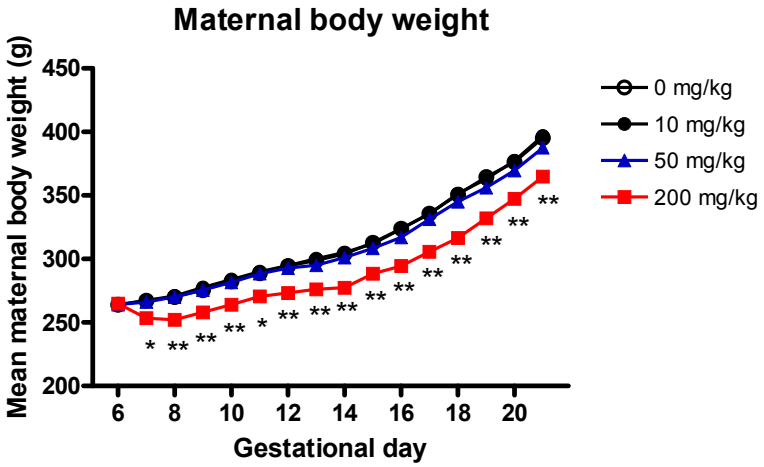

* Significantly different from control, p<0.05
** Significantly different from control, p<0.01

Mean adjusted body weight change and uterine weight (g)

Parameter	Dose (mg/kg)			
	0	10	50	200
Uterus weight (g)	93.16	93.66	86.27	78.65**
Carcass weight (g)	302.18	303.26	301.25	286.18*
Net body weight change (g) from GD 6	38.12	39.47	37.25	21.64**

* p<0.05 ** p<0.01

Food Consumption

- Food consumption was significantly decreased in the 200 mg/kg group compared to controls

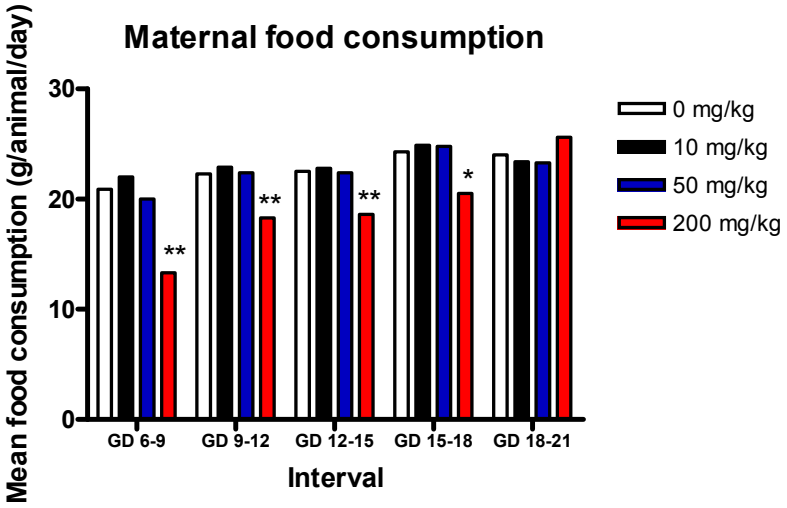

* Significantly different from control, p<0.05
** Significantly different from control, p<0.01

Toxicokinetics

Blood samples were collected on GD 17 from the 0 mg/kg group at ~1, 4, and 7 hours after dosing and from the 10, 50, and 200 mg/kg groups at ~ 1, 2, 4, 7, and 24 hours after dosing. Blood samples were analyzed for PF-02341066 concentrations.

- C_{max} and AUC $_{(0-24)}$ increased with increased dose
- Mean t_{max} was between 2-4 hours

(Excerpted from sponsor)

Dose (mg/kg/day)	Cmax (ng/mL)			tmax (h)			AUC(0-24) (ng*h/mL)		
	Mean	S.D.	n	Mean	S.D.	n	Mean	S.D.	n
10	107	46.6	5	2.8	1.1	5	670	313	5
50	570	95.7	5	2.0	0.0	5	4980	534	5
200	1360	332	5	4.0	2.7	5	20800	6260	5

Necropsy

Unremarkable

Cesarean Section Data

Results of the uterine examinations are presented in the table below.

Dose (mg/kg)	0	10	50	200
Number of surviving pregnant females	20	20	20	19
Number of corpora lutea				
Total	279	273	270	270
Mean number per female	13.9	13.7	13.5	14.2
Number of implantations				
Total	261	258	253	245
Mean number per female	13.1	12.9	12.7	12.9
Pre-implantation loss				
Total	18	15	17	25
Mean number per female	0.9	0.8	0.8	1.3
Post-implantation loss				
Early resorptions	6	8	19	17
Late resorptions	0	1	0	0
Dead fetuses	0	0	0	0
Total	6	9	19	17
Mean number per female	0.3	0.5	0.9	0.9
Number of live fetuses				
Total	255	249	234	228
Mean number per female	12.8	12.4	11.7	12.0

Offspring

Fetal observations are presented in the tables below.

Number of fetuses and weights

Dose (mg/kg)	0	10	50	200
Number of live fetuses				
Total	255	249	234	228
Mean number per female	12.8	12.4	11.7	12.0
Sex distribution				
Males	131	123	97	124
Females	124	126	137	104
Mean % male fetuses	51.5	49.7	43.0	54.1
Mean fetal weight	5.5	5.8	5.5	5.0**

** $p<0.01$

A detailed external examination (external and oral cavity) was conducted on all viable fetuses. One half of the viable fetuses from each litter were examined internally (visceral exam) and the other half of each litter was eviscerated and fixed in 95% ethanol for skeletal examination. Skeletal variations of wavy ribs and unossified metatarsals were observed in the 200 mg/kg group, however, the incidence was minimal. No teratogenicity was observed in this study.

Fetal skeletal variations

Dose (mg/kg)	No. of fetuses affected (No. of litters affected)			
	0	10	50	200
Total number of litters examined	20	20	20	19
Total number of fetuses examined	132	130	122	120
Wavy ribs	-	-	1 (1)	2 (1)
Unossified metatarsals	4 (3)	3 (3)	-	10 (7)

- = variation not observed in this group

Study title: Oral dose range-finding study of PF-02341066 in pregnant rabbits

Study no.: 09GR350
Study report location: M4.2.3.5.2
Conducting laboratory and location: Pfizer Global Research & Development
Drug Safety Research & Development
Eastern Point Rd.
Groton, CT
Date of study initiation: September 29, 2009
GLP compliance: No
QA statement: No
Drug, lot #, and % purity: PF-02341066, lot # GR02806, purity: 99.7%

Key Study Findings

- PF-02341066 produced maternal toxicity including decreased body weight and food consumption and mortality at ≥ 75 mg/kg.
- All the females in the 175 and 350 mg/kg groups either died or were euthanized moribund.
- There were no PF-02341066 related effects on any cesarean-section parameter, fetal body weights, or fetal external examinations.

Methods

Doses: 0, 25, 75, 175, or 350 mg/kg
Frequency of dosing: Once daily gestation days (GD) 7-19
Dose volume: 2 mL/kg
Route of administration: Oral gavage
Formulation/Vehicle: 0.5% methylcellulose
Species/Strain: New Zealand White rabbits
Number/Sex/Group: 6 females/group
Satellite groups: None
Study design: 6 females/group were dosed GD 7-19 with the day that the rabbits were bred as GD 0 and euthanized on GD 29
Parameters and endpoints evaluated: Females: Clinical signs, body weight, gravid uterine weights, food consumption, necropsy,

and number of corpora lutea, implantation sites, late and early resorptions, and viable and dead fetuses
Fetuses: Fetal weight and fetal external examinations

Results

Mortality

- Mortality was observed at doses ≥75 mg/kg PF-02341066. All mortalities observed in this study are listed in the table below.
- All females in the 175 and 350 mg/kg groups either died or were euthanized moribund.

Dose of PF-02341066	Animal #	Died or euthanized	GD	Important observations related to euthanization or death
75 mg/kg	017	Euthanized	18	• Feces decreased or absent and decreased activity • Stomach erosion/ulcer
175 mg/kg	019	Died	12	• Feces decreased and decreased activity • Stomach focus
	020	Euthanized	12	• Feces decreased or watery and decreased activity • Stomach focus
	021	Euthanized	12	• Feces absent • Stomach focus
	022	Euthanized	12	• Feces decreased or watery and decreased activity • Stomach focus
	023	Died	12	• Feces absent and decreased activity • Stomach focus
	024	Died	11	• Stomach focus
350 mg/kg	025	Died	9	• Stomach focus
	026	Died	9	• Stomach focus
	027	Died	9	• Stomach focus
	028	Euthanized	9	• Activity decreased, cool to the touch, and breathing pattern slow • Stomach focus
	029	Euthanized	9	• No findings reported
	030	Died	9	• Stomach focus

Clinical Signs

The clinical signs observed for each group are listed in the table below. Clinical signs observed in rabbits that died or were euthanized are noted in the mortality table above.

Clinical signs	No. of animals affected				
Dose (mg/kg)	0	25	75	175	350
Number of animals examined	6	6	6	6	6
Decreased activity	-	-	1	4	1
Feces absent	-	-	1	2	-
Feces decreased	-	-	1	3	-
Feces soft	-	-	1	-	-
Feces watery	-	-	-	2	-
Cool to touch	-	-	-	-	1
Breathing pattern slow	-	-	-	-	1

- = Clinical sign not observed in this group

Body Weight

- The 175 and 350 mg/kg groups lost weight (16.2% and 9.8%, respectively) from the start of treatment of PF-02341066 until death or moribund euthanasia.
- Body weight was slightly decreased in the 75 mg/kg group compared to controls during the dosing period (GD 7-20). Average maternal net weight gain corrected for the gravid uterine weight was reduced for the 75 mg/kg group compared to controls.

(Excerpted from Sponsor)

Figure 47: Maternal Body Weight (Rabbit Dose Range)

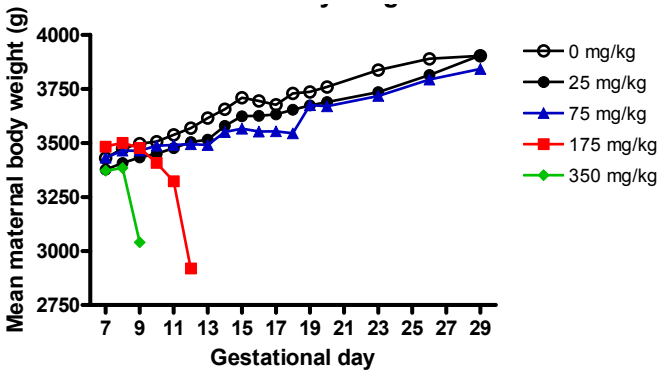

Table 44: Mean adjusted body weight change and uterine weight (g)

Parameter	Dose (mg/kg)		
	0	25	75
Uterus weight (g)	521.72	509.70	525.40
Carcass weight (g)	3,381.48	3,395.13	3,316.80
Net body weight change (g) from GD 7	-48.12	17.97	-92.20

Food Consumption

- Maternal food consumption was dramatically decreased for both the 175 and 350 mg/kg groups prior to death or moribund euthanasia.

- For the 350 mg/kg group, the mean maternal food consumption was 3.0 g for GD 7-8 and 0.0 g for GD 8-9 with a mean of 1.5 g for the 2 days. This was only 1% of the mean food consumption for the control group for GD 7-10 (147.4 g).
- For the 175 mg/kg group, the mean maternal food consumption was 17.4 g for GD 7-10, only 12% of the mean food consumption for the control group for GD 7-10 (147.4 g).
- Food consumption was decreased during the dosing period in the 75 mg/kg group compared to controls as shown in the figure below. The mean food consumption for the 75 mg/kg group across the dosing interval of GD 7-20, including the data for animal that was euthanized on GD 18, was 118.8 g compared to 144.2 g for the control group, a decrease of 17.6%.

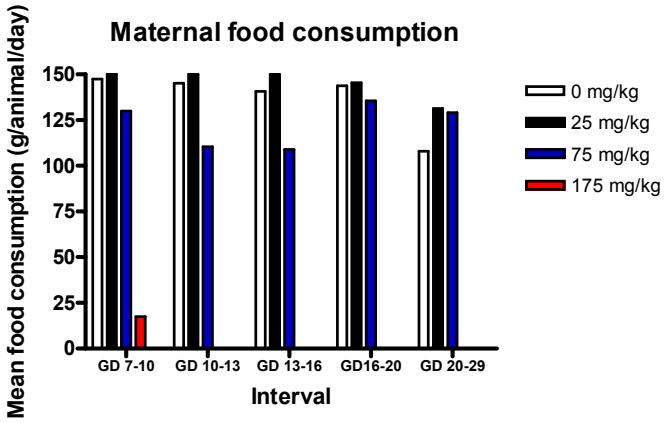

Toxicokinetics

Not conducted

Necropsy

Gross necropsy findings are listed by group in the table below. All gross necropsy findings were observed in the females that died or were euthanized early.

Gross necropsy findings	No. of animals affected				
Dose (mg/kg)	0	25	75	175	350
Number of animals examined	6	6	6	6	6
Stomach erosion/ulcer	-	-	1	-	-
Stomach focus	-	-	-	6	5

- = Necropsy finding not observed in this group

Cesarean Section Data

Results of the uterine examinations are presented in the table below. There is no data for the 175 and 350 mg/kg groups, since all females either died or were euthanized moribund. One female in the control group was not pregnant and one female in the 75 mg/kg group was euthanized on GD 18.

Dose (mg/kg)	0	25	75
Number of surviving pregnant females	5	6	5
Number of corpora lutea			
Total	48	63	47
Mean number per female	9.6	10.5	9.4
Number of implantations			
Total	47	59	43
Mean number per female	9.4	9.8	8.6
Pre-implantation loss			
Total	1	4	4
Mean number per female	0.2	0.7	0.8
Post-implantation loss			
Early resorptions	0	3	1
Late resorptions	2	0	0
Dead fetuses	0	0	0
Total	2	3	1
Mean number per female	0.4	0.5	0.2
Number of live fetuses			
Total	45	56	42
Mean number per female	9.0	9.3	8.4

Offspring

The mean fetal weights are presented in the table below. No abnormalities were observed in the fetal external examinations in this study.

Fetal weight

Dose (mg/kg)	0	25	75
Mean fetal weight	40.6	40.2	45.0

Study title: Oral embryo-fetal development study of PF-02341066 in rabbits

Study no.: 10GR073
Study report location: M4.2.3.5.2
Conducting laboratory and location: Pfizer Global Research & Development
Drug Safety Research & Development
Eastern Point Rd.
Groton, CT
Date of study initiation: June 21, 2010
GLP compliance: Yes
QA statement: Yes
Drug, lot #, and % purity: PF-02341066, lot # E010010728, purity: 99.5%

Key Study Findings

- Maternal toxicity was not observed in this study with doses up to 60 mg/kg PF-02341066.
- A slight increase post-implantation loss was observed in the 60 mg/kg group.

- Fetal body weight was decreased in the 60 mg/kg group compared to controls.
- Visceral (carotid artery left from innominate, absent gallbladder, small gallbladder) and skeletal (misaligned caudal centrum, hyoid bent arch, and skull extra ossification site) variations were observed in the PF-02341066-treated groups, however, the incidence was minimal and within the range of historical controls.
- No teratogenicity was observed in this study.

Methods

Doses:	0, 10, 25, or 60 mg/kg
Frequency of dosing:	Once daily gestation days (GD) 7-19
Dose volume:	2 mL/kg
Route of administration:	Oral gavage
Formulation/Vehicle:	0.5% methylcellulose
Species/Strain:	New Zealand White rabbits
Number/Sex/Group:	20 females/group
Satellite groups:	Toxicokinetic groups: 3 females/group for 0 mg/kg group, 5 females/group for 10, 25, and 60 mg/kg groups
Study design:	20 females/group were dosed GD 7-19 with the day that the rabbits were bred as GD 0 and euthanized on GD 29
Parameters and endpoints evaluated:	Females: Clinical signs, body weight, gravid uterine weights, food consumption, necropsy, and number of corpora lutea, implantation sites, late and early resorptions, and viable and dead fetuses Fetuses: Fetal weight and fetal examinations (external, visceral, and skeletal abnormalities)

Results

Mortality and Pregnancy

- Mortality: One female in the control group (Animal #5) died due to a dosing error on GD 9.
- Pregnancy: Several females were not pregnant in this study. The number of females not pregnant in each group is listed in the table below.

Dose (mg/kg)	No. of females not pregnant			
	0	10	25	60
Main study animals	6	3	3	1
Toxicokinetic animals	1	1	2	0

Clinical Signs

Unremarkable

Body Weight

- Mean uterine weight in the 25 mg/kg group was significantly increased compared to the control group, however, there were a larger number of live fetuses in this group

Table 45: Mean adjusted body weight change and uterine weight (g)

Parameter	Dose (mg/kg)			
	0	10	25	60
Uterus weight (g)	458.93	479.69	537.40*	489.26
Carcass weight (g)	3,053.15	3,009.37	2,966.42	2,998.90
Net body weight change (g) from GD 7	41.0	-3.75	-7.87	-5.26

* p <0.05

Food Consumption

Unremarkable

Toxicokinetics

Blood samples were collected on GD 19 from the control group at 1, 4, and 7 hours after dosing and from the dosing groups at ~ 0, 1, 2, 4, and 7 hours after dosing. Blood samples were analyzed for PF-02341066 concentrations (see tables excerpted from the sponsor's submission). Although 0 hour samples were collected predose, these samples were also analyzed as 24 hour time points and the same values appear to be used for both the 0 and 24 hour values according to the individual plasma concentration table.

- C_{max} and AUC $_{(0-24)}$ increased with increased dose; increases were greater than dose proportional
- Mean t_{max} was between 1.5-2.0 hours

Mean toxicokinetic parameters

Dose (mg/kg/day)	Cmax (ng/mL)			tmax (h)			AUC(0-24) (ng*h/mL)		
	Mean	S.D.	n	Mean	S.D.	n	Mean	S.D.	n
10	150	105	4	1.5	0.6	4	571	341	4
25	435	177	3	2.0	0.0	3	2730	1090	3
60	1640	376	5	1.6	0.5	5	12600	2680	5

Only values from pregnant animals were included in the mean and SD.

Individual plasma concentration data (ng/mL)

Dose (mg/kg/day)	Animal	Plasma Concentration (ng/mL) by Time (h)					
		0	1	2	4	7	24
0	81	--	BLQ	--	BLQ	BLQ	--
	82[a]	--	BLQ	--	BLQ	BLQ	--
	83	--	BLQ	--	BLQ	BLQ	--
10	84[a]	BLQ	6.55	27.7	19.2	6.38	BLQ
	85	3.59	129	117	27.9	13.7	3.59
	86	4.83	40.9	102	19.1	8.12	4.83
	87	6.01	302	234	61.2	19.7	6.01
	88	5.55	65.0	66.2	12.0	6.95	5.55
25	89	18.9	203	232	130	61.9	18.9
	90[a]	10.1	421	400	173	77.7	10.1
	91[a]	43.8	226	549	257	103	43.8
	92	13.5	389	515	189	90.0	13.5
	93	32.4	304	557	345	156	32.4
60	94	158	1820	1870	1620	704	158
	95	78.6	856	1220	905	452	78.6
	96	193	2160	1950	947	372	193
	97	84.3	904	1550	971	465	84.3
	98	167	1400	1290	961	463	167

-- = No sample as per protocol, amendment, or communication from the Study Director.
BLQ = Below the limit of quantitation (<3.00 ng/mL).
[a]Animal was not pregnant (no viable fetus) and was excluded from group mean and SD.

Necropsy

- Abnormal content in the trachea and abnormal color of the lung were observed in the female in the control group (Animal #5) that died due to a dosing error on GD 9.

Cesarean Section Data

Results of the uterine examinations are presented in the table below.

Dose (mg/kg)	0	10	25	60
Number of surviving pregnant females	13	17	17	19
Number of corpora lutea				
Total	119	165	173	188
Mean number per female	9.2	9.7	10.2	9.9
Number of implantations				
Total	108	149	160	177
Mean number per female	8.3	8.8	9.4	9.3
Pre-implantation loss				
Total	11	16	13	11
Mean number per female	0.8	0.9	0.8	0.6
Post-implantation loss				
Early resorptions	4	1	2	4
Late resorptions	1	2	0	3
Dead fetuses	0	1	0	1
Total	5	4	2	8
Mean number per female	0.4	0.2	0.1	0.4
Number of live fetuses				
Total	103	145	158	169
Mean number per female	7.9	8.5	9.3	8.9

Offspring

Fetal observations are presented in the tables below.

Number of fetuses and weights

Dose (mg/kg)	0	10	25	60
Number of live fetuses				
Total	103	145	158	169
Mean number per female	7.9	8.5	9.3	8.9
Sex distribution				
Males	58	66	79	86
Females	45	79	79	83
Mean % male fetuses	55.8	44.2	49.8	50.5
Mean fetal weight	42.0	40.2	41.8	39.4

Visceral variations

Dose (mg/kg)		0	10	25	60
Total number of litters examined		13	17	17	19
Total number of fetuses examined		103	145	158	169
Carotid artery left from innominate	Litters affected	-	4	2	5
	Fetuses affected	-	12	4	8
	% per litter	-	7.4	2.3	4.3
Absent gallbladder	Litters affected	-	1	-	1
	Fetuses affected	-	1	-	1
	% per litter	-	0.7	-	0.7
Small gallbladder	Litters affected	1	4	2	4
	Fetuses affected	1	4	2	4
	% per litter	1.1	3.6	1.2	2.4

- = Variation not observed in this group

Skeletal variations

Dose (mg/kg)		0	10	25	60
Total number of litters examined		13	17	17	19
Total number of fetuses examined		103	145	158	169
Misaligned caudal centrum	Litters affected	-	2	3	4
	Fetuses affected	-	3	3	4
	% per litter	-	2.1	1.7	2.6
Hyoid bent arch	Litters affected	-	2	2	1
	Fetuses affected	-	2	3	1
	% per litter	-	2.0	1.8	0.6
Skull extra ossification site	Litters affected	-	2	-	3
	Fetuses affected	-	2	-	4
	% per litter	-	1.2	-	2.9

- = Variation not observed in this group

9.3 Prenatal and Postnatal Development

No prenatal and postnatal development studies were submitted.

10 Special Toxicology Studies

Study title: 4-week oral gavage exploratory electroretinography study of PF-02341066 in male Long-Evans rats

Study no.:	10GR201
Study report location:	M4.2.3.2
Conducting laboratory and location:	Pfizer Global Research & Development Drug Safety Research & Development Eastern Point Rd. Groton, CT
Date of study initiation:	June 22, 2010 (Animals ordered)
GLP compliance:	No
QA statement:	No
Drug, lot #, and % purity:	PF-02341066, lot # E010010728

Key Study Findings

- PF-02341066 (100 mg/kg) significantly reduced the rate of retinal dark adaptation as demonstrated by a reduction in the amplitude of the electroretinogram *b*-wave on treatment Days 15 and 29 during the initial 16 and 32 minutes of dark adaptation, respectively.
- PF-02341066 was detected in the vitreous humor at a concentration 0.66 fold the concentration in the plasma

Methods

Doses:	0 or 100 mg/kg
Frequency of dosing:	Once daily for 29 days
Route of administration:	Oral gavage
Dose volume:	10 mL/kg
Formulation/Vehicle:	0.5% methylcellulose (w/v)
Species/Strain:	Long-Evans rat
Number/Sex/Group:	8 males/group
Age:	8-9 weeks at dose initiation
Weight:	280-310 g at dose initiation
Satellite groups:	Toxicokinetics: 6 males/group (100 mg/kg only)

Low grade visual disturbances have been observed with daily administration of PF-02341066 in clinical trials, however, no treatment-related ophthalmic findings were observed in nonclinical rat and dog studies up to 3 months in duration. This study was designed to evaluate the effects of PF-02341066 on electroretinogram (ERG) measurements as a biomarker for changes in ocular/retinal function in male Long-Evans (pigmented) rats after 4-weeks of daily dosing.

Observations and times:

Mortality:	Three times a day (predose, ~ 2 hours postdose, and near the end of the workday)
Clinical signs:	Three times a day (predose, ~ 2 hours postdose, and near the end of the workday)
Body weights:	Weekly (Days 1, 8, 15, 22, and 29)
Food consumption:	Weekly
ERG:	Days 15 and 29
Ophthalmic examinations:	Once prior to study and twice during the treatment period
Toxicokinetics:	Days 1 and 29 at ~1, 2, 4, 7, and 24 hours after dosing

The scheduled euthanization and necropsies occurred ~27 hours after the final dose. At necropsy the left eye of each animal was kept for possible histopathology and the right eye was dissected for vitreous fluid for subsequent PK analysis. The animal found dead was examined to determine a cause of death. No histopathology data is presented in the report.

Electroretinography (ERG) Procedure

ERG was conducted during Week 2 on Day 15 and during Week 4 at the end of the study on Day 29. The sessions were 2-4 hours after dosing (morning session) or 6-8 hours after dosing (afternoon session). Rats were dark-adapted for ~ 2 hours and than anesthetized just prior to ERG sessions with an i.p. injection of ketamine (30 mg/kg) and xylazine (2.5 mg/kg). Mydriacyl solution was applied to the eyes to dilate the pupils and an ERG contact lens was placed onto the surface of both eyes. A platinum needle reference electrode was inserted subcutaneously into the midline of the back of the head and a ground electrode clip was placed on the tail. An LKC UTAS-E 3000 Visual Electrodiagnostics System was used to acquire the ERG signals. ERG signals were high-pass filtered at 0.3 Hz and low-pass filtered at 500 Hz. Five ERG protocols were applied to test scotopic and photopic luminance responses, photopic and scotopic adaptometry and photopic flicker responses. ERG waveforms were analyzed with LKC-provided software using the International Society for Clinical Electrophysiology of Vision (ISCEV) guidelines. The schedule of ERG testing is shown in the figure below (excerpted from sponsor's submission).

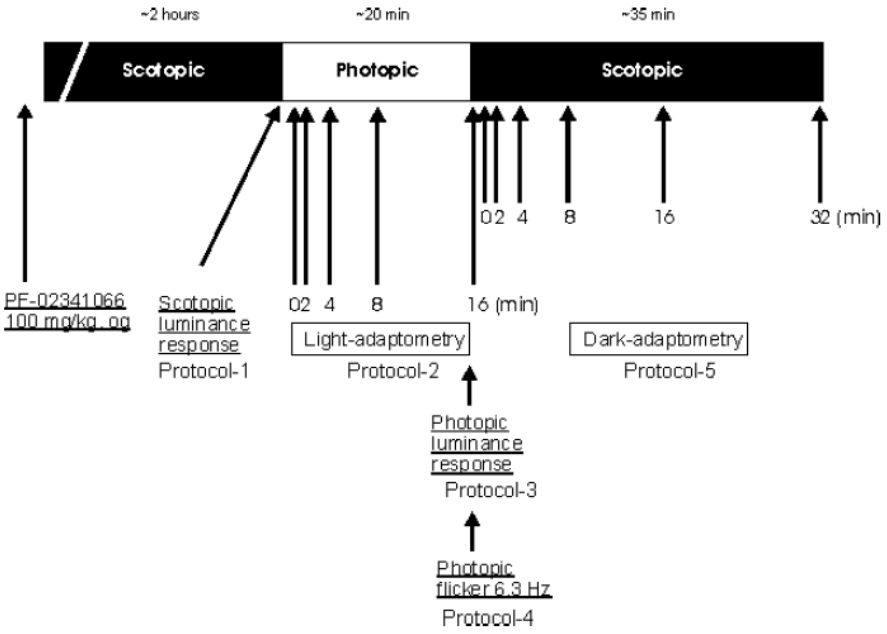

Results

Mortality

One rat in the main study 100 mg/kg group (#16) was found dead on Day 21. During necropsy, a large mass was observed in the underside of the right forelimb. Histopathology of the tissue showed marked acute inflammation with necrosis and hemorrhage, suggesting acute trauma. All other tissues were grossly normal and microscopic evaluation was conducted only on the mass. The cause of death was undetermined by the pathologist.

Clinical Signs

Rough haircoat was observed for rat #16 treated with 100 mg/kg on Day 21 prior to being found dead. No treatment-related clinical signs were observed for surviving rats.

Body Weights

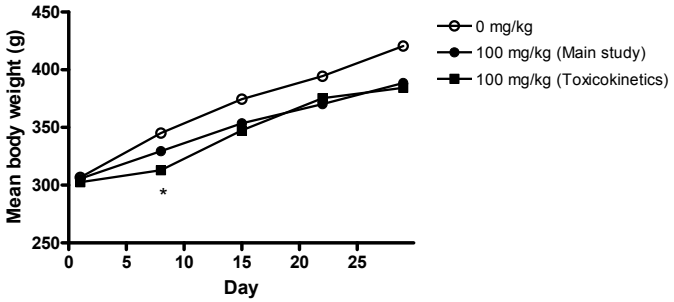

* Significantly different from control, p≤0 05

Food Consumption

Food consumption was significantly decreased by 19% in the toxicokinetic 100 mg/kg group compared to main study controls Days 1-8. This decrease corresponds to a significantly lower body weight compared to controls on Day 8.

Ophthalmic examinations

Unremarkable

Electroretinography (ERG)

The mean *b*-wave amplitude was significantly smaller in rats treated with 100 mg/kg PF-02341066 compared to controls during the first 16 minutes of dark adaptation on Day 15 and during the first 32 minutes of dark adaptation on Day 29. The decrease in *b*-wave amplitude was similar for Day 15 and Day 29 and is shown in Figure 48. After 2 hours of dark adaptation, b-wave amplitudes were not different between treated rats and controls, suggesting that PF-02341066 affects rate, rather than the final magnitude of dark adaptation. No treatment-related effects were observed on other ERG parameters including responses during light adaptation, scotopic (dark-adapted) luminance responses, photopic (light-adapted) luminance responses, and photopic flicker responses.
(Excerpted from Sponsor)

Figure 48: ERG b-Wave Amplitude in Male Rats

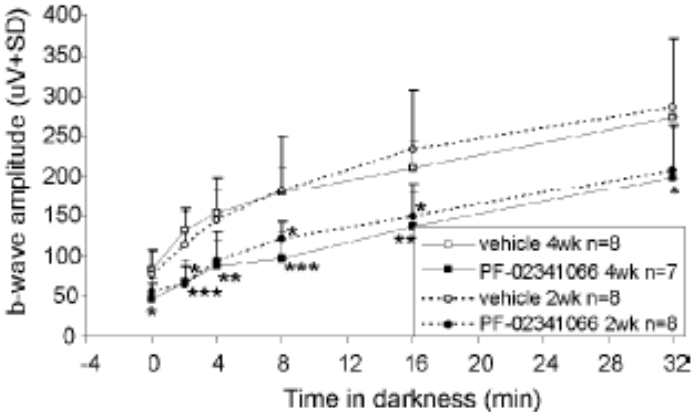

* p<0.05 ** p<0.01 *** p<0.001

Toxicokinetics

The toxicokinetics of PF-02341066 (100 mg/kg) were evaluated on Days 1 and 29 with samples collected at 1, 2, 4, 7, and 24 hours after dosing in toxicokinetic animals. Additionally, the levels of PF-02341066 in the vitreous humor of the eye were measured from samples taken at necropsy and were compared to plasma samples taken at necropsy in main study animals.

- C_{max} and AUC were higher on Day 29 than Day 1, indicating drug accumulation
- The mean PF-02341066 concentration in vitreous humor was lower than in plasma with a vitreous humor/plasma ratio of 0.66.

Mean plasma toxicokinetic parameters (excerpted from sponsor's submission)

Dose (mg/kg/day)	Study Day	Cmax (ng/mL) Mean	Tmax (Hours) Mean	AUC(0-24) (ng•h/mL) Mean
100	1	1470	4.0	22500
	29	2820	2.0	37600

Additional Information:
C_{max} = Maximum observed plasma concentration; T_{max} = Time to reach C_{max}; AUC = Area under the plasma concentration-time curve from time zero to 24 hours postdose.

Table 46: Vitreous Humor to Plasma Ratio

(excerpted from sponsor's submission)

Dose (mg/kg/day)	Total Days On Study[a]	Subject No.[b]	Vitreous Humor (ng/mL)	Plasma (ng/mL)	Vitreous Humor:Plasma Ratio
100	33	09	202	182	1.1
	33	10	72.1	192	0.38
	32	11	195	771	0.25
	32	12	162	198	0.81
	31	13	219	327	0.67
	31	14	402	727	0.55
	30	15	1070	1310	0.82
		Mean	**332**	**530**	**0.66**
		SD	**340**	**427**	**0.29**
		n	**7**	**7**	**7**

Additional Information:
SD = Standard deviation; n = Number of animals.
[a]First dosing, corresponding to study Day 1, was varied among the animals. Final necropsy was on the same study day for each animal. The last dose was administered to all animals approximately 26 to 27.5 hours prior to terminal blood collection and necropsy.
[b]Animal No. 16 was found dead on Day 21; therefore, a terminal blood sample was not taken and data are not reported.

Study title: Determination of the phototoxic potential of PF-02341066 in the 3T3 neutral red uptake (NRU) phototoxicity assay

Study no.: 05195
Study report location: M4.2.3.7.7
Conducting laboratory and location: Pfizer Global Research & Development
Amboise
Safety Sciences Europe
Route des Industries, Poce-sur-Cisse
37400 Amboise, France
Date of study initiation: July 13, 2005
GLP compliance: Yes
QA statement: Yes
Drug, lot #, and % purity: PF-02341066, batch # RR-100802-79-1, Purity: 98.9%

Key Study Findings

- Under the conditions of this experiment, PF-02341066 had probable phototoxic potential *in vitro* in the 3T3 neutral red uptake assay

Methods

Cells:	Balb/c 3T3, clone 31 mouse fibroblast cells
Concentrations:	0.002, 0.01, 0.08, 0.5, 3.4, 22.5, 150, and 1000 µg/mL
Formulation/vehicle:	DMSO (1% v/v) in (b) (4) Salt Solution
Negative controls:	Sodium Lauryl Sulfate (0.547-70 µg/mL)
Positive control:	Chlorpromazine (0.003-250 µg/mL)

To test the phototoxic potential of PF-02341066, the *in vitro* 3T3 neutral red uptake assay was conducted with Balb/c 3T3 clone 31 mouse fibroblast cells, in which cells were treated with various concentrations of PF-02341066 for 1 hour and then irradiated with 5 joules/cm^2 of UVA light (365 nm). Parallel cultures were prepared under similar conditions and kept in the dark. The cell viability was measured approximately 24 hours after the irradiation. Each concentration of PF-02341066 was tested 6 times. The cytotoxicity response curve of the test groups were compared, and the IC_{50} values were determined to calculate a photo-irritancy factor (PIF) to determine any phototoxicity.

$$PIF = \frac{IC_{50}\ (\text{without UV})}{IC_{50}\ (\text{with UV})}$$

The photo effect (MPE) was also calculated and is based on the comparison of the concentration-response curves for PF-02341066 with and without UV on a grid of concentrations chosen from a common range of dark and light experiments. Criteria used for determination of photoxicity:

Determination	Criteria
Not phototoxic	PIF= <2 and/or MPE= <0.1
Probable phototoxic	PIF= 2-5 and/or MPE=0.1-0.15
Phototoxic	PIF= >5 and/or MPE= >0.15

Results

Drug	IC_{50} without UV (µg/mL)	IC_{50} with UV (µg/mL)	PIF	MPE
Chlorpromazine (positive control)	12.6	0.400	31.4	0.269
Sodium Lauryl Sulfate (negative control)	14.8	15.7	0.94	0.008
PF-02341066	2.723	0.804	3.4	0.1

The PIF of PF-02341066 was 3.4 and the MPE was 0.1, therefore, based on the evaluation criteria, PF-02341066 was determined to have probable phototoxic potential.

Study title: 1-month oral toxicity study of PF-02341066 in rats

Study no.:	10GR100
Study report location:	M4.2.3.7
Conducting laboratory and location:	Pfizer Global Research & Development Drug Safety Research & Development Eastern Point Rd. Groton, CT and (b) (4) (Toxicokinetics)
Date of study initiation:	March 30, 2010
GLP compliance:	Yes
QA statement:	Yes
Drug, lot #, and % purity:	PF-02341066, lot # 00703371-053-2, Purity: 97.9%

Key Study Findings

- Target organs of toxicity included the kidney, liver (males only), heart, and pancreas.
- Toxicities observed in this study with 50 mg/kg were similar to those observed at the mid-dose in males (30 mg/kg) and females (50 mg/kg) in the 3-month repeat-dose study in rats (Study # 09GR347).
- Impurities (b) (4) are qualified based on higher doses of impurity in batch 00703371-053-2 than the proposed specifications.
- Impurities (b) (4) are not qualified based on the lower doses of impurity in batch 00703371-053-2 than the proposed specifications.

Methods

Doses:	0, 10 or 50 mg/kg
Frequency of dosing:	Once daily for 28 days
Route of administration:	Oral gavage
Dose volume:	10 mL/kg
Formulation/Vehicle:	0.5% methylcellulose (w/v)
Species/Strain:	Sprague-Dawley rat
Number/Sex/Group:	10/sex/group
Age:	9 weeks at dose initiation
Weight:	Males: 267-325 g at dose initiation Females: 180-217 g at dose initiation
Satellite groups:	Toxicokinetics: 3/sex/group (0 mg/kg group), 4/sex/group (10 and 50 mg/kg groups)

The purpose of this study was to qualify impurities anticipated to be present in clinical lots of PF-02341066, at levels that were not present in previous non-clinical toxicology studies.

Observations and times:

Mortality:	Once daily during pretreatment period, three times daily during dosing period (predose and at least twice), and once on day of necropsy
Clinical signs:	Once daily during pretreatment period, three times daily during dosing period (predose and at least twice), and once on day of necropsy
Body weights:	During pretreatment period, Day 1, and weekly during dosing period
Food consumption:	Weekly
ECG:	Not conducted
Ophthalmoscopy:	Pretreatment and Day 27
Hematology:	Prior to necropsy on Day 29
Clinical chemistry:	Prior to necropsy on Day 29
Coagulation:	Prior to necropsy on Day 29
Urinalysis:	Prior to necropsy on Day 29
Gross pathology:	At necropsy on Day 29
Organ weights:	At necropsy on Day 29
Histopathology:	At necropsy on Day 29
Toxicokinetics:	Days 1 and 28 at ~2, 4, 7, and 24 hours after dosing

Results

Mortality

No mortality was observed in this study.

Clinical Signs

Unremarkable

Body Weights

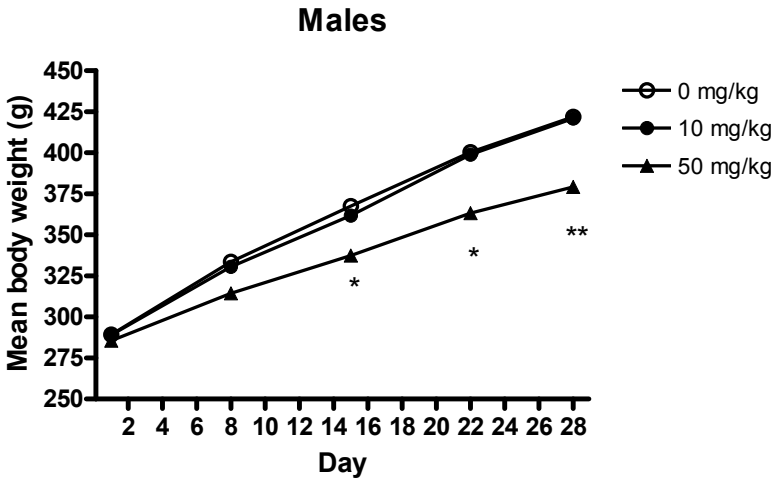

* Significantly different from control, p≤0.05
**Significantly different from control, p≤0.01

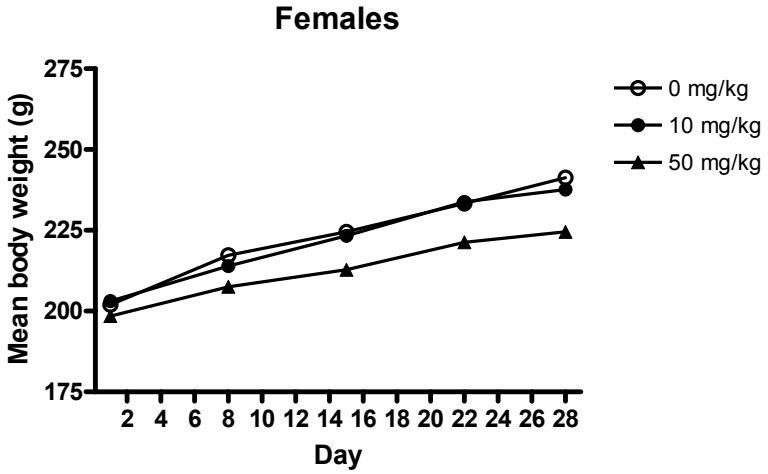

Food Consumption

While not statistically significant, there was a slight decrease in the food consumption for Days 1-28 (6-7%) in both males and females at 50 mg/kg that corresponds to decreased body weight gain. The mean food consumption values for Days 1-28 are shown in the table below.

Days 1-28	Mean food consumption (g)		
	0 mg/kg	10 mg/kg	50 mg/kg
Males	659.58	662.94	616.14
Females	444.95	437.96	416.35

Ophthalmoscopy

Unremarkable

ECG

Not conducted

Hematology and coagulation

Index	Mean		Percentage deviation from Control			
	Control 0 mg/kg		10 mg/kg		50 mg/kg	
Sex	Males	Females	Males	Females	Males	Females
Eosinophils	0.066	0.067	↑44	↑33	↑59	↑109
APTT	14.48	13.00	-	-	↓11	-

↑= increase ↓=decrease - = no test-article related changes; * p≤0.05 **p≤0.01

Clinical Chemistry

Index	Mean	Percentage deviation from Control	
	Control 0 mg/kg	10 mg/kg	50 mg/kg
Sex	Males	Males	Males
ALT	30.5	-	↑97**
AST	82.6	-	↑61**

↑= increase ↓=decrease - = no test-article related changes; * p≤0.05 **p≤0.01

Urinalysis

Index	Mean	Percentage deviation from Control	
	Control 0 mg/kg	10 mg/kg	50 mg/kg
Sex	Males	Males	Males
Specific gravity	1.0288	↓1.3*	↓1.6*
Urine volume	14.50	↑85	↑95

↑= increase ↓=decrease - = no test-article related changes; * p≤0.05 **p≤0.01

Gross Pathology

Unremarkable

Organ Weights

Group and Dose		Mean		Percentage deviation from Control			
		Control 0 mg/kg		10 mg/kg		50 mg/kg	
Sex		Males	Females	Males	Females	Males	Females
Number of animals examined		10	10	10	10	10	10
Liver	Absolute (g)	10.80	6.00	-	-	↓15*	-
	Relative Brain (%)	5.05	3.06	-	-	↓13*	-
Thymus	Absolute (g)	0.5225	0.4365	-	-	↓26**	↓25**
	Relative Brain (%)	0.2429	0.2232	-	-	↓23**	↓24*

↑= increase ↓=decrease - = no test-article related changes
* p≤0.05 **p≤0.01

Histopathology

Adequate Battery: Yes

Peer Review: Yes

Histological Findings

Treatment-Related Microscopic Findings			No. of animals affected					
			Males			Females		
Dose (mg/kg)			0	10	50	0	10	50
Number of animals examined			10	10	10	10	10	10
Organ	Finding							
Kidney	Chronic progressive nephropathy	Minimal	1	NE	4	-	NE	1
Liver	Hyperplasia, bile duct	Minimal	-	-	1	-	-	-
	Vacuolation, bile duct	Total	-	-	10	-	-	-
		Minimal	-	-	9	-	-	-
		Mild	-	-	1	-	-	-
	Single cell necrosis	Minimal	-	-	3	-	-	-
	Hepatocyte vacuolation	Minimal	-	-	-	-	-	2
Heart	Inflammation, pericardium	Mild	-	-	-	-	-	1
	Myonecrosis/myofibrosis	Total	1	-	6	-	-	-
		Minimal	1	-	5	-	-	-
		Mild	-	-	1	-	-	-
Pancreas	Inflammation/necrosis	Moderate	-	-	1	-	NE	-
	Chronic inflammation	Mild	-	-	-	-	-	1

- = no test-article related changes
NE=Not examined, tissue not examined in this group

Toxicokinetics

The toxicokinetics of PF-02341066 (10 or 50 mg/kg) were evaluated on Days 1 and 28 with samples collected at 2, 4, 7, and 24 hours after dosing in toxicokinetic animals.

- C_{max} and $AUC_{(0-24)}$ increased with increasing dose; increases were greater than dose proportional in males.
- In general, exposure ($AUC_{(0-24)}$) to PF-02341066 was higher in males than females, particularly at 50 mg/kg.
- Exposures to PF-02341066 were similar for females on Days 1 and 28, while exposures were higher on Day 28 than Day 1 for males, indicating drug accumulation.
- T_{max} ranged from 2-4 hours.

Mean toxicokinetic parameters (excerpted from sponsor's submission)

			Cmax (ng/mL)			tmax (h)			AUC(0-24) (ng*h/mL)		
Dose (mg/kg/day)	Study Day	Gender	Mean	SD	n	Mean	SD	n	Mean	SD	n
10	1	Males	81.6	21.7	4	4.0	0.0	4	618	170	4
		Females	122	20.9	4	3.5	1.0	4	912	279	4
		Overall	102	29.2	8	3.8	0.71	8	765	265	8
	28	Males	209	52.8	4	4.0	0.0	4	1660	425	4
		Females	221	63.3	4	2.0	0.0	4	1390	540	4
		Overall	215	54.4	8	3.0	1.1	8	1530	472	8
50	1	Males	1020	152	4	4.0	0.0	4	13700	1950	4
		Females	826	210	4	2.5	1.0	4	7230	1110	4
		Overall	921	198	8	3.3	1.0	8	10500	3740	8
	28	Males	1440	424	4	2.5	1.0	4	17900	4960	4
		Females	745	130	4	2.5	1.0	4	6370	633	4
		Overall	1090	470	8	2.5	0.93	8	12100	6970	8

Impurity qualification

This study is being used to qualify impurities [redacted] (b) (4) that have proposed specifications above the ICH qualification threshold of 0.15%. These impurities were present in batch 00703371-053-2 used in this study. Toxicities observed in this study with 50 mg/kg were similar to those observed at the mid-dose in males (30 mg/kg) and females (50 mg/kg) in the 3-month repeat-dose study in rats (Study # 09GR347). The dose of each impurity based on body surface area (mg/m^2) at the recommended clinical dose using the proposed specifications and the levels of the impurities present in batch 00703371-053-2 are presented in the table below. At the doses used in this study (10GR100) the doses of impurities [redacted] (b) (4) were higher than the expected clinical doses at the proposed specifications, therefore, these impurities are qualified. Impurities [redacted] (b) (4) are not qualified as the doses administered to animals in the current study were lower than the expected clinical doses at doses the proposed specifications for these impurities.

Table 47: Impurity Qualification

Impurity	NDA 202570 Proposed Specifications		Impurity qualification study in rats (10GR100) Batch 00703371-053-2		Qualification Determination
	%	Dose (mg/m^2)	%	Dose (mg/m^2)	
[redacted] (b) (4)					Not qualified
					Qualified
					Qualified
					Not qualified

11 Integrated Summary and Safety Evaluation

Crizotinib is an orally administered kinase inhibitor that has been developed clinically in patients with ALK-positive advanced non-small cell lung cancer. ALK is expressed at high levels in the nervous system during embryogenesis and is involved in neural development and differentiation. In humans, ALK has a restricted distribution in normal cells and is detected in rare scattered neural cells, pericytes, and endothelial cells in the adult brain. Translocations can affect the ALK gene resulting in the expression of oncogenic fusion proteins. The formation of fusion proteins results in activation and dysregulation of ALK expression and signaling leading to increased cell-proliferation and survival. Nonclinical pharmacology, pharmacokinetic, and toxicology studies have been submitted to support the approval of crizotinib for this indication.

The C_{max} observed in humans at the recommended clinical dose of 250 mg BID was 1061 nM (478 ng/mL). Pharmacokinetic results show the unbound fraction of crizotinib in human plasma *in vitro* was 0.093 (9.3%), indicating that 91% of crizotinib is bound to human plasma proteins *in vitro*. Based on this information, crizotinib is capable of inhibiting those kinases for which it has IC_{50} values approximately less than [redacted] (b) (4). Therefore, crizotinib is a kinase inhibitor with activity at c-Met/HGFR, ALK, and RON.

Pharmacology

In vitro and *in vivo* studies were conducted to investigate the pharmacologic and anti-tumor activity of crizotinib. Crizotinib was tested in *in vitro* recombinant biochemical enzyme assays and cell-based kinase assays to evaluate the potency and selectivity of the compound by determining the IC_{50} or EC_{50} values for various kinases. Crizotinib was shown to be an ATP-competitive inhibitor of recombinant, human c-Met/HGFR kinase activity with a mean K_i of 4 nM. Crizotinib inhibited HGF-stimulated or constitutive tyrosine phosphorylation of wild-type c-Met/HGFR with a mean IC_{50} value of 11 nM across a panel of human tumor and endothelial cell lines. This included inhibition of HGF-stimulated phosphorylation of c-Met/HGFR in A549 lung carcinoma cells at an IC_{50} value of 8.6 nM. In preliminary kinase selectivity screens, the IC_{50} value for Anaplastic Lymphoma Kinase (ALK) in Karpas 299 lymphoma cells was 24 nM, and the IC_{50} value for RON in engineered Ron-NIH3T3 cells was 189 nM. Other kinases with IC_{50} values in the nM range in cell-based assays were Axl (IC_{50}=294 nM), Tie2 (IC_{50}=448 nM), Trk A (IC_{50}=580 nM), and Trk B (IC_{50}=399 nM).

Additional cellular assays were conducted to assess the ability of crizotinib to inhibit the phosphorylation of EML4-ALK variants, NPM-ALK, c-Met/HGFR and RON in cell lines expressing these targets. Crizotinib showed similar inhibition of the various variants of EML4-ALK (V1, V2, V3a, and V3b) with EC_{50} values ranging from 27-74 nM. Additionally, crizotinib inhibited c-Met/HGFR phosphorylation in A549 lung carcinoma cells (EC_{50}=5 nM) and inhibited RON and RONΔ160 phosphorylation (EC_{50}=80 nM and 65 nM) in NIH-3T3 cells engineered to express human RON or RONΔ160.

Biochemical enzyme and cell assays investigating the inhibition of ALK, c-Met/HGFR, and RON activity were also conducted with the human metabolites of crizotinib. The activities of the metabolites in the cell-based assays were consistent with those observed in the enzyme assays. The two O-desalkyl crizotinib metabolites (PF-06268935 and PF-03255234) did not inhibit EML4-ALK, c-Met/HGFR, or RON activity at concentrations up to 10 µM, however, the two lactam metabolites (PF-06270079 and PF-06270080) demonstrated potentially pharmacologically relevant inhibitory activity for phosphorylation of EMLK-ALK, c-Met/HGFR and RON kinase in cell-based assays. The data indicate that PF-06270079 and PF-06270080 are less potent than crizotinib for ALK and c-Met/HGFR. In cells, PF-06270079 and crizotinib showed similar potencies for the inhibition of RON phosphorylation, while PF-06270080 was 2-fold more potent than crizotinib against RON.

Further *in vitro* studies showed the effects of crizotinib on cell growth/proliferation and survival. Crizotinib inhibited HGF-stimulated human NCI-H441 lung carcinoma cell migration and invasion (IC_{50s} of 11 nM and 6.1 nM, respectively). In the EML4-ALK V1 positive NCI-H3122 cell line, crizotinib completely inhibited cell proliferation (EC_{50}=54 nM) and induced apoptosis demonstrated by a 4-fold increase in Caspase 3/7 activity with a mean EC_{50} value of 110 nM. In the EML4-ALK V3a/b positive NCI-H2228 cell line, crizotinib only partially inhibited cell proliferation with a mean EC_{50} value of 34 nM and induced apoptosis associated with a 2-fold increase in Caspase 3/7 activity.

In vivo effects of crizotinib were demonstrated in various human tumor xenograft models in athymic mice. The GTL-16 human gastric carcinoma xenograft model was used extensively to investigate the *in vivo* effects of crizotinib on c-Met/HGFR activity. In the GTL-16 xenograft model, oral administration of crizotinib for 11 days dose-dependently inhibited both tumor growth and c-Met/HGFR phosphorylation at doses of 12.5, 25, and 50 mg/kg/day (37.5, 75, and 150 mg/m^2/day), with complete inhibition observed at 50 mg/kg/day (150 mg/m^2/day). The inhibition of tumor growth corresponded to both the percentage and duration of the inhibition of c-Met/HGFR phosphorylation. Immunoblotting studies showed that treatment with 25 or 50 mg/kg/day (75 or 150 mg/m^2/day) crizotinib for 12 days produced dose-dependent inhibition of phosphorylated HGFR (activation loop and docking site), Erk, AKT, and Gab-1 in GTL-16 tumors. Crizotinib (25 and 50 mg/kg/day; 75 and 150 mg/m^2/day) also inhibited cell proliferation in the GTL-16 model as measured by the percentage of Ki67 postive cells in these tumors. A significant dose-dependent reduction in immunostaining for CD31, a tumor endothelial cell marker, was observed at 12.5, 25, and 50 mg/kg/day (37.5, 75, and 150 mg/m^2/day) in GTL-16 tumors, indicating that crizotinib may have anti-angiogenic effects. Based on these results, crizotinib has multiple effects *in vivo* in the GTL-16 human gastric carcinoma xenograft model, including inhibition of tumor growth, phosphorylation of c-Met/HGFR and other signaling proteins, and cell proliferation. A dose of 50 mg/kg/day (150 mg/m^2/day) crizotinib appears to be the maximally efficacious dose in the GTL-16 xenograft model.

Crizotinib was also studied in xenograft models associated with ALK activity including the Karpas 299 human lymphoma and NCI-H3122 lung adenocarcinoma models. In the Karpas 299 model, crizotinib dose-dependently inhibited tumor growth and NPM-ALK phosphorylation at 25, 50, and 100 mg/kg/day (75, 150, and 300 mg/m^2/day). At 100 mg/kg/day (300 mg/m^2/day), 100% tumor regression was observed. These findings are similar to those observed in the GTL-16 xenograft model, with tumor growth corresponding to the percent inhibition of NPM-ALK phosphorylation in Karpas 299 tumors. Crizotinib also demonstrated dose-dependent inhibition of PLC-γ1, MAPK 44/42, AKT and STAT3 phosphorylation and inhibition of Cyclin-A, -B, and -D1, c-myc, c-fos, and c-jun expression in Karpas 299 human lymphoma xenografts. The maximally efficacious dose of crizotinib in the Karpas 299 model was 100 mg/kg/day (300 mg/m^2/day), which was higher than the 50 mg/kg/day (150 mg/m^2/day) maximally efficacious dose in the GTL-16 model.

A series of experiments using the NCI-H3122 lung adenocarcinoma model harboring the EML4-ALK V1 fusion gene were conducted to investigate the effects of crizotinib on EML4-ALK activity *in vivo*. Consistent with the findings in other models, 13 days of treatment with crizotinib (25, 50, 100, and 200 mg/kg/day; 75, 150, 300, and 600 mg/m^2/day) dose-dependently inhibited both tumor growth and EML4-ALK phosphorylation. In immunoblot studies, crizotinib (50, 100, and 200 mg/kg/day; 150, 300, and 600 mg/m^2/day) dose-dependently inhibited phosphorylated EML4-ALK (activation loop and docking site), STAT3, ERK1/2, AKT, PLCγ, and c-Myc in NIH-H3122 xenografts following 4 days of crizotinib administration. Additionally, the same doses of crizotinib inhibited c-Met/HGFR phosphorylation in NCI-H3122 xenografts.

Immunohistochemistry results showed that crizotinib (25-200 mg/kg/day; 75-600 mg/m^2/day) dose-dependently inhibited phospho-ALK staining following 14 days of treatment. A significant reduction in the number of Ki67 positive tumor cells was observed at 200 mg/kg/day (600 mg/m^2/day), suggesting that crizotinib inhibited cell proliferation in the H3122 model. Finally, compared to vehicle treatment, a significant induction of activated caspase-3 levels was observed following treatment of mice with 50, 100, and 200 mg/kg/day (150, 300, and 600 mg/m^2/day) crizotinib for 4 days in the NCI-H3122 model, suggesting crizotinib may induce apoptosis. Based on these results, crizotinib also has multiple effects *in vivo* in the NCI-H3122 lung adenocarcinoma xenograft model, including inhibition of tumor growth, inhibition of phosphorylation of EML4-ALK, c-Met/HGFR and other signaling proteins, and inhibition of cell proliferation. A dose of 200 mg/kg/day (600 mg/m^2/day) crizotinib appears to be the maximally efficacious dose in the NCI-H3122 xenograft model.

In vitro secondary pharmacology studies were conducted to evaluate the potential off-target effects of crizotinib at various receptor subtypes, primarily GPCRs, including those for neurotransmitters. In initial receptor binding and cellular function assays, crizotinib showed inhibitory activity for a number of receptors including the α_1 (non-selective) adrenergic receptor and the 5-HT$_{2B}$ and 5-HT$_{4e}$ serotonin receptors. Follow-up studies were then initiated to investigate the functional consequences of inhibition of receptor binding for receptors with the highest crizotinib affinity. Included in these investigations were the 5-HT$_{2B}$, 5-HT$_{2A}$ and 5-HT$_{1B}$ receptors, the rat adrenergic $\alpha_{1A,}$ receptor, and the M1, M2, and M3 muscarinic receptors. Crizotinib inhibited agonist binding at the 5-HT$_{2B}$ receptor with an IC$_{50}$ of 1.7 E-07 M (170 nM) and Ki of 1.6 E-07 M (160 nM). Crizotinib did not demonstrate potential agonist activity at any of the other receptors examined in functional assays at the concentrations tested. In addition, crizotinib did not demonstrate antagonist activity at the 5-HT$_{2A}$ (tested up to 10 μM), 5-HT$_{1B}$ (tested up to 1 μM), or M1, M2, and M3 muscarinic (tested up to 1 μM) receptor subtypes. Crizotinib was shown to be an antagonist at the rat adrenergic α_{1A} receptor with an EC$_{50}$ value of 159.73 nM and a calculated apparent dissociation constant (K$_B$) value of 40.73 nM. Crizotinib's potential agonist activity at the 5-HT$_{2B}$ receptor and inhibition of the rat adrenergic α_{1A} receptor occurred at concentrations higher than but similar to clinically relevant concentrations of 114 nM. Activity of crizotinib at these receptors could result in a wide range of effects including neurologic effects as the drug appears to efficiently cross the blood brain barrier. For example the α_1 adrenergic receptors, including α_{1A}, are involved in vasoconstriction of coronary arteries and veins and decrease motility of smooth muscle in the gastrointestinal tract, therefore, as an antagonist, crizotinib could cause vasodilation of coronary arteries and veins and increase motility of the smooth muscle of the gastrointestinal tract; however, vasodilation would lead to a decrease in blood pressure, which was not observed in either the non-clinical or clinical studies. There were no adverse effects noted in clinical trials that clearly relate to the off target binding of crizotinib at these receptors.

Safety Pharmacology

Both *in vitro* and *in vivo* safety pharmacology studies were conducted to assess the effects of crizotinib on neurological, cardiovascular, and pulmonary functioning.

Neurological function, including observational assessment, neuromuscular testing, and reflex/activity monitoring, was assessed in Sprague-Dawley rats starting 3 or 4 hours after a single oral dose of crizotinib (0, 10, 75, or 500 mg/kg; 0, 60, 450, or 3000 mg/m^2). Treatment with crizotinib reduced locomotor activity at the mid and high doses (450 and 3000 mg/m^2), and produced salivation and dyspnea at the highest dose (3000 mg/m^2). The C_{max} values observed at the mid (2.57 µM) and high dose (5 µM), were higher than the C_{max} (1.061 µM; 478 ng/mL) observed in humans at the recommended clinical dose. To assess the potential for seizures, the effects of PF-02341066 (0.3, 1, and 3 µM) on the neuronal Nav1.1 sodium channel were studied in an *in vitro* assay in HEK293 cells expressing the Nav1.1 channel. Crizotinib produced a concentration-dependent inhibition of the Nav1.1 current with IC_{50s} of 0.85 µM and 0.87 µM for the closed and inactivated states of the Nav1.1 channel, respectively. Therefore, crizotinib has the potential to inhibit the Nav1.1 channel at the C_{max} (1.061 µM; 478 ng/mL) observed in humans at the recommended clinical dose.

The effects of crizotinib on cardiovascular function were assessed in multiple *in vitro* studies and an *in vivo* study in anesthetized dogs. To assess the potential for delayed repolarization and prolongation of the QT interval, the effects of crizotinib (0.1, 0.3, 1, 3, and 10 µM) were studied in an *in vitro* hERG assay in HEK293 cells expressing the hERG potassium channel. Crizotinib inhibited the hERG channel at all concentrations tested with an IC_{50} of 1.1 µM. To evaluate the potential for blood pressure changes, the effects of crizotinib (0.1, 1, and 10 µM) on vascular Ca^{2+} channel function were studied in the rat aorta isometric tension model. Crizotinib produced a concentration-dependent relaxation of a 45 mM KCl-induced contraction with an IC_{50} of 0.83 µM, indicating that crizotinib can act as a calcium channel antagonist at concentrations below at and below the C_{max} (1.061 µM) observed in humans at the recommended clinical dose. The effects of crizotinib (1, 3, 10, 30, and 100 µM) on the cardiac L-type calcium channel current ($I_{Ca,L}$) were investigated using the whole-cell patch clamp technique to record $I_{Ca,L}$ in freshly isolated guinea pig ventricular myocytes. Crizotinib inhibited the L-type calcium channel current in a concentration-dependent manner with an IC_{50} of 14.6 µM. An *in vitro* study in dog isolated Purkinje fibres was conducted to evaluate the effects of crizotinib (0.01, 0.1, 1, and 10 µM) on cardiac action potentials evoked at stimulation frequencies of 0.3, 1, and 3 Hz. At the highest concentration tested (10 µM), crizotinib produced effects on the cardiac action potential including reductions in the action potential duration at 50% repolarization (APD_{50}) at all stimulation frequencies and the action potential duration at 90% repolarization (APD_{90}) at 1 and 3 Hz. To assess the potential for prolongation of the QRS or PR intervals, the effects of crizotinib (0.3, 1, 3, and 10 µM) on the Nav1.5 sodium channel were studied in another *in vitro* assay in CHO cells expressing the Nav1.5 sodium channel. Crizotinib inhibited the Nav1.5 current in a concentration-dependent manner with an IC_{50} value of 1.56 µM.

In a hemodynamic and electrophysiological study in anesthetized dogs, arterial blood pressure, left ventricular pressure, monophasic action potentials, and lead II ECG parameters were monitored following intravenous infusion of crizotinib or vehicle. Each dose of crizotinib or vehicle was administered as a 10 minute loading infusion (0, 0.134, 0.295, 1.192, and 1.907 mg/kg; 0, 2.68, 5.9, 23.84, and 38.14 mg/m^2) followed by a 25

minute maintenance infusion (0, 0.00939, 0.0207, 0.0834, 0.134 mg/kg/min; 0, 0.1878, 0.414, 1.668, and 2.68 mg/m^2/min). Changes in hemodynamic parameters included significant decreases in heart rate and increases in left ventricular end diastolic pressure (LVEDP) at the two highest doses of crizotinib compared to vehicle treatment. Additionally, there were significant differences in myocardial contractility (LV+dP/dt) at the highest dose. Changes in ECG parameters included significant increases in the PR-, QRS-, and QT-intervals at the two highest doses of crizotinib.

The effects of crizotinib on pulmonary function were evaluated in an *in vivo* rat study. Respiratory parameters (minute volume, respiratory rate, and tidal volume) were monitored for approximately 2 hours starting 3 hours after a single oral administration of crizotinib (0, 10, 75, or 500 mg/kg; 0, 60, 450, or 3000 mg/m^2). At the high dose of 3000 mg/m^2, mean minute volume and mean respiratory rate were significantly lower and tidal volume was significantly increased compared to vehicle controls during the first 24 minute observation interval starting 3 hours after dosing. These respiratory findings are at the same dose that decreased activity in the neurofunctional evaluation study with a C_{max} higher than the C_{max} observed in humans at the recommended clinical dose.

Phamacokinetics

The pharmacokinetics of crizotinib were studied in multiple species including the rat and dog, the non-clinical species tested for toxicity. In an *in vitro* binding assay assessing the binding of crizotinib to plasma proteins, the average unbound fraction of crizotinib was 0.057 (5.7%) in the rat plasma, 0.043 (4.3%) in the dog plasma, and 0.093 (9.3%) in human plasma. These results indicate that 91% of crizotinib is bound to human plasma proteins *in vitro*. A distribution study in rats following a single oral dose of crizotinib (10 mg/kg; 60 mg/m^2) showed that distribution of crizotinib was extensive with C_{max} occurring at 4 or 8 hours after dosing in most tissues. High concentrations of crizotinib were observed in the eye and associated tissues (Harderian gland, lacrimal gland, and uveal tract), pituitary gland, liver, kidney, adrenal gland, and spleen. Exposure in the eye was long with crizotinib present through 504 hours after dosing with an estimated elimination $t_{1/2}$ of 576 hours. The kidney, liver, pituitary, and spleen were target organs of toxicity in the rat, and visual impairment was observed in rats and in the clinical studies. These findings suggest that crizotinib produces toxicity in organs with high concentrations of the drug. Excretion studies in rats and dogs following a single oral dose of crizotinib (10 mg/kg; 60 mg/m^2 in rats and 200 mg/m^2 in dogs) showed that with oral administration crizotinib is primarily eliminated in the feces and bile (62-99% total; 35-53% in feces and 38-62% in bile in rats), with some excretion in the urine (2-6%). A metabolism study in rats showed that crizotinib underwent oxidation of the piperdine ring, direct sulfate conjugation, and *O*-dealkylation, with subsequent Phase 2 conjugation of *O*-dealkylated metabolites. In the dog study, crizotinib underwent metabolism on the piperdine ring by oxidative pathways and *N*-dealkylation. In a study performed using rat, dog, monkey, and human hepatocytes (not fully reviewed) there were no human metabolites that were not also detected in at least 1 animal species. The major human metabolites tested in the pharmacology studies were the crizotinib

lactam diasteromers (PF-06270079 and PF-06270080), pO-desalkyl crizotinib (PF-03255243), and O-desalkyl lactam crizotinib (PF-06268935).

General toxicology

Crizotinib was assessed in repeat dose oral toxicology studies including a 7-day study in rats and one- and three-month studies in both rats and dogs. In the 7-day toxicology study, Sprague-Dawley rats (n=3/sex/group) were administered crizotinib (0, 50, 150, or 500 mg/kg; 0, 300, 900, or 3000 mg/m^2) daily for 7 days. Mortality was observed in all animals in the high dose group, with one male found dead on Day 4 and the remaining males and females euthanized on Day 4 due to poor clinical condition. Body weight was decreased compared to Day 1 of treatment, and clinical signs of diarrhea, dyspnea, and oral discharge were observed. Target organs of toxicity were the bone marrow (sternum), gastrointestinal tract (ileum, jejunum, and stomach), kidney, liver, ovary, pancreas, spleen, salivary gland, and thymus. Ovarian toxicity consisting of decreased ovary weight and, in one female, necrosis of the ovary was observed at the high dose (500 mg/kg; 3000 mg/m^2).

The one-month repeat dose toxicology studies in rats and dogs were previously reviewed under IND 73544. In the one-month studies crizotinib was administered by oral gavage daily for 28 days in rats (0, 10, 50, or 150 mg/kg; 0, 60, 300, or 900 mg/m^2) and in dogs (0, 1, 6, or 20 mg/kg; 0, 20, 120, or 400 mg/m^2). Recovery was not assessed in these studies and no treatment related mortality was observed in either study. In the rat study, toxicity was primarily observed in males. Toxicokinetics showed that exposure to crizotinib was greater in males than females with $AUC_{(0-24)}$ values 1.6-2.9 fold higher in males compared to females. Target organs of toxicity were the bone marrow, bone (joint), kidney, prostate, spleen, seminal vesicle, testes, and thymus in male rats only. Vacuolation of renal cortical tubules, atrophy of the prostate and thymus, and degeneration of pachytene spermatocytes in the testes were observed at $\geq$ 50 mg/kg ($\geq$ 300 mg/m^2). At the 150 mg/kg (900 mg/m^2) dose level, hypocellularity of the bone marrow, decreased bone at the primary spongiosa of the joint, atrophy of the seminal vesicle, and lymphoid depletion of the spleen were also observed. The decreased bone formation was observed only in high dose males who had higher crizotinib exposure than females; as immature rats were used in this study this finding may have significance in a pediatric population. In the dog study, crizotinib-related effects included emesis and diarrhea in both males and females at doses $\geq$ 6 mg/kg ($\geq$ 120 mg/m^2), and decreased cellularity of the thymus in males at 20 mg/kg (400 mg/m^2). ECG results showed that QT/QTc intervals before or after dosing on Day 22 were increased compared to pre-study values in 2 dogs (1 male and 1 female) at the 20 mg/kg dose level.

In a three-month oral study crizotinib was administered to rats daily for 90 days with a 57-day recovery period. Based on the results of the one-month rat study, lower doses of crizotinib were administered to males (0, 10, 30, or 100 mg/kg; 0, 60, 180, or 600 mg/m^2) than females (0, 10, 50, or 250 mg/kg; 0, 60, 300, or 1500 mg/m^2). Mortality was observed in 4 females treated at the high dose (250 mg/kg; 1500 mg/m^2). Though

the sponsor attributes 3 of these deaths to gavage error, the fact that all deaths occurred at the high dose suggests that the cause of death may in fact be treatment-related. Target organs of toxicity include the bone marrow, gastrointestinal tract (cecum, colon, duodenum, ileum, and jejunum), heart, liver, lung, mesenteric lymph node, pituitary, mandibular salivary gland, and thymus. Myeloid cell debris in the bone marrow was observed in all high dose males (100 mg/kg; 600 mg/m^2) and females (250 mg/kg; 1500 mg/m^2) at the end of dosing, however, this finding was reversible. Increased incidence and severity of myonecrosis in the heart and alveolar histiocytosis in the lung were also observed in high dose males (100 mg/kg; 600 mg/m^2) and females (250 mg/kg; 1500 mg/m^2) at the end of dosing. Vacuolation was observed in multiple organs including the gastrointestinal tract (cecum, colon, duodenum, ileum, and jejunum), liver, pituitary, and prostate, and foamy macrophages were observed in the mesenteric lymph node. The vacuolation was reversible and the foamy macrophages were also observed in controls following recovery. Based on ultrastructural evaluation and immunohistochemical staining for adipophilin (a protein that forms the membrane around non-lysosomal lipid droplets) conducted on representative tissues of the liver (bile duct), duodenum (enterocyte), and mesenteric lymph node (macrophage), cellular vacuolation and the presence of foamy macrophages observed in the histopathology appear to be due to phospholipidosis. As in the one-month rat study, exposure to crizotinib was higher in males than females with C_{max} and $AUC_{(0-24)}$ values similar between males and females or higher in males than females despite higher mid and high dose levels in females than males.

The sponsor conducted a three-month oral study in dogs in which crizotinib (0, 1, 5, or 25 mg/kg; 0, 20, 100, or 500 mg/m^2) was administered daily for 91 days with a 57-day recovery period. Target organs of toxicity were the bone marrow, mesenteric lymph node, jejunum, and stomach. Clinical signs were similar to those observed in the one-month dog study and included emesis and watery/mucoid feces at $\geq$ 5 mg/kg (100 mg/m^2). QT/QTc intervals were increased from baseline to Week 6 or 13 pre-dose measurements in males at doses $\geq$ 5 mg/kg (100 mg/m^2) and in females at the 25 mg/kg (500 mg/m^2) dose level. This finding is consistent with the increases in QT/QTc intervals observed in the one-month dog study. Hematological findings included increases in eosinophils in both males and females at 25 mg/kg (500 mg/m^2) and corresponded to increased eosinophil cellularity in bone marrow observed in the same dose group. Toxicokinetic results showed that in general, exposure to crizotinib was similar between male and female dogs. These results are consistent with the toxicokinetic findings in the on-month dog study, and differ from the sex difference in exposure to crizotinib observed in rats.

Genetic Toxicology

Crizotinib was tested for mutagenicity in an *in vitro* reverse mutation (Ames) assay, and did not increase the number of revertant colony counts of any strain in the absence or presence of S-9 activation. Therefore, PF-02341066 was not mutagenic in this valid assay. In an *in vitro* structural chromosome aberration assay in human peripheral lymphocytes, crizotinib was genotoxic as evidenced by significant increases in the

percentage of structural and numerical chromosomal aberrations both with and without S-9 activation in this valid assay. Structural chromosomal aberrations were increased at 3 hours of treatment both with and without S-9 activation. Numerical chromosomal aberrations were increased at 3 hours of treatment both with and without S-9 activation and at 24 hours of treatment without S-9 activation. An exploratory *in vitro* micronucleus assay with kinetochore analysis of crizotinib was conducted in Chinese hamster ovary (CHO) cultures without metabolic activation to determine if the genotoxic activity of crizotinib is clastogenic (chromosome breakage) or aneugenic (whole chromosome loss). Crizotinib induced micronuclei in CHO-WBL cells with the presence of kinetochore staining, indicating that the genotoxic activity of the drug is aneugenic in nature.

Crizotinib was tested for micronucleus induction in two separate *in vivo* micronucleus studies conducted in the rat. In the first, crizotinib was positive for micronucleus induction in male rats treated with ≥250 mg/kg as evidenced by significant increases in micronucleated polychromatic erythrocytes in bone marrow. Crizotinib treatment (250-1000 mg/kg) resulted in increased micronucleated polychromatic erythrocytes in female rats as well, but not to a level outside of the historical range. Since exposure to crizotinib was higher in males than females, sex-related differences in exposure may have contributed to differential effects on micronucleus formation in males and females. In the second study, crizotinib significantly increased micronucleated polychromatic erythrocytes in males treated with 250 mg/kg, however, the value was within the historic control range. Though both *in vivo* studies showed a positive trend for micronucleus formation and, thus, clatogenicity, in each study bone marrow was collected for micronucleus assessment at only a single time point, 24 hours after the second dose of crizotinib, making the studies technically invalid. Since the guidance for anticancer pharmaceutical development states that if the *in vitro* assays for genotoxicity are positive, an *in vivo* assay might not be warranted, additional validated micronucleus studies are not required to support the NDA.

Carcinogenicity

Carcinogenicity studies have not been conducted.

Reproductive and Developmental Toxicology

The embryo-fetal development effects of crizotinib were studied in the rat and rabbit. In the range finding study in the rat, female Sprague-Dawley rats (n=6/group) were administered crizotinib (0, 50, 250, or 500 mg/kg; 0, 300, 1500, or 3000 mg/m^2) once daily on GD 6-17 and euthanized on GD 21. Treatment with crizotinib produced maternal toxicity including decreased body weight and food consumption at doses ≥1500 mg/m^2. All females in the high dose group (3000 mg/m^2) were euthanized on GD 12 due to clinical signs of morbidity as well as decreases in body weight and food consumption and were not included for further reproductive analysis. Fetal body weight was decreased by 15% compared to controls in the 1500 mg/m^2 group. Forelimb hyperflexion was observed in all 14 fetuses of a single litter in the 1500 mg/m^2 group

and was associated with extremely low birth weight. In the pivotal embryo-fetal development study in the rat, female rats (n=20/group) were dosed daily with crizotinib (0, 10, 50, or 200 mg/kg; 0, 60, 300, or 1200 mg/m^2) GD 6-17 and euthanized on gestation Day 21. Maternal toxicity including decreased body weight and food consumption was observed at 1200 mg/m^2, and one female in this group was euthanized on GD 12. Increased post-implantation loss consisting of early resorptions was observed at doses $\geq$ 300 mg/m^2. Fetal body weight was decreased compared to controls in the 1200 mg/m^2 group. A skeletal variation of unossifed metatarsals was observed in the 1200 mg/m^2 group, however, the incidence was minimal. No teratogenicity was observed in this study.

In the range finding study in the rabbit, female New Zealand White rabbits (n=6/group) were administered crizotinib (0, 25, 75, 175, or 350 mg/kg; 0, 300, 900, 2100, or 4200 mg/m^2) once daily on GD 7-19 and euthanized on GD 29. Treatment with crizotinib produced maternal toxicity including decreased body weight, decreased food consumption, and mortality at $\geq$900 mg/m^2. All females in the 2100 and 4200 mg/m^2 groups either died or were euthanized moribund. There were no crizotinib related effects on any cesarean-section parameter, fetal body weights, or fetal external examinations in this study in surviving rabbits treated with doses of 300 or 900 mg/m^2. In the pivotal embryo-fetal development study in the rabbit, female rabbits (n=20/group) were dosed daily with crizotinib (0, 10, 25, or 60 mg/kg; 0, 120, 300, or 720 mg/m^2) GD 7-19 and euthanized on gestation Day 29. Maternal toxicity was not observed in this study with doses up to 720 mg/m^2 crizotinib. A slight increase post-implantation loss was observed in the 720 mg/m^2 group compared to controls. Additionally, fetal body weight was decreased compared to controls in the 720 mg/m^2 group. Visceral variations (carotid artery left from innominate, absent gallbladder, and small gallbladder) and skeletal variations (misaligned caudal centrum, hyoid bent arch, and skull extra ossification site) were observed in the crizotinib-treated groups, however, the incidence was within the range of historical controls. No teratogenicity was observed in this study. Dedicated fertility and pre- and post-natal studies were not required and were not conducted with crizotinib, though findings from the general toxicology studies suggest that crizotinib can negatively impact fertility. Pregnancy category D is recommended.

Special toxicology

One of the most common adverse events observed in the clinical studies with crizotinib was visual disorder including diplopia (double vision), photopsia, blurred vision, visual impairment, and vitreous floaters. No treatment-related ophthalmic findings were observed in the one- or three-month general toxicology studies in the rat or dog. A dedicated study was conducted to evaluate the potential effects of crizotinib on electroretinogram (ERG) measurements as a potential biomarker for changes in ocular/retinal function in male Long-Evans (pigmented) rats after 4-weeks of daily administration of crizotinib (0 or 100 mg/kg; 0 or 600 mg/m^2). Treatment with crizotinib (600 mg/m^2) significantly reduced the rate of retinal dark adaptation as demonstrated by a reduction in the amplitude of the electroretinogram *b*-wave on treatment Days 15 and 29 during the initial 16 and 32 minutes of dark adaptation, respectively. Crizotinib was

detected in the vitreous humor at a concentration 0.66 fold the concentration in the plasma.

To test the phototoxic potential of crizotinib, the *in vitro* 3T3 neutral red uptake assay was conducted with Balb/c 3T3, clone 31 mouse fibroblast cells, in which cells were treated with various concentrations of crizotinib for 1 hour and then irradiated with 5 joules/cm^2 of UVA light. Under the conditions of this assay, crizotinib was determined to have probable phototoxic potential.

Summary of Safety Pharmacology Studies

Study #/Organ System	Method of Administration	Species/cells	Doses/ concentrations	Gender/n	Findings
PF02341066NA11/CNS	*In vitro*	HEK293 cells expressing Nav1.1 gene	0, 0.3, 1, and 3 µM PF-02341066	NA/n=4-7	Nav1.1 sodium channel inhibited with an IC_{50} of 0.85 µM for the closed state and 0.87 µM for the inactivated state
3660/CNS	Oral	Rat	0, 10, 75, or 500 mg/kg (0, 60, 450, or 3000 mg/m^2) PF-02341066	Male/n=8	450 and 3000 mg/m^2: ↓ locomotor activity 3000 mg/m^2: salivation and dyspnea
PF02341066HERG/ cardiovascular	*In vitro*	HEK293 cells expressing hERG gene	0, 0.1, 0.3, 1, 3, and 10 µM PF-02341066	NA/n=5	hERG channel inhibited with an IC_{50} of 1.1 µM
PF02341066AORTA Amendment/ cardiovascular	*In vitro*	Descending thoracic aorta of male Sprague-Dawley rats	0, 0.1, 1, and 10 µM PF-02341066	NA/n=5-6	Relaxation of a 45 mM KCl-induced contraction with an IC_{50} of 0.83 µM
04-2796-01/ cardiovascular	*In vitro*	Guinea pig ventricular myocytes	0, 1, 3, 10, 30 and 100 µM PF-02341066	NA/n=3-6	L-type calcium channel inhibited with an IC_{50} of 14.6 µM
IC00104/ cardiovascular	*In vitro*	Beagle dog Purkunje fibres	0, 0.01, 0.1, 1, and 10 µM PF-02341066	NA/n=5	10 µM reduced the cardiac action potential duration at 50% repolarization (APD_{50}) at

Study #/Organ System	Method of Administration	Species/cells	Doses/ concentrations	Gender/n	Findings
					0.3, 1, and 3 Hz and at 90% (APD_{90}) repolarization at 1 and 3 Hz in canine isolated cardiac purkinje fibres
PF02341066NA15 and PF02341066NA15 Amendment 1/ cardiovascular	*In vitro*	CHO cells expressing Nav1.5 gene	0, 0.3, 1, 3, and 10 µM PF-02341066	NA/n=2-6	Nav1.5 sodium channel inhibited with an IC_{50} of 1.56 µM
PF02341066/CG/003/04/ cardiovascular	Intravenous	Dog (anesthetized)	Loading infusions: 0, 0.134, 0.295, 1.192, and 1.907 mg/kg (0, 2.68, 5.9, 23.84, and 38.14 mg/m^2) over 10 minutes Maintenance infusions: 0, 0.00939, 0.0207, 0.0834, 0.134 mg/kg/min (0, 0.1878, 0.414, 1.668, and 2.68 mg/m^2/min) for ~25 minutes	Male/n=4, (2 groups, drug-treated and vehicle-treated)	Two highest doses: ↓ heart rate, ↑ left ventricular end diastolic pressure, and ↑ PR-interval, QRS-interval, and QT-interval Highest dose: ↓ myocardial contractility
3622/Pulmonary	Oral	Rat	0, 10, 75, or 500 mg/kg (0, 60, 450, or 3000 mg/m^2) PF-02341066	Male/n=8	3000 mg/m^2: ↓ mean minute volume and mean respiratory rate and ↑ tidal volume during the first 24 minute observation interval starting 3 hours after dosing

General Toxicology Summary:

Repeat Dose Toxicity Studies				
Species	**Route Duration**	**N/sex/ dose**	**mg/kg (mg/m^2)**	**Significant findings**
Rat	Oral Daily x 7 days	3 (MS)	50 (300) 150 (900) 500 (3000)	300 mg/m^2: Gurgled/raspy breathing, ↓ body weight gain, ↓ kidney and liver weights, ↓ spleen and thymus weight in males, liver glycogen depletion in 1 female 900 mg/m^2: Gurgled/raspy breathing, dyspnea, lethargy, oral discharge, ↓ body weight/body weight gain, ↓ kidney and liver weights, ↓ spleen and thymus weight in males, hydronephrosis in kidney in 1 male, liver glycogen depletion in females, thymus atrophy in 1 female 3000 mg/m^2: Mortality in all 3 males and 3 females, diarrhea, dyspnea, oral discharge, ↓ body weight, ↓WBC count and % lymphocytes, ↑ % neutrophils and monocytes, ↑ ALT and AST, ↑ glucose in males, ↑ creatine kinase, ↓ total protein and albumin, ↑ urine volume, ↓ kidney and liver weights, ↓ spleen weight, ↓ thymus weight in males, ↓ ovary weight in females, hypocellularity in bone marrow, ileum and jejunum lymphoid depletion and necrosis in males, liver glycogen depletion, ovary necrosis in 1 female, pancreas zymogen depletion, spleen lymphoid depletion in males, spleen depletion extramedullary hematopoiesis, salivary gland secretory depletion and single cell necrosis, stomach edema, thymus atrophy
Rat	Oral Daily x 28 days (1 month)	10 (MS)	10 (60) 50 (300) 150 (900)	Exposures ($AUC_{(0-24h)}$) were 1.6-2.9 fold greater in males than females 300 mg/m^2: Increased salivation, ↑ platelets and neutrophils in males, ↓APTT, ↓ PT in males, ↑ AST and ALT in males, ↓ urine pH in males, ↓ kidney weight in males, tubule vacuolation in kidney in males, prostate atrophy in 1 male, thymus atrophy in 1 male, degeneration of spermatocytes in testes in 1 male, 900 mg/m^2: Increased salivation, piloerection in males, chromodacryorrhoea, ↓ body weight and food consumption in males, ↑ in neutrophils, ↑ platelets and monocytes in males, ↓ APTT, ↓ PT in males, ↑ AST and ALT, ↑ GGT in males, ↓ potassium, ↑ urea in males, ↓ urine pH, ↓ kidney weight, ↓ liver, prostate, spleen and thymus weights in males, hypocellularity in bone marrow in males, decreased bone primary spongiosa of the joint in males, tubule vacuolation in kidney in males, atrophy of prostate and seminal vesicle in males, spleen lymphoid depletion in males, thymus atrophy in males, degeneration of spermatocytes in testes in males
Rat	Oral Daily x 90 days (3 months) 57-day (2-month) recovery	10 (MS) 5 (Recov.)	Males: 10 (60) 30 (180) 100 (600) Females: 10 (60) 50 (300) 250 (1500)	Exposure was higher in males than females with C_{max} and $AUC_{(0-24h)}$ values similar between males and females or higher in males than females despite higher mid and high doses in females than males 60 mg/m^2: Decreased skin tugor in males, ↑ ALT and AST in males 180 mg/m^2 (males): Decreased skin tugor, ↑ ALT and AST, ↓ urine pH, myeloid cell debris in bone marrow in 1 male, extrahepatic bile duct vacuolation in duodenum, ↑

Repeat Dose Toxicity Studies				
Species	**Route Duration**	**N/sex/ dose**	**mg/kg (mg/m^2)**	**Significant findings**
				incidence of myonecrosis in heart, bile duct vacuolation in liver, vacuolation in ileum 300 mg/m^2 (females): ↑ BUN, extrahepatic bile duct vacuolation in duodenum, bile duct vacuolation in liver, vacuolation in ileum 600 mg/m^2 (males): Decreased skin tugor, ↓ body weight gain and food consumption, ↓ hemoglobin and hematocrit, ↓ reticulocytes, ↑ platelets and neutrophils, ↑ ALT, AST, and ALP, ↓ glucose, ↑ BUN and creatinine, ↓ urine pH, ↓ kidney, liver, spleen, and thymus weights, myeloid cell debris in bone marrow, extrahepatic bile duct vacuolation in duodenum, ↑ incidence and severity of myonecrosis in heart, bile duct vacuolation in liver, vacuolation in gastrointestinal tract (cecum, colon, duodenum, ileum, and jejunum), ↑ incidence and severity of alveolar histiocytosis in lung, foamy macrophages in mesenteric lymph node, vacuolation in pituitary, acinar cell swelling in salivary gland, lymphocytolysis in thymus 1500 mg/m^2 (females): Mortality in 4 females, decreased skin tugor, activity decreased, chromodacryorrhea, edema, eye partially closed, lame/limping forelimb, hunched posture, ↓ body weight gain and food consumption, ↑ platelets, WBC count, neutrophils, and monocytes, ↑ ALT, AST, and ALP, ↓ glucose, ↑ BUN, ↑ heart weight, ↓ kidney, spleen, and thymus weights, myeloid cell debris and ↑ cellularity in bone marrow, extrahepatic bile duct vacuolation in duodenum, bile duct vacuolation in liver, vacuolation in gastrointestinal tract (cecum, colon, duodenum, ileum, and jejunum), ↑ incidence and severity of alveolar histiocytosis in lung, lung congestion in 2 females with mortality, foamy macrophages in mesenteric lymph node, vacuolation in pituitary, acinar cell swelling in salivary gland, lymphocytolysis in thymus
Dog	Oral Daily x 28 days (1 month)	3 (MS)	1 (20) 6 (120) 20 (400)	120 mg/m^2: Emesis, diarrhea, ↓ albumin in females 400 mg/m^2: Emesis, diarrhea, ↑ QT/QTc interval in 1 male and 1 female, ↓ RBC count, hemoglobin, and hematocrit in females, ↑WBC count and neutrophils in females, ↓ albumin, ↓ cellularity of thymus in males
Dog	Oral Daily x 91 days (3 months) 57-day (2-month) recovery	3 (MS) 2 (Recov.)	1 (20) 5 (100) 25 (500)	20 mg/m^2: ↑ GGT in females, ↑ ALP in males, ↓ total protein and albumin in males, erythrophagocytosis in mesenteric lymph node 100 mg/m^2: Emesis, watery/mucoid feces, ↑ eosinophils in females, ↑ ALP, ↑ AST and GGT in females, ↓ total protein and albumin in males, jejunum congestion in 1 female, stomach congestion in 1 male, erythrophagocytosis in mesenteric lymph node 500 mg/m^2: Emesis, watery/mucoid feces, salivation, ↑ QT/QTc interval, ↓ RBC count, hemoglobin, and hematocrit %, ↑ reticulocytes in males, ↑ platelets and fibrinogen, ↑ WBC count, neutrophils, lymphocytes, monocytes, and eosinophils, ↑ ALT, AST, and ALP, ↑ GGT, ↓ albumin, ↓ total protein and calcium in males, ↑

Repeat Dose Toxicity Studies				
Species	**Route Duration**	**N/sex/ dose**	**mg/kg (mg/m^2)**	**Significant findings**
				BUN in males, ↑ eosinophil cellularity in bone marrow, skin ulcer in 1 female, erythrophagocytosis in mesenteric lymph node

MS=Main study
Recov.=Recovery groups

Genetic Toxicology Summary

Title	Study #	Without Metabolic Activation	With Metabolic Activation
Bacterial reverse mutation assay of PF-2341066	3565	Negative at concentrations of 31.3-500 µg/plate for *Salmonella typhimurium* strains TA98, TA100, TA1535, and TA1537 and at concentrations of 62.5-1000 µg/plate for *Escherichia coli* strain WP2*uvr*A	Negative at concentrations of 31.3-500 µg/plate for *Salmonella typhimurium* strains TA98, TA100, TA1535, and TA1537 and at concentrations of 62.5-1000 µg/plate for *Escherichia coli* strain WP2*uvr*A
In vitro structural chromosome aberration assay of PF-2341066 in human peripheral lymphocytes	3554	Positive for genotoxicity: Increased structural chromosomal aberrations at 3 hours (2.5 and 7.5 µg/mL) Increased numerical chromosomal aberrations at 3 hours (2.5, 5, and 7.5 µg/mL) and 24 hours (1, 1.5, and 2.5 µg/mL)	Positive for genotoxicity: Increased structural (10 µg/mL) and numerical (5 and 10 µg/mL) chromosomal aberrations at 3 hours
In vitro micronucleus assay with kinetochore analysis of PF-2341066 in Chinese hamster ovary (CHO) cultures	PG 0135	Positive for aneugenicity in CHO-WBL cells at concentrations of 0.20-0.30 µg/mL	Not conducted
In vivo micronucleus study of PF-2341066 in rats	3665	Positive for genotoxicity in the male rats at doses of 250, 500, or 1000 mg/kg (1500, 3000, or 6000 mg/m^2) at 24 hrs; negative in female rats at same doses Micronucleus assessment conducted at a single time point, study invalid	
In vivo micronucleus study of PF-2341066 in male rats	3746	Significant increase in micronucleus induction in male rats at 250 mg/kg, however, the value was within the historic control range Micronucleus assessment conducted at a single time point, study invalid	

Reproductive and Developmental Toxicity Summary

	Embryonic Fetal Development			
Study #	**09GR345**	**10GR072**	**09GR350**	**10GR073**
Title	Oral dose range-finding study of PF-02341066 in pregnant rats	Oral embryo-fetal development study of PF-02341066 in rats	Oral dose range-finding study of PF-02341066 in pregnant rabbits	Oral embryo-fetal development study of PF-02341066 in rabbits
Methods	Females dosed once daily GD 6-17 and euthanized on GD 21	Females dosed once daily GD 6-17 and euthanized on GD 21	Females dosed once daily GD 7-19 and euthanized on GD 29	Females dosed once daily GD 7-19 and euthanized on GD 29
Key Findings	PF-02341066 produced maternal toxicity including ↓ body weight and food consumption at ≥1500 mg/m^2 All females in the 3000 mg/m^2 group were euthanized on GD 12 Fetal body weight ↓ in the 1500 mg/m^2 group compared to controls	PF-02341066 produced maternal toxicity including ↓ body weight and food consumption at 1200 mg/m^2 One female in the 1200 mg/m^2 group was euthanized on GD 12 Post implantation loss (early resorptions) ↑ at ≥ 300 mg/m^2 Fetal body weight ↓ in the 1200 mg/m^2 group compared to controls No teratogenicity was observed in this study	PF-02341066 produced maternal toxicity including ↓ body weight and food consumption and mortality at ≥ 900 mg/m^2 All females in the 2100 and 4200 mg/m^2 groups either died or were euthanized moribund	Maternal toxicity was not observed in this study with doses up to 720 mg/m^2 PF-02341066 Post implantation loss ↑ at 720 mg/m^2 Fetal body weight ↓ in the 720 mg/m^2 group compared to controls No teratogenicity was observed in this study
Species	Sprague-Dawley rat	Sprague-Dawley rat	New Zealand White rabbit	New Zealand White rabbit
Doses	0, 50, 250, or 500 mg/kg (0, 300, 1500, or 3000 mg/m^2)	0, 10, 50, or 200 mg/kg (0, 60, 300, or 1200 mg/m^2)	0, 25, 75, 175, or 350 mg/kg (0, 300, 900, 2100, or 4200 mg/m^2)	0, 10, 25, or 60 mg/kg (0, 120, 300, or 720 mg/m^2)
Mortality and Clinical Signs	3000 mg/m^2: All females were euthanized on GD 12 due to clinical signs of ↓ activity, oral/nasal chromorhinorrhea, and piloerection as well as ↓ in body weight and food consumption	1200 mg/m^2: One female was euthanized on GD 12 due to clinical signs of oral/nasal chromorhinorrhea and rough haircoat as well as ↓ in body weight and food consumption	900 mg/m^2: One female was euthanized on GD 18 with clinical signs of ↓ activity and ↓ or absent feces 2100 mg/m^2: All females died or were euthanized moribund on GD 11 or 12 with clinical signs of ↓ activity and watery, ↓, or absent feces	No treatment related mortality or clinical signs

			4200 mg/m^2: All females died or were euthanized moribund on GD 9 with clinical signs of ↓ activity, cool to touch, and breathing pattern slow	
Body Weight/Food Consumption	1500 mg/m^2: Lost weight GD 6-8, ↓ body weight gain compared to controls with ↓ net weight gain corrected for gravid uterine weight; ↓ food consumption 3000 mg/m^2: On GD 12 body weight was ↓ 16% compared to GD 6 and ↓26% compared to controls; ↓ food consumption	1200 mg/m^2: ↓ body weight gain compared to controls GD 7-21; ↓ gravid uterine weight, corrected maternal body weight, and net body weight gain corrected for gravid uterine weight; ↓ food consumption	900 mg/m^2: Slight ↓ in body weight compared to controls GD 7-20 with ↓ net body weight gain corrected for gravid uterine weight; food consumption ↓ 17.6% compared to controls for the GD 7-20 interval 2100 mg/m^2: Lost 16.2% of body weight from start of treatment until death or euthanasia; food consumption ↓ 88% compared to controls for GD 7-10 interval 4200 mg/m^2: Lost 9.8% of body weight from start of treatment until death or euthanasia; food consumption on GD 7-9 ↓ 99% compared to controls for GD 7-10 interval	No findings
Necropsy	3000 mg/m^2: Dilated stomach in 2 females and dilated cecum in another female	No findings	900 mg/m^2: Stomach erosion/ulcer in euthanized female 2100 mg/m^2: Stomach focus in all females 4200 mg/m^2: Stomach focus in 5 of 6 females	No treatment related findings
Cesarean section/fetal exams	1500 mg/m^2: Fetal weight ↓ 15%; forelimb hyperflexion observed in all fetuses of a	Post implantation loss (early resorptions) ↑ at both 300 and 1200 mg/m^2	No findings	720 mg/m^2: Post implantation loss ↑, fetal weight ↓

	single litter.	1200 mg/m^2: Fetal weight ↓; skeletal variations of unossifed metatarsals were observed with minimal incidence		Visceral (carotid artery left from innominate, absent gallbladder, small gallbladder) and skeletal (misaligned caudal centrum, hyoid bent arch, and skull extra ossification site) variations were observed in the PF-02341066-treated groups, however, the incidence was minimal

---

This is a representation of an electronic record that was signed electronically and this page is the manifestation of the electronic signature.

/s/

BRENDA J GEHRKE
08/10/2011

WHITNEY S HELMS
08/10/2011

PHARMACOLOGY/TOXICOLOGY FILING CHECKLIST FOR NDA/BLA or Supplement

NDA/BLA Number: 202570 **Applicant: Pfizer Inc.** **Stamp Date: 3/30/2011**

Drug Name: Crizotinib **NDA/BLA Type: NME**

On **initial** overview of the NDA/BLA application for filing:

	Content Parameter	Yes	No	Comment
1	Is the pharmacology/toxicology section organized in accord with current regulations and guidelines for format and content in a manner to allow substantive review to begin?	✓		NDA is submitted in the eCTD format
2	Is the pharmacology/toxicology section indexed and paginated in a manner allowing substantive review to begin?	✓		Electronic submission
3	Is the pharmacology/toxicology section legible so that substantive review can begin?	✓		
4	Are all required (*) and requested IND studies (in accord with 505 b1 and b2 including referenced literature) completed and submitted (carcinogenicity, mutagenicity, teratogenicity, effects on fertility, juvenile studies, acute and repeat dose adult animal studies, animal ADME studies, safety pharmacology, etc)?	✓		• Carcinogenicity: Not conducted/submitted and not required • Mutagenicity: Submitted • Teratogenicity: Submitted, both rat and rabbit • Effects on fertility: Not conducted/submitted and not required • Juvenile studies: Not conducted and not required • Acute dose animal studies: Not conducted/submitted • Repeat dose animal studies: Submitted, studies include 3 month rat and 3 month dog • ADME: Submitted • Safety Pharmacology: Submitted
5	If the formulation to be marketed is different from the formulation used in the toxicology studies, have studies by the appropriate route been conducted with appropriate formulations? (For other than the oral route, some studies may be by routes different from the clinical route intentionally and by desire of the FDA).	✓		Oral formulations were used in pivotal clinical and nonclinical studies
6	Does the route of administration used in the animal studies appear to be the same as the intended human exposure route? If not, has the applicant submitted a rationale to justify the alternative route?	✓		Same route of administration

PHARMACOLOGY/TOXICOLOGY FILING CHECKLIST FOR NDA/BLA or Supplement

	Content Parameter	Yes	No	Comment
7	Has the applicant submitted a statement(s) that all of the pivotal pharm/tox studies have been performed in accordance with the GLP regulations (21 CFR 58) or an explanation for any significant deviations?	✓		
8	Has the applicant submitted all special studies/data requested by the Division during pre-submission discussions?	✓		
9	Are the proposed labeling sections relative to pharmacology/toxicology appropriate (including human dose multiples expressed in either mg/m2 or comparative serum/plasma levels) and in accordance with 201.57?	✓		A substantive labeling review will be conducted after review of the submitted nonclinical program
10	Have any impurity – etc. issues been addressed? (New toxicity studies may not be needed.)	✓		There are 4 impurities in the drug substance that have proposed specifications above the ICH qualification thresholds that will need to be qualified A one month study to qualify impurities was conducted and submitted
11	Has the applicant addressed any abuse potential issues in the submission?			Not applicable
12	If this NDA/BLA is to support a Rx to OTC switch, have all relevant studies been submitted?			Not applicable

IS THE PHARMACOLOGY/TOXICOLOGY SECTION OF THE APPLICATION FILEABLE? ____Yes____

If the NDA/BLA is not fileable from the pharmacology/toxicology perspective, state the reasons and provide comments to be sent to the Applicant.

Please identify and list any potential review issues to be forwarded to the Applicant for the 74-day letter.

File name: 5_Pharmacology_Toxicology Filing Checklist for NDA_BLA or Supplement 010908

PHARMACOLOGY/TOXICOLOGY FILING CHECKLIST FOR NDA/BLA or Supplement

Brenda J. Gehrke, Ph.D.	5/2/2011
Reviewing Pharmacologist	Date
Whitney S. Helms, Ph.D.	5/2/2011
Acting Team Leader/Supervisor	Date

File name: 5_Pharmacology_Toxicology Filing Checklist for NDA_BLA or Supplement 010908

This is a representation of an electronic record that was signed electronically and this page is the manifestation of the electronic signature.

/s/

BRENDA J GEHRKE
05/02/2011

WHITNEY S HELMS
05/02/2011